University of St Andrews

Properties of Free Radicals Incorporating Thiophene, Cubane and Fullerene Units.

A thesis presented by Philip Mallon, B.Sc., to the University of St. Andrews in application for the degree of Doctor of Philosophy.

October 1992.

Declarations

I, Philip Mallon, hereby certify that this thesis has been composed by myself, that it is a record of my own work and that it has not been accepted in partial or complete fulfilment of any other degree or professional qualification.

Signed _____ _____ Date 26ᵗʰ October 1992

I was admitted to the Faculty of Science of the University of St. Andrews under Ordinance General No. 12 on the 1ˢᵗ of October 1989 and as a candidate for the degree of Ph.D. on the 1ˢᵗ of October 1990.

Signed _____ Date 26ᵗʰ October 1992

We hereby certify that the candidate has fulfilled the conditions of the Resolution and Regulations appropriate to the Degree of Ph.D.

Signature of _____ Date 26ᵗʰ Oct. 1992

Supervisors _____ Date 26ᵗʰ Oct 1992

Declaration.

In submitting this thesis to the University of St. Andrews, I understand that I am giving permission for it to be made available for its use in accordance with the regulations of the University library for the time being in force, subject to any copyright vested in the work not being affected thereby. I also understand that the title and abstract will be published, and that a copy of the work may also be made and supplied to any *bona fide* library or research worker.

Contents

Part One
Thiophene-Based Polyradicals.

Chapter One
Introduction to Radical Polythiophenes.

Chapter Two
Preparation and Study of Radical-Thiophene Monomers.

Part Two
The Cubyl and Cubylcarbinyl Radicals, and Homolytic Reactions of Cubane.

Chapter Three
Introduction to the Chemistry of Cubane.

Part Three
The Behaviour of Fullerene Radicals.

Chapter Six
Introduction to the Fullerenes.

Chapter Seven
The Behaviour of Fullerene Radicals.

Acknowledgements

Postgraduate Courses

The Department of Chemistry requires that a number of courses are attended, these courses are;

"Free Radicals" (Dr. J.C. Walton), "Cyclic Voltammetry" (Dr. J.A. Crayston), "Semi-conductor Growth Technology" (Prof. D.J. Cole-Hamilton), "Asymmetric Synthesis" (Dr. R.A. Aitken), "Frontier Orbital Theory" (Dr. F.G. Riddell), "Molecular Rearrangements" (Dr. J.C. Walton).

List of Abbreviations

δ	Relative To Tetramethylsilane
CB	Conduction Band
COSY	COrrelated SpectroscopY
CV	Cyclic Voltammetry
DMF	Dimethylformamide
DMSO	Dimethyl Sulphoxide
DPPH	2,2-Diphenyl-1-picrylhydrazyl
EI-MS	Electron Impact Mass Spectrometry
EPR	Electron Paramagnetic Resonance
ESR	Electron Spin Resonance
FAB-MS	Fast Atom Bombardment Mass Spectrometry
GC-MS	Gas Chromatographic Mass Spectrometry
hfs	Hyperfine Splittings
HPLC	High Performance Liquid Chromatography
IR	Infra-Red
IPR	Isolated Pentagon Rule
LUMO	Lowest Unoccupied Molecular Orbital
NBMO	Non Bonding Molecular Orbital
NHE	Normal Hydrogen Electrode
NMR	Nuclear Magnetic Resonance
PRV	Pressure Release Valve
SCE	Standard Calomel Electrode
SCF-MO	Self-Consistent Field Molecular Orbital
SE	Strain Energy
SOMO	Semi-Occupied Molecular Orbital
TBAHFP	Tetrabutylammonium hexafluorophosphate
TBAT	Tetrabutylammonium Triflate

TDAE	Tetrakis(dimethylamino)ethylene
TEMPO	2,2,6,6-Tetramethyl-1-piperidinyloxy, free radical
THF	Tetrahydrofuran
TOF-MS	Time-Of-Flight Mass Spectrometry
UV	Ultra Violet
VB	Valence Band

Abstract

Two routes to thiophene-3,4-dicarboxylic acid were compared. A series of thiophenenaphthoquinones was then prepared by cyclic diacylation of substituted benzenes with thiophene-3,4-dicarbonyl chloride and aluminium trichloride, and their radical anions characterised by CV and EPR spectroscopy. The polymerisation of these monomers was probed by a variety of chemical and electrochemical techniques. The preparation of the thiophene analogue of the 1,1,3,3-tetramethylisoindolin-2-yloxyl radical via the imide was investigated, and the reaction of thiophene-3-carboxaldehyde examined.

A series of 4-substituted cubyl radicals was generated by bromine atom abstraction from the corresponding bromocubanes. The cubyl radicals were shown to abstract secondary hydrogen atoms from triethylsilane and to terminate mainly by means of second order combination reactions. t-Butoxyl radicals abstracted hydrogen atoms from cubane at a rate in excess of 26 times that from cyclopropane at -90°C, with electron-withdrawing substituents on the cubane greatly reducing this. The cubyl hydrogen atoms of methylcubane were abstracted in preference to the primary methyl hydrogens. Bromine atoms reacted with cubane at the carbon atoms, directly by homolytic substitution, prompting a series of rearrangements which ended with the precipitation of cis,cis-3,4,7,8-tetrabromo-syn-tricyclo[4.2.0.0^{2,5}]octane from solution. In contrast cubane and chlorine reacted mainly by hydrogen abstraction. EPR spectroscopy showed that the cubylcarbinyl radical rearranged by a cascade of three β-scissions, with a rate constant $\geq 5\times10^9$ s^{-1} at 25°C. The intermediate tricycloallyl radical was characterised by EPR spectroscopy. The initial β-scission of the α-hydroxycubylcarbinyl radical proceeded at one thousandth the rate of the parent cubylcarbinyl radical, allowing the α-hydroxycubylcarbinyl radical and its rearrangement product to be observed by EPR spectroscopy.

Fullerenes 60 and 70 were observed to react with photolytically generated alkyl and haloalkyl radicals (such as methyl, ethyl, benzyl, trichloromethly and

fluorodichloromethyl radicals) to produce $R\text{-}C_{60}{}^{\bullet}$ and $R\text{-}C_{70}{}^{\bullet}$ radical adducts. These were observed by EPR spectroscopy and the ^{13}C interactions of the $Cl_3C\text{-}C_{60}{}^{\bullet}$ radical adduct were obtained. This shows that the unpaired electron is mainly restricted to two fused six-membered rings of the fullerene 60, with the R substituent at one point of this fusion. The behaviour of fullerene 60 with the diradical produced by the extrusion of nitrogen from 2,3-diazabicyclo[2.2.1]hept-2-ene was examined. EPR spectroscopy was used to monitor the abstraction of bromine from $C_{60}Br_2$.

"I love it when a plan comes together."

- Hannibal Smith,

The A-Team.

Part One:

Thiophene-Based

Polyradicals.

Chapter One

Introduction to Radical Polythiophenes

In general it has been supposed that organic polymers are better suited to applications requiring good insulative properties, as opposed to conductive properties. In fact the electronics industry has traditionally used such materials in packing and insulating roles, in order to protect the electronically active components of an electrical circuit or device. This view is, however, rapidly changing as new polymeric materials with a range of electrical and optical properties are becoming available.

The modern era of conducting polymers began in 1977 when Heeger and MacDiarmid discovered that polyacetylene, $(CH)_n$[1], could undergo a twelve orders of magnitude increase in conductivity upon charge-transfer oxidative coupling[2]. The essential structural characteristic of a conducting polymer is a conjugated π-system extending over a large number of repeating monomer units. This results in low-dimensional materials with a high anisotropy of conductivity which is higher along the chain direction. Polyacetylene is the simplest example of this type of polymer and is the subject of much theoretical and experimental work[3], despite its environmental instability, which is a major obstacle to practical applications.

A major group of conjugated organic polymers are the poly(heterocycles). These can be treated as $sp^2 p_x$ carbon chains in which the structure, analogous to that of cis-$(CH)_n$, is stabilised by the heteroatom (Figure 1.1). Poly(heterocycles) differ from polyacetylene in several ways: (i) their non-degenerate ground state is related to the non-energetic equivalence of their two limiting mesomeric forms, aromatic and quinoid, (ii) their higher environmental stability, and (iii) their structural versatility which allows their electronic and electrochemical properties to be manipulated.

Great interest in the development of conjugated poly(heterocycles) was generated in 1979. Diaz *et al*. showed that highly conducting and homogeneous free standing films of polypyrrole could be produced by oxidative electropolymerisation of
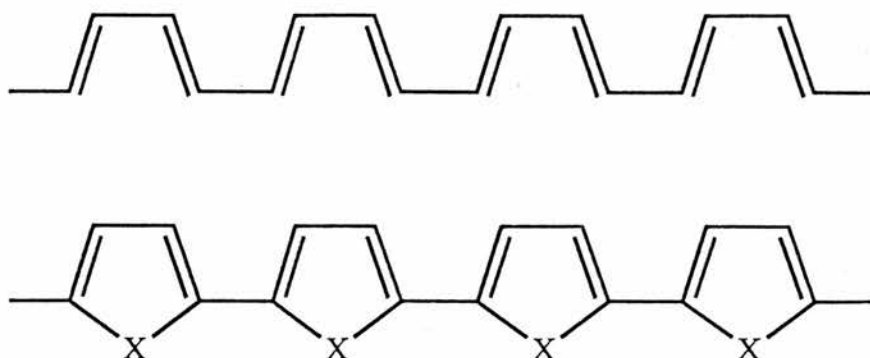
Figure 1.1

cis-(CH)$_x$ compared to a poly(heterocycle).

pyrrole[4]. The synthesis of polypyrrole in aqueous sulphuric acid was reported in 1969[5] but the poor mechanical and electrical properties of the material did not give rise to further developments. The electrochemical polymerisation has since been extended to include other aromatic compounds such as thiophene[6,7], furan, indole[7], carbazole, azulene, pyrene[8], benzene[9], fluorene[10] and aniline[11].

The doping process, in the case of a poly(heterocycle), produces polaron and bipolaron sites (Figure 1.2). To begin with, an electron is removed from the π-system of the polymer backbone thereby creating a free radical and a cation. These are coupled to each other by way of a local bond rearrangement, which takes the form of a sequence of quinoid-like rings. This quinoid-like lattice distortion is of higher energy than the remaining benzene-like polymer backbone. As a result of the high energy requirement for creating and separating these defects, the number of quinoid-like rings which can link together the radical and cation is limited. This combination of a charged site coupled to a free radical via a local lattice distortion is called a polaron and can take the form of a radical cation or a radical anion. Polaron formation results in the production of new localised electronic states in the polymer bandgap (Figure 1.3), with the lower energy states being occupied by single unpaired electrons, consequently a polaron has spin.

With further oxidation another electron can be removed from the polaron or
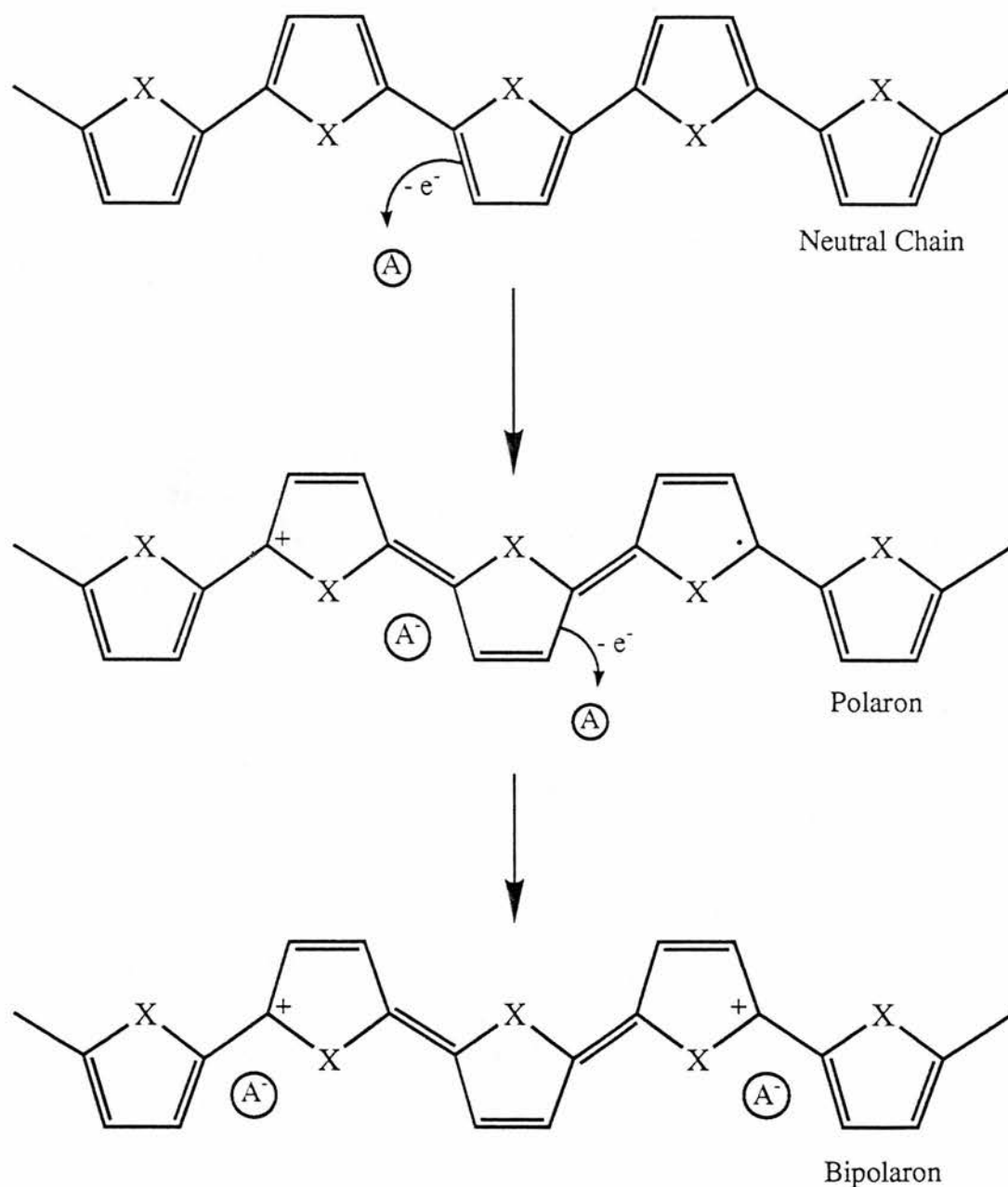
Figure 1.2

Oxidation of a poly(heterocycle) and the creation of

polaron and bipolaron states.

the remaining neutral polymer chain. When the electron is removed from the

polaron, a dication is formed which consists of two positive charges coupled through

a lattice distortion. This spinless defect is termed a bipolaron. Removal of another

electron from a different region of the neutral polymer chain, on the other hand,

produces a second polaron. Bipolaron formation causes a larger reduction in ionisation energy compared to the formation of two polarons. Therefore bipolaron formation is thermodynamically favoured. Persistent high doping of the polymer creates additional bipolaron states, which, at high doping levels, can overlap to produce continuous bipolaron bands (Figure 1.3). The polymer bandgap is increased
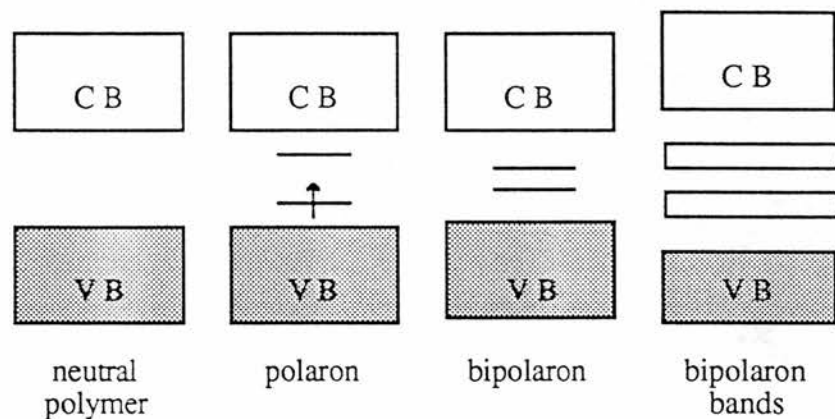
Figure 1.3

The bandgap, conduction and valence bands of

the various polymer states.

during this process and the newly formed bipolaron sites are produced at the expense of the band edges. For conjugated polymers that can be heavily doped, it is theoretically conceivable that the upper and lower bipolaron bands will merge with the conduction and valence bands (CB and VB) to produce partially filled bands and metallic conductivity.

In order for commercial applications of a polymer to be developed, it is imperative that it exhibits a good environmental stability and is amenable to a variety of processing techniques. The state of these attributes, with the levels of conductivity after suitable oxidative doping, for several representative conjugative polymers is shown in Table 1.1.
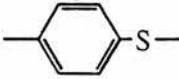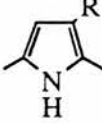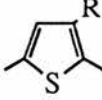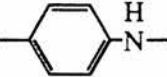
Polymer	Conductivity $(\Omega^{-1}cm^{-1})$	Stability (doped state)	Processing Possibilities
Polyacetylene -HC=CH-	10^3 to 10^5	poor	limited
Polyphenylene	1000	poor	limited
Poly(p-phenylene sulphide)	100	poor	excellent
Poly(phenylene vinylene)	1000	poor	limited
Polypyrroles	100	good	good
Polythiophenes	100	good	excellent
Polyaniline	10	good	good

Table 1.1

Stability and processability of representative conducting polymers.

"Limited" processability means that the polymer can only be processed into

usable forms by specialised methods, whereas "excellent" indicates that a number of different conventional processing techniques are suitable. A polymer with "poor" stability is essentially unstable in its doped state under normal atmospheric conditions. The conductivity of such materials may decrease by as much as an order of magnitude every few months at room temperature and much faster at higher temperatures. Conversely, materials that exhibit "good" stability only display minor changes in conductivity, even after exposure in air to temperatures of up to 200°C for long periods of time. Thus it can be seen that in general, conducting polymers based on polythiophene exhibit the best overall stability and processability, with polypyrrole a close second[12]. The stability of these poly(heterocycles) can be enhanced by the introduction of an electron donating substituent at C-3 or C-4. This has the effect of lowering the oxidation potential of the polymer and stabilising its positively charged bipolaron states[13].

Based on polythiophene's high environmental stability and its structural versatility, which has led to multiple developments aimed at applications such as conductors, electrode materials and organic semiconductors, we too decided to use thiophene units as the polymer backbone in our materials.

1.1   Stable Organic Free Radicals

A free radical is an atom, molecule or complex which contains one or more unpaired electrons. The first authenticated free radical to be discovered was the triphenylmethyl radical in 1900 by Gomberg[14]. Examples of other stable free radicals soon followed, such as Piloty and Schwerin's nitroxide porphyrexide[15] (Figure 1.4).

There are a variety of routes by which one can produce free radicals. Those that exist as stable, pure substances can be obtained by conventional chemical methods. The more reactive radicals are produced by thermal decomposition, irradiation techniques, electron transfer reactions or by electrode processes. Most of the free radicals obtained by these techniques are highly reactive and have lifetimes in

the range of micro- or milliseconds, unless they are stabilised in some way. Here we are only concerned with stable, that is long-lived, organic free radicals.

The concept of stability, when applied to free radicals, has proven to be a rather imprecise term, with no exact definition. It can be said that the stability of a radical is dependent on its chemical environment. The methyl radical, for example, can be stabilised almost indefinitely in an argon matrix at very low temperatures, although it irreversibly disappears on warming the matrix[16]. In contrast to this is the diphenylpicrylhydrazyl (DPPH) radical (Figure 1.4), which is able to exist permanently as a free radical in the solid state[17]. It can be crystalised, isolated and treated as a normal organic compound, although in the presence of other organic radicals it usually disappears rapidly. These two examples obviously exhibit differing degrees of stability, yet they have both been described as "stable" radicals. Therefore some definition of what actually is a stable radical is required. Griller and
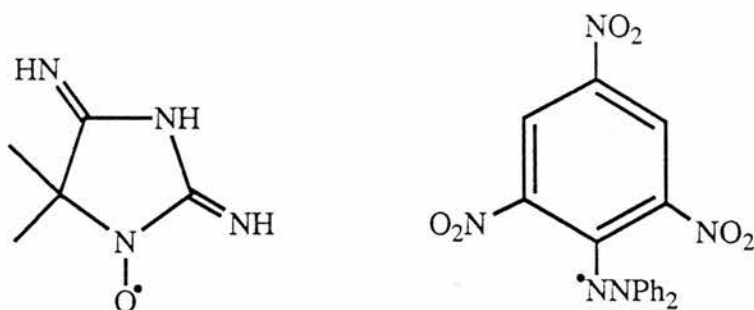
Figure 1.4

Nitroxide porphyrexide (left) and the
2,2-diphenyl-1-picrylhydrazyl radical (right).

Ingold[18] have looked at this and produced a definition for the description of radical stability. They suggested that the term "stable" should only be applied to a radical which is so persistent and unreactive to air and moisture etc. under normal laboratory conditions, that the pure radical can be handled with no special precautions being

needed.   Other radicals that have a lifetime significantly greater than the methyl radical, under the same conditions, are termed "persistent".

Highly stabilised organic free radicals are known to derive their stability from factors such as the delocalisation of the unpaired electron and a sterically hindered radical centre which reduces the rate of possible intermolecular reactions.   The lack of any reactive group, such as a labile hydrogen atom, close to the radical centre is also of great importance.

The stable radicals concerning us are the semiquinone radical anion, the nitroxide and the nitronyl nitroxide radicals.

1,4-Quinones are a special example of cross-conjugated enediones.   The dipolar ion (zwitterion) form (Figure 1.5) was considered to contribute to the structure of the molecule.   It is now known however that quinones have little aromatic character.   X-ray crystallographic data show that the bond lengths correspond to values expected for the classical diketone structures[19].
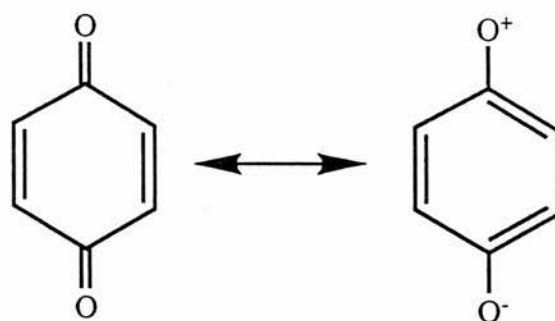
Figure 1.5

1,4-Benzoquinone and its dipolar ion.

The major difference between quinones and their acyclic counterparts is their ease of reduction.   The driving force is the formation of a fully aromatic system (Figure 1.6).   The quinone can accept an electron to produce the semiquinone radical anion, followed by another electron to form the dianion.   This ability is the overriding

feature of quinone chemistry.
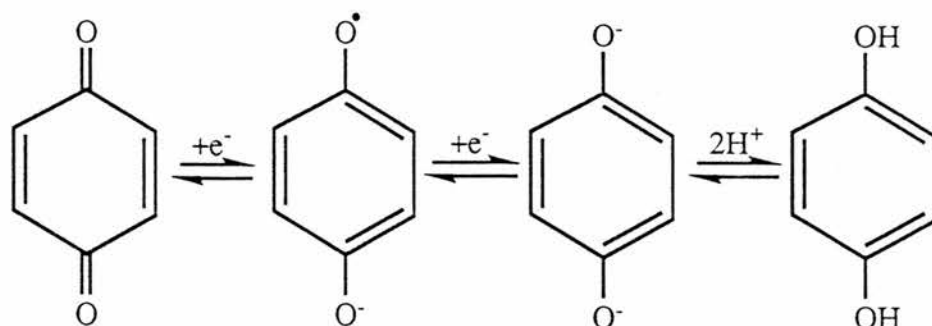
Figure 1.6

Reduction of quinones.

The ability to accept an electron to form the semiquinone radical anion can be measured polarographically as the halfwave potential $(E^{1/2})$[20]. The values for some common 1,4-quinones are given in Table 1.1, which shows the change in electron affinity with structure. The high electron affinity and the stability of the resulting radical anions are the reasons for the large number of charge-transfer complexes which are formed between quinones and electron donors[21]. An example of such a complex is the 1:1 pyrene-1:4-benzoquinone complex, which has been examined in some detail[22].

Nitroxides, or more correctly aminoxyl radicals, with no α-hydrogens are probably the most stable free radicals known. With the exception of the bis-(trifluoromethyl)-nitroxyl radical[26], all nitroxides show no tendency to dimerise or react with air. Nitroxides may be viewed as derivatives of the stable inorganic radical nitric oxide, the stability of which to dimerisation has been attributed to its hybrid structure (Figure 1.7). It has also been represented as a structure with five bonding electrons, that is a σ-bond and a three-electron bond between the atoms[27]. This structure is supported by the small dipole moment, the bond length of 1.15 Å (which is intermediate between the values calculated for N=O and $N^+\equiv O$, and between

Quinone	m.p. / °C	$E^{1/2}$ / V[a]	E^{0} / V
1,4-Benzoquinone	116	-0.51	0.711[b,23]
2,3,5,6-Tetrachloro-1,4-benzoquinone	290	+0.01	0.742[b,23]
2,3-dichloro-5,6-dicyano-1,4-benzoquinone	213	+0.51	*ca.* 1.00[b,24]
1,4-Naphthoquinone	125	-0.71	0.484[c,25]
1,4-Anthraquinone	218	-0.75	0.451[c,25]

Table 1.1

Physical properties of quinones.

[a] MeCN solvent, $Et_4N^+ClO_4^-$ as supporting electrolyte.

[b] C_6H_6 solvent. [c] EtOH solvent.

values for N_2 and O_2) and the infrared spectrum (the infrared vibration (1876 cm^{-1}) also being intermediate between that of N_2 (2330 cm^{-1}) and O_2 (1556 cm^{-1})). Linnett
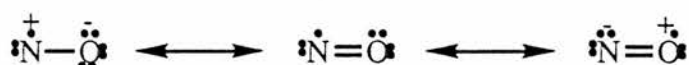
Figure 1.7

The hybrid structures of nitric oxide.

explains these observations with his double quartet hypothesis[28], in which the electrons are shared in such a way that both atoms have an octet. Thus interelectronic repulsion is minimised and there are five bonding electrons between the atoms. As a result, dimerisation is not favoured because the number of bonding electrons would not be increased and the interelectronic repulsion would be.

Thus, by analogy, one may represent nitroxides in three different ways

(Figure 1.8): by resonance hybrids, by a structure with a three-electron bond[29] or by the double quartet hypothesis[28]. From an organic viewpoint the resonance hybrid

(1)

(2)   (3)
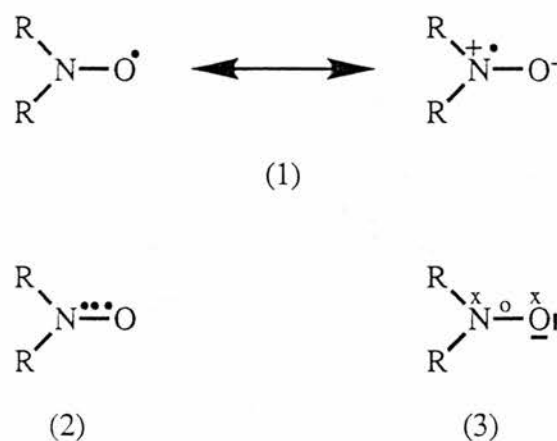
Figure 1.8

The three nitroxide forms: resonance hybrids (1), a three-electron bonded structure (2), and the double quartet hypothesis form (3).

representation is the most convenient to use.

A particularly stable group of nitroxides is that of the nitronyl nitroxides. The preparation of this type of nitroxide has been thoroughly studied (Figure 1.9)[30]. Nitroxides based on 1-hydroxyimidazole-3-oxides have also been examined. These are formed by the reaction of 2,3-butanedione with aldehyde oximes[31], nitrile oxides
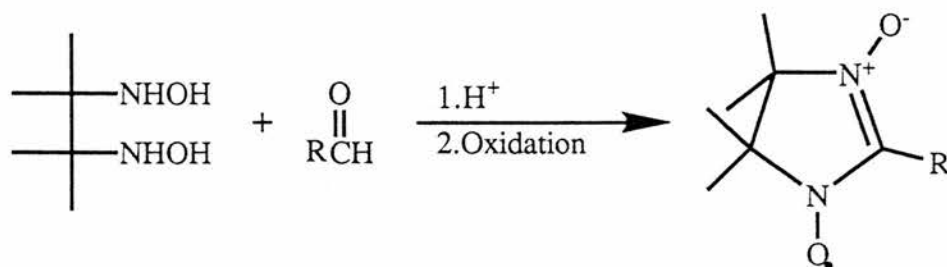
Figure 1.9

General preparation of nitronyl nitroxides[30].

19

with aromatic nitroso derivatives[32] and by the original preparation by LaParola, of dimethylglyoxime with aldehydes[33] (Figure 1.10).
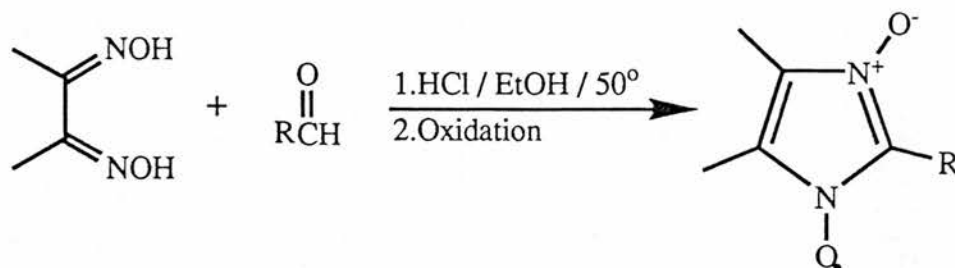
Figure 1.10

LaParola's preparation of imidazole nitronyl nitroxides[33].

The stability of the nitroxide function in the nitronyl nitroxides is so great that many chemical reactions, such as ring expansions, can be carried out whilst leaving this functionality intact.

1.2   **Polyradicals**

To begin with, all organic polymers had at least one property in common, that is they were diamagnetic. This changed in 1956 when Henglein and Boysen reported the preparation of the first polyradical[34]. They had incorporated hydrazine side groups on to polymers by irradiating them with gamma rays in the presence of DPPH, and subsequently oxidised this to the radical.

The preparation of several polyradicals by the modification of existing polystyrenes soon followed this initial report. These include poly(4-fluoro-3,5-dinitrostyrene) with DPPH pendant groups[35], poly(triarylmethyl) radicals from the polymerisation of diarylhydroxymethylstyrenes[36] and the synthesis of a polystyrene containing verdazyl units reported by Kurusu et al.[37] in 1967 and Kinoshita et al.[38] in 1968.

In 1967 Griffith and co-workers published the first report which featured the

direct polymerisation of free radical monomers[39]. This report described the polymerisation of a nitroxide monomer containing the 2,2,6,6-tetramethyl-1-piperidinyloxy (TEMPO) free radical in the form of the methacrylate ester of the alcohol TEMPOL (Figure 1.11). The average weight of the polymer formed was
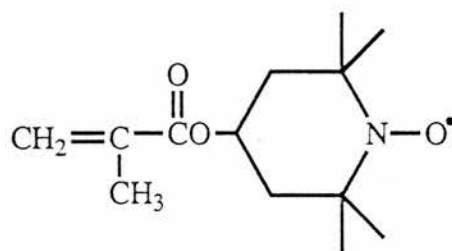
Figure 1.11

The methacrylate ester of 2,2,6,6-tetramethylpiperidin-4-ol (TEMPOL).

1050 or 1950 depending on the solvent used in the preparation. This methacrylate ester polymerisation was repeated in 1982 by Kamachi and co-workers using the same technique but with reported molecular weights of over 140 000[40]. Griffith *et al.* also reported details of the attachment of TEMPO units to the commercial maleic anhydride-methyl vinyl ether (1:1) coploymer in a similar strategy to that used for the polystyrene based polyradicals.

TEMPO polyradicals were further examined by Kurosaki and co-workers[41,42]. These involved the preparation of 4-methacroyl derivatives of 2,2,6,6-tetramethylpiperidine monomers (Figure 1.12), which were polymerised using the appropriate radical initiator. The resultant polymer was then oxidised to produce polymers with stable pendant nitroxyl free radicals. Thus polynitroxides with molecular weights in excess of 100 000 and possessing a high spin density were formed.

Over the past decade most of the polyradicals prepared and reported have involved nitroxides as the radical unit. Using a similar strategy to Kurosaki *et al.*[41],

21
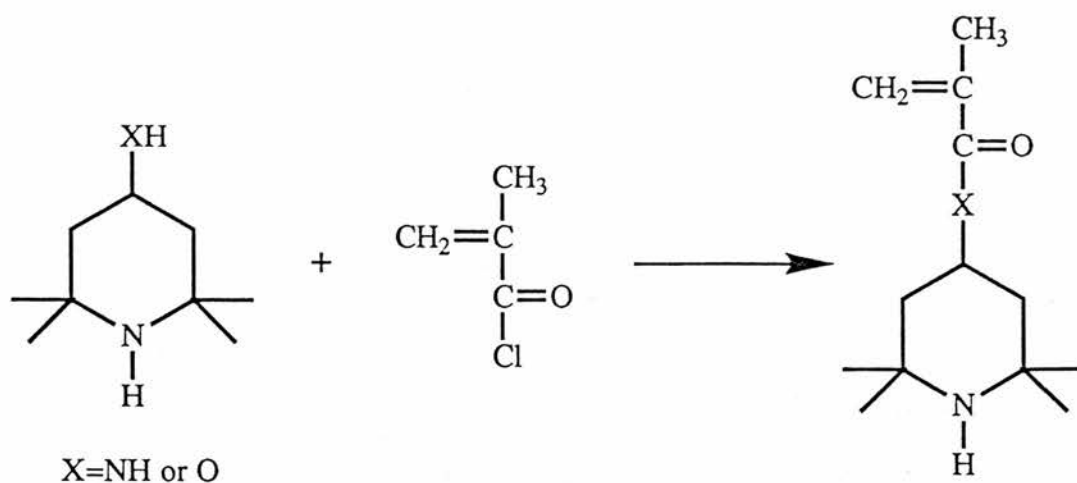
Figure 1.12

Preparation of 4-methacroyl derivatives of 2,2,6,6-tetramethylpiperidine[41].

4-O-vinylbenzyloxyTEMPO polymers (Figure 1.13) were prepared by Miyazawa and Endo[43]. Ovchinnikov and co-workers reported the thermal, photochemical and glow discharge treatment of the 4,4'-(butadiyne-1,4-diyl)-bis-(2,2,6,6-tetramethyl-4-hydroxypiperidin-1-oxyl) diradical (Figure 1.14) to form a black polymer[44]. They
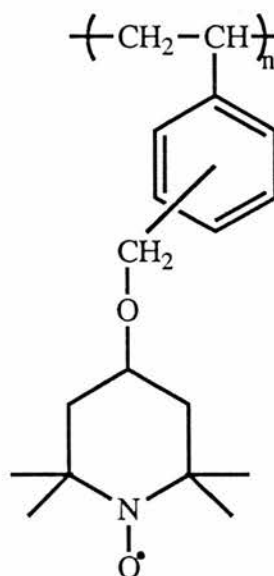
Figure 1.13

Generalised structure of the 4-O-vinylbenzyloxyTEMPO polymer[43].

showed that some samples displayed field dependent magnetisation corresponding to an "insignificant" amount (0.1%) of a ferromagnet. This low yield of a ferromagnetic fraction was put down to a number of side reactions, including radical annihilation, on polymerisation.
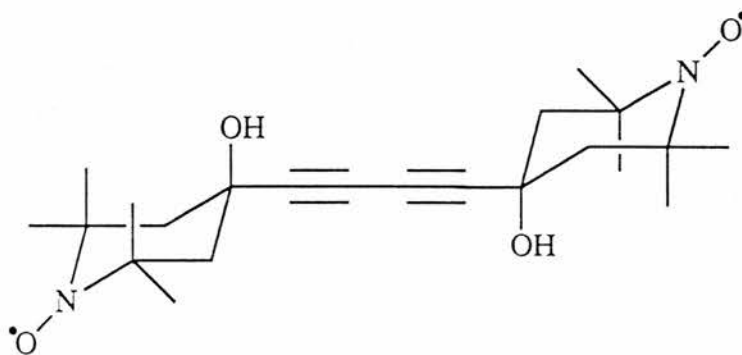
Figure 1.14

The 4,4'-(butadiyne-1,4-diyl)-bis-(2,2,6,6-tetramethyl-
4-hydroxypiperidin-1-oxyl) diradicals.

More recently, a new TEMPO containing polymer, poly(2,2,6,6-tetramethyl-piperidinyl-N-oxyl-4-acrylic ester, has been synthesised by anionic polymerisation of the monomer alkene[45] and was shown to act as an efficient catalyst for the electrochemical oxidation of amines.

An example of a polyradical where the radical unit is carbon centred and not a nitroxide is poly[(4-ethynylphenyl)diphenylmethyl][46] (Figure 1.15). This polymer displayed a high concentration of free spins and a reversible increase in spin concentration with increasing temperature. However, compared to the theoretical spin concentration of 10^{21} spins g^{-1}, the highest spin concentration exhibited by this polymer was 10^{18} spins g^{-1}. It was suggested that this was due to spin pairing by dimerisation of triphenylmethyl radicals, although no firm evidence for this was obtained.

Finally, there are a few polyradicals where the radical group is in close
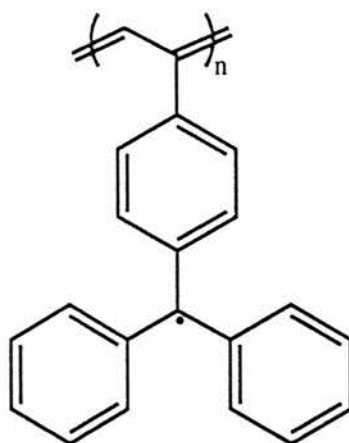
Figure 1.15

Poly[(4-ethynylphenyl)diphenylmethyl].

proximity to the polymer backbone itself. Examples of such polyradicals are the corresponding polyradicals formed from poly(N-hydroxyaniline)[47], poly(N-hydroxypyrrole)[48,49] and poly(3-phenyl-N-hydroxypyrrole)[48,49] (Figure 1.16). The hydroxypyrroles were polymerised both chemically and electrochemically. The

(1)

(2)

(3)
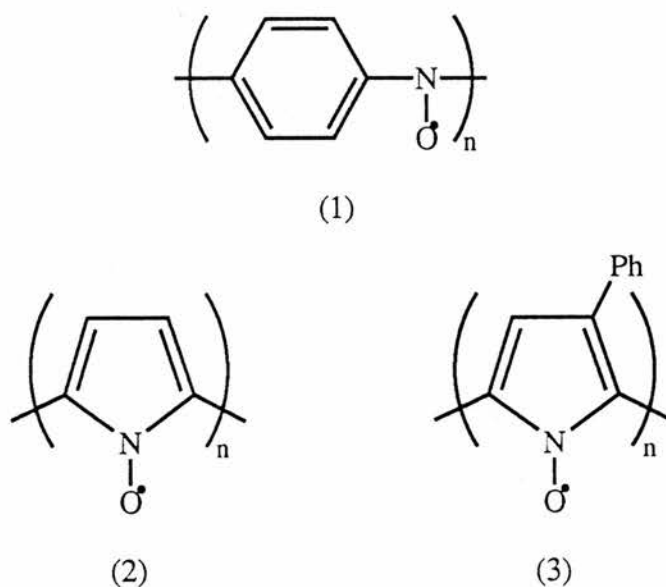
Figure 1.16

Poly(aniline-N-oxyl) (1), poly(pyrrolyl-1-oxyl) (2) and

poly(3-phenylpyrrolyl-1-oxyl) (3).

oxygen functionality on the nitrogen lowers the conductivity in both the pyrrole and aniline polymers compared to the unsubstituted parent polymers. Further oxidation of these polymers produced materials which were effectively insulators.

In summary it can be seen that there are essentially only two strategies for the production of a polyradical. One is the modification of an existing conventional polymer by the attachment of pendant radical groups along its chain. The other is the synthesis of a monomer containing a free radical group or a group which can be readily converted into a radical, and the polymerisation of this to produce the polyradical. At the moment the latter method of direct polymerisation of a radical monomer is favoured and is most widely utilised.

1.3   Applications of Polyradicals

Initially stable radicals were investigated as they were known to be good scavengers of radicals and were therefore potentially useful as antioxidants. Some stable radicals are known to abstract certain types of reactive hydrogen atoms and thereby promote certain chemical transformations. Examples of such radicals are 4,4'-dinitrodiphenylnitroxide and porphyrexide which are capable of oxidising phenols to quinones[50]. The latter radical will also oxidise thiols and can be used as a standard reagent for the estimation of thiol groups in proteins[51].

With respect to the chemical uses of polynitroxides, a large proportion of interest has centred not on the reactions of the radical centre itself but on the oxidised form, the oxoammonium (or oxoaminium) cation. The oxoammonium salt of TEMPO derivatives, the 1-oxo-2,2,6,6-tetramethylpiperidinium salt (Figure 1.17), has been shown to be a versatile oxidising agent[52-54]. It can oxidise the hydroxide ion to hydrogen peroxide, with the regeneration of the radical nitroxide group[52], alcohols to their corresponding carbonyl compounds[53], with the oxoammonium salt being reduced to the hydroxylamine, and amines to aldehydes and ketones (in aqueous media) and nitriles (in anhydrous acetonitrile)[54], with the oxoammonium salt again being reduced to the hydroxylamine. The hydroxylamine and nitroxide
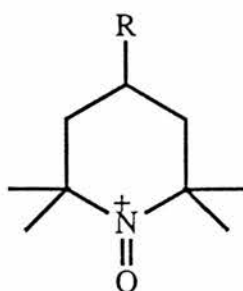
Figure 1.17

produced by these processes can readily be converted back to the oxoammonium salt by chemical or electrochemical oxidation[55]. Thus, a polymer which has these properties and can easily be regenerated has obvious synthetic potential.

Since the discovery of polyradicals there has been speculation as to their magnetic properties and potential as ferro, ferri or antiferromagnetic materials. π-Conjugated polyradicals are of interest as potential superparamagnetic species with possible uses as organic magnetic information storage materials[55]. One example which exhibits these properties is the black polymer of Ovchinnikov's[44] mentioned earlier which contains an "insignificant amount" of a ferromagnet.

Chapter Two

Preparation and Study of Radical-Thiophene
Monomers

As mentioned in Chapter One, the polymers which we sought to prepare are based on thiophene. The aim was to attach a pendant stable radical group, such as a quinone, nitroxide or nitronyl nitroxide group, onto the thiophene molecule to produce a polyradical monomer. Thiophene and its derivatives have been shown to undergo electrochemical polymerisation with a certain amount of ease[6,56-59], and therefore this was to be our favoured route to the polymer.

Thus the compounds which were targeted by us can be divided into three categories. These are the thienonaphthoquinones, the fused thiophene nitroxides and the thienyl nitronyl nitroxides. Each of these will be dealt with separately in this chapter, followed by a summary of the conclusions drawn and details of the experimental work carried out.

2.0   Thienonaphthoquinones

The initial target thienonaphthoquinone molecule has a structure comprised of a thiophene ring fused to a naphthoquinone ring system (Figure 2.1). This type of structure is accessible from the thiophene-3,4-dicarboxylic acid as demonstrated by MacDowell and Wisowaty[60] in 1972. Two methods for the preparation of thiophene-3,4-dicarboxylic acid were examined. The first method is that used by Kornfeld and Jones[61] (Figure 2.2). This synthesis involves the ring closure of 1-formyl-2-diethoxymethylsuccinate with phosphorus pentasulphide, with the ester thereby produced being hydrolysed by heating in ethanolic aqueous sodium hydroxide solution. The overall yield for these two steps is quoted as being 35%, although we could only achieve 24%. The second route is the synthesis favoured by us, as it produces material of superior quality and in a greater yield. This method starts with
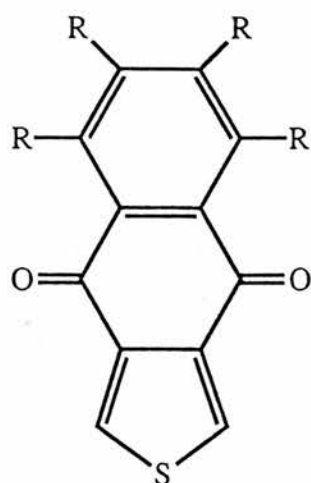
Figure 2.1

the cheap and readily available tetrabromothiophene and incorporates the method used by MacDowell and Wisowaty[60] to produce the desired dicarboxylic acid in an overall yield of approximately 59% (Figure 2.3). An attempt was made to improve this
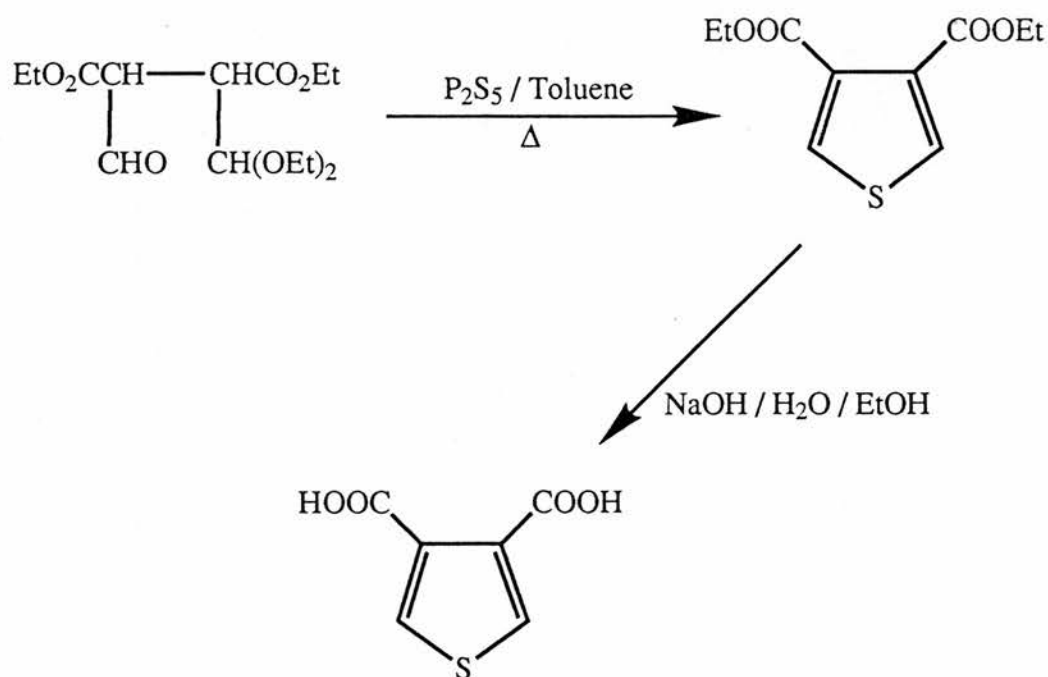
Figure 2.2

Kornfeld and Jones' route to thiophene-3,4-dicarboxylic acid[61].
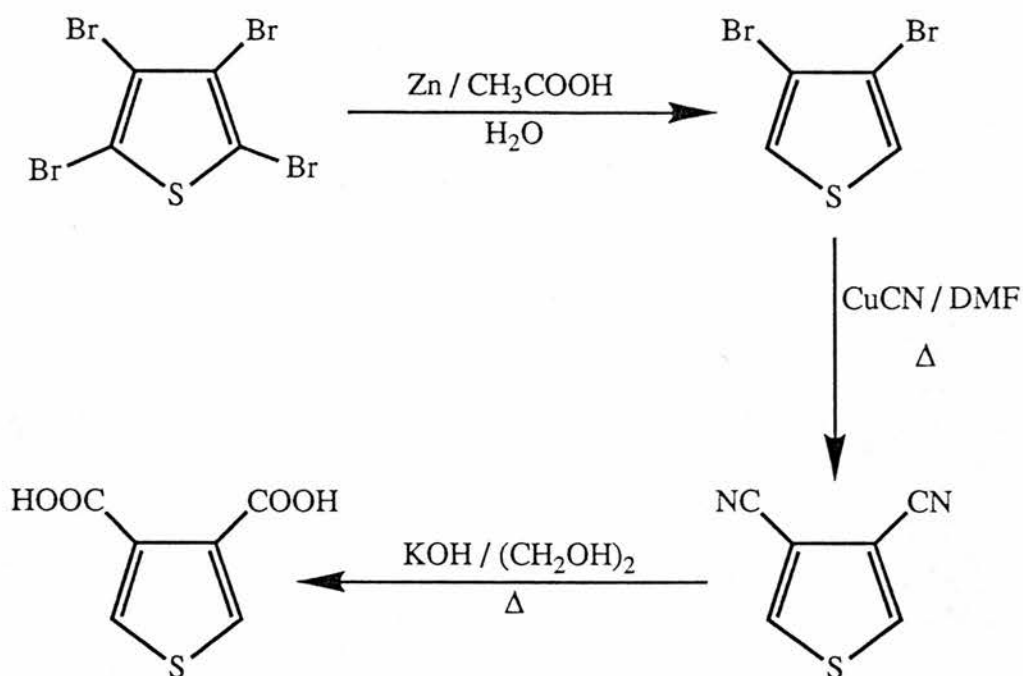
Figure 2.3

The favoured route to thiophene-3,4-dicarboxylic acid[60,62].

synthesis by converting the dibromothiophene directly to the dicarboxylic acid and thereby reducing the synthesis by one step. This involved the use of halogen-metal
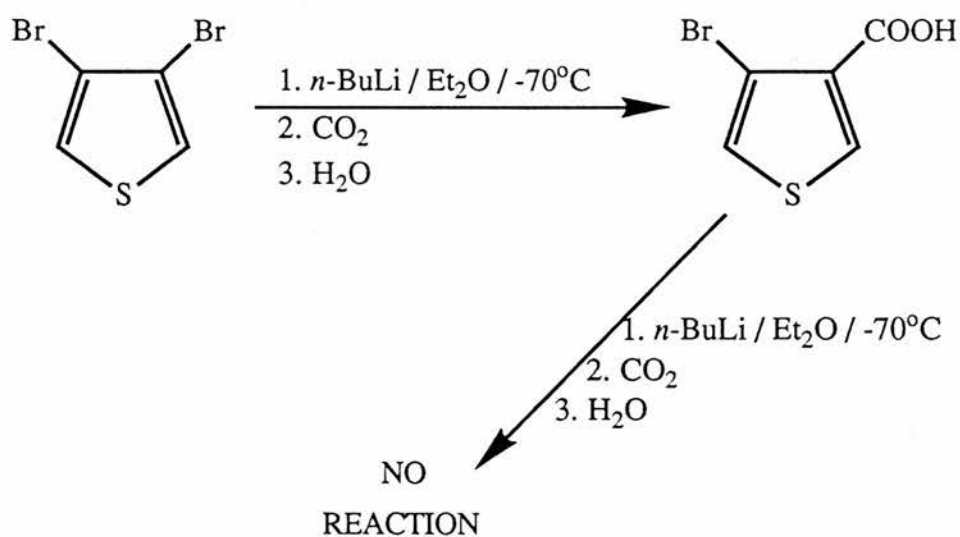
Figure 2.4

Halogen-metal exchange in 3,4-dibromothiophene.

exchange[63] in 3,4-dibromothiophene with *n*-butyllithium, followed by the bubbling of carbon dioxide through the reaction mixture and quenching with water. However on examination of the product it was found that only one bromine atom had exchanged, to yield 3-bromothiophene-4-carboxylic acid (Figure 2.4). This on further treatment with *n*-butyllithium produced no further reaction, and so this method was abandoned in favour of that shown in Figure 2.3.

The thiophene-3,4-dicarboxylic acid thus produced was then used to prepare substituted 4,9-dihydronaphtho[2,3-*c*]thiophene-4,9-diones. This was achieved by diacylation of substituted benzenes with the dicarboxylic acid and aluminium trichloride (Figure 2.5). By means of this methodology three thienonaphthoquinones

1. $R_1=R_2=H$
2. $R_1=R_2=Me$
3. $R_1=H, R_2=OMe$
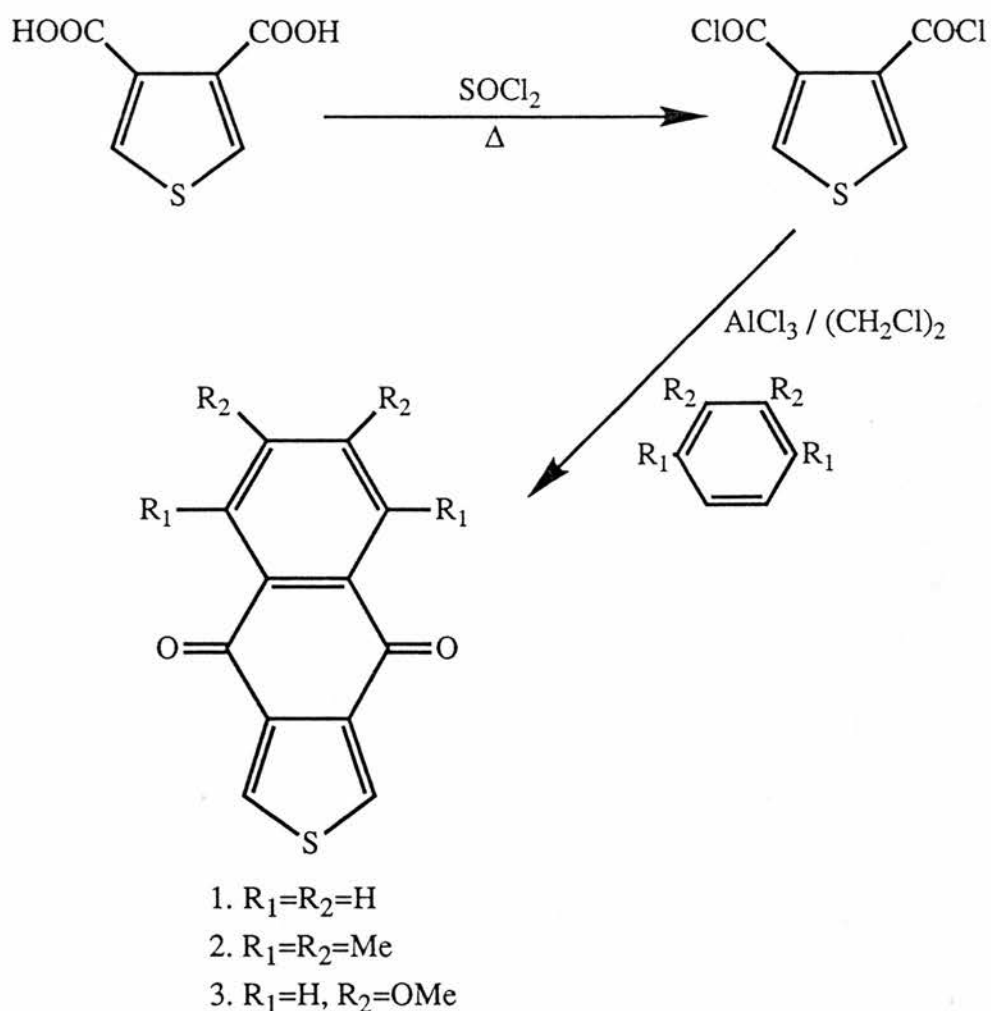
Figure 2.5

Preparation of substituted 4,9-dihydronaphtho[2,3-*c*]thiophene-4,9-diones.

of this structural type were prepared and fully characterised (see Experimental Section). For the reasons of simplicity we shall refer to these three compounds as the tetrahydrothienonaphthoquinone (1), the tetramethylthienonaphthoquinone (2) and the dimethoxythienonaphthoquinone (3). The preparation of other derivatives by the diacylation of pyrrole, cyclohexene and 1,4-dicyanobenzene was also attempted.
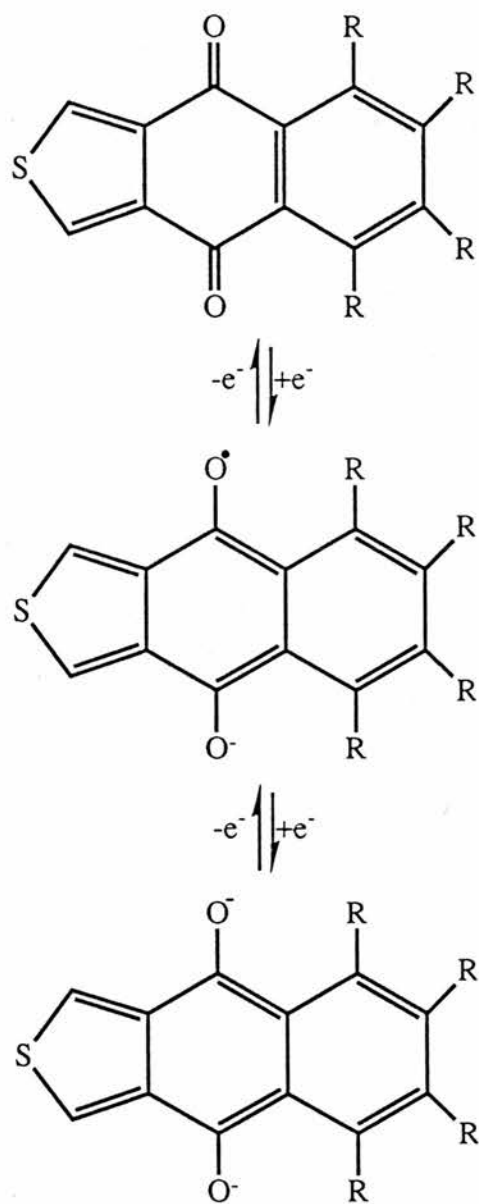
Figure 2.6

Electrochemical oxidation and reduction of the quinone function.

However these produced no thienonaphthoquinone structures and the starting thiophene-3,4-dicarboxylic acid was reclaimed in each case.

The thienonaphthoquinones were examined by ESR and CV. The cyclic voltammetric investigation provided the reduction potentials for the production of the quinone radical anion and dianion (Figure 2.6). The CV's of these compounds are displayed in Figure 2.7, with the potentials for the formation of the radical anion in Table 2.1.

Thienonaphtho-quinone	Radical Anion $E^{o'\,a}$/Volts
Tetrahydro (1)	-1.14[b]
Tetramethyl (2)	-1.66[c]
Dimethoxy (3)	-1.65[c]

Table 2.1

[a] vs. Ag/Ag+, [b] In MeCN and TBAT, ΔE=220mV,

[c] In MeCN and TBAHFP, ΔE=80mV.

These potentials were then used to electrochemically generate the radical anion of the thienonaphthoquinones using the electrochemical ESR cell (Figure 2.8). By the use of this cell, with solutions of the thienonaphthoquinones identical to those used to obtain their cyclic voltammograms, the radical anions were generated by the application of the appropriate potential across the cell. Thus by placing the cell in the cavity of the ESR spectrometer the radical could be directly observed as it was generated. Well resolved second derivatives of the spectra of all three thienonaphthoquinones were observed and recorded by this method (Figure 2.9). These ESR spectra are fully consistent with what one would expect on the basis of the structure of the radical anions. The tetrahydrothienonaphthoquinone produces a five peak ESR spectrum due to the coupling to four protons. These protons are the two
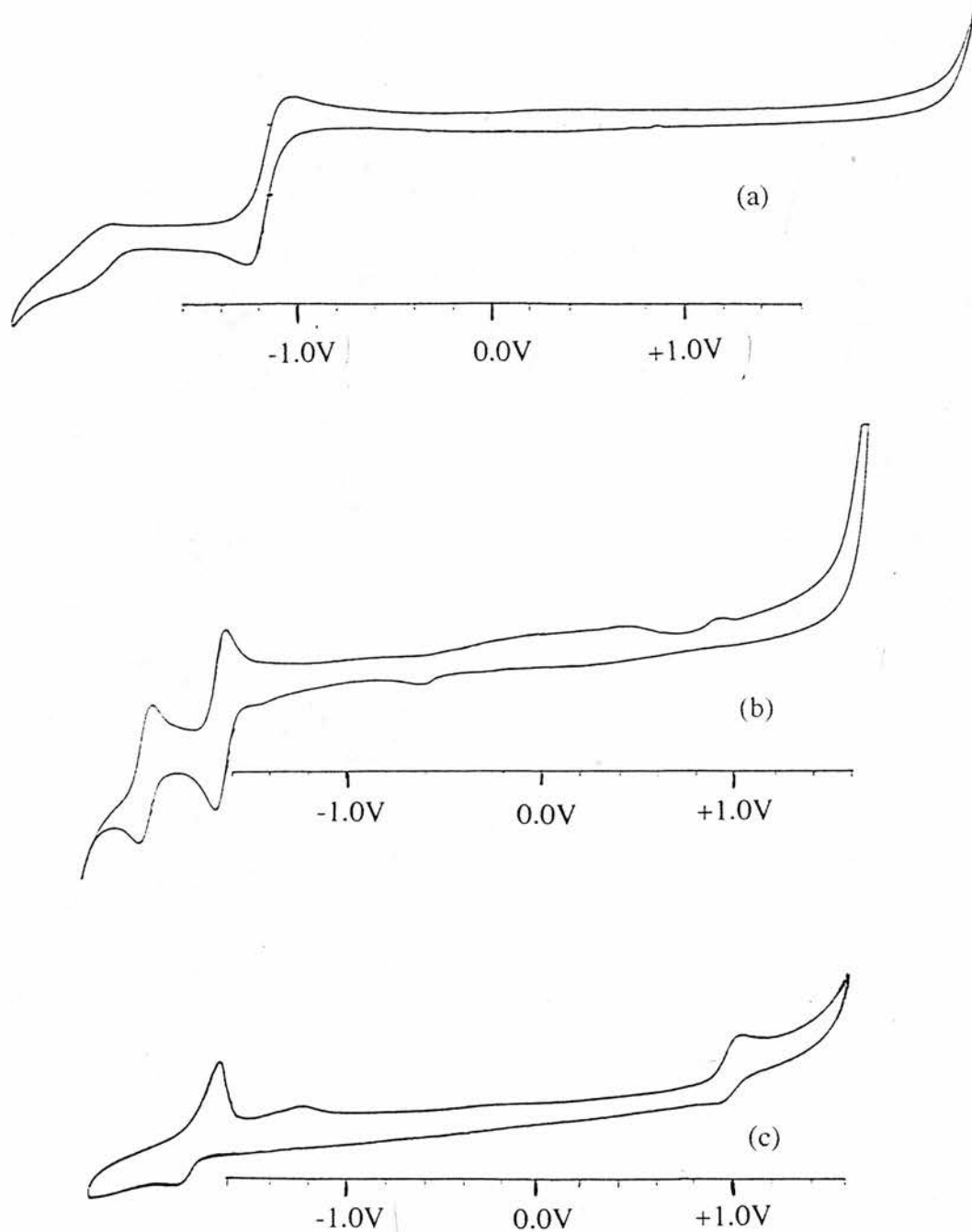
Figure 2.7

Cyclic voltammagrams of the thienonaphthoquinones. Tetrahydrothieno-
naphthoquinone in MeCN and 0.1M TBAT, volts vs. Ag/Ag$^+$ and ΔE=220mV (a),
tetramethyl-thienonaphthoquinone (b) and dimethoxythienonaphthoquinone (c) in
MeCN and 0.1M TBAHFP, volts vs. Ag/Ag$^+$ and ΔE=80mV.

Silver Reference Electrode

Flattened square
quartz window

Platinum Gauze
Working Electrode

Tungsten Loop
Counter Electrode

To syringe for
ease of loading
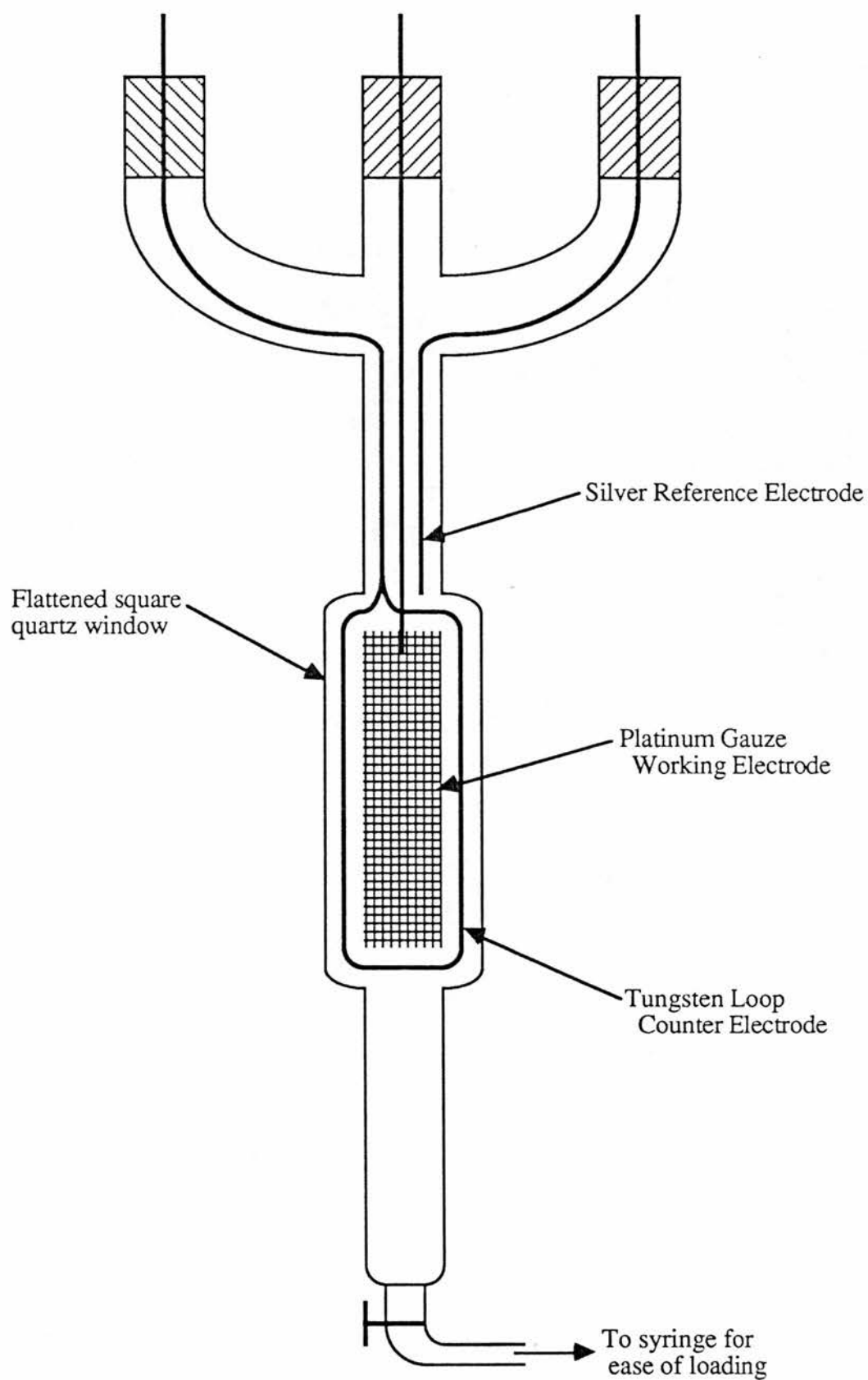
Figure 2.8

Schematic drawing of the electrochemical ESR cell.
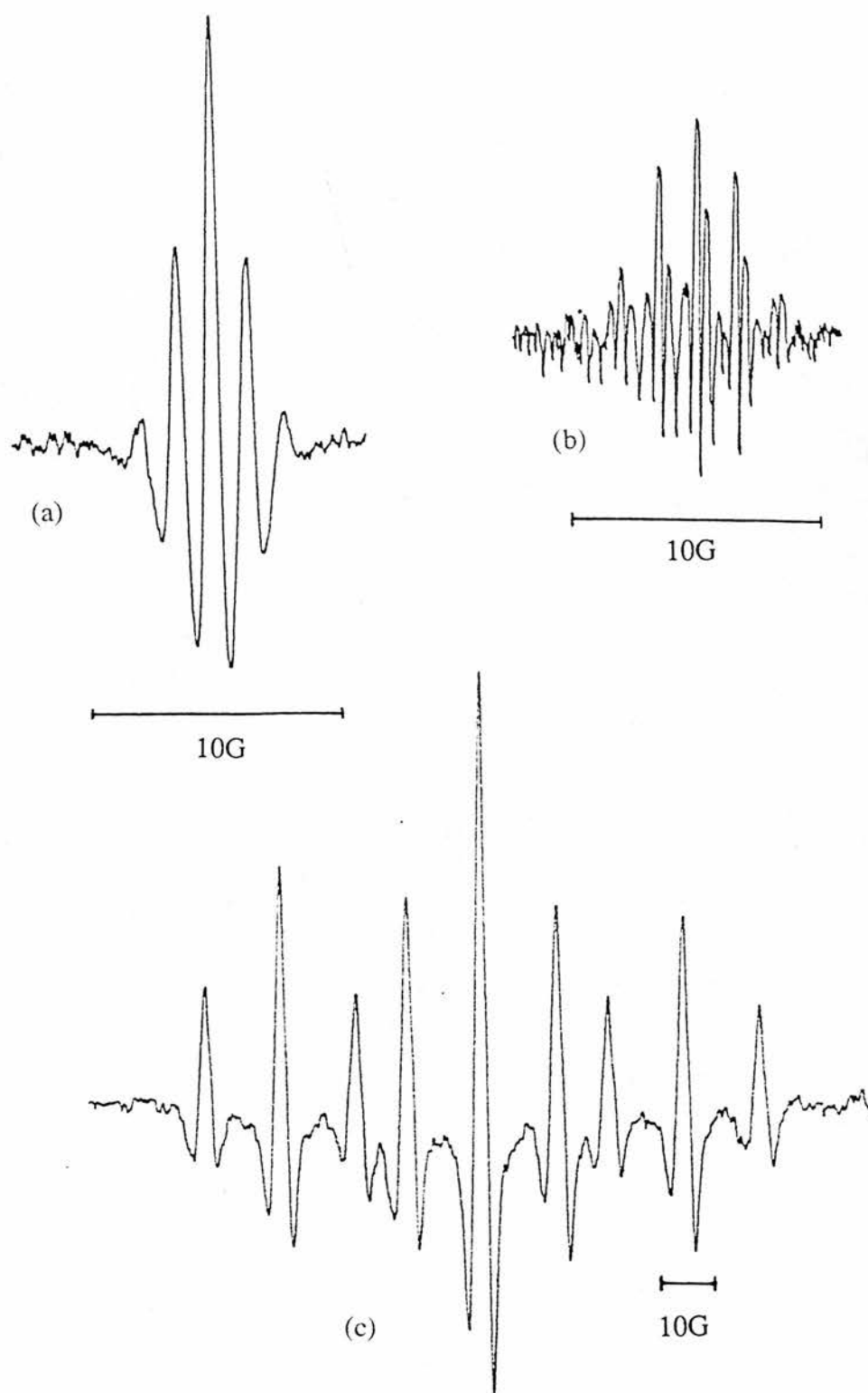
Figure 2.9

9.3GHz second derivative ESR spectra of the electrochemically generated radical anions of the thienonaphthoquinones.Tetrahydrothienonaphthoquinone in DMF and 0.1M TBAT, volts vs. Ag/Ag+ (a), tetramethylthienonaphthoquinone (b) and dimethoxythienonaphthoquinone (c) in MeCN and 0.1M TBAT, volts vs. Ag/Ag+.

thienyl protons and the two nearest phenyl protons which have identical hyperfine couplings. The tetramethyl derivative of the radical anion produces a septet of triplets, from the coupling of the two thienyl protons being further split by the six protons of the two nearest methyl groups on the benzene ring. Finally, the ESR of the dimethoxy derivative displays a triplet of triplets due to two discrete pairs of protons (the thienyl and phenyl protons). The presence of the two methoxy groups on the benzene ring alters the environment of the phenyl protons such that their hyperfine coupling constants are no longer equivalent to those of the thienyl protons. The hfs of these radical anions are shown in Table 2.2, with those of similarly substituted 9,10-anthrasemiquinones[64] (Figure 2.10).

From Table 2.2 it can be seen that the effect of substituting the tetrahydro-thienonaphthosemiquinone with methyl or methoxy groups mirrors that exhibited by substituting 9,10-anthrasemiquinone with the same groups. The substituted thieno-

Compound	Splitting constants / G
Tetrahydrothienonaphtho-semiquinone (1)	1.5 (4H)[a,b]
Tetramethylthienonaphth-semiquinone (2)	0.5 (2H)[a], 1.5 (6H)
Dimethoxythienonaphtho-semiquinone (3)	0.6 (2H)[a], 1.6 (2H)[b]
9,10-Anthrasemiquinone	0.65 (4H)[c,d], 1.04 (4H)[e,f]
1,4-Dimethyl-9,10-anthra-semiquinone	0.4 (2H)[d], 0.9 (2H)[f], 0.8 (6H), 1.2 (2H)[e]
2,3-Dimethoxy-9,10-anthra-semiquinone	0.6 (2H)[d], 1.0 (2H)[f], 0.8 (2H)[c]

Table 2.2

[a] Thienyl protons, [b] Phenyl protons, [c] H_1 and H_4,
[d] H_5 and H_8, [e] H_2 and H_3, [f] H_6 and H_7.
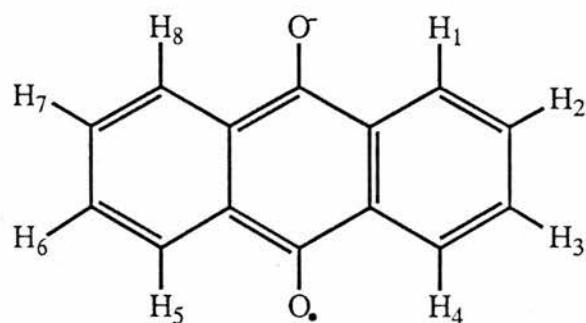
Figure 2.10

9,10-Anthrasemiquinone, with the positions labelled for clarity.

naphthosemiquinones display less spin density in the thiophene ring and a slight increase in spin density in the phenyl ring. This trend is the same as that shown by the 9,10-anthrasemiquinones (*ie.* the substituted phenyl ring shows an increase in spin density and the unsubstituted one a decrease).

Attempts at the polymerisation of the thienonaphthoquinones all failed. Both chemical and electrochemical methods were investigated. Electrochemical polymerisation was attempted by the use of solutions of the monomers in acetonitrile containing supporting electrolyte (both TBAT and TBAHFP were used). These solutions were left to cycle between approximately -2.0V and +2.0V (see Figure.2.7
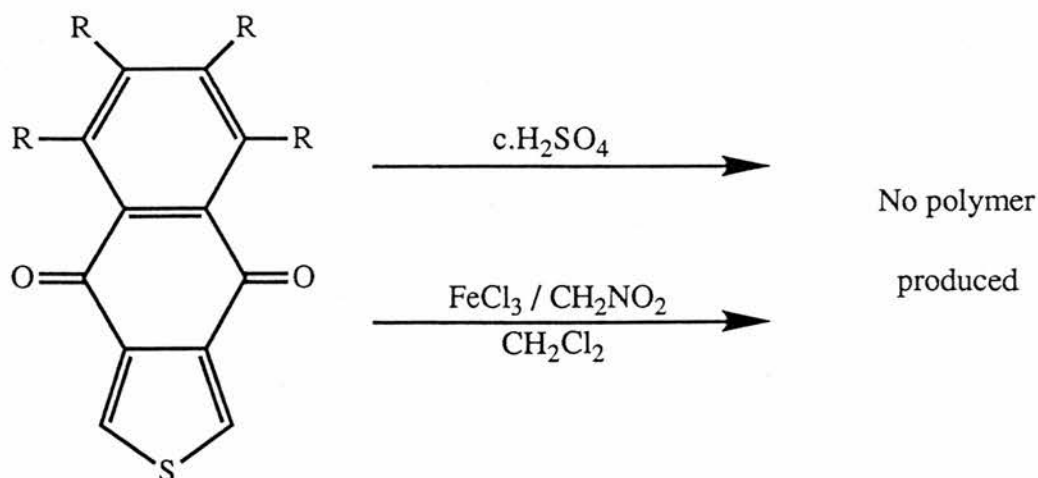
Figure 2.11

Attempts at chemical polymerisation.

37

for the exact values for each thienonaphthoquinone), 0V to +2.0V and held at a constant potential of approximately +2.0V. Despite these efforts no polymer was observed for any of the thienonaphthoquinones. Chemical attempts involved the use of concentrated sulphuric acid[57] and ferric chloride (Figure 2.11). Neither of these methods however produced the desired polymers, despite the appearance of a distinctive red colour, believed to be due to the thiophene cation which is intermediate in the polymerisation of thiophene, when the monomer was treated with sulphuric acid.

The inability of these compounds to polymerise can be explained by the close proximity of the quinone carbonyl groups to the thiophene ring. These carbonyl groups have the effect of withdrawing electron density from the thiophene ring and thus making the removal of an electron from that ring, which is required for polymerisation, much more difficult. This withdrawal of electron density can be partially offset by having electron donating groups on the benzene ring of the molecule. This is the case with the tetramethyl and dimethoxythieno-naphthoquinones, however these substituents did not reduce the adverse effects sufficiently for polymerisation to occur. A final attempt at obtaining a polymer was made by chemical modification of the monomer. As the thiophene ring was too electron deficient, the aim was to attach a further thiophene unit at both the two and five positions of the existing monomer thiophene ring. This was to be achieved by the use of transition metal catalysed cross coupling of 2-bromothiophene with a zinc chloride derivative of the thienonaphthoquinone[65] (Figure 2.12). It was expected that the newly formed monomer would then be more likely to polymerise. This method was only attempted with the tetramethyl derivative, which failed to produce anything of interest.

Thus it can be seen that this kind of thienonaphthoquinone structure is a very poor candidate for polymerisation. Therefore the structure of the target quinone monomer was modified in order to place the quinone ring further from the thiophene ring (Figure 2.13), and thereby reduce the electron withdrawing effect on the latter.
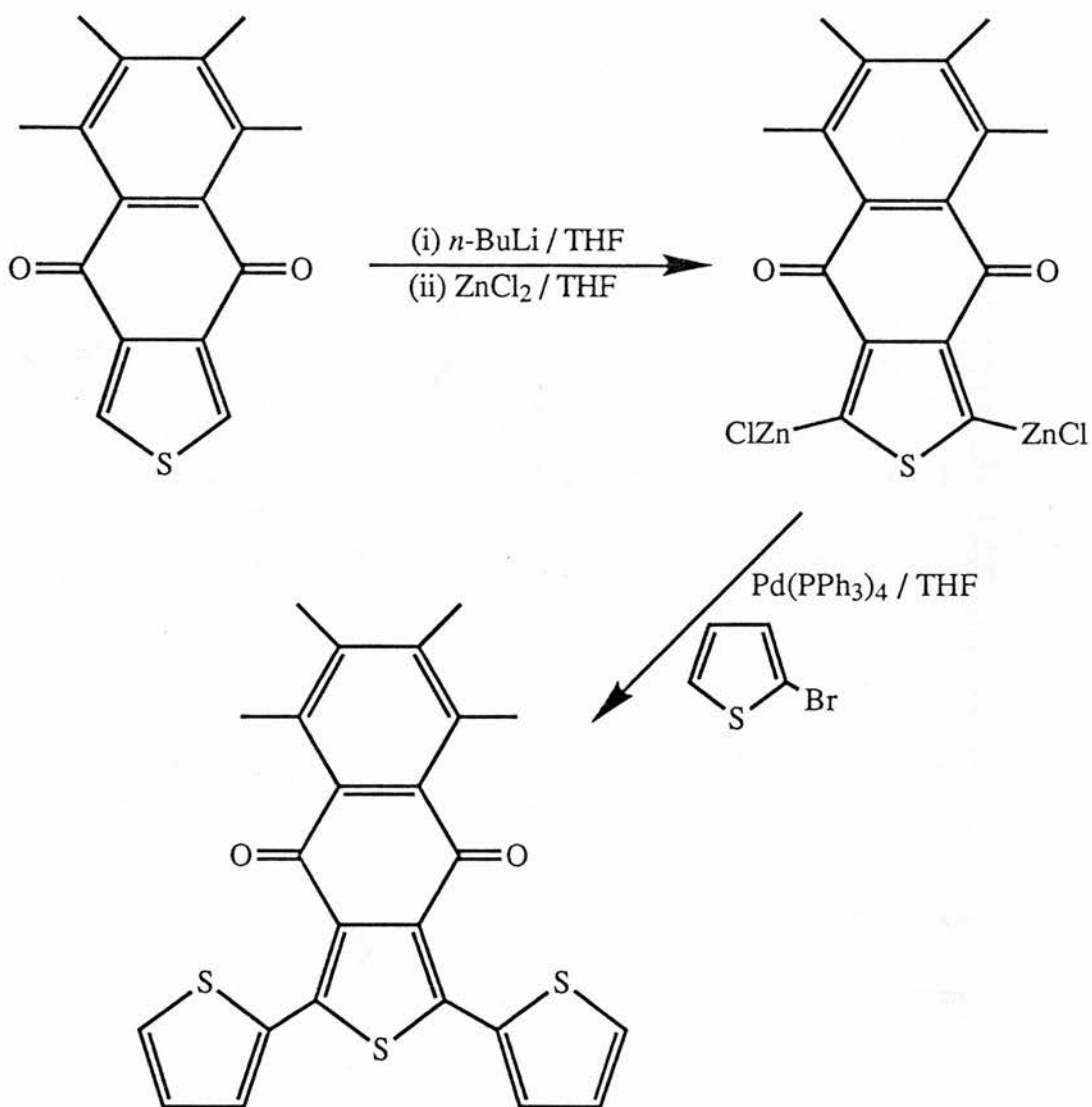
Figure 2.12

A synthetic route to this structure can be devised based on the chloromethylation of
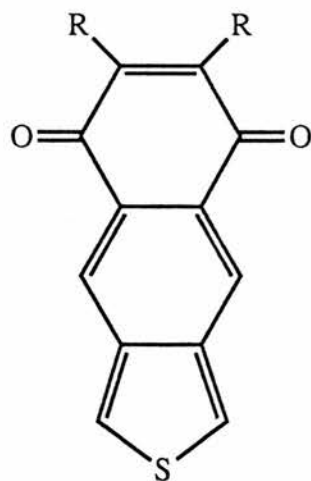
Figure 2.13

naphthoquinone followed by ring closure with sodium sulphide[66] and oxidation to the sulphoxide[67] and finally to the thiophene (Figure 2.14). Unfortunately the chloro-
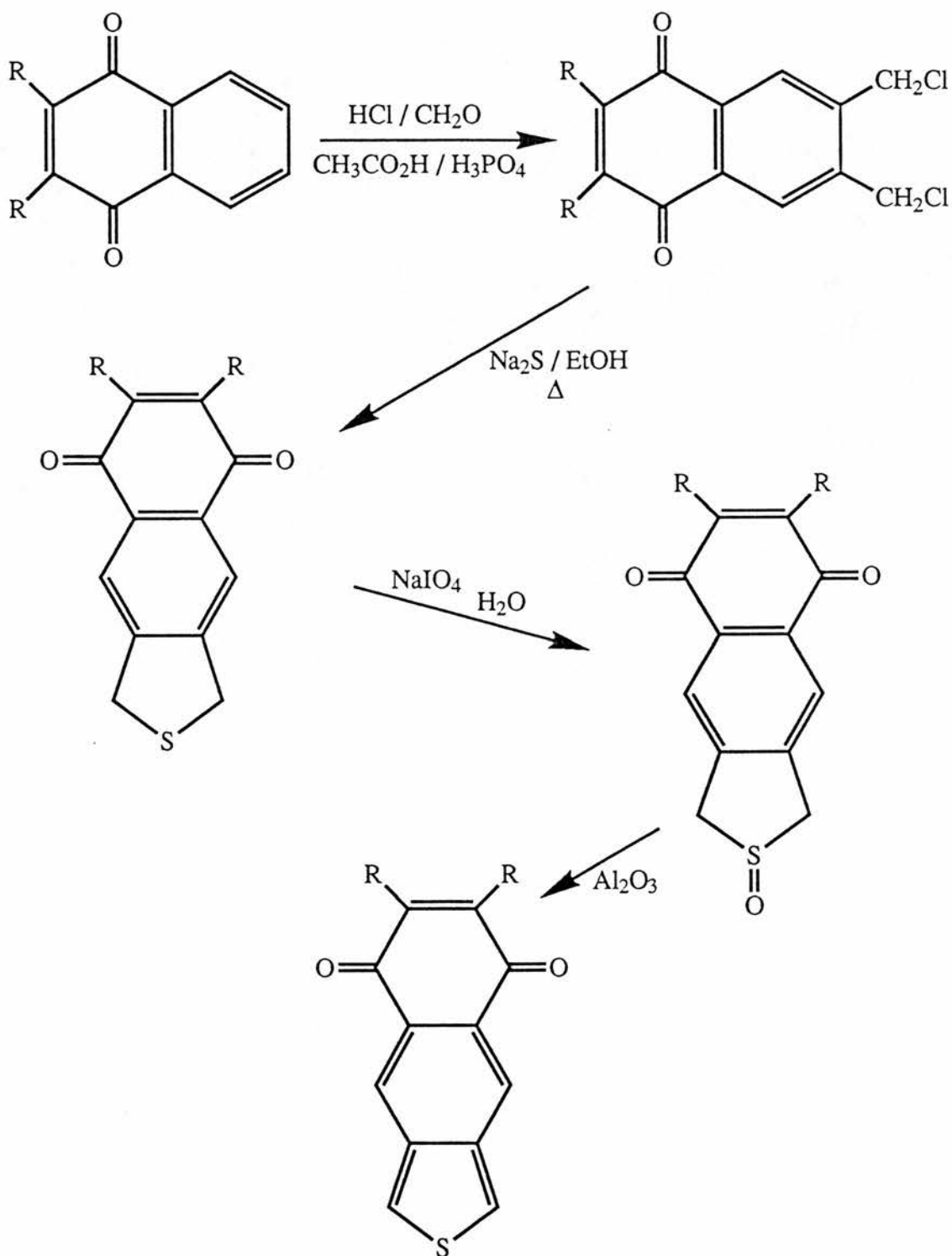
Figure 2.14

methylation step could not be carried out satisfactorily, but further work should enable this problem to be rectified permitting progress to the final monomer structure.

2.1   Fused Thiophene Nitroxides

As with the thienonaphthoquinones the aim here was to produce a thiophene monomer with a radical group fused across the 3- and 4- ring positions, in this instance a nitroxide-containing ring. The synthetic pathway to such a molecule was based on the preparation of 1,1,3,3-tetramethylisoindolin-2-yloxyl radical scavenger (Figure 2.15) by Griffiths and co-workers[68].
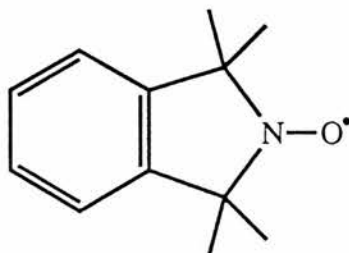
Figure 2.15

1,1,3,3-tetramethylisoindolin-2-yloxyl.

The initial route to this type of structure makes use of the thiophene-3,4-dicarboxylic acid prepared with the view of producing the thienonaphthoquinones (Figure 2.16). The preparation of the thiophenedicarboxylic anhydride was straight-forward and proceeded in a quantitative manner. However a problem arose when the conversion of this to the ring closed benzylimide structure was undertaken. The methods investigated to produce the ring closed imide from the thiophenedicarboxylic anhydride are summarised in Figure 2.18. All the attempts to produce this cyclic imide resulted in the production of the ring-opened structure. The structure and connectivity of this ring-opened compound was finally verified by the use of 2D COSY NMR Spectroscopy (200MHz), using DMSO-d^6 as solvent. This COSY
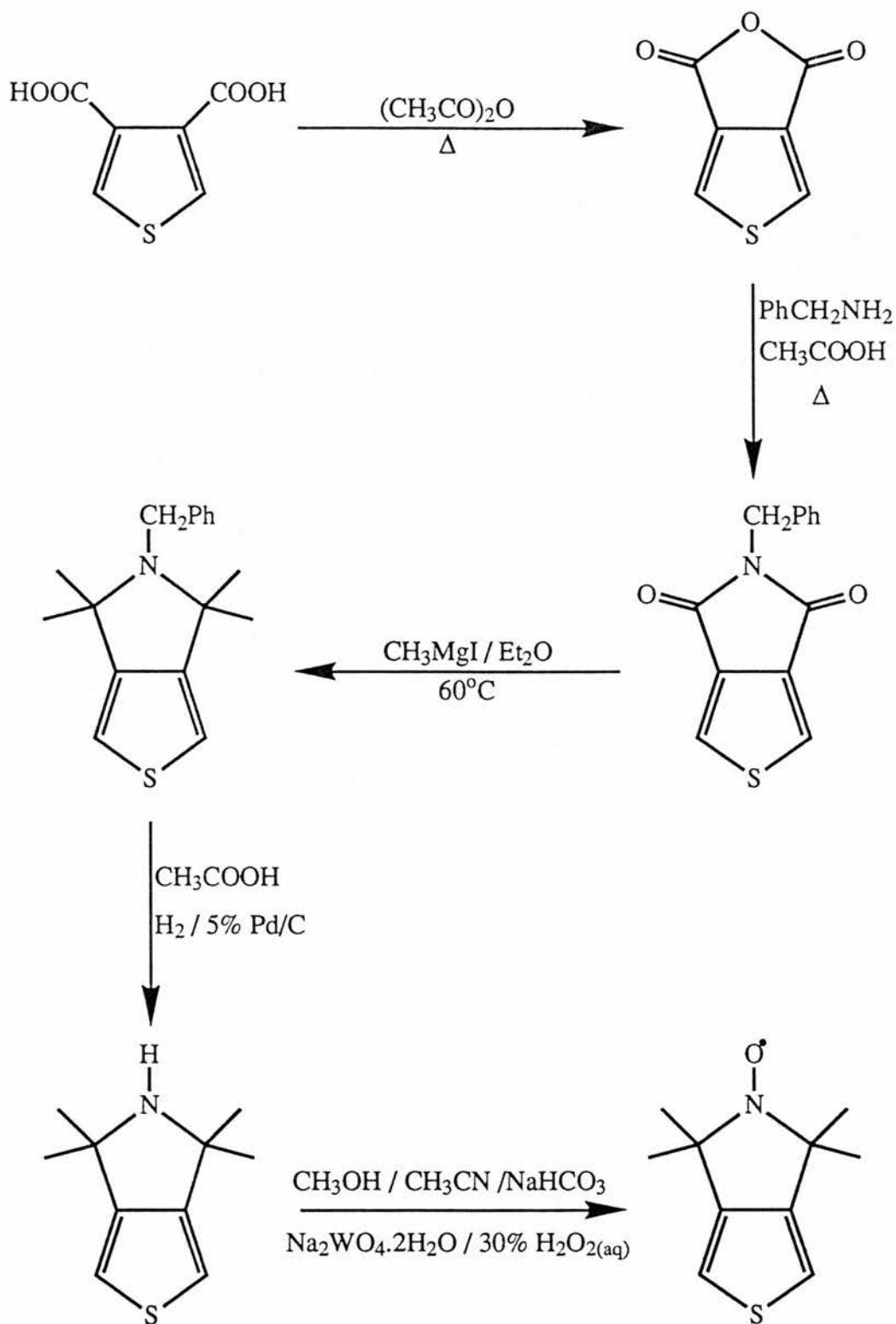
Figure 2.16

spectrum contour plot is displayed in Figure 2.17 and can be explained as follows.

The doublet at 4.50δ (2H) couples strongly to the triplet at 9.48δ (1H) and weakly to

the phenyl protons at 7.37δ (5H), as these are more distant. Both the phenyl protons

and the single proton at 9.48δ couple only to this doublet. Therefore this fraction of
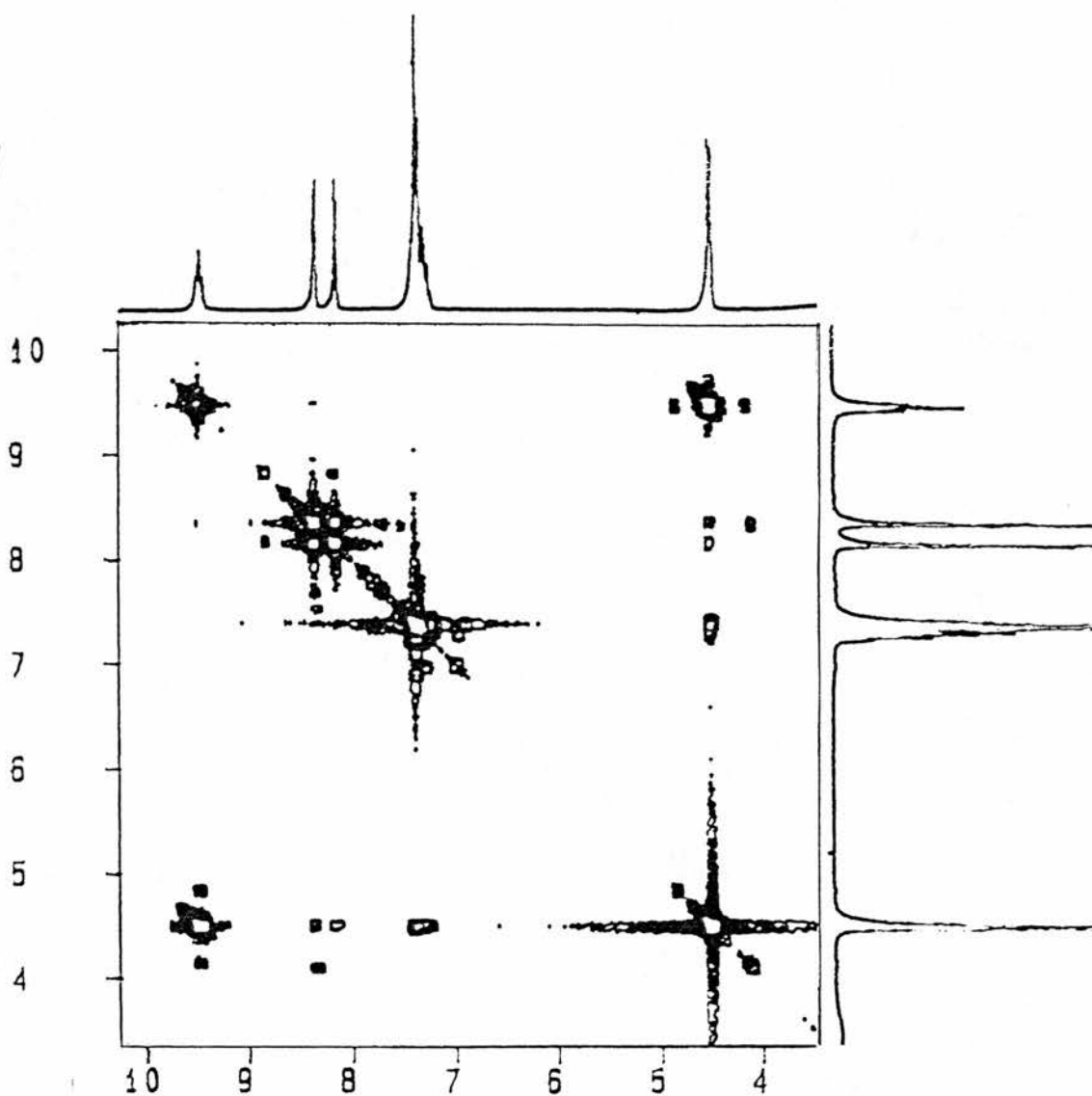
Figure 2.17

2D COSY NMR (200MHz) contour plot of the

ring-opened thiophene amide (below).
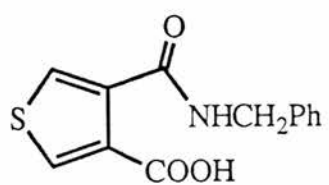
the molecule can be identified as Ph-CH₂-NH-CO-. The thienyl protons produce a pair of doublets at 8.15δ and 8.35δ, which can be seen to couple exclusively to each other, as would be expected for a thiophene ring which is substituted in the 3 and 4 positions. Therefore the structure of the ring-opened amide is established, with the acidic proton not being observed. As this ring-opened product has both an amide and a carboxylic acid group in close proximity one may expect the structure to ring close, given a little persuasion. This is the case with 3-nitrophthalic anhydride, which also reacts with primary amines to yield the ring-opened amide. This then undergoes

Figure 2.18

44
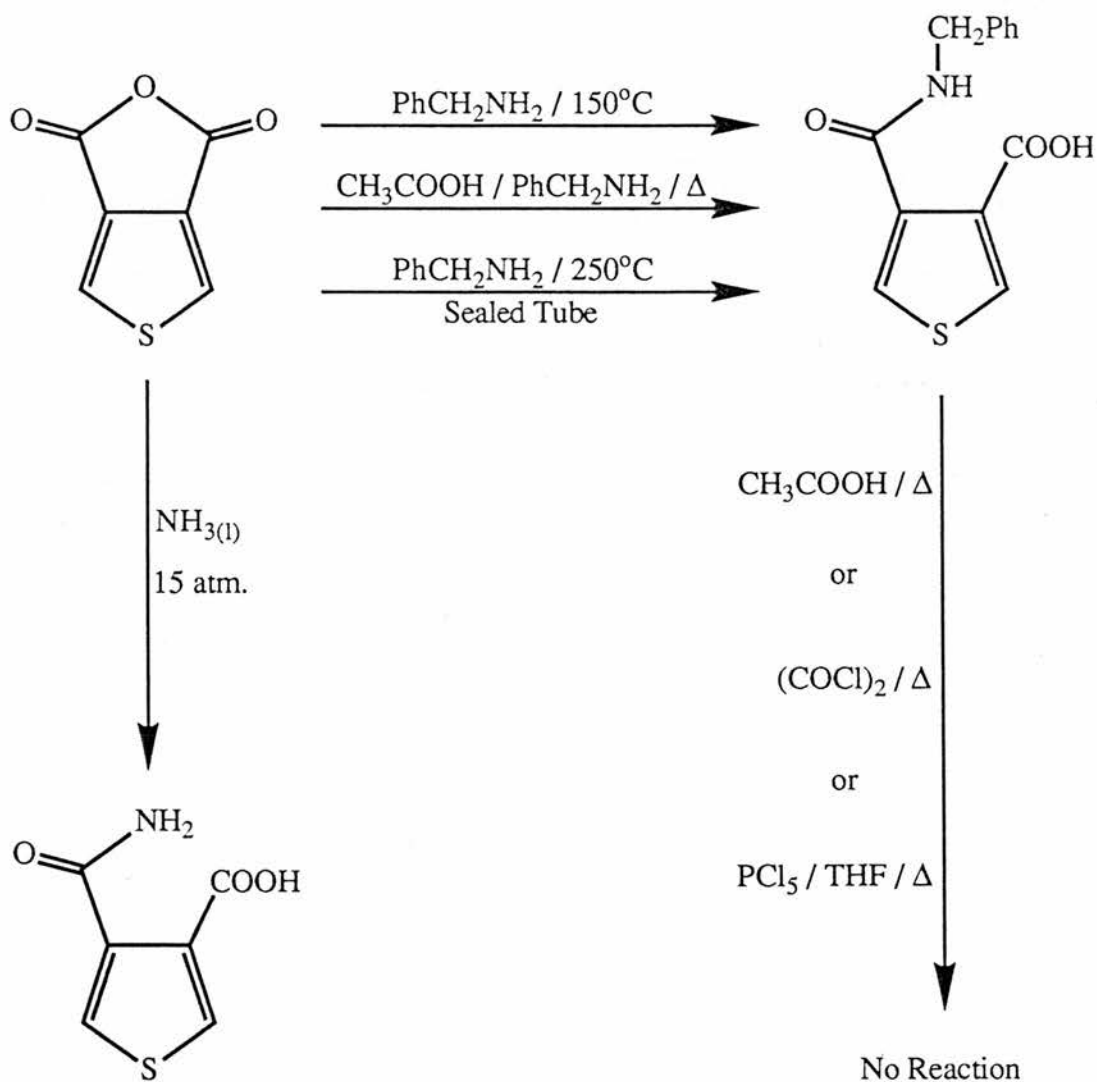
dehydration to produce the N-substituted 3-nitrophthalimide when heated to 145°C[69].
However on heating our thiophene derivative to 150°C, and even up to 250°C in a
sealed tube, no ring-closed product was obtained. Further attempts at ring-closure
were made (Figure 2.18), however the structure remained unchanged and intact. The
reaction of the thiophenedicarboxylic anhydride with liquid ammonia at high pressure
(15 atmospheres) was also examined. In line with the benzylamine reactions
however, this too produced only the ring-opened product.

As a result of the lack of success with the anhydride, preparation of the N-
benzylimide directly from thiophene-3,4-dicarboxylic acid was examined. Several
techniques were investigated (Figure 2.19), including an adaptation of the Schotten-

HOOC   COOH

S

(i) $SOCl_2$ / Δ
(ii) $NaOH_{(aq)}$ / $PhCH_2NH_2$

or

(i) $SOCl_2$ / Δ
(ii) $PhCH_2NH_2$ / THF

or

(i) PCl_5 / THF / Δ
(ii) $PhCH_2NH_2$ / THF

No Reaction
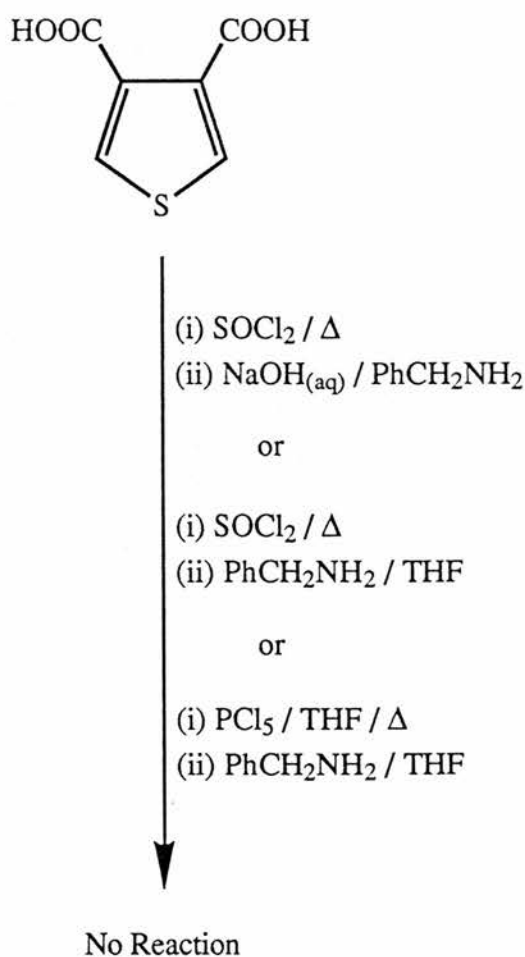
Figure 2.19

Baumann method using aqueous sodium hydroxide solution. Initially the second method tried ((i) $SOCl_2/\Delta$, (ii) $PhCH_2NH_2/THF$) used only a 10% excess of benzylamine, and produced what was thought to be a mixture of the starting dicarboxylic acid and the ring-opened amide product. However it was then realised that the formation of the ring opened amide from thiophene-3,4-dicarbonyl chloride and benzylamine would also produce one molecule of hydrochloric acid. This acid would then combine with unreacted benzylamine to produce benzylammonium chloride ($PhCH_2NH_3^+Cl$), thereby reducing the amount of benzylamine available for reaction with the thiophenedicarbonyl chloride. Likewise the production of the imide would yield two molecules of benzylammonium chloride. Therefore further reactions involving thiophene-3,4-dicarbonyl chloride were carried out using a 320% excess of benzylamine. This, however produced no advancement, in fact no reaction was observed and the thiophene-3,4-dicarboxylic acid was reclaimed.

Thus the production of a fused thiophene nitroxide reached an impasse and no further advance towards preparing the final molecule was made.

2.2 Thiophene Nitronyl Nitroxides

The thiophene nitronyl nitroxide structure was to be accessed in a one step reaction from thiophene-3-carboxaldehyde according to the analogous reaction of LaParolas with benzaldehyde[33] (Chapter One, Figure 1.10).

LaParolas' method involved bubbling hydrogen chloride through a solution of dimethyl glyoxime and the aldehyde in alcohol at room temperature. However this produced no appreciable change. Refluxing with concentrated hydrochloric acid in methanol provided no real progress. The thiophene-3-carboxaldehyde was reclaimed, however a small fraction was obtained which appeared to consist of the starting aldehyde plus a dimethyl compound of some description (which was not dimethyl glyoxime). Unfortunately this fraction was too small to purify and identify the unknown compound. Thus the reaction time was increased from 2.5 hours to 7.0 hours in an attempt to increase the amount of the dimethyl compound formed. This

produced no improvement however and so the reaction temperature was elevated by refluxing in ethanol, as opposed to methanol. This produced sufficient material for the compound to be purified by column chromatography. In this way a white crystalline solid of melting point 74°C was isolated. On analysis this was identified as biacetylmonoxime (literature melting point 76°C[70]), that is one of the oxime groups had been hydrolysed to the carbonyl (Figure 2.20) and no reaction had taken place with the thiophene-3-carboxaldehyde.
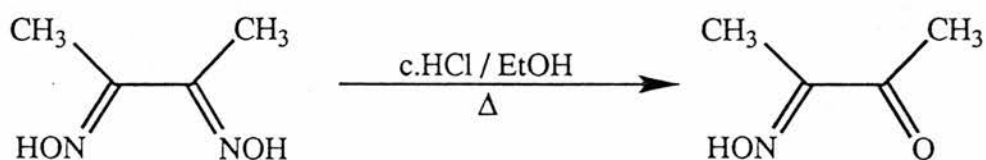
Figure 2.20

Hydrolysis of dimethyl glyoxime to the monoxime.

The corresponding reaction with diphenyl glyoxime (benzil dioxime) also failed to yield the desired nitronyl nitroxide, although in this case the dioxime was not hydrolysed to the monoxime (Figure 2.21). The final product of this reaction was a pale yellow crystalline solid of melting point 103°C. This was analysed by ^{1}H, ^{13}C and 2D COSY NMR, IR, EIMS and elemental analysis. The information from these examinations revealed the presence of approximately two equivalent phenyl groups, one thienyl group, two non-equivalent carbonyl groups, one acidic hydroxyl group and the total absence of nitrogen from the molecule. Initially it was envisaged that the benzil dioxime had been hydrolysed to the diketone which then underwent a benzilic acid type rearrangement to produce benzilic acid. The latter could then interact with thiophene-3-carboxylic acid (produced by the oxidation of the aldehyde) so as to produce the ester structure shown in Figure 2.22.

On further examination by EIMS, electrospray and FAB-MS (under both neutral and acidic conditions and after addition of sodium) however, it was revealed
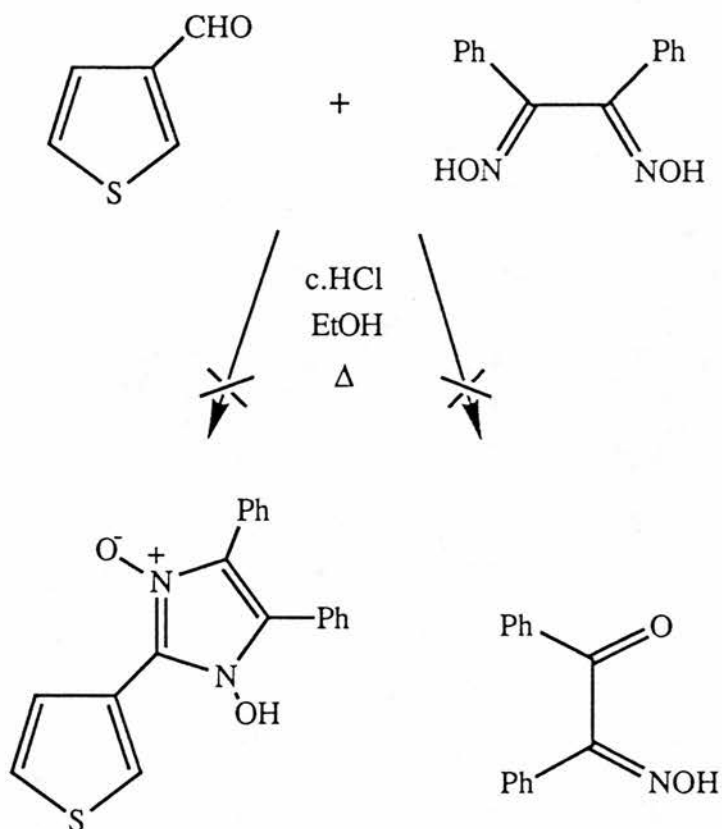
Figure 2.21

that the material was in fact a mixture consisting mainly of benzoic acid and thiophene-3-carboxylic acid. FAB-MS also showed the presence of trace amounts of
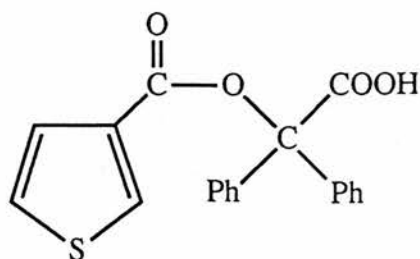
Figure 2.22

compounds produced by the condensation of the two carboxylic acids (examples of these type of structures are given in Figure 2.23). The mass and empirical formula of
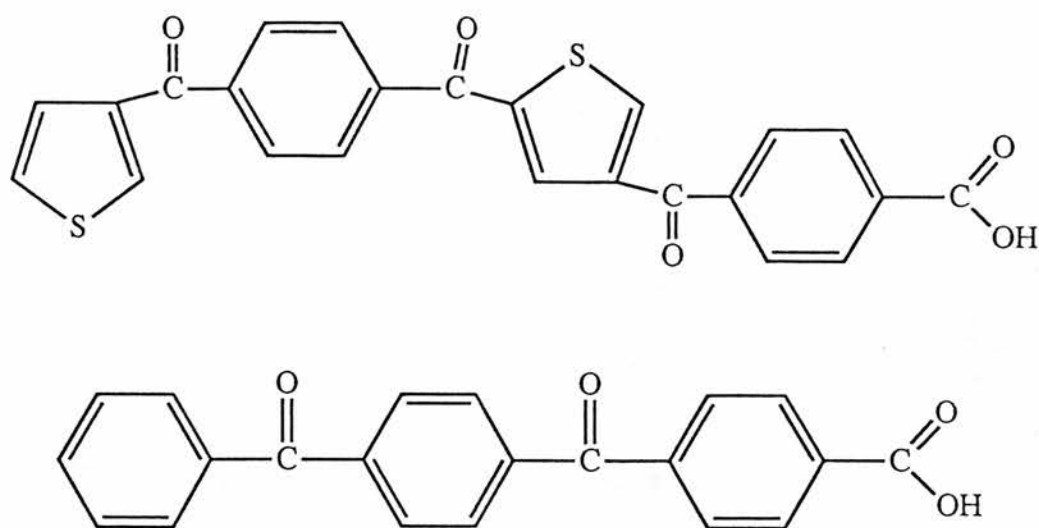
Figure 2.23

these trace compounds are shown in Table 2.3.

Mass	Formula
330	$C_{21}H_{14}O_4$
336	$C_{19}H_{12}O_4S$
422	$C_{26}H_{14}O_4S$
446	$C_{24}H_{14}O_5S_2$
660	$C_{36}H_{20}O_7S_3$
752	$C_{47}H_{28}O_8S$

Table 3.2

The mass and empirical formula of the structures of the type shown

in Figure 2.23, identified by FAB-MS.

By ignoring the trace structures one can obtain a crude value for the ratio of the two carboxylic acids by using the elemental analysis. From this a ratio of approximately 3:1 (benzoic acid to thiophene-3-carboxylic acid) is obtained.

Therefore it would appear that the main products of this reaction are benzoic acid and thiophene-3-carboxylic acid, which on work up of the reaction co-crystallise to produce the material isolated.

2.3   Conclusions

The main conclusion which can be drawn from this work is that one should be careful as to what groups are attached to the thiophene ring, as the removal of electron density from the thiophene ring system fatally inhibits the polymerisation of the monomer.   One method of circumventing this may be copolymerise reluctant monomers with thiophene or 3-alkylthiophenes, however it would then be difficult to ascertain exactly to what degree the radical monomer is incorporated into the copolymer.   Therefore it would be more advisable to prepare monomers with the radical group remote from the thiophene ring and with an electron donating group also attached to the thiophene to facilitate polymerisation.

2.4　　　　　　　　Experimental Section

^{1}H NMR spectra were recorded using a Varian EM-360 NMR Spectrometer (60 MHz), a Bruker WP80 NMR Spectrometer (80 MHz), a Varian Gemini-200 Spectrometer (200 MHz) and a Bruker AM300 NMR Spectrometer (300 MHz). ^{13}C NMR spectra were recorded using a Varian Gemini-200 Spectrometer (50 MHz) and a Bruker AM300 NMR Spectrometer (75.5 MHz) using DEPT-135 pulse techniques to assign peaks when necessary. 2D COSY NMR contour plots were recorded using a Varian Gemini-200 Spectrometer (200MHz).

IR spectra were recorded using a Perkin-Elmer 1420 Infra-Red Spectrometer, FT-IR using a Perkin-Elmer 170 Infra-Red Fourier Transform Spectrometer, and were run as liquid film, nujol mull, or KBr disc samples.

Mass spectra were recorded using an AEI MS902 Spectrometer. GC-MS were measured on a Finnigan Incos 50 Quadrupole Mass Spectrometer coupled to a Hewlet-Packard HP5890 Gas Chromatograph. The FAB-MS and electrospray investigation was carried out by D.J. Cooper at the Wellcome Research Laboratories, Kent.

Cyclic Voltammetric data was recorded using a Pine Instruments RDE 4 (EG & G, Wokingham, UK) with a Graphtec XY Recorder WX2300.

ESR spectra were recorded using a Bruker ER200D ESR Spectrometer operating at 100KHz modulation, with the potentials across the electrochemical ESR cell being generated with a potentiostat.

Elemental analyses were carried out in house at St. Andrews by Mrs. Sylvia Smith.

Melting points were determined using a Gallenkamp melting point apparatus.

The diethyl 1-formyl-2-diethoxymethylsuccinate was graciously provided by Dr. Ahmed Iraqi.

Thiophene-3,4-dicarboxylic Acid, via diethyl thiophene-3,4-dicarboxylate[61]. Dry toluene (210 ml) , diethyl 1-formyl-2-diethoxymethyl-

succinate (50.0g, 164.5 mmol) and phosphorus pentasulphide (35.48g, 79.8 mmol) were placed in a flask fitted with a stirrer and reflux condenser. The mixture was stirred rapidly under reflux for 2 hours. After cooling the toluene was decanted off from the dark resin. The resin was washed with fresh toluene and this too was decanted off. The combined toluene solutions were washed with water (*ca.* 160 ml) and twice with ice cold 2M sodium hydroxide solution (2 x *ca.* 160 ml). The toluene solution was then dried over magnesium sulphate and evaporated to dryness. The residual liquid was distilled and the fraction boiling from 100°C to 160°C at 5 mm Hg was collected. This was hydrolysed by heating with a solution of sodium hydroxide (6.46g, 161.5 mmol) in 16ml of water and 16ml of ethanol for 30 minutes. The red solution was then evaporated to dryness at reduced pressure. 50 ml of warm water was added to the solid residue and the resulting solution acidified with concentrated hydrochloric acid, and chilled. The precipitate which separated was filtered and washed with cold ether. This yielded 6.79g (39.44 mmol, 24.0%) of thiophene-3,4-dicarboxylic acid, which was used without further purification. ^{1}H NMR (200 MHz) δ(DMSO-d[6]) 8.20 (s, 2H), 8.05 (br s, 2H); ^{13}C NMR (50 MHz) δ(DMSO-d[6]) 135.54 (CH), 136.18 (C), 164.94 (COOH).

3,4-Dibromothiophene[62]. Tetrabromothiophene (50.0g, 125 mmol), zinc powder (50.0g, 765 mmol), 50ml of glacial acetic acid and 155ml of water were placed in a flask fitted with a reflux condenser and dropping funnel. The mixture was heated until the reaction had begun. The heating mantle was then removed and once the reaction had subsided the condenser was rearranged for distillation. The mixture was then distilled. After every 50 ml of distillate the heavier organic layer was separated and the aqueous layer returned to the reaction vessel via the dropping funnel. When no more organic phase distilled with the water the combined organic phases were dried over sodium carbonate and fractionally distilled at the water pump. This gave two fractions, the lower boiling fraction being a mixture of 3-bromo-thiophene and 3,4-dibromothiophene. The second fraction, distilling at 93°C to

104°C and 11 mmHg, was identified as 24.73g (102.22 mmol, 81.8%) of pure 3,4-dibromothiophene. ^{1}H NMR (300 MHz) δ(CDCl$_3$) 7.25 (s, 2H); ^{13}C NMR (75.5MHz) δ(CDCl$_3$) 113.73 (C-Br), 123.61 (CH).

3,4-Dicyanothiophene[60].   3,4-Dibromothiophene (22.36g, 92.4 mmol) and cuprous cyanide (24.10g, 269.0 mmol) in 25ml of dry DMF was stirred under reflux for 4 hours.   The dark solution thereby formed was poured into a solution of hydrated ferric chloride (93.0g in 162ml of 1.7M hydrochloric acid), and maintained at 60°C to 70°C for 30 minutes.   When cool this mixture was extracted five times with methylene chloride, each extract being washed successively with two portions of 6.0M hydrochloric acid, water, saturated sodium bicarbonate solution and again with water.   The methylene chloride layers were combined, dried over magnesium sulphate and then evaporated to dryness.   The crude solid produced was then sublimed at 0.1 mmHg to give 10.01g (74.60 mmol, 80.8%) of 3,4-dicyano-thiophene.   Infra-Red (nujol mull) 2210 cm^{-1} (CN).

Thiophene-3,4-dicarboxylic Acid[60].   3,4-Dicyanothiophene (8.44g, 62.9mmol) and potassium hydroxide (23.30g, 415.3 mmol) in 90ml of ethylene glycol were stirred under reflux for 4 hours.   On cooling this was poured into water and the resulting solution washed with ether.   The aqueous phase was cooled in an ice bath and acidified with 12.0M hydrochloric acid.   The white precipitate produced was filtered and taken up in ether.   The aqueous filtrate was extracted thoroughly with ether and all the ethereal solutions combined and dried over magnesium sulphate.   Removal of the solvent yielded 9.70g (56.34 mmol, 89.6%) of thiophene-3,4-dicarboxylic acid.   This was not purified further. ^{1}H NMR (60MHz) δ(DMSO-d^6) 10.18 (br s, 2H), 8.25 (s, 2H).   Infra-red (nujol mull) 1690 cm^{-1} (C=O).

Attempted Preparation of Thiophene-3,4-dicarboxylic Acid by Halogen-Metal Exchange[63].   To a stirred solution of butyllithium (18.4ml,

2.5M in hexane), at -70°C under a dry nitrogen atmosphere, was added 3,4-dibromothiophene (5.0g, 20.67 mmol) in 50ml of dry diethyl ether, over a period of 10 minutes. The resulting mixture was stirred at -70°C for 20 minutes. Carbon dioxide was then bubbled through the solution for approximately 2.5 hours, at which point water was added and the solution washed with ether. The ether layers were washed with water and the combined aqueous layers acidified with 1.0M hydrochloric acid and left at 5°C overnight. No precipitate separated and thus the solution was extracted with ether and dried over magnesium sulphate. Removal of the solvent produced 3.95g (18.59 mmol, 89.9%) of material in which only one bromine atom had exchanged. ^{1}H NMR (60MHz) δ(DMSO-d^6) 12.4 (s, 1H), 8.4 (m, 2H). Infrared (nujol mull) 1710 cm^{-1} (C=O). EIMS m/z (relative intensity) 208 (36), 206 (36), 191 (29), 189 (31), 128 (22), 111 (28), 82 (23), 81 (31), 73 (15), 60 (28), 59 (19). This singly exchanged compound was then treated with 1.2 equivalents of butyllithium and carbon dioxide once more, however no reaction was observed and the 4-bromothiophene-3-carboxylic acid was reclaimed. In retrospect this is not surprising as two molar equivalents is required due to the formation of the lithium salt with the acid group already present.

4,9-Dihydronaphtho[2,3-c]thiophene-4,9-dione (Tetrahydrothieno-naphthoquinone)[60]. Thiophene-3,4-dicarboxylic acid (2.0g, 11.62 mmol) in 5ml of thionyl chloride was stirred under reflux for 1 hour. The excess thionyl chloride was distilled off at reduced pressure, with the final traces being removed by azeotroping with benzene. The dark brown material thereby obtained was then left under vacuum in a desiccator for 1 hour.

The dicarbonyl chloride was then taken up in 12ml of dry 1,2-dichloroethane and added, in a dropwise manner, to a stirred suspension of aluminium chloride (3.49g, 26.17 mmol) in 12ml of dry 1,2-dichloroethane, maintained at 4°C. This mixture was stirred at 4°C for 10 minutes, at which point a solution of dry benzene (1.10ml, 12.31 mmol) in 6ml of dry 1,2-dichloroethane was slowly added. The

resulting solution was stirred at room temperature for approximately 18 hours. The solution was then poured into a mixture of ice and hydrochloric acid (15ml, 2M). Chloroform was added and the solution shaken vigorously. The solution was then extracted with chloroform and the organic extracts washed with saturated sodium bicarbonate solution, followed by water and dried over magnesium sulphate. This was concentrated down to about 70ml of solution, loaded onto a column of neutral alumina (Brockmann type 1) and eluted with 400 to 450ml of chloroform. The chloroform was removed and the product recrystallised from methylene chloride to yield 0.24g (1.12 mmol, 9.6%) of the tetrahydrothienonaphthoquinone. Melting point 283°C (with slight sublimation). ^{1}H NMR (300MHz) δ(CDCl$_3$) 7.8 (m, 2H), 8.3 (m, 2H), 8.37 (s, 2H). ^{13}C NMR (75.5MHz) δ(CDCl$_3$) 127.73 (CH), 132.76 (CHS), 134.12 (CH), 134.78 (C), 137.25 (C), 179.25 (C=O). Infra-red (nujol mull) 1670 cm^{-1}. EIMS m/z (relative intensity) 214 (82), 186 (92), 158 (100), 114 (46), 113 (32), 93 (18), 82 (21), 81 (20), 79 (22), 76 (21), 74 (14), 69 (21). Mass calculated for C$_{12}$H$_6$O$_2$S: 214.0089, found to be: 214.0087. Elemental analysis calculated for C$_{12}$H$_6$O$_2$S: C 67.27%, H 2.82%, found to be: C 66.22%, H 2.34%.

Other thienonaphthoquinones were prepared by this method by the reaction of thiophene-3,4-dicarbonyl chloride with benzene derivatives. The yields and characterisation data of these compounds are given below.

Tetramethylthienonaphthoquinone[71]. The crude product was recrystallised from ethyl acetate to produce the desired product in a yield of 10.8%. Melting point 238°C. ^{1}H NMR (300MHz) δ(CDCl$_3$) 2.37 (s, 6H), 2.71 (s, 6H), 8.14 (s, 2H). ^{13}C NMR (75.5MHz) δ(CDCl$_3$) 17.72 (CH$_3$), 19.01 (CH$_3$), 130.50 (CH), 132.99 (C), 138.38 (C), 138.81 (C), 143.05 (C), 183.00 (C=O). EIMS m/z (relative intensity) 270 (100), 269 (41), 255 (38), 227 (21), 226 (11), 199 (20), 198 (13), 196 (12), 184 (18), 165 (15), 152 (10), 145 (10), 127 (11), 115 (12), 111 (11). Mass calculated for C$_{16}$H$_{14}$O$_2$S: 270.0715, found to be: 270.0712. Elemental analysis calculated for C$_{16}$H$_{14}$O$_2$S: C 71.08%, H 5.22%, found to be: C 70.69%, H 5.09%.

Dimethoxythienonaphthoquinone[71]. The crude material was recrystallised from ethyl acetate followed by recrystallisation from methylene chloride for further purification. This produced the final product in a yield of 16.3%. Melting point 260°C. ^{1}H NMR (60MHz) δ(CDCl$_3$) 4.03 (s, 6H), 7.60 (s, 2H), 8.20 (s, 2H). EIMS m/z (relative intensity) 274 (98), 259 (21), 203 (68), 160 (50), 132 (37), 131 (22), 111 (38), 110 (39), 82 (49), 81 (43), 77 (20), 69 (27), 63 (45), 62 (44), 53 (60), 50 (72). Mass calculated for C$_{14}$H$_{10}$O$_4$S: 274.0300, found to be 274.0294.

Electrochemical Polymerisation of the Thienonaphthoquinones. Saturated solutions (approximately 0.6mM) of the thienonaphthoquinones in acetonitrile with TBAT or TBAHFP as supporting electrolyte were prepared. Three techniques were then attempted, with each solution, to polymerise the monomers.

(i) The solutions were subjected to a potential repeatedly scanning from -2.0V to +2.0V.

(ii) The solutions were subjected to a potential repeatedly scanning from 0.0V to +2.0V.

(iii) The solutions were subjected to a constant potential of about +2.0V.

However there was no polymer formation observed in any of these instances.

Chemical Polymerisation of the Thienonaphthoquinones.

1. Sulphuric Acid[57]. 1ml of concentrated sulphuric acid was added to the tetra-hydrothienonaphthoquinone (10mg, 0.047 mmol), the colour instantly changing from yellow to crimson, and stirred overnight. The reaction mixture was then poured into 20ml of methanol and stirred overnight. No polymer precipitated from the solution. Therefore the solution was thoroughly extracted with chloroform and the starting material reclaimed.

2. Ferric Chloride. Tetrahydrothienonaphthoquinone (0.10g, 0.47 mmol) and ferric chloride (0.038g, 0.23 mmol) were taken up in 0.5ml of nitromethane and 25ml

of methylene chloride and stirred for 48 hours. The solid precipitate was then separated. Examination revealed this precipitate to be the starting thienonaphthoquinone, which had presumably precipitated due to solvent evaporation. However if the procedure is repeated with more solvent to account for this then no precipitate is produced and no polymer isolated.

Attempted Cross Coupling Between 2-Bromothiophene and Tetra-methylthienonaphthoquinone Zinc Chloride[64a]. To a stirring solution of tetramethylthienonaphthoquinone (0.10g, 0.37 mmol) in 40ml of dry THF, at 0°C under a dry nitrogen atmosphere, was added 1.6M n-butyllithium solution (0.5ml, 0.80mmol) in hexane. This mixture was stirred at 0°C for 3.5 hours and then added, via a double ended catheter, to a stirring solution of zinc chloride (0.11g, 0.81 mmol) in 30ml of dry THF, under dry nitrogen at room temperature. This solution was then stirred for a further 1 hour. Note, in order to ensure that the zinc chloride was moisture free it was heated at 150°C with stirring under a dry nitrogen atmosphere for 30 minutes prior to use.

Meanwhile, *tetrakis*-triphenylphosphine palladium (0) (5.6mg, 0.0048 mmol) was placed in a 3-necked flask, under dry nitrogen, and 2-bromothiophene (0.12g, 0.74 mmol) added. The thienyl-zinc chloride solution was then added to this, again via a double ended catheter, and the resulting solution stirred for 30 minutes. The temperature was then gently raised to about 50°C and the solution stirred at this temperature for 24 hours. Dilute hydrochloric acid (5ml, 0.1M) was added to the cooled reaction mixture followed by extraction with ether. The combined organic extracts were washed with saturated sodium bicarbonate solution, water and dried over magnesium sulphate. Removal of the solvent produced the crude material, which was found to consist of 2-bromothiophene and the tetramethylthionaphthoquinone.

Attempted Chloromethylation of Naphthoquinone. 1,4-Naphthoquinone

(5.0g, 31.62 mmol), paraformaldehyde (2.53g, 84.33 mmol), 8ml of glacial acetic acid, 8ml of concentrated hydrochloric acid and 4ml of syrupy phosphoric acid was stirred at 100°C for 4.5 hours. The reaction mixture was then poured into 50ml of cold water, extracted with chloroform and dried over magnesium sulphate. Removal of the solvent produced crude material, which on examination proved to be devoid of chlorine. Therefore it is obvious that no chloromethyl groups were incorporated into the naphthoquinone structure.

Thiophene-3,4-dicarboxylic Anhydride. Thiophene-3,4-dicarboxylic acid (5.0g, 29.0mmol) in 200ml of acetic anhydride was stirred under reflux for three hours. The acetic anhydride was then distilled off at atmospheric pressure, with the final traces being removed at reduced pressure. The crude material was then recrystallised from ethanol to yield 4.23g (27.44 mmol, 94.6%). ^{1}H NMR (200MHz) δ(CDCl$_3$) 8.12 (s, 2H). ^{13}C NMR (50MHz) δ(CDCl$_3$) 129.91 (CH), 135.83 (C), 156.33 (C=O). EIMS m/z (relative intensity) 154 (16), 110 (100), 82 (56), 81 (32), 50 (22), 45 (24), 38 (15), 37 (18).

Attempted Preparation of the Ring Closed N-Benzylimide from the Thiophene-3,4-dicarboxylic Anhydride.

1. Benzylamine and Acetic Acid. The thiophenedicarboxylic anhydride (0.62g, 4.02mmol) and benzylamine (0.70g, 6.53 mmol) in 7.5ml of glacial acetic acid were stirred under reflux for 30 minutes. The solution was then allowed to cool and the product filtered. The solid product was shaken vigorously with chloroform, filtered and washed with fresh chloroform. The chloroform washings were found to contain starting anhydride, benzylamine and some minor impurities. The solid was dried in a vacuum desiccator to leave 0.44g (1.66 mmol, 41.9%) of the ring opened amide. ^{1}H NMR (200MHz) δ(DMSO-d^6) 4.50 (d (J=5.5Hz), 2H), 7.37 (m, 5H), 8.15 (d (J=3.7Hz), 1H), 8.35 (d (J=3.7Hz), 1H), 9.48 (t (J=5.3Hz), 1H), the acidic proton was not resolved. ^{13}C NMR (50MHz) δ(DMSO-d^6) 42.99 (CH$_2$), 127.15

58

(CH), 127.56 (CH), 128.58 (CH), 131.28 (CH), 133.04 (C), 136.24 (CH), 136.33 (C), 139.13 (C), 163.76 (C=O), 164.30 (C=O).   EIMS m/z (relative intensity) 244 (16), 243 (90), 225 (58), 215 (14), 214 (48), 198 (13), 186 (25), 139 (34), 136 (25), 112 (12), 111 (38), 110 (49), 105 (13), 104 (100), 91 (39), 90 (11), 89 (13), 83 (17), 82 (42), 81 (32), 78 (12), 77 (38), the parent ion not being observed.   The identity of this substrate was also confirmed using 2D-COSY NMR.

2. Benzylamine at 150°C.   Thiophenedicarboxylic anhydride (0.6g, 3.89 mmol) and benzylamine (0.6ml, 6.95 mmol) were stirred at 150°C (oil bath at 155° to 160°C) for 30 minutes.   Once cool 10ml of chloroform was added and the solution shaken.   The precipitate was filtered and washed with chloroform.   The chloroform washings were examined and found to contain benzylamine with a trace amount of the thiophenedicarboxylic anhydride.   Meanwhile the solid was dried to yield 0.91g (3.45 mmol, 89.5%) of the ring opened product. ^{1}H NMR (300MHz) δ(DMSO-d^6) 4.60 (d,2H), 7.40 (m, 5H), 8.13 (d, 1H), 8.30 (d, 1H), 9.70 (t, 1H), 13.26 (br s, 1H).

3. Benzylamine at 250°C.   The thiophenedicarboxylic anhydride (10mg, 0.065 mmol) and benzylamine (1.0ml, 11.58 mmol) were sealed in a NMR tube and heated to 250°C for 1 hour, using the oven of a Kugelrohr distillation apparatus.   Once cool the tube was broken open and placed on a sinter funnel.   The excess benzylamine was washed away with chloroform.   The remaining solid was taken up in DMSO-d^6 and examined by NMR.   This showed it to be the ring opened product (see above for spectral data).

Reaction of the Thiophenedicarboxylic Anhydride with Ammonia. Thiophenedicarboxylic anhydride (0.10g, 0.65 mmol) and a magnetic stirrer bar were placed in a high pressure reaction vessel and cooled to -80°C.   10ml of liquid ammonia was then added to this and the vessel sealed.   The solution was stirred and allowed to reach room temperature (the ammonia therefore vapourising until a pressure of 15 atmospheres was established).   The resulting solution was stirred at

room temperature overnight. The reaction vessel was then cooled to -80°C and the seal opened. With no stirring the solution was allowed to warm slowly to room temperature, the ammonia therefore evaporating leaving a solid residue. This solid, 0.11g (0.64 mmol, 98%), was examined by NMR and found to contain one acid group and therefore identified as the ring opened product. ^{1}H NMR (200MHz) δ(DMSO-d^6) 8.00 (d (J=4.4Hz), 1H), 8.16 (d (J=4.4Hz), 1H), 11.33 (br s, 1H), the amine peak was not observed.

Attempted Preparation of the Ring Closed N-Benzyl Thienylimide from Thiophene-3,4-dicarboxylic Acid.

1. Thionyl Chloride and Benzylamine. Thiophene-3,4-dicarboxylic acid (0.50g, 2.90 mmol) in 5ml of thionyl chloride was stirred under reflux for 1 hour. The thionyl chloride was then distilled off at reduced pressure, with the final traces being removed by azeotroping with benzene. The thiophene-3,4-dicarbonyl chloride was then placed under vacuum in a dessicator for 1 hour.

The dicarbonyl chloride was taken up in 70ml of dry THF, under a dry nitrogen atmosphere, and benzylamine (1.00g, 9.33 mmol) in 20ml of dry THF was slowly added. The resulting solution was stirred overnight and filtered, to remove the insoluble PhCH$_2$NH$_3$$^{+-}$Cl formed. The filtrate was dried over magnesium sulphate and evaporated to yield 0.54g (2.07 mmol, 71.4%) of the ring opened amide. Spectral details given earlier.

2. Phosphorus Pentachloride and Benzylamine. Thiophene-3,4-dicarboxylic acid (0.50g, 2.90 mmol) and phosphorus pentachloride (1.20g, 5.80mmol) in 40ml of dry THF was stirred under reflux for 2 hours. The THF and phosphorus oxychloride were removed by distillation and the thiophene-3,4-dicarbonyl chloride sucked dry under high vacuum.

The dicarbonyl chloride was taken up in 70ml of dry THF, under a dry nitrogen atmosphere, and benzylamine (1.00g, 9.33 mmol) in 20ml of dry THF was slowly added. The resulting solution was stirred overnight and filtered, to remove

the insoluble $PhCH_2NH_3^+Cl^-$ formed. The filtrate was dried over magnesium sulphate. Removal of the solvent yielded 0.67g (2.57 mmol, 88.6%) of the ring opened amide. Spectral details given earlier.

3. The Schotten-Baumann Method. Thiophene-3,4-dicarboxylic acid (0.50g, 2.90 mmol) in 5ml of thionyl chloride was stirred under reflux for 1 hour. The thionyl chloride was then distilled off at reduced pressure, with the final traces being removed by azeotroping with benzene. The thiophene-3,4-dicarbonyl chloride was then placed under vacuum in a desiccator for 1 hour.

The dicarbonyl chloride was then added to a mixture of 5ml of 15% sodium hydroxide solution and benzylamine (0.32g, 2.99 mmol) and stirred vigorously for 30 minutes. This solution was extracted with chloroform, which was then washed with water and dried over magnesium sulphate. Removal of the chloroform yielded only 0.29g (90.6% of that used) of benzylamine. The aqueous layers were therefore washed with ether (the ether layer being examined and found to contain nothing of interest) and carefully acidified. The solution was then extracted with ether, and the extracts dried over magnesium sulphate. Removal of the solvent produced 0.46g (92.0% of that used) of the starting thiophene-3,4-dicarboxylic acid.

Attempted Ring Closure of the Ring Opened Thiophene Amide.

1. Acetic Acid. The ring opened thiophene amide (0.10g, 0.38 mmol) in 10ml of glacial acetic acid was stirred under reflux for 3 hours. The solution was then cooled and the solid filtered. This solid was washed with chloroform and dried under high vacuum. Examination of the solid showed it to be unchanged starting material, whilst the chloroform washings were found to contain traces of acetic acid only.

2. Oxalyl Chloride. The ring opened thiophene amide (0.20g, 0.76 mmol) in 2ml of oxalyl chloride were stirred under reflux for 3 hours, under a dry nitrogen atmosphere. The oxalyl chloride was then removed by distillation at atmospheric pressure, with the final traces being removed at the oil pump. The residue was shaken vigorously with methylene chloride and filtered. Examination of the

methylene chloride extract by NMR yielded nothing of interest, whereas the solid residue was identified as the starting amide.

3. Phosphorus Pentachloride.   The ring opened thiophene amide (0.50g, 1.90mmol) and phosphorus pentachloride (0.40g, 1.92 mmol) in 25ml of dry THF was stirred under reflux for 3 hours, under a dry nitrogen atmosphere.   The THF and phosphorus oxychloride were then removed by distillation and the residue sucked dry at the oil pump.   The residue was then shaken vigorously with chloroform and filtered.   Examination of the chloroform filtrate showed that it contained nothing of interest.   The solid residue was examined and identified as the starting thiophene amide.

Attempted Preparation of the Thienyldimethylimidazole Nitronyl Nitroxide.

1. Hydrogen Chloride.   Thiophene-3-carboxaldehyde (1.00g, 8.92mmol) and dimethyl glyoxime (1.04g, 8.96mmol) were dissolved in 100ml of methanol. Hydrogen chloride gas was bubbled through the solution for approximately 40 minutes.   The methanol was then removed to give the crude material which was taken up in chloroform and filtered.   The chloroform was removed to produce a clear oil. Both the solid and the oil were examined by NMR.   The solid proved to be dimethyl glyoxime, ^{1}H NMR (60MHz) δ(DMSO-d^6) 1.97 (s, 6H), 11.36 (s, 2H).   The oil was identified as the starting thiophene-3-carboxaldehyde, ^{1}H NMR (200MHz) δ(CDCl$_3$) 7.24 (d (J=4.4Hz), 1H), 7.41 (t (J=5.0Hz), 1H), 8.03 (d (J=4.2Hz), 1H), 9.79 (s, 1H).

2. Concentrated Hydrochloric Acid in Methanol.   Thiophene-3-carboxaldehyde (1.00g, 8.92mmol), dimethyl glyoxime (1.04g, 8.96mmol) and 1.6ml of concentrated hydrochloric acid in 100ml of methanol was stirred under reflux for 2.5 hours.   The methanol was removed and the residue taken up in methylene chloride.   The insoluble material was filtered and identified as dimethyl glyoxime.   The methylene chloride solution was washed with saturated sodium

hydrogen carbonate solution, water and dried over magnesium sulphate.

The methylene chloride was removed to produce a crude oil which was distilled at the water pump. This produced 0.84g (7.49mmol, 84.0%) of thiophene-3-carboxaldehyde at 90 to 92°C and 19 mmHg, and 20mg of material at 125 to 135°C and 15 mmHg which appeared to consist mainly of the aldehyde with a small proportion of material which produced a methyl signal in the ^{1}H NMR. Attempts to purify this further by preparative tlc failed.

The reaction was repeated with a reflux time of seven hours, however this produced no appreciable difference in the outcome of the reaction.

3. Concentrated Hydrochloric Acid in Ethanol. Thiophene-3-carboxaldehyde (4.00g, 35.67mmol), dimethyl glyoxime (4.18g, 35.99mmol) and 20ml of concentrated hydrochloric acid in 400ml of ethanol were stirred under reflux for 4.5 hours. The ethanol was then removed and the residue taken up in chloroform. This solution was then washed with saturated sodium hydrogen carbonate solution, water and dried over magnesium sulphate.

Removal of the solvent produced the crude material which was purified by column chromatography, on silica gel 60 using 40-60 petrol followed by 5% diethyl ether in 40-60 petrol. This yielded 0.16g (1.58mmol, 4.4%) of white crystalline material which was identified as diacetyl monoxime (2,3-butanedione monoxime). Melting point 74°C (lit. value 76°C[69]). ^{1}H NMR (200MHz) δ(CDCl$_3$) 1.97 (s, 3H), 2.38 (s, 3H), 8.66 (br s, 1H). ^{13}C NMR (50MHz) δ(CDCl$_3$) 8.55 (CH$_3$), 25.58 (CH$_3$), 157.69 (C=NOH), 197.76 (C=O). FTIR (KBr disc) 3200 cm^{-1} (br s, OH), 1675 cm^{-1} (vs, C=O), oxime C=N bands are usually very weak and therefore this is probably obscured by the carbonyl absorption. EIMS m/z (relative intensity) 101 (7), 58 (4), 43 (100), 42 (22), 41 (8), 40 (4), 36 (3), 31 (3), 28 (12), 26 (3). Elemental analysis calculated for C$_4$H$_7$O$_2$N: C 47.52%, H 7.05%, N 13.85%, found to be: C 45.70%, H 6.95%, N 13.38%.

Attempted Preparation of the Thienyldiphenylimidazole Nitronyl

Nitroxide. This was carried out by the same method employed above with the dimethyl analogue using concentrated hydrochloric acid in ethanol, with the exception that benzil dioxime (8.66g, 36.00mmol) was used in the place of dimethyl glyoxime.

The crude material was purified by recrystallisation from ethanol followed by recrystallisation from methylene chloride. This yielded 1.47g of a pale yellow crystalline material. ^{1}H NMR (200MHz) δ(CDCl$_3$) 7.25 (d (J=5.0Hz), 1H), 7.47 (m, 4H), 7.62 (m, 2H), 7.67 (t (J=2.0Hz), 1H), 8.15 (m, 4H), 8.23 (d (J=2.0Hz), 1H), 12.47 (br s, 1H). ^{13}C NMR (50MHz) δ(CDCl$_3$) 126.85 (CH), 127.96 (C), 129.00 (CH), 129.88 (CH), 130.71 (CH), 131.49 (C), 134.32 (CH), 135.15 (C), 169.20 (C=O), 170.31 (C=O). 2D COSY NMR (200MHz) provided no information of consequence, that is it only revealed that the three thienyl protons were coupled to each other and that the phenyl protons were coupled to each other. IR (nujol mull) 1700 cm^{-1} (C=O). EIMS m/z (relative intensity) 128 (20), 122(63), 111 (42), 105 (100), 83 (6), 77 (72), 51 (27), 50 (21), 45 (18), 39 (19), 38 (10), 37 (6). On further examination by electrospray and FAB-MS techniques the material was identified as a mixture of benzoic acid and thiophene-3-carboxylic acid. Elemental analysis calculated for C$_{26}$H$_{22}$O$_8$S (a ratio of 3:1 of benzoic acid : thiophene-3-carboxylic acid): C 63.15%, H 4.48%, found to be: C 63.55%, H 4.20%.

Part One References

1. Ito, T. ; Shirakawa, H. ; Ikeda, S. *J. Polym. Sci., Chem. Ed.*, **1974**, *12*, 11.

2. Chiang, C.K. ; Park, Y.W. ; Heeger, A.J. ; Shirakawa, H. ; Louis, E.J. ; MacDiarmid, A.G. *Phys. Rev. Lett.*, **1977**, *39*, 1098.

3. Proceedings of ICSM '88 *Synth. Met.*, **1989**, vol. 27 to 29.

4. Diaz, A.F. ; Kanazawa, K.K. ; Gardini, G.P. *J. Chem. Soc., Chem. Commun.*, **1979**, 635.

5. Dall'Ollio, A. ; Dascola, Y. ; Gardini, G.P. *C.R. Acad. Sci.*, **1969**, *267*, 4336.

6. Diaz, A.F. *Chem. Scr.*, **1981**, *17*, 142.

7. Tourillon, G. ; Garnier, F. *J. Electroanal. Chem.*, **1982**, *135*, 173.

8. Bargon, J. ; Mohamand, S. ; Waltman, R.J. *IBM J. Res. Develop.*, **1983**, *27*, 330.

9. Delamar, M. ; Lacaze, P.C. ; Dumousseau, J.Y. ; Dubois, J.E. *Electrochim. Acta.*, **1982**, *27*, 61.

10. Rault-Bertholet, J. ; Simonet, J. *J. Electroanal. Chem.*, **1985**, *182*, 187.

11. (a) Diaz, A.F. ; Logan, J.A. *J. Electroanal. Chem.*, **1980**, *111*, 111.   (b) MacDiarmid, A.G. ; Chiang, J.C. ; Halpern, M. ; Huang, H.S. ; Mu, S.L. ; Somasiri, N.L.D. ; Wu, W. ; Yaniger, S.I. *Mol. Cryst. Liq. Cryst.*, **1985**, *121*, 173.   (c) Genies, E.M. ; Tsintaris, C. ; Syed, A.A. *Mol. Cryst. Liq. Cryst.*, **1985**, *121*, 181.

12. Druy, M.A. ; Rubner, M.F. ; Walsh, S.P. *Synth. Met.*, **1986**, *13*, 207.

13. Elsenbaumer, R.L. ; Jen, K.-Y. ; Eckhardt, H. ; Shacklette, L. ; Jow, R. *Electronic Properties of Conjugated Polymers*, p. 400, Kuzmany, H. ; Mehring, M. ; Roth, S. Ed., Springer-Verlag, Berlin (1987).

14. Gomberg, M. *Ber.*, **1900**, *33*, 3150 ; *J. Am. Chem. Soc.*, **1900**, *22*, 757.

15. Piloty, O. ; Scherwin, B.G. *Ber.*, **1901**, *34*, 1870 and 2354.

16. Andrews, W.L.S. ; Pimental, G.C. *J. Chem. Phys.*, **1966**, *44*, 2527.

17. (a) Goldschmidt, S. ; Renn, K. *Ber.*, **1922**, *55*, 628.   (b) Goldschmidt, S. ; Graef, F. *Ber.*, **1928**, *61*, 1858.   (c) Poirer, R.H. ; Kahler, E.J. ; Benington, F. *J. Org. Chem.*, **1952**, *17*, 1437.

18. Griller, D. ; Ingold, K.U. *Acc. Chem. Res.*, **1976**, *9*, 13.

19. Dewar, M.J.S. ; Gleicher, G.J. *J. Chem. Phys.*, **1966**, *44*, 759.

20. Peover, M.E. *J. Chem. Soc.*, **1962**, 4540.

21. Foster, R. *Organic Charge Transfer Complexes*, Academic, London, 1969.

22. Bernstein, J. ; Reger, H. ; Herbstein, F.H. ; Main, P. ; Rizvi, S.H. ; Sasvari, K. ; Turcsanyi, B. *Proc. Roy. Soc. London, Ser. A*, **1976**, *347*, 419.

23. Clark, W.M. *Oxidation-Reduction Potentials in Organic Systems*, Williams and Wilkins, Baltimore, 1960.

24. Jackman, L.M. *Adv. Org. Chem.*, **1960**, *2*, 329.

25. *Encyclopaedia of Chemical Technology* (Kirk-Othmer), vol. 16, p. 899, Interscience, New York, 1968.

26. (a) Makarov, S.P. ; Yakubovich, A.Y. ; Dubov, S.S. ; Medvedev, A.N. *Dokl. Akad. Nauk SSSR*, **1965**, *160*, 1319.   (b) Blackley, W.D. ; Reinhard, R.R. *J. Am. Chem. Soc.*, **1965**, *87*, 802.

27. Pauling, L. *The Nature of the Chemical Bond*, p. 343, Cornell University Press, New York, 1960.

28. Linnett, J.W. *J. Am. Chem. Soc.*, **1961**, *83*, 2643.

29. Anderson, B. ; Anderson, P. *Acta. Chem. Scand.*, **1966**, *20*, 2728.

30. (a) Osiecki, J.H. ; Ullman, E.F. *J. Am. Chem. Soc.*, **1968**, *90*, 1078.   (b) Boocock, D.G.B. ; Darcy, R. ; Ullman, E.F. *J. Am. Chem. Soc.*, **1968**, *90*, 5945.   (c) Boocok, D.G.B. ; Ullman, E.F. *J.Am. Chem. Soc.*, **1968**, *90*, 6873.   (d) Ullman, E.F. ; Call, L. ; Osiecki, J.H. *J. Org. Chem.*, **1970**, *35*, 3623.

31. Wright, J.B. *J. Org. Chem.*, **1964**, *29*, 1620.

32. Minisci, F. ; Galli, R. ; Quilico, A. *Tetrahedron Lett.*, **1963**, *4*, 785.

33. LaParola, G. *Gazz. Chim. Ital.*, **1945**, *75*, 216.

34. Henglein, A. ; Boysen, M. *Makromol. Chem.*, **1956**, *20*, 83.

35. Braun, D. ; Loflund, I. ; Fischer, H. *J. Polym. Sci.*, **1962**, *58*, 667.

36. (a) Braun, D. ; Neumann, W. ; Faust, J. *Makromol. Chem.*, **1965**, *85*, 143.

     (b) Braun, D. ; Faust, J. *Angew. Chem., Int. Ed. Engl.*, **1966**, *5*, 838.

37. Kurusu, Y. ; Yoshida, H. ; Okawara, M. *Tetrahedron Lett.*, **1967**, *8*, 3595.

38. Kinoshita, M. ; Schultz, R.C. *Makromol. Chem.*, **1968**, *111*, 137.

39. Griffith, O.H. ; Keana, J.F.W. ; Rottschaeffer, S. ; Warlick, T.A. *J. Am. Chem. Soc.*, **1967**, *89*, 5072.

40. Kamachi, M. ; Tamaki, M. ; Morishama, Y. ; Nozakura, S. ; Mai, W. ; Kishita, M. *Polym. J. (Tokyo)*, **1982**, *14*, 363.

41. Kurosaki, T. ; Lee, K.W. ; Okawara, M. *J. Polym. Sci., Polym. Chem. Ed.*, **1972**, *10*, 3295.

42. Kurosaki, T. ; Takahashi, O. ; Okawara, M. *J. Polym. Sci., Polym. Chem. Ed.*, **1974**, *12*, 1407.

43. Miyazawa, T. ; Endo, T. *J. Polym. Sci., Polym. Chem. Ed.*, **1985**, *23*, 2487.

44. (a) Korshak, Y.V. ; Ovchinnikov, A.A. ; Shapiro, A.M. ; Medvedeva, E.V. ; Specktor, V.N. *Pisma Zh. Eksp. Teor. Fiz*, **1986**, *43*, 309. (b) Korshak, Y.V. ; Medvedeva, T.V. ; Ovchinnikov, A.A. ; Specktor, V.N. *Nature*, **1987**, *326*, 370.

45. MacCorquodale, F. ; Crayston, J.A. ; Walton, J.C. ; Worsfold, D.J. *Tetrahedron Lett.*, **1990**, *31*, 771.

46. (a) Alexander, C. ; Feast, W.J. *Polym. Bull.*, **1991**, *26*, 245. (b) Alexander, C. ; Feast, W.J. ; Friend, R.H. ; Sutcliffe, L.H. *J. Mater. Chem.*, **1992**, *2*, 459.

47. Crayston, J.A. ; Kakouris, C. ; Walton, J.C. (in preparation).

48. Crayston, J.A. ; Kakouris, C. ; Walton, J.C. *Magn. Res. Chem.*, **1992**, *30*, 77.

49. Kakouris, C. ; Crayston, J.A. ; Walton, J.C. *Synth. Metals*, **1992**, *48*, 65.

50.   Forrester, A.R. ; Thomson, R.H. *J. Chem. Soc. (C)*, **1966**, 1844.

51.   Chinard, F.P. ; Hellerman, L. *Methods of Biochemical Analysis*, vol. 1, p. 1, Glick, D. Ed., Interscience, New York, 1954.

52.   Endo, T. ; Miyazawa, T. ; Shiihashi, S. ; Okawara, M. *J. Am. Chem. Soc.*, **1984**, *106*, 3877.

53.   (a) Goluber, V.A. ; Rozantsev, E.G. ; Neiman, M.B. *Bull. Acad. Sci. USSR*, **1965**, 1898.   (b) Rozantsev, E.G. ; Sholle, V.D. *Synthesis*, **1971**, 401.   (c) Miyazawa, T. ; Endo, T. ; Shiihashi, S. ; Okawara, M. *J. Org. Chem.*, **1985**, *50*, 1332.

54.   Semmelhack, M.F. ; Schmid, C.R. *J. Am. Chem. Soc.*, **1983**, *105*, 6732.

55.   Lahti, P.M. *Am. Chem. Soc. Polym. Preprints*, **1990**, *31 (1)*, 710; and references therein.

56.   Kaneto, K. ; Kohno, Y. ; Yoshino, K. *J. Chem. Soc., Chem. Commun.*, **1983**, 382.

57.   Wudl, F. ; Kobayashi, M. ; Heeger, A.J. *J. Org. Chem.*, **1984**, *49*, 3382.

58.   (a) Hotta, S. ; Hosaka, T. ; Shimotsuma, W. *Synth. Metals*, **1983**, *6*, 317. (b) Tourillon, G. ; Garnier, F. *J. Polym. Sci., Polym. Phys. Ed.*, **1984**, *22*, 33.   (c) Sato, M.-A. ; Tanaka, S. ; Kaeriyama, K. *J. Chem. Soc., Chem. Commun.*, **1985**, 713.

59.   Grimshaw, J. ; Perera, S.D. *J. Electroanal. Chem.*, **1990**, *278*, 287.

60.   MacDowell, D.W.H. ; Wisowaty, J.C. *J. Org. Chem.*, **1972**, *37*, 1712.

61.   Kornfeld, E.C. ; Jones, R.G. *J. Org. Chem.*, **1954**, *19*, 1671.

62.   Gronowitz, S. *Acta. Chem. Scand.*, **1959**, *13*, 1045.

63.   MacDowell, D.W.H. ; Jeffries, A.T. *J. Org. Chem.*, **1970**, *35*, 871.

64.   Pedersen, J. A. *CRC Handbook of EPR Spectra From Quniones and Quinols*, CRC Press Inc. 1985.

65.   (a) Pelter, A. ; Rowlands, M. ; Clements, G. *Synthesis*, **1987**, 51.   (b) Pelter, A. ; Rowlands, M. ; Jenkins, I.H. *Tetrahedron Lett.*, **1987**, *28*, 5213. (c) Pelter, A. ; Maud, J.M. ; Jenkins, I.H. ; Sadeka, C. ; Coles, G.

Tetrahedron Lett., **1989**, *30*, 3461.

66. King, J.F. ; Hawson, A. ; Huston, B.L. ; Danks, L.J. ; Komery, J. *Can. J. Chem.*, **1971**, *49*, 943.

67. King, J.F. ; Du Manoir, J.R. *Can. J. Chem.*, **1973**, *51*, 4082.

68. Griffiths, P.G. ; Moad, G. ;Rizzardo, E. ; Solomon, D.H. *Aust. J. Chem.*, **1983**, *36*, 397.

69. Furniss, B.S. ; Hannaford, A.J.; Smith, P.W.G. ; Tatchell, A.R. *Vogel's Textbook of Practical Organic Chemistry, 5th Ed.*, p. 1276, Longman Scientific & Technical, 1989.

70. Rappoport, Z. *Handbook of Tables for Organic Compound Identification, 3rd Ed.*, p.161.

71. For preparative details see the synthesis of 4,9-dihydronaphtho[2,3-c]-thiophene-4,9-dione.

Part Two:

The Cubyl and Cubyl-

Carbinyl Radicals, and

Homolytic Reactions

of Cubane.

Chapter Three

Introduction to the Chemistry of Cubanes

Of the five convex Platonic solids[1], shown in Figure 3.1, only the carbocyclic $(C-H)_n$ analogues of the tetrahedron, the cube and the dodecahedron are potentially accessible to the synthetic organic chemist. It should be said that a Platonic solid is defined as being a solid made up of identical regular polygonal faces, with each vertex therefore being congruent with every other vertex. In reality, all three "cage"
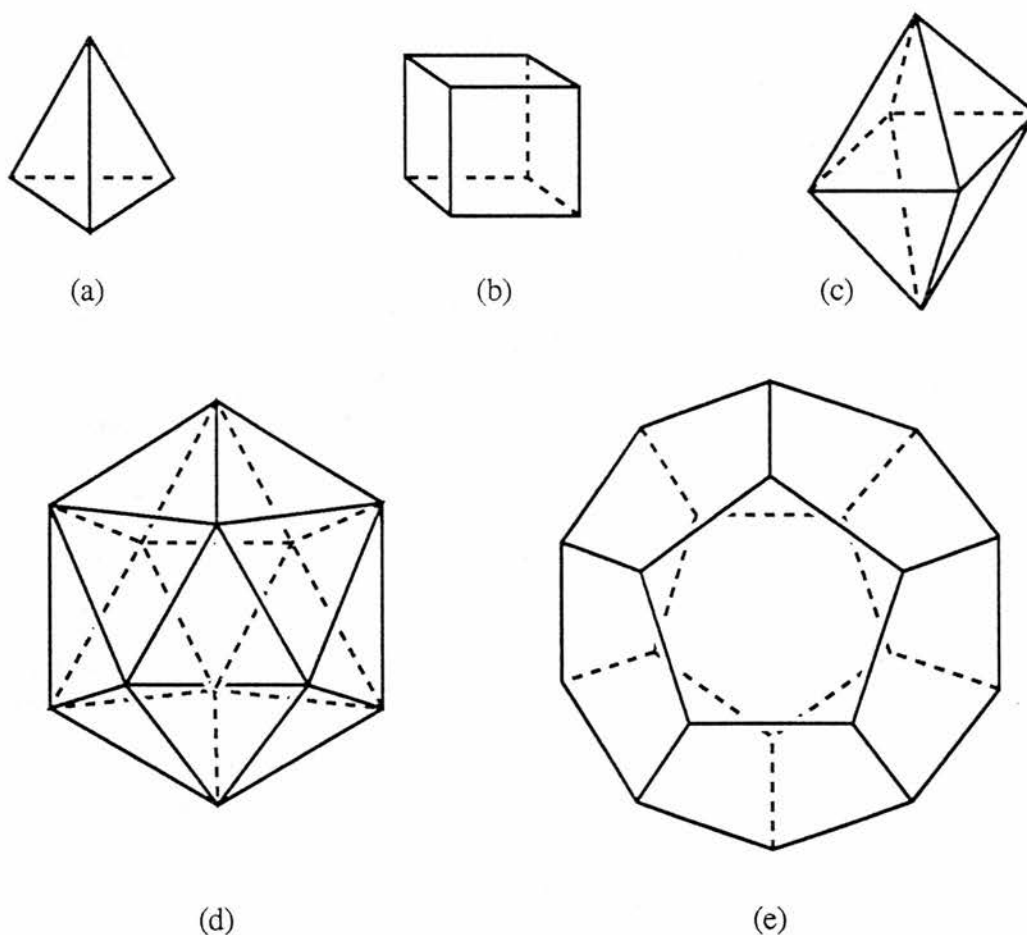
Figure 3.1 ; The Platonic Solids

The tetrahedron (a), cube (b), octahedron(c),

dodecahedron (d) and icosahedron (e).

systems, "tetrahedrane" (n=4)[2,3], "cubane" (n=8)[4] and "dodecahedrane" (n=20)[5], or derivatives thereof, are synthetically known. Octahedrane and icosahedrane are excluded as the former is formally an allotropic form of carbon, and the latter requires pentavalent carbon.

Tetrahedrane, the simplest Platonic hydrocarbon is unknown. The system is highly strained, and pathways for its decomposition are readily available, such as protonation and bond opening to form a di-radical. This supports the possibility that some of the many attempts at synthesis of tetrahedrane may have in fact been successful, but that the molecule failed to survive.[6] However, tetra substituted derivatives, such as tetra-*tert*-butyltetrahedrane[2] and tetralithiotetrahedrane[3] (Figure 3.2), have been isolated. The fact that these are fully substituted may have much to do with their greater stability.
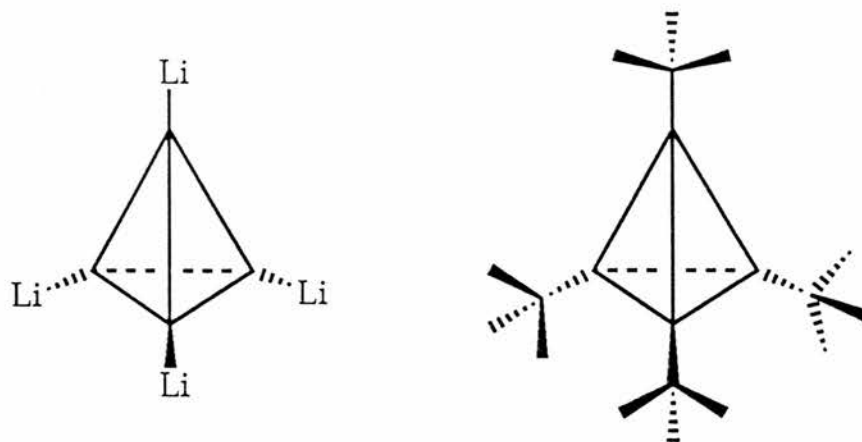
Figure 3.2

Tetralithiotetrahedrane and Tetra-*tert*-butyltetrahedrane

On the other hand, dodecahedrane, the largest of the Platonic solids is much less strained, with a strain energy of less than 100 kcal mol^{-1} (based on heats of formation[7] or the sum of the strains[8]). Even so, it was not until recently that the structure was synthetically realised. The total synthesis of the parent hydrocarbon in

twenty-three steps was reported by Paquette and co-workers[5(a)-(b)] soon after their successful preparation of the monomethyl[9] and 1,16-dimethyl[10] derivatives. This was more recently followed by the preparation of dodecahedranes from [1.1.1.1] pagodanes by Fessner *et al*[5(c)], although dodecahedrane itself is only obtained in low yield.

The first of the "Platonic Hydrocarbons" to be prepared from a rational synthesis however was pentacyclo[4.2.0.0.^{2,5}0.^{3,8}0.^{4,7}]octane, or cubane, its synthesis being solved by Eaton and Cole in 1964.[4] Since then many derivatives of cubane have been isolated and their behaviour studied extensively.

3.1 Preparation of Cubanes

There are two apparent routes to the cubane skeleton. These are: (i) the cycloaddition of functionalised noncage precursors, and (ii) the ring contraction of functionalised cage precursors.

Intramolecular [2+2] photocyclisations of appropriately constructed dienes would appear to be a most attractive technique with which to access the cubane structure. In general however, this photocyclisation does not occur. Explanations of why this should be include: accounts of why the photocyclisation should be symmetry forbidden[11-13], the expected effects of strain in the product against the corresponding effects in the reactant[14], and the large non-bonded distance (approximately 3.05 Å) separating the two carbon-carbon double bonds.[14]

With the right choice of substituent however, this photocyclisation has been observed in a few cases, such as the preparation of *octakis*(trifluoromethyl)cubane by photolysing either *syn-* or *anti-octakis*(trifluoromethyl)-tricyclo-[4.2.0.0.^{2,5}]-octa-3,7-diene[15] (Figure 3.3).

Ring contractions of homocubanes and *bis*-homocubanes were invaluable in the first successful synthesis of the cubane skeleton[4]. The preparation was achieved by utilising the base-promoted "quasi-Favorskii" or "semibenzilic acid" rearrangement of α-haloketones in the way displayed in Figure 3.4. Many cubane preparations

followed which were based on the Eaton and Cole method. Among these are the photochemical preparations of cubane-1,3-dicarboxylic acid[16] and dimethylcubane-1,3-dicarboxylate[17]. From these and other[18-20] reports, it has become clear that (i) the nature of the substrate and its leaving group, and (ii) the reaction conditions, are crucial to the success of the base-promoted semibenzilic acid rearrangements[21]. Despite this, the "Favorskii-like" contraction of a bromoketone is still the most successful method for gaining entry to the cubane system.
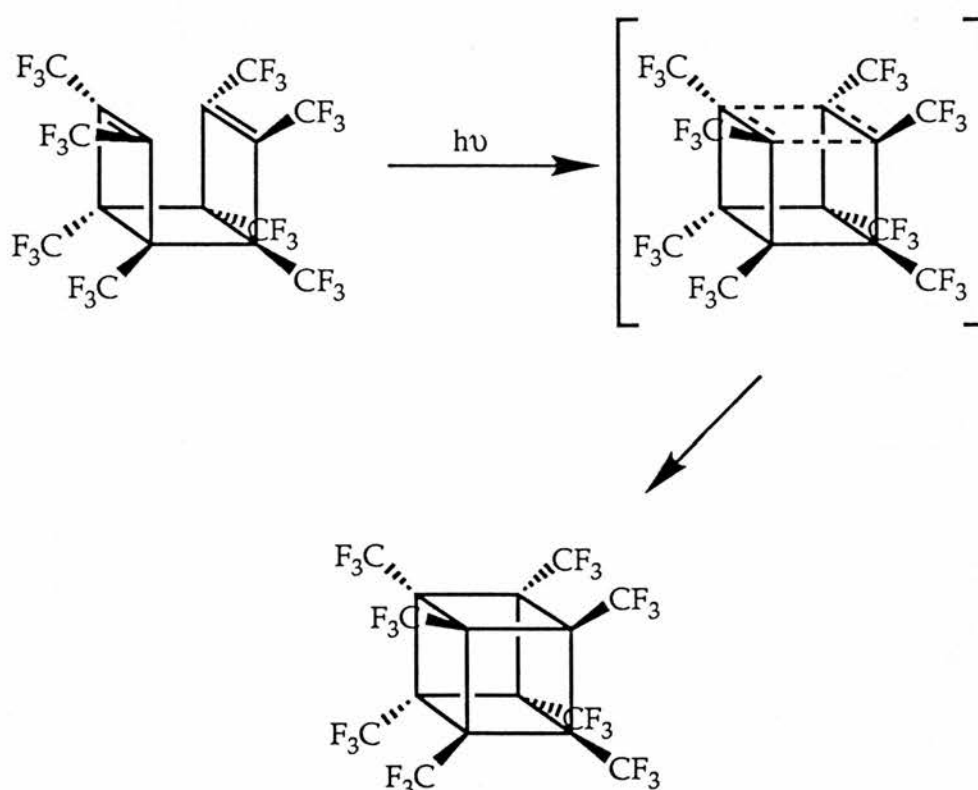
Figure 3.3

Irradiation of *syn-octakis*(trifluoromethyl)tricyclo[4.2.0.0.^{2,5}]-

octa-3,7-diene, to produce *octakis*(trifluoromethyl)cubane.

Derivatives of cubane are usually prepared by direct substitution on the cubane cage. Initially functionalisation centred around the manipulation of the carboxylic acid groups by standard techniques (as the acid and di-acid were the first substituted

74
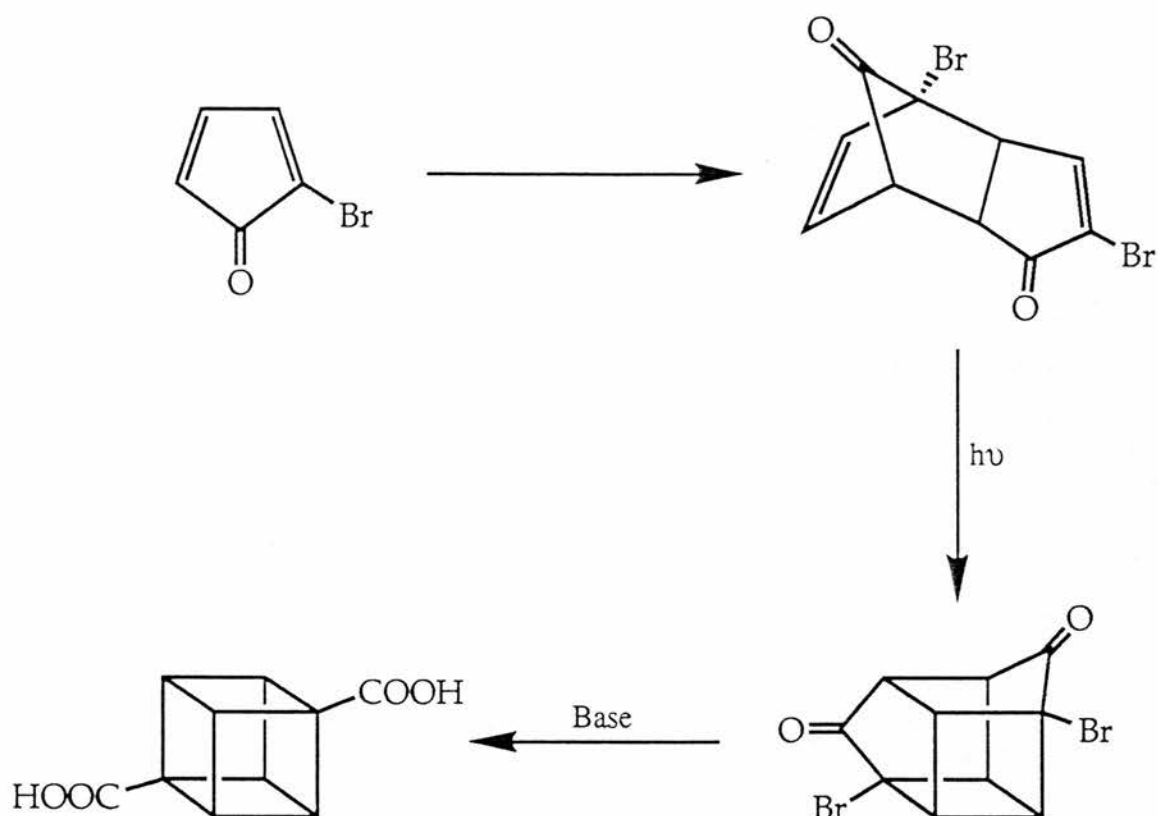
Figure 3.4

Eaton and Coles' preparation[4], using the base-promoted

"Favorskii-like" contraction of an α-haloketone.

cubanes isolated). For example, iodinative decarboxylation has been used to produce

iodocubanes[22], which can then be oxidatively deiodinated to yield new, substituted

cubanes[23]. The major breakthrough in cubane functionalisation came however,

when Eaton directly metalated the cubane skeleton[24], followed by the indirect

metalation by Della *et al*[25]. These latter achievements have now renewed the interest

of researchers in cubane and its derivatives, as has their potential as an important new

class of energetic materials[26].

3.2   Reactions of Cubanes

Substituted cubanes have the facility to react in many ways. However, for

the sake of simplicity these will be summarised in four types of reaction only. These

are: those resulting in the fragmentation or ring expansion of the cubane cage, rearrangements promoted by transition metals, and direct substitution and functionalisation of the cubane structure itself.

Despite the considerable strain introduced into a molecule by the bond deformations needed to accommodate eight sp^3-hybridised methine carbons at the vertices of a cube (166 kcal mol^{-1} [27,28], approximately 14 kcal mol^{-1} per carbon carbon bond[7]), cubane displays an unusual thermal stability. The molecule survives unchanged at temperatures of up to *ca.* 200°C[28]. It has been pointed out that this thermal stability is a result of the cage's inability to undergo bond reorganisation in a *concerted* manner in the ground state. However, when there is the opportunity for reorganisation via a *nonconcerted* process, then a fast cage fragmentation reaction may take place, even at low temperatures[29]. Cage-opening reactions, which derive some driving force from the release of strain by cleaving a carbon-carbon σ bond in the cubane system, include hydrogenolysis, base-promoted reactions and thermal reactions.

Stober and Musso[30] have investigated the hydrogenolysis of cubane and have found that up to three carbon-carbon bonds will undergo hydrogenolysis in a sequential manner under the correct conditions. In each case hydrogenolysis occurs at the most highly strained carbon-carbon bond, releasing 50 kcal mol^{-1}, 34 kcal mol^{-1} and 45 kcal mol^{-1} [30b] of strain energy successively. Thus the three products accessible by the hydrogenolysis of cubane are tetracyclo-[4.2.0.0[2,5].0[3,8]]-octane ("secocubane"), which further reduces to tricyclo-[4.2.0.0[4,7]]-octane ("nortwistbrendane") and finally bicyclo-[2.2.2]-octane (Figure 3.5).

Base-promoted reactions of cubanes such as homoketonisation[31] and homoallylic rearrangements[32], which lead to ring opening, have also been investigated.

It has been mentioned that cubane is stable up to 200°C, but under static pyrolysis in the temperature range 230 to 260°C[33] the cage fragments. The pyrolysis products thereby formed are acetylene, benzene, cyclooctatetraene, styrene and 1,2-,
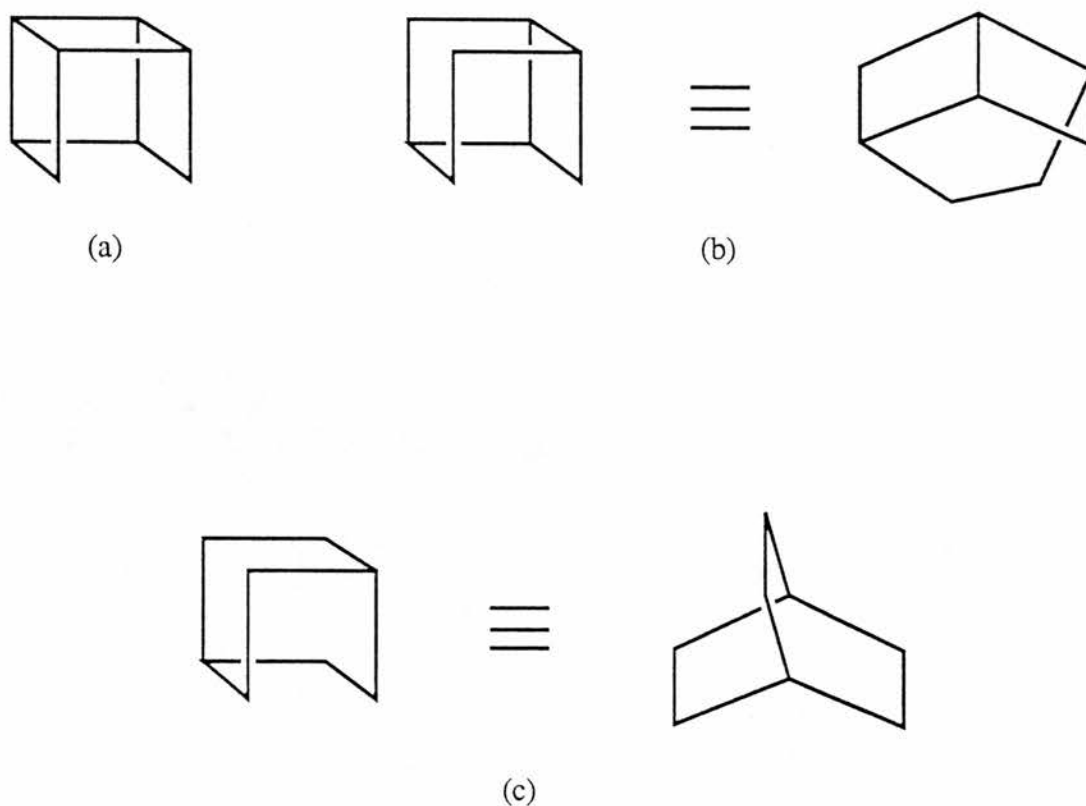
Figure 3.5

(a) Tetracyclo-[4.2.0.0^{2,5}.0^{3,8}]-octane ("secocubane"),

(b) Tricyclo-[4.2.0.0^{4,7}]-octane ("nortwistbrendane"),

(c) Bicyclo-[2.2.2]-octane.

1,4- and 1,5-dihydropentalenes. Benzene and acetylene are the dominant products at low pressures, and cyclooctatetraene predominates at high pressures.

In solution at 200°C cubane is converted, albeit very slowly, to cyclooctatetraene[34], via cuneane and semibullvalene. It is not known whether this slow thermolysis (*ca.* two weeks) proceeds uncatalysed or if it requires traces of transition metal ions. It is known however, that transition metal ions (such as Ag$^+$, Pd^{2+}, and Rh$^+$)[35-37] at high concentrations, induce very rapid ring opening and/or rearrangement reactions (Figure 3.6). The reason for this innate stability is probably the lack of symmetry allowed pathways for ring opening of the cubane structure itself,

whereas substituents and/or reagents (such as metal ions) open other pathways for the system to rearrange.
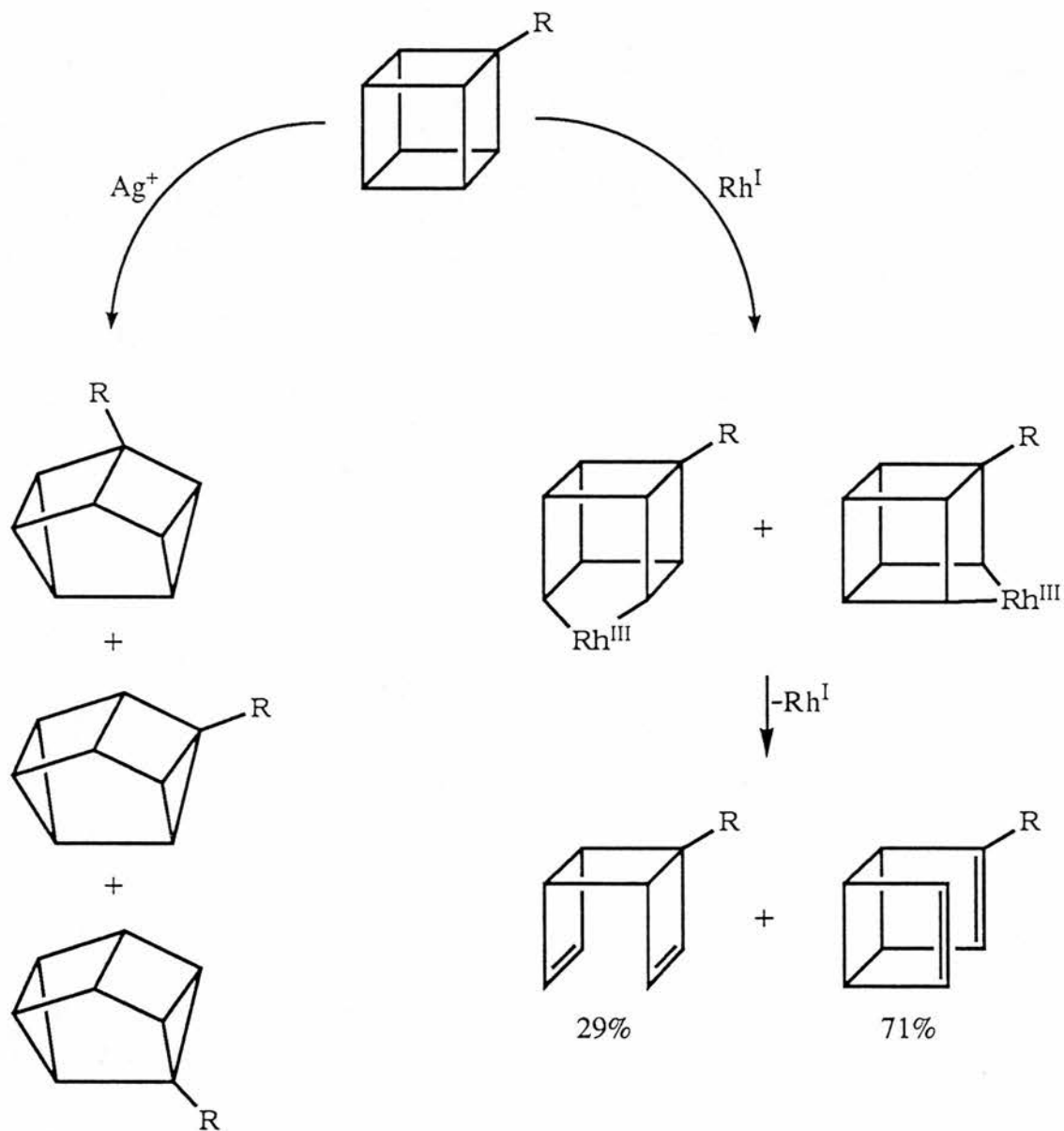
Figure 3.6

Argentiation induces rearrangement to cuneane[35]

(Palladium (II) behaves in a similar way[36]). Rhodium (I)

triggers opening of the cubic frame to the *syn*-tricyclooctadiene system[37].

78

Direct substitution and functionalisation of the cube itself was mentioned in Section 3.1. The cubane functionality is converted into other substituents by the use of a whole range of more or less standard synthetic techniques[19,20,38-43].

3.3 Physical Studies

The physical aspects of the chemistry of cubanes have been thoroughly investigated. The crystal structure[44], thermochemistry[27], carbon hybridisation[45], kinetic acidity[46], NMR spectra[38b,47], photoelectron spectrum[48], far UV, IR and Raman spectra[49], appearance potentials[27,50], valence isomerisations[36,37], electrochemical oxidation[35], and transmission of substituent effects[51,52] have all been examined.

The s-character of the carbon bonding orbital has been correlated to the one-bond bridgehead carbon-proton couplings $^1J(^{13}C\text{-}H)$ for polycyclic hydrocarbons[45]. This correlation accords with to the empirical relationship described by Muller and Pritchard[53]:

$$\% \text{ s-character} = \frac{J(^{13}C\text{-}H)}{5}$$

Della *et al.* report a $^1J(^{13}C\text{-}H)$ coupling of 153.8 Hz[45], whereas Eaton and Cole measure it as 160.0 Hz[4a], these values producing results of 30.8% and 32.0% respectively for the s-character of the carbon-hydrogen bond. As expected these values are quite high, because the magnitude of the bridgehead carbon-proton couplings grows as the strain at the bridgehead increases. The small size of the cubane bridgehead skeletal angles produces an increase in the p-character of the endocyclic hybrid orbitals (that is the C-C bonds) of the carbon atom, with a corresponding increase in the s-character of the exocyclic hybrid orbital (that is the C-H bond).

Other NMR experiments have been carried out by Farrell and co-workers to examine the substituent effects on the cube[38b,52]. This was accomplished by looking at the magnitudes of the couplings between the cubyl protons of 1,4-disubstituted cubanes (Figure 3.7). The ortho couplings are small, as the cubane H-C-C' bond angles are considerably greater than those in nonfused cyclobutanes[54]. Meta
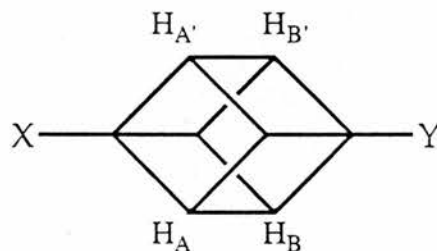
$$J_{AB}, J_{A'B'} = J_{ortho}$$

$$J_{AA'}, J_{BB'} = J_{meta}$$

$$J_{A'B}, J_{AB'} = J_{para}$$

Figure 3.7

couplings are larger than the cross-ring couplings of nonfused cyclobutanes, mainly due to the approximately planar "W" pathways connecting these positions in cubane[55]. Para couplings are unusually large in cubanes, because the cube has the ideal geometry for back-lobe overlap between these positions[38b]. The large effect of substituents in the four position (para) displayed by this is reinforced by the study of the solvolysis of cubyl trifluoromethanesulphonate by Kevill *et al*[56].

3.4   **The Cubyl Cation**

The cubyl cation has the appearance of a most unfavourable species.
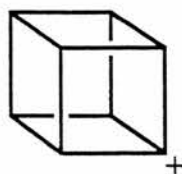
Carbocations prefer to have a planar arrangement, but the geometry of the cation carbon here is far from being planar. The pyramidalisation angle of a planar cation is 0°, whereas if one assumed that the cubane cation had the same geometry as the parent hydrocarbon, it would then have a pyramidalisation angle of 35° [57].

As previously mentioned, the exocyclic orbitals in cubane are rich in s-character (approximately 31 to 32% [4a,45]). Therefore the formation of the cubyl cation would be expected to be difficult, because forming a cation from a hybrid orbital becomes more arduous as the s-character of that orbital increases.

Should the cation be formed, then despite the fact that the vicinal carbon-hydrogen bonds eclipse the empty orbital, hyperconjugation would still require high-energy cubene-like structures.[58] Thus stabilisation through hyperconjugation is not expected.

Despite all of these indications as to how challenging the generation of a cubyl cation is, there are numerous observed reactions that might involve the intermediacy
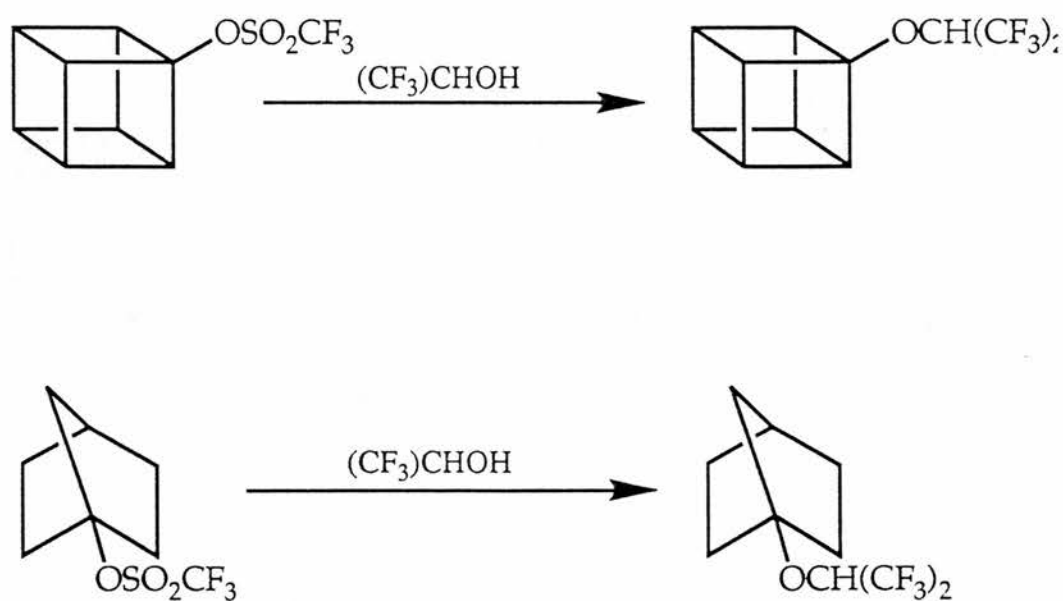
Figure 3.8

Solvolysis of cubyl and norbornyl triflates.

of a cubyl cation, such as the decomposition of cubyl diazonium salts[59], photolytic solvolysis of iodocubanes[23,60] and the solvolysis of cubyl triflates[61]. The latter study shows that cubyl triflate is solvolysed at least 100 000 times faster than the norbornyl triflate, in hexafluoropropan-2-ol (Figure 3.8).

Why should the cubyl cation be more accessible than the 1-norbornyl cation? Several groups have furnished possible answers to this question[61,62]. One such theory is that the delocalisation of the positive charge might occur via interaction with strained cubane carbon-carbon bonds, as resonance hybrids. One example of this, which might be important, is the cyclopropylcarbinyl-cyclobutyl cation system[63].
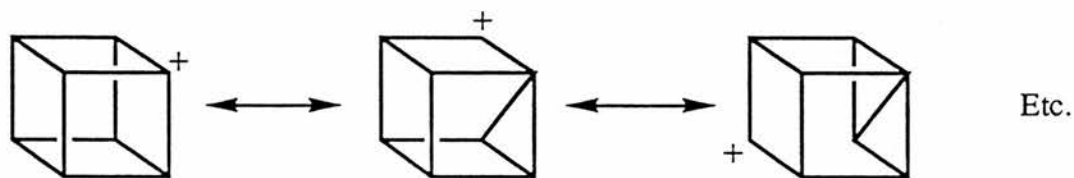
A similar explanation for the solvolysis at 120°C of 4-bromohomocubane in hexafluoropropan-2-ol has been suggested by Ruchardt and co-workers[64].

3.5   The Cubyl Radical

Removing a bridgehead hydrogen atom from the parent hydrocarbon produces the cubyl radical, $C_8H_7 \cdot$. This is a neutral bridgehead species possessing exceptional symmetry. The cubyl radical is of the β-methine category of bridgehead radicals, that is the radical centre is directly bonded to three bridgehead methine groups. Other examples of this type of radical are the dodecahedryl and prismyl radicals.

Spectroscopic and theoretical studies have shown that simple alkyl radicals are not strictly planar, and that the *tert*-butyl radical has a degree of pyramidal character[65-68]. The difference in energy however between the planar and pyramidal forms of the simple carbon free radicals is actually quite small[68]. As a result, for all intents and

purposes the *tert*-butyl radical can be assumed to be planar. In contrast, bridgehead radicals are permanently pyramidal, and can neither undergo inversion nor become planar. Consequently they are expected to be less stable than the corresponding acyclic tertiary radicals.

In this type of radical, the β-carbons of the bridgehead are "held back" and constrained by the cage structure, leaving the radical centre sterically uncongested. This leaves the radical more vulnerable and thus increases its reactivity. This pyramidal arrangement of the radical centre ensures that the SOMO is a σ-orbital with a high s-character. In addition, the orientation of the SOMO with respect to the other bonds in the cubyl radical is different from that of nearly planar alkyl radicals, which will affect the unimolecular reactions of the radical, such as decomposition and rearrangement. The decomposition rate is slower as a result of the stronger carbon-carbon bonds in the molecule, due to the greater s-character, and from the reduced opportunity for the development of polar character in the transition state in the reactions of these radicals. The redox properties when compared to acyclic tertiary radicals are also expected to be affected by the extent of the s-character, making the cubyl radical more nucleophilic in behaviour. In addition to the orientation of the SOMO relative to the β C-H bond orbitals being less favourable for overlap than in acyclic tertiary radicals, and the rigid structure preventing any rotation improving this, hyperconjugation structures will contain extremely strained double bridgehead alkene
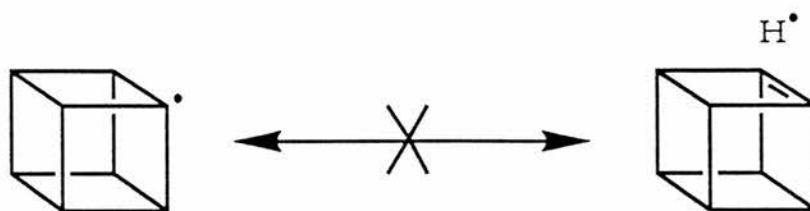
structures. Therefore hyperconjugative structures do not contribute to the stability of the ground electronic state of the cubyl radical.

Cubyl radicals give g-factors the same as those found in other hydrocarbon radicals, but the hyperfine splittings (hfs) produced differ markedly . In comparison with the *tert*-butyl radical, the cubyl radical has much smaller $a(H_\beta)$ values. The β-hydrogen hfs in *tert*-butyl radicals are large (22.9G) due to hyperconjugation, the SOMO and the C_β-H bond orbitals overlap effectively. Thus, although the dihedral angle ϕ (Figure 3.9) for the cubyl radical is zero, implying a favourable overlap and therefore large hfs, hyperconjugation would produce high energy anti-Bredt cubenes. Thus $a(H_\beta)$ is small as there is no hyperconjugation in the cubyl radical. Larger long-
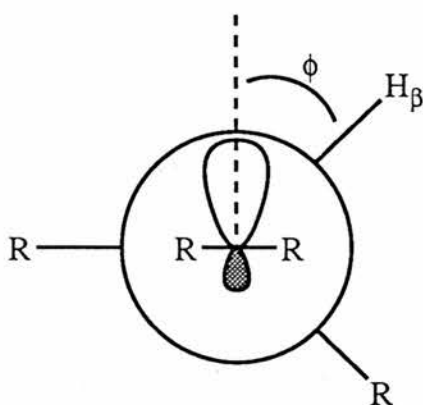
Figure 3.9

range hfs are demonstrated by the cubyl radical, particularly from the 4-position ("para" to the radical centre). One could attribute this to the fact the SOMO, and the orbitals of the C_δ-H bond, are exactly in line and at an angle of 180°. In general bridgehead radicals show a decrease in $a(H_{br})$ as r[C$\cdot$-C_{br}] increases up to approximately 2.1 Å (H_{br} being a bridgehead hydrogen). This decrease is likely to be due to the reduction in the through-space effects with increasing distance, agreeing with evidence showing that through-space effects are unimportant beyond 2.1 Å in radicals[69,70]. The through-bond effect should also diminish as the number of intervening bonds increases. All of this implies that coupling to the δ-hydrogen (which is approximately 2.65 Å from the radical centre[71]) in cubane should not be

large, which is not the case.   So it would appear that there is some orbital arrangement for the cubyl radical which allows a significant amount of spin density to reach the bridgehead δ-hydrogen

The chemistry of bridgehead radicals has been actively investigated[72], the thermal decomposition of the peresters[73,74], with the selectivity of the radicals in halogen atom abstractions[74-76] receiving particular attention.   These halogen atom abstraction studies have revealed that the cubyl radical is much less selective in its reactions than other acyclic and monocyclic aliphatic radicals[76].   The lower steric requirement of the cubyl radical obviously plays an important role in this reduced selectivity[74], this being in agreement with Giese, who indicated that less sterically crowded radicals are usually less selective[77].   Surprisingly though, the least hindered radical, the cubyl radical, shows the greatest selectivity.   This may be as a result of variations in the polar character of the transition state for the halogen transfer, this being less well developed in the halogen atom abstraction reaction of the cubane than, for example, of the adamantane[76].

The cubyl radical and radical cation have been observed directly by ESR, the latter being in a neon matrix at 4K[78].   The cubyl radical and 4-fluorocubyl radical
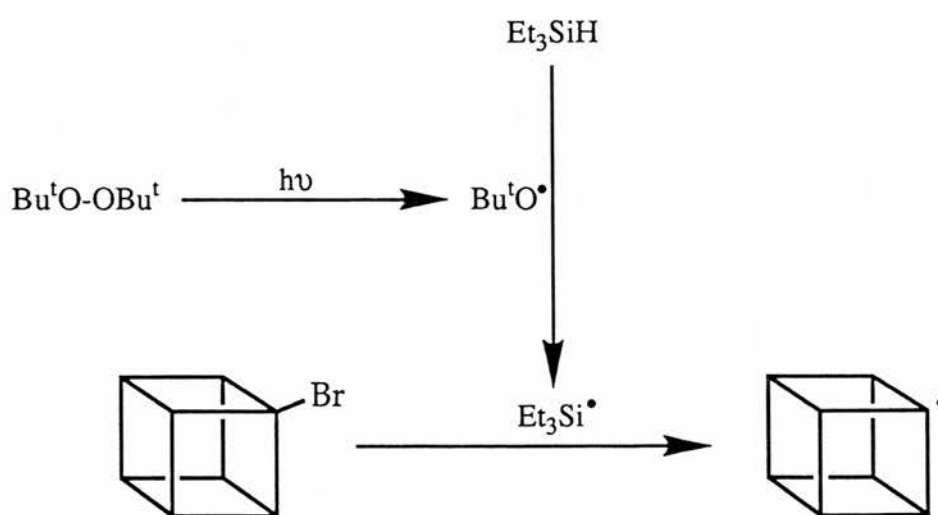
Figure 3.10

were observed by bromine abstraction using triethylsilyl radicals generated in the ESR cavity at 150K[71] (Figure 3.10).   The cubyl radical was also accessed directly by hydrogen abstraction using *tert-* butyl peroxide.   This shows that cubyl carbon-hydrogen bonds are open to homolytic cleavage, agreeing with the study of polyiodination of cubane using *tert*-butyl hypoiodite[79].

Usually free radicals containing three- or four-membered rings readily undergo β-scission under normal solution conditions.   However with cubane this does not appear to be the case.   The cubyl radical, which contains approximately 14 kcal mol^{-1} of strain energy per carbon-carbon bond (compared to *ca.* 6 kcal mol^{-1} per carbon-carbon bond for cyclobutyl) takes part in reactions at temperatures greater than 100°C without rearrangement.   This can easily be explained as β-scission of the cubyl radical would result in the production of a high energy bridgehead alkene.
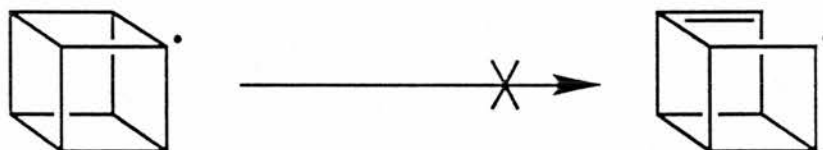
Related to the cubyl system is the cubylcarbinyl system.   The cubylcarbinyl cation is very unstable and undergoes a Wagner-Meerwein 1,2-bond shift very rapidly, even when the cationic carbon is stabilised by two phenyl groups. Rearrangement to the homocubyl system is driven by concomitant release of strain[80] (Figure 3.11).

The cubyl radical however does not rearrange in this manner[81].   The cubylcarbinyl radical was generated by abstraction of bromine from the corresponding bromide using a tin centred radical.   Eaton and Yip proposed that the rearrangement begins with the rupture of a strained cubane bond, producing the methylene secocubyl radical, which is similar to the familiar cleavage of the cyclobutylcarbinyl radical to the pent-4-enyl radical[82].   This is followed by other bond cleavages, as demonstrated in
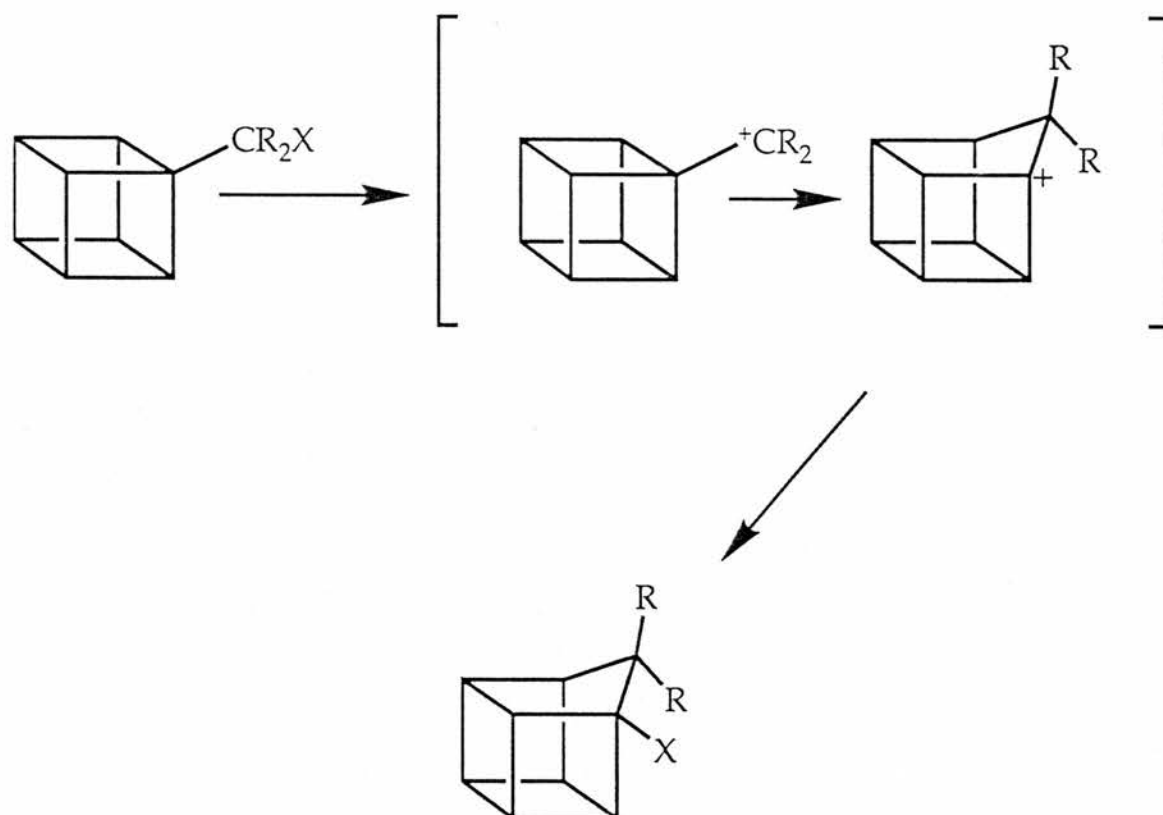
Figure 3.11

Rearrangement of the cubylcarbinyl cation.

Figure 3.12, until the final allylic radical accepts hydrogen from the tri-*n*-butyltin hydride to give the final two olefins. These two products were isolated and characterised by Eaton and Yip[81]. In order to demonstrate the fantastic rate at which the cubylcarbinyl radical rearranges, they attempted to trap the radical using selenophenol, which is known to transfer hydrogen most efficiently[83]. The selenophenol trapped the radical marked A (Figure 3.12), the rate constant for the formation of which was calculated to be about 2.0×10^{10} s^{-1} at 20°C, although this is a lower limit as some of the products were lost to polymerisation[81]. Despite this, the rate of the ring opening of the cubylcarbinyl radical is in excess of two orders of magnitude greater than that of the cyclopropylcarbinyl radical, measured at about 1.0×10^8 s^{-1} [84]. This makes the rearrangement of the cubylcarbinyl radical the fastest known to date.
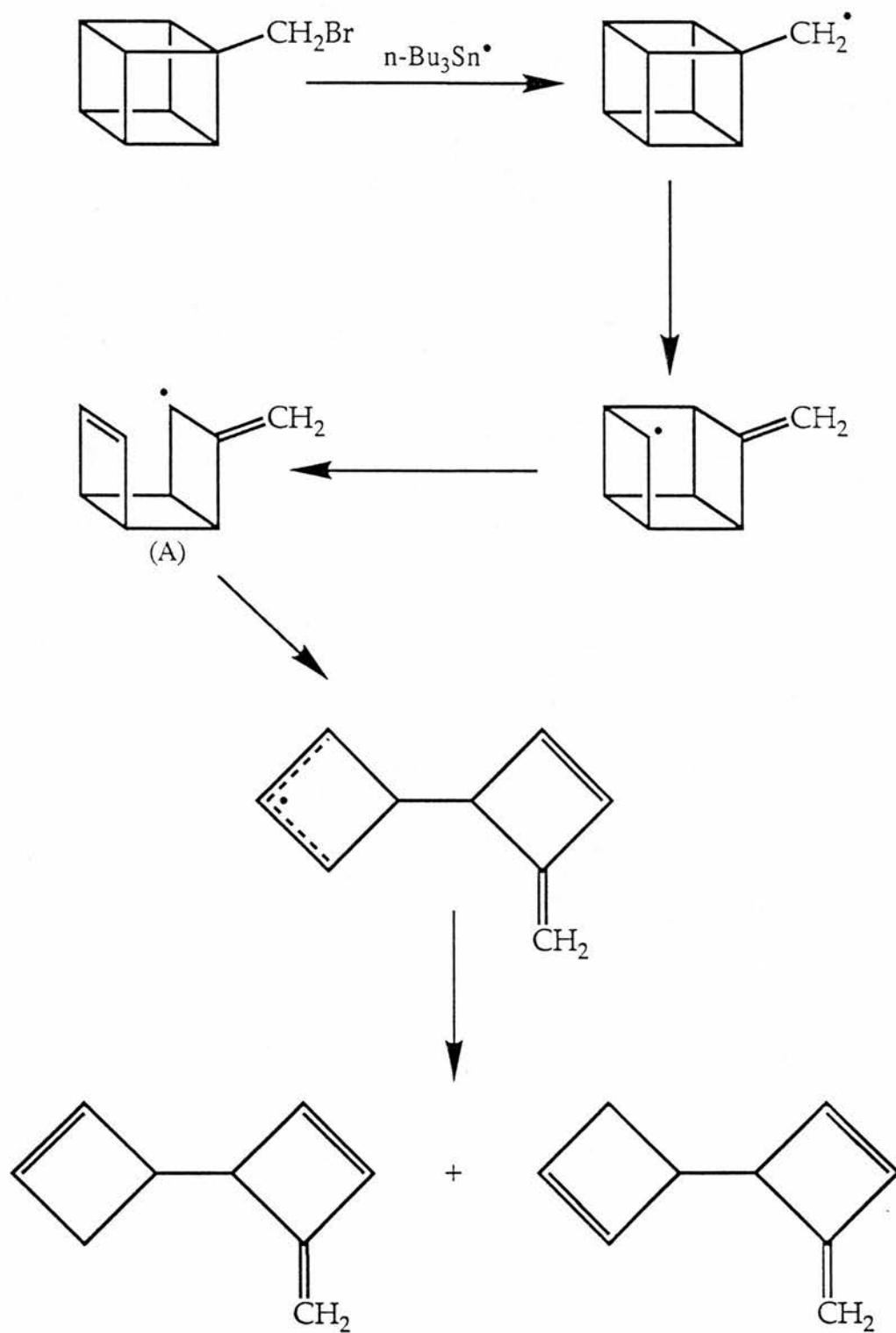
Figure 3.12

Rearrangement of the cubylcarbinyl radical.

Radical A is trapped when selenophenol is employed at high concentration.

Chapter Four

The Cubyl and Cubylcarbinyl Radicals

4.0   **The Preparation of 4-substituted Cubanes**

All of the cubane structures examined in this study were synthesised by Ernest.W. Della and Nick J. Head, our co-workers on this cubane project. The only exception to this was the preparation of the unstable cubylcarbinyl bromide, which was prepared from fresh from the hydroxymethylcubane.

A summary of the preparation of the previously unknown 4-substituted bromocubanes is shown using known methodolgy[85] (Figure 4.1)[86].
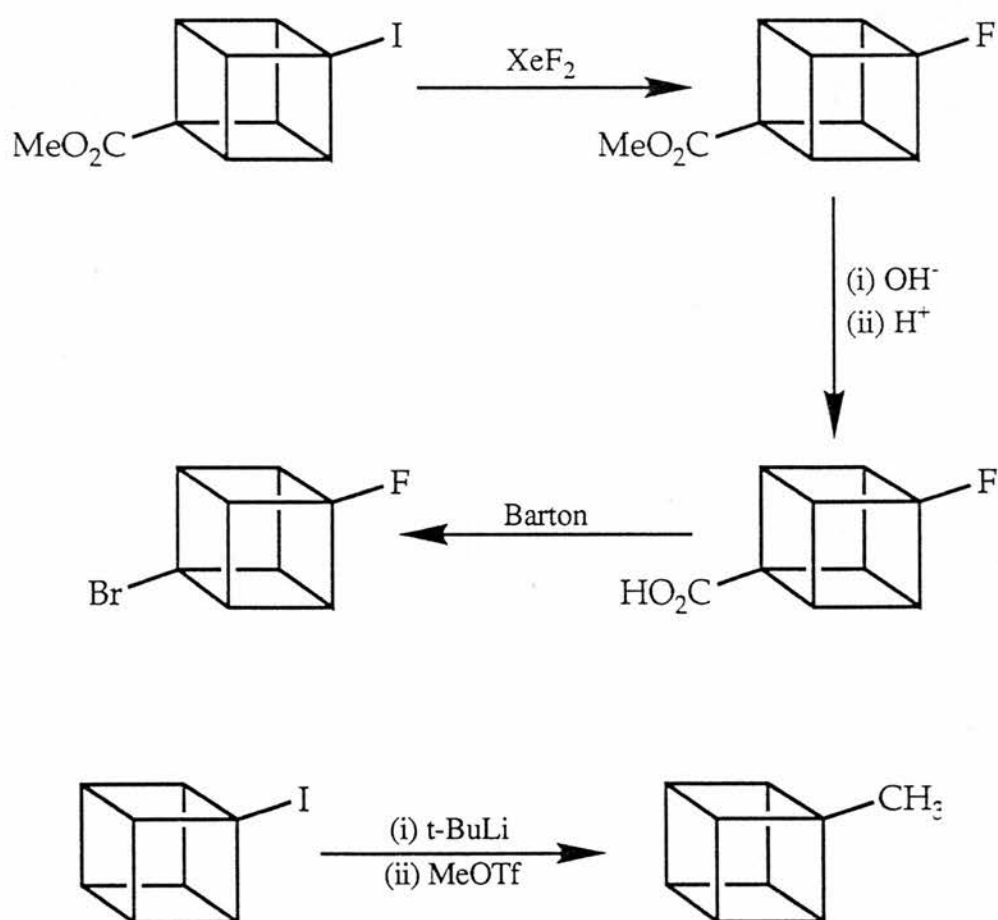
Figure 4.1 continues over the page.
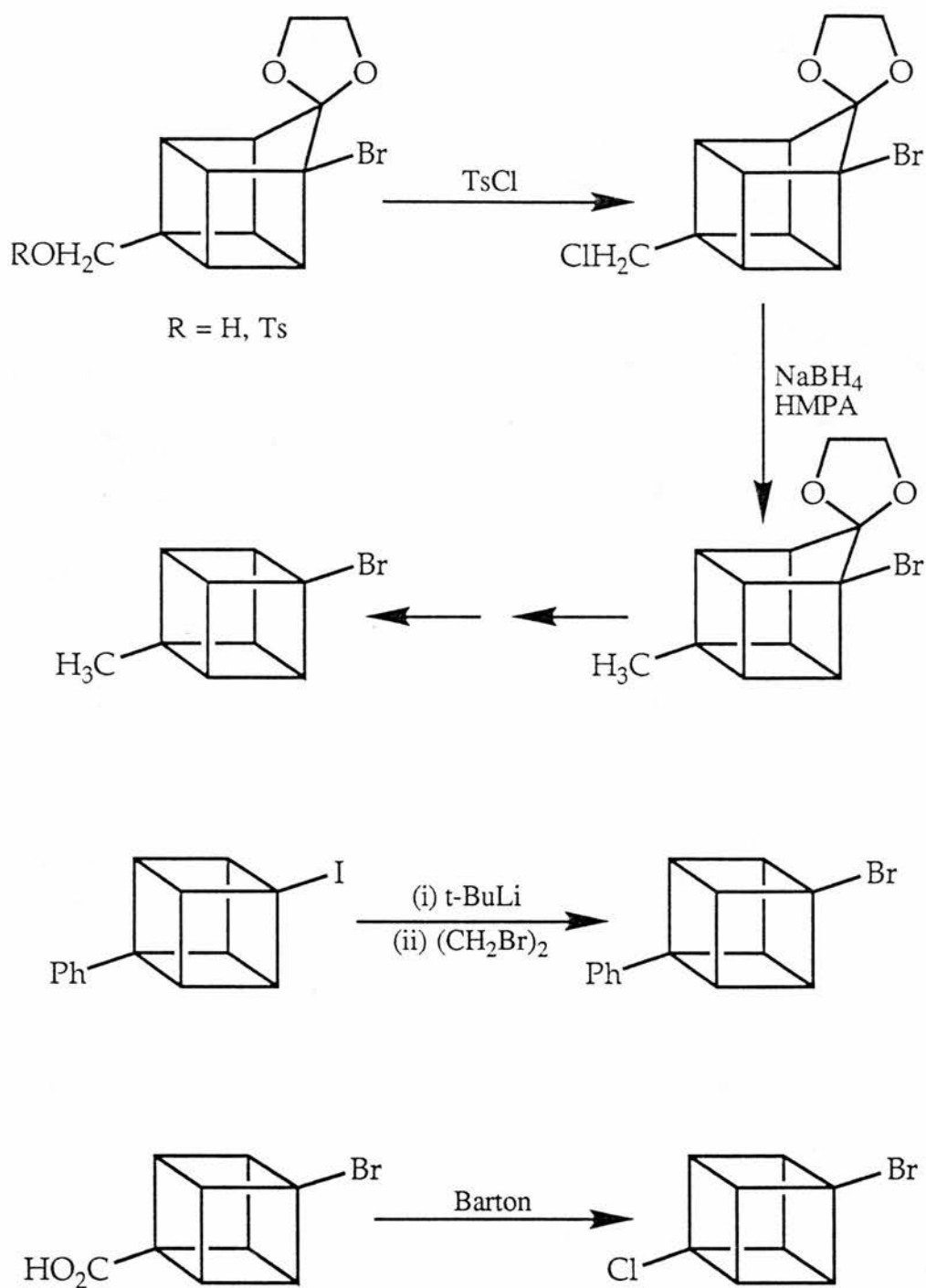
Figure 4.1

A summary of the preparation of the hitherto unknown substituted

cubanes studied.

Hydroxymethylcubane (cubylcarbinol)[87], bromocubane[85b], 1,4-dibromo-

cubane[85b] and methyl 4-bromocubanecarboxylate (4-carbomethoxycubyl bromide)[85b] were all prepared according to known literature procedures.

The compounds thus prepared were >99% pure and fully characterised by ^{1}H and ^{13}C NMR, mass spectral and elemental analysis data[86].

As mentioned in Chapter Three, the cubane skeleton contains about 166 kcal mol^{-1} of strain energy[27,28]. However despite this, the cubyl radical does not rearrange in solution but maintains its structural integrity under a range of conditions. Therefore it does not seem unreasonable to assume that a whole range of substituted cubyl radicals should be observable using EPR spectroscopy.

There are two obvious routes to the cubyl radical; those of hydrogen abstraction and bromine abstraction. To this end both cubyl and bromocubyl derivatives were prepared, as detailed above, and examined by EPR spectroscopy.

4.1   Hydrogen Atom Abstraction from Cubanes

The solvent used for hydrogen abstraction was cyclopropane. The carbon-hydrogen bonds of cyclopropane are strong, with about 32% s-character, so that hydrogen abstraction from this solvent is difficult. The strength of the carbon-hydrogen bonds in cubane has not been measured, but the bond does contain approximately 31 to 32 % s-character[4a,45]. Consequently one would expect the rate of hydrogen abstraction from cubane to be of a similar order of magnitude to that from cyclopropane. Nevertheless, when hydrogen was abstracted from cubane in cyclopropane, using photochemically generated *tert*-butoxyl radicals, the radical concentration ratio [cubyl]/[cyclopropyl] was measured to be 1.7, at -90°C. From this it can be seen that the k_H(cubyl)/k_H(cyclopropyl) $\geq$ 26 (or $\geq$ 19.5 on statistical correction), where k_H is the rate constant for the abstraction of hydrogen from each hydrocarbon by *tert*-butoxyl radicals, that is

$$t\text{-BuO}^\bullet + \text{R-H} \xrightarrow{ k_H } t\text{-BuOH} + \text{R}^\bullet$$
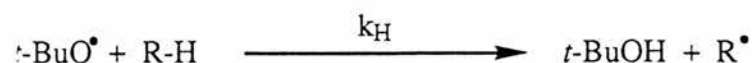
This result is a lower limit, as some of the cubane had crystalised out at -90°C. This higher rate constant for the abstraction of hydrogen from cubane demonstrates that the carbon-hydrogen bond dissociation energy in cubane may actually be less than that of cyclopropane (106.3 kcal mol^{-1})[88], and not as similar as was first suggested by the comparable s-characters of these bonds in cubane and cyclopropane.

Following this, it seemed that the abstraction of a primary hydrogen should be compared with that of a cubyl hydrogen. With this in mind methylcubane was examined.

The EPR spectrum from methylcubane was obtained by photolysing a solution of methylcubane and di-*tert*-butyl peroxide in cyclopropane at -120°C. The spectrum thus acquired is shown in Figure 4.2 (upper spectrum).

From the spectrum it can be seen that no cyclopropyl radicals are formed, as was found when hydrogen was abstracted from cubane in this manner[71]. It is also apparent that no cubylcarbinyl radicals, nor any of the species which this rearranges into are present (Section 4.3), as would be the case if a hydrogen had been abstracted from the methyl group. Thus the circumstantial evidence implies that it is a cubyl hydrogen which has in fact been removed. By comparing this spectrum with that obtained by the abstraction of a bromine atom from 4-methylcubyl bromide (Section 4.2), the 4-methylcubyl radical can readily be identified. Therefore it appears that hydrogen abstraction from methylcubane results in a mixture of radicals. It also seems reasonable that as the cubyl hydrogen in the 4-position is removed, the other cubyl hydrogens may also be abstracted, and that this radical mixture is in actual fact made up of the three methylcubyl radicals: 2-methyl-, 3-methyl- and 4-methyl-cubyl radicals (Figure 4.3).

In order to prove this, these three radicals were simulated using the hfs from the 4-methylcubyl radical as a guide (section 4.2). Many different sets of hfs and relative radical concentrations were used until a good fit was produced. This was achieved with the hfs displayed in Table 4.1 and with the radical concentrations in the
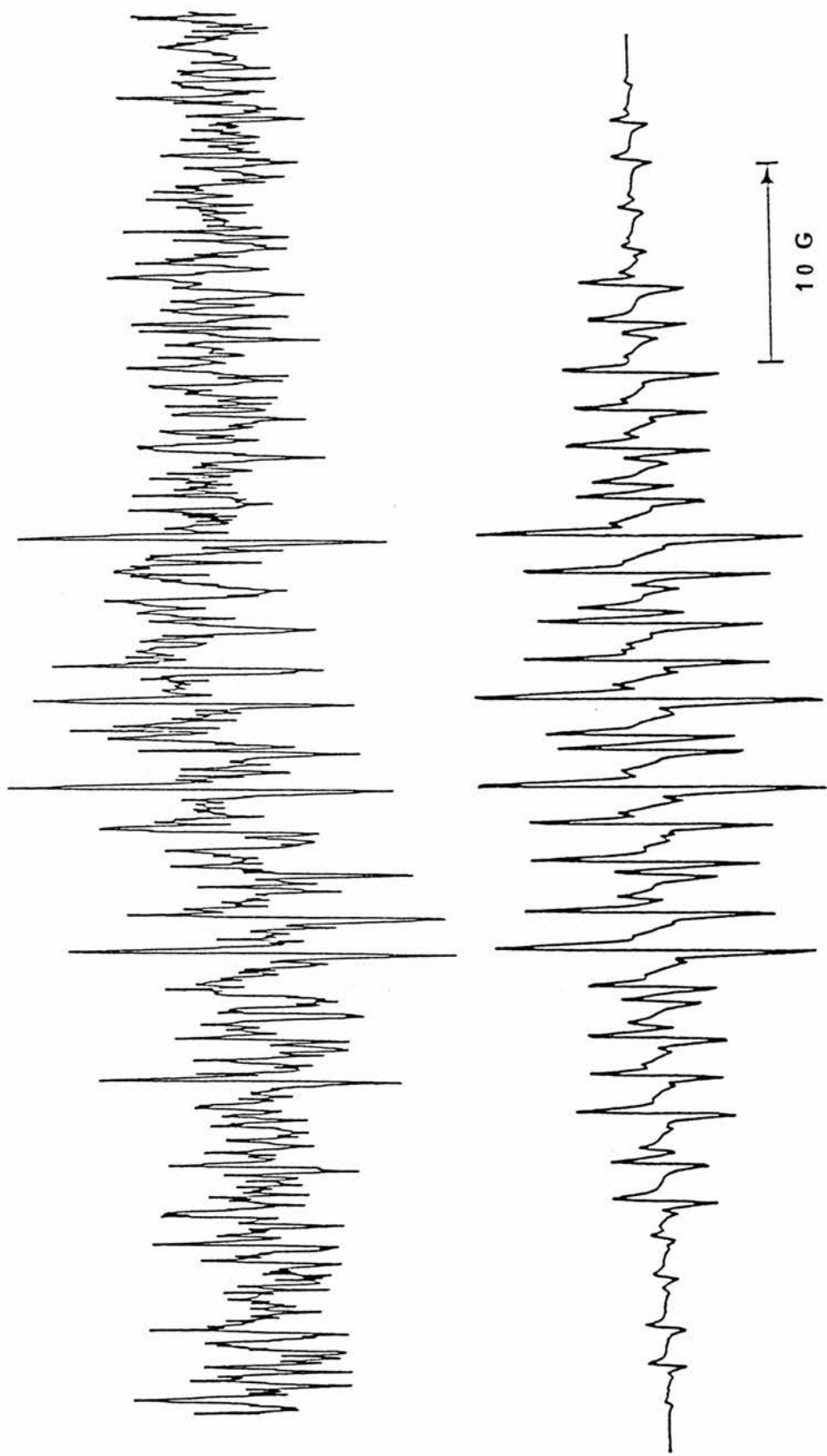
Figure 4.2

Upper: 9.3 GHz EPR spectrum obtained by hydrogen abstraction, with *t*-butoxyl radicals, from methylcubane in cyclopropane at -120°C.

Lower: The simulation of the upper spectrum comprising of the 2-methyl-, 3-methyl- and 4-methyl-cubyl radical in the ratio 3:3:1 respectively.
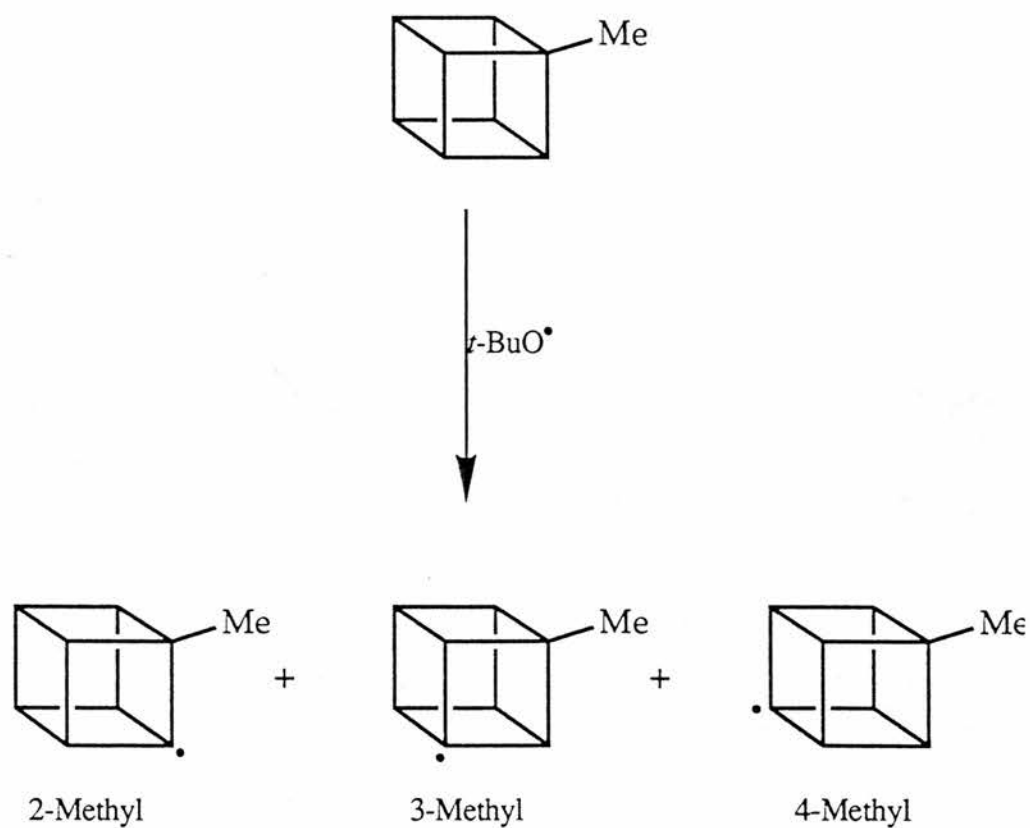
Figure 4.3

Preparation of the 2-, 3- and 4-methylcubyl radicals.

ratio expected if the hydrogens were abstracted statistically. That is, three 2-methylcubyl radicals to three 3-methylcubyl radicals to one 4-methylcubyl radical, as

Radical	$a(H_\beta)$	$a(H_\gamma)$	$a(H_\delta)$	$a(CH_3)$
4-Methyl	12.3 (3H)	7.9 (3H)	---	0.18
3-Methyl	12.4 (3H)	8.0 (2H)	6.3	1.85
2-Methyl	12.4 (2H)	8.0 (3H)	6.3	2.4

Table 4.1

EPR parameters of the methylcubyl radicals.

hfs in G, g-factors 2.0027 ± 0.001.

there are three hydrogens in the 2-position, three in the 3-position and only one in the 4-position. The simulations of the individual radicals are shown in Figure 4.4, with the simulation of the mixture in the 3:3:1 ratio, which is also displayed in Figure 4.2 for direct comparison with the observed spectrum.

It is probable that the radical with the largest $a(CH_3)$ is the 2-methylcubyl radical and furthermore that, due to the differing numbers of β–hydrogens, H(2,6,8), and γ- hydrogens, H(3,5,7), between the 2-methyl- and 3-methyl-cubyl radicals, the 12.4G hfs ought to be assigned to the β-hydrogens and the 8.0G hfs to the γ-hydrogens. These assignments are in agreement with the conclusions drawn by Michl[89].

That the *tert*-butoxyl radicals abstract the cubyl hydrogens in preference to the methyl hydrogens is quite surprising. The bond dissociation energy for the methyl hydrogens in ethane is 100.5 kcal mol^{-1} [90] and, based on the knowledge that the bond dissociation energy for the methyl hydrogens in methylcyclopropane is actually lower by 2 to 3 kcal mol^{-1} than those of primary hydrogens[91], one might then expect a value in this region for the methyl hydrogens of methylcubane. Despite this the experimental observations point towards a cubane carbon-hydrogen bond dissociation energy of much less than this. Yet a recent ab-initio calculation with a 6-31G* basis set predicted that the formation of the cubyl radical from cubane would only require 11.0 kcal mol^{-1} more energy than formation of the *tert*-butyl radical from 2-methylpropane[62] would need. Taking the experimental value of $DH^o(Me_3C-H)$[89] of 95.9 kcal mol^{-1}, one can combine it with the ab-initio result to produce a value for $DH^o(cubyl-H)$ of 106.9 kcal mol^{-1}, which is much greater than that suggested by the simple interpretation of the methylcubane result.

Hydrogen abstraction by *tert*-butoxyl radicals was also attempted from 1,4-dicarbomethoxycubane, 1,4-dibromocubane and 4-methylcubyl bromide (Figure 4.5). In all three cases the only radicals detected, with cyclopropane as solvent, were cyclopropyl radicals (Figure 4.6). When dichloro-difluoromethane was used as the solvent, no radicals whatsoever were detected in the temperature range -130 to -70°C.
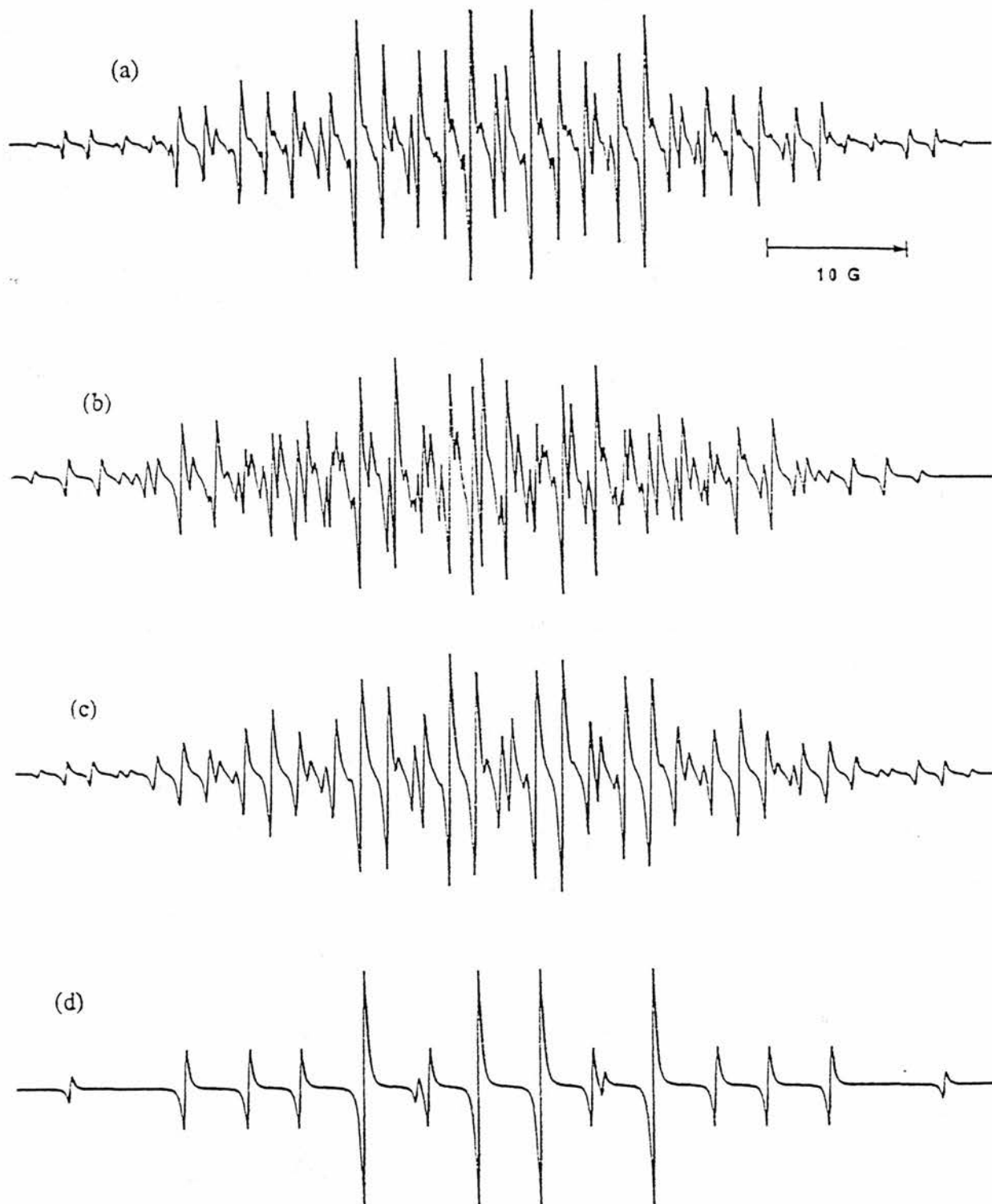
Figure 4.4

(a) The simulation of the 3:3:1 mixture of 2-methyl-,3-methyl- and 4-methylcubyl radicals, as shown in Figure 4.2 (lower).   (b), (c) and (d) Simulations of the 2-methyl- (b), 3-methyl- (c) and 4methyl- (d) cubyl radicals.

Also when neat di-*tert*-butyl peroxide at -40°C was used, no interpretable spectra were obtained. It would appear therefore that electron-withdrawing groups, such as bromine and carbomethoxy groups, deactivate the cube to hydrogen abstraction.
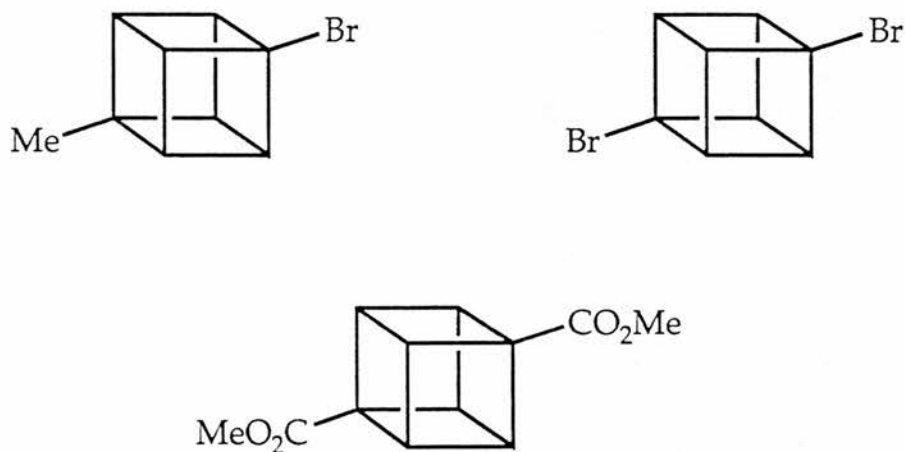
Figure 4.5

4-Methylcubyl Bromide, 1,4-Dibromocubane and

1,4-Dicarbomethoxycubane.

Therefore, from this data it can be said that no cyclopropyl radicals are observed in the methylcubane case, but with cubane itself, the k_H(methylcubane) > k_H(cubane). In addition, because only cyclopropyl radicals were observed in the three cases where electron-withdrawing substituents were on the cube, then k_H(cubane) > k_H(cubyl-A), where A represents an electron-withdrawing substituent.

So by simple interpretation of the idea of the relation between *tert*-butoxyl hydrogen abstraction rate data and carbon-hydrogen bond dissociation energies, one could say that,

$$k_H(\text{Cubyl-Me}) > k_H(\text{Cubyl-H}) > k_H(\text{Cubyl-A})$$
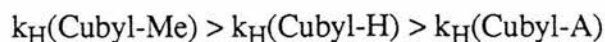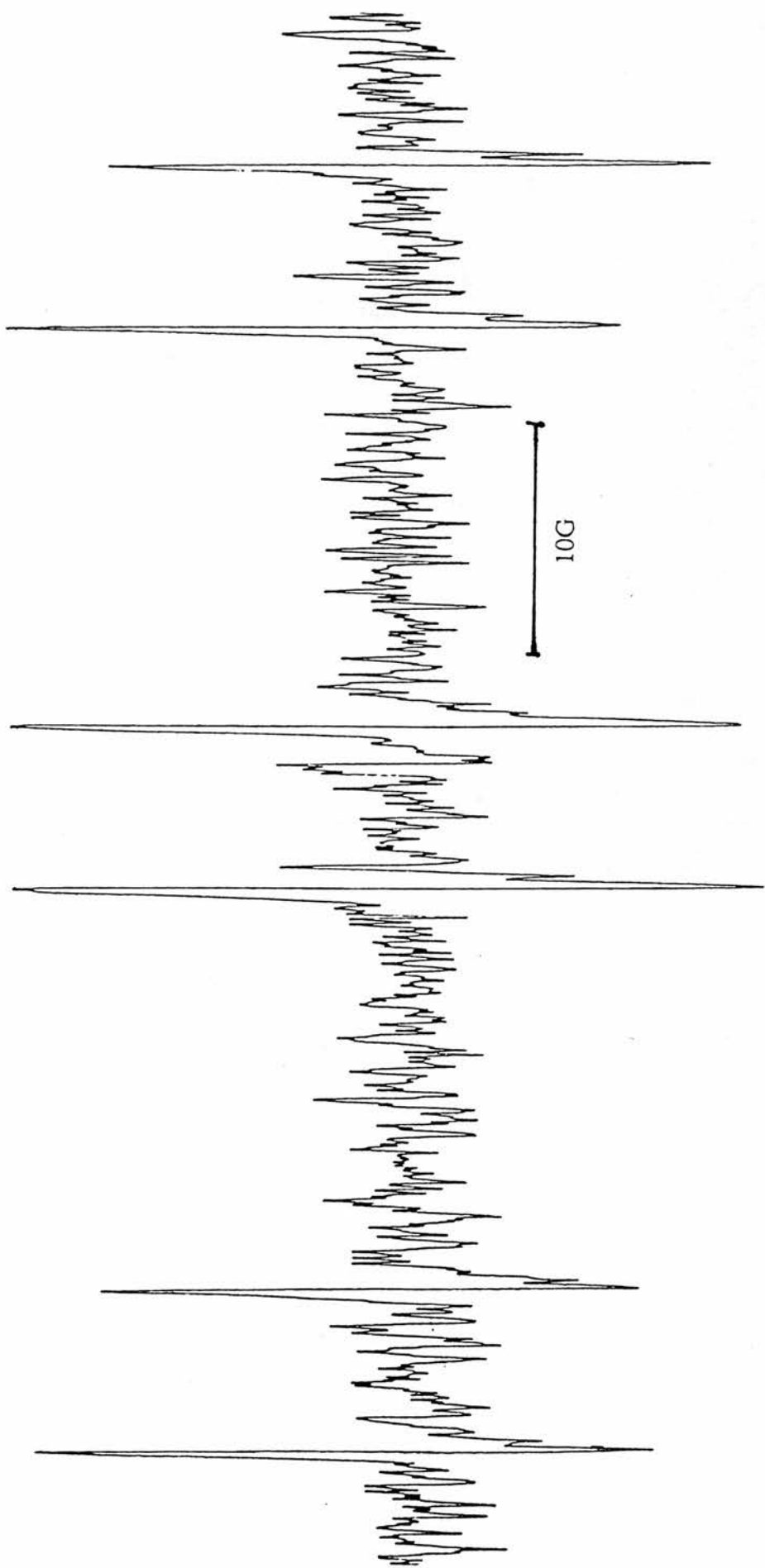
Figure 4.6

9.3 GHz EPR spectrum (the central region only) of cyclopropyl radicals formed by hydrogen abstraction from cyclopropane with *t*-butoxyl radicals at -120°C.

98

4.2   Bromine Atom Abstraction from Cubanes

The generation of cubyl and 4-fluorocubyl radicals from their corresponding bromides has already been reported[71]. Both photochemically produced trimethyltin and triethylsilyl radicals were used, but the former produced no EPR signals which could be attributed to the cubyl system. As a result of this we favoured the use of triethylsilyl radicals (produced by hydrogen abstraction from triethylsilane with photochemically generated *tert*-butoxyl radicals) to abstract bromine atoms from the compounds examined. Again the solvent used was cyclopropane, as this behaves well at the temperature range at which these radicals are observed.

The cubane compounds examined by bromine abstraction, and discussed in this section, are shown in Figure 4.7, with the EPR spectra of the corresponding radicals being displayed at the end of this section (Figures 4.13 to 4.17). With the exception of the 4-carbomethoxycubyl radical (Figure 4.14), all of the EPR spectra degraded quite quickly, and no radicals, without exception, were observed when trimethyltin radicals were used as the bromine abstracting species.

The hfs for these radicals are displayed in Table 4.2. The cubyl and 4-fluorocubyl radicals produce well-defined hfs from the δ-hydrogen and δ-fluorine atoms respectively[92]. The δ-^{35}Cl hfs of the 4-chlorocubyl radical is also easily discernible (Figure 4.13) this probably being the longest range chlorine hfs resolved to date, although the spectra were too weak for the hfs of the ^{37}Cl isotope to be distinguished. Under high resolution conditions the small hfs from the ε-hydrogens of the methyl group in the 4-methylcubyl radical were also visible (Figure 4.15). The spectra of the 4-phenylcubyl and 4-bromocubyl radicals (Figures 4.16 and 4.17 respectively) were extremely weak, making only a tentative analysis of the EPR spectrum of the latter possible.

Previously, in the cases of the cubyl and 4-fluorocubyl radicals, the larger quartet hfs had been assigned to the γ-hydrogens and the smaller quartet hfs to the β-hydrogens, because semi-empirical INDO and AM1 SCF-MO calculations predicted larger spin densities at the γ-hydrogens[71]. Recently however, Michl and co-workers

Bromocubane[92]

4-Fluorocubyl Bromide[92]

4-Chlorocubyl Bromide

4-Methylcubyl Bromide

4-Phenylcubyl Bromide

1,4-Dibromocubane

4-Carbomethoxycubyl Bromide
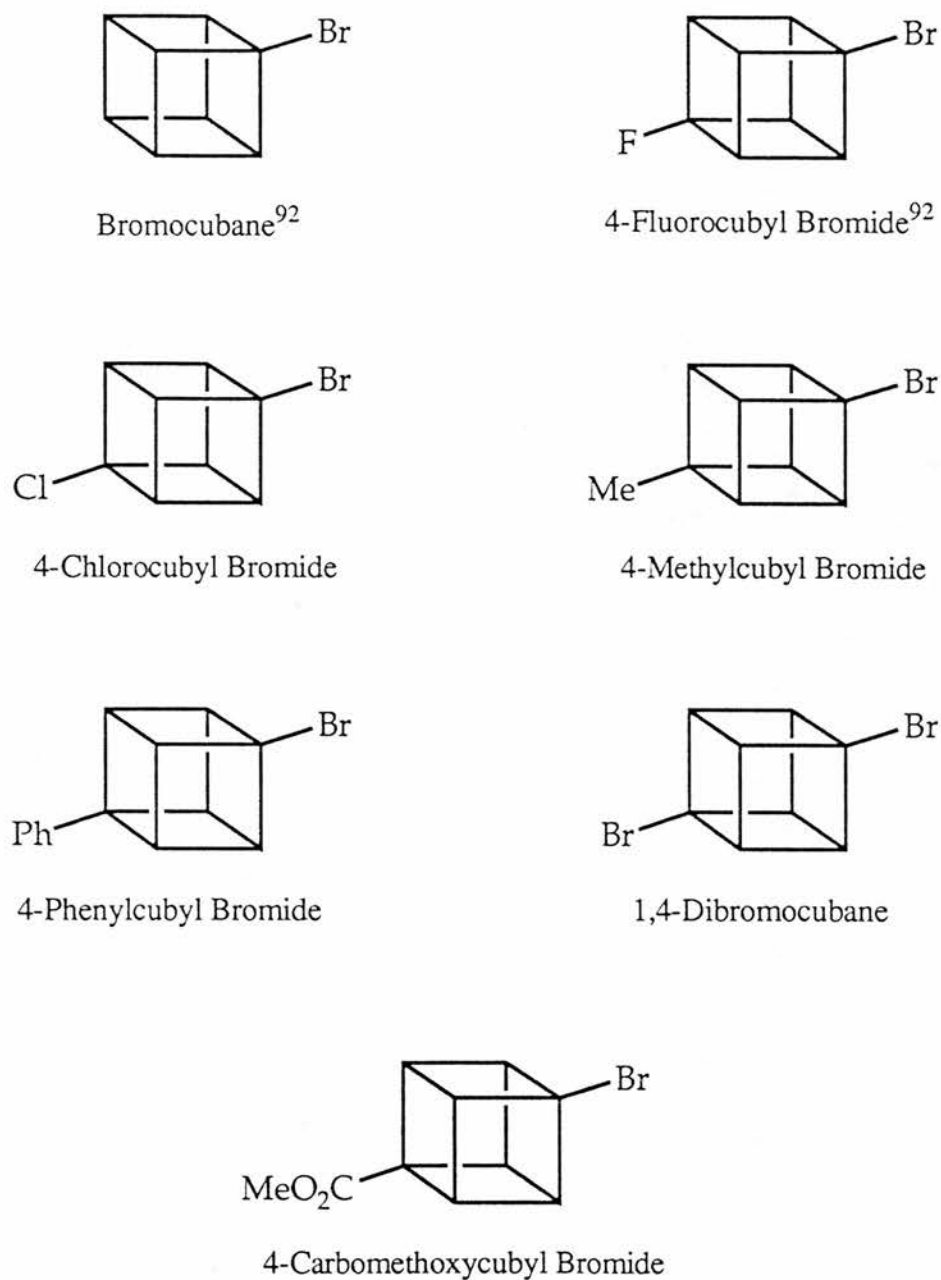
Figure 4.7

The 4-substituted cubanes examined by EPR.

demonstrated that spectra of deuterium labelled cubyl radicals imply the reverse assignment[89], the results with 2-methylcubyl and 3-methylcubyl radicals being in agreement and confirming this (Section 4.1). Therefore, this recent information has been taken into account and the hfs assigned accordingly. It should be pointed out that the small size of the β-hydrogen hfs indicates that, as was expected,

100

hyperconjugation is unimportant in cubyl radicals.

Radical	$a(3H_\beta)$[a]	$a(3H_\gamma)$[b]	a(other)
4-H	12.4	8.2	6.3 (H_δ)
4-Fluoro	10.8	6.2	29.1 (F)
4-Chloro	10.9	7.0	4.3 (^{35}Cl)
4-Bromo	*12.2*[c]	*8.0*[c]	----
4-Methyl	12.3	7.9	0.18 (CH$_3$)
4-Phenyl	12.2	7.7	----
4-Carbomethoxy	12.3	7.8	----

Table 4.2

EPR parameters of cubyl and 4-substituted cubyl radicals.

In cyclopropane at -120°C, hfs in G, g-factors 2.0027 ± 0.001

[a]H(2,6,8), [b]H(3,5,7), [c]Tentative values.

As can be seen from Table 4.2, the variations in the magnitude of the β-hydrogen and γ-hydrogen hfs are really quite small as the substituent at the 4-position is changed, and there is no discernible trend to these hfs changes. Also, neither the β-hydrogen nor the γ-hydrogen hfs correlate with the σ_p, σ_I, or $\sigma\cdot$ parameters of their corresponding 4-substituents. AM1 calculations failed to provide an explanation of the hfs variations in terms of the computed spin density changes or structural changes as the 4-substituent was varied. However this is not surprising when one takes into account the inability of the semi-empirical SCF-MO methods to correctly order the spin densities at the β-carbon and γ-carbon atoms. In addition, this type of computation is an extremely severe test of the computational methods as it involves open shell species containing highly strained four-membered rings and bridgehead carbon atoms, taking AM1 well beyond the limits of its parameterisation.

Initially all of the EPR spectra showed the presence of a second radical in addition to the expected cubyl radicals. Based on information built up from several spectra, this second radical was eventually identified as the 1-(diethylsilyl)-ethyl radical, with the spectrum being assigned as follows: $a(3H)=25.5G$, $a(1H)=20.4G$ and $a(1H)=12.0G$ (Figure 4.18). On reduction of the amount of triethylsilane used in the EPR samples, the concentration of the 1-(diethylsilyl)-ethyl radical also decreased. In this way spectra of the cubyl radicals were obtained which were almost completely free of this interference. The formation of this radical is surprising. Usually carbon-centred radicals, with various cyclopropyl radicals[93] among them, selectively abstract the weakly bound silyl hydrogen in preference to the secondary hydrogens of the ethyl group to produce the triethylsilyl radical. This latter radical, $Et_3Si\cdot$, is not usually detected by EPR spectroscopy when an organic bromide is present as its stationary concentration is kept below the detection limit of the spectrometer by its rapid abstraction of bromine from the organic bromide. In the
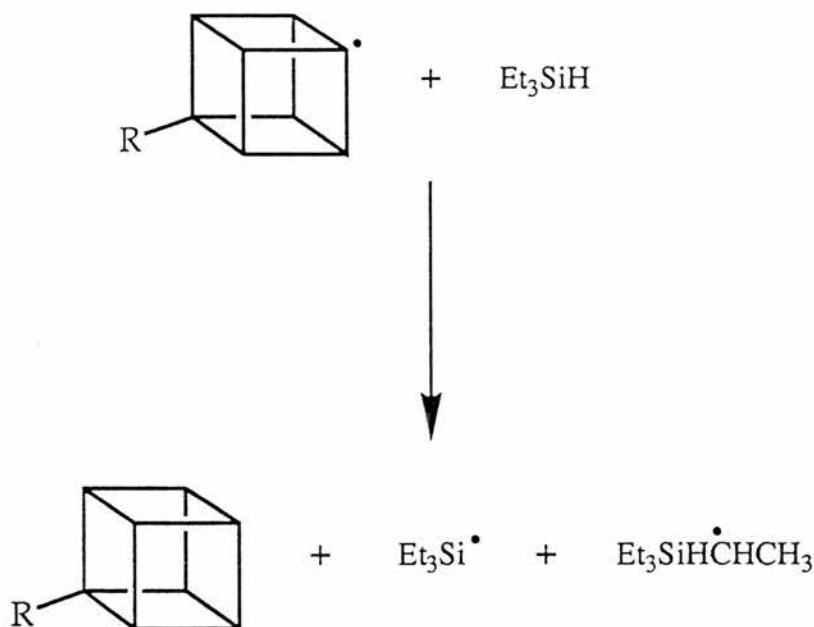
Figure 4.8

Competitive abstraction of secondary ethyl hydrogens and silyl hydrogens from triethylsilane by cubyl radicals.

absence of an organic bromide however this radical can be observed[94]. Thus it would appear that cubyl radicals abstract a secondary hydrogen from the ethyl groups of triethylsilane in competition with the abstraction of the silyl hydrogen (Figure 4.8). Trialkylsilyl groups are known to act as electron-attractors in free radical reactions[95], and one could interpret the formation of the 1-(diethylsilyl)-ethyl radical as indicating that cubyl radicals are strongly nucleophilic, the transition state for hydrogen atom abstraction being stabilised by structures such as

$$\overset{\delta-}{Et_3(H)Si(Me)CH} - - - - \overset{\delta+}{H} - - -\overset{\delta-}{\text{(cubyl)}}$$
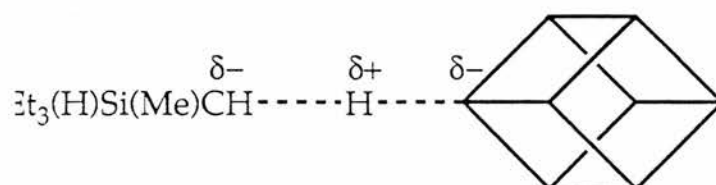
Alternatively, the production of the 1-(diethylsilyl)-ethyl radical may simply be a result of the high reactivity and low selectivity of the cubyl radical in comparison with alkyl radicals[76].

When the photolysis beam was shuttered, most of the cubyl radicals examined decayed within the response time of the spectrometer, that is the radical lifetimes were less than about 10^{-3} seconds. However, four radicals had sufficiently strong EPR signals for the exponent of the light intensity n to be determined by measuring the change in signal height on attenuating the light beam with calibrated gauzes. The signal height and light intensity data with their logarithms for the 4-methylcubyl and 4-carbomethoxycubyl radicals are displayed in Tables 4.3 and 4.4, with their corresponding graphs in Figures 4.9 and 4.10. The accuracy was limited due to the rapid degradation of the spectra, but the values of the exponent of the light intensity obtained are noted in Table 4.5. These experimental exponents only marginally exceed the theoretical value of 0.5 for second-order processes. Disproportionation involving two cubyl radicals can probably be ruled out as this would involve the formation of the unstable bridgehead cubene[58]. On the other hand dimerisation

EPR Peak Height / m	$\log_{10}$ (peak height)	Relative Light Intensity (I)	$\log_{10}$ I
0.127	-0.896	1.00	0.000
0.090	-1.046	0.59	-0.229
0.074	-1.131	0.42	-0.377
0.064	-1.194	0.32	-0.495

Table 4.3

EPR peak height data at various light intensities for the

4-methylcubyl radical.
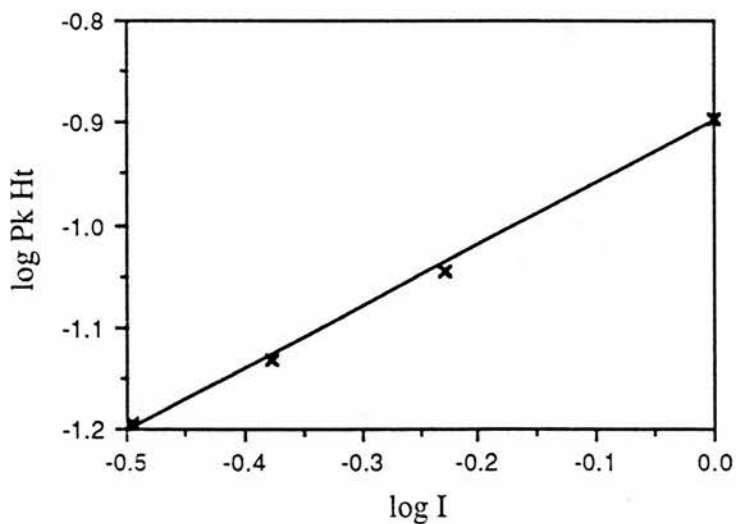
Figure 4.9

The graph of log EPR peak height against log light intensity for

the 4-methylcubyl radical.

EPR Peak Height / m		$\log_{10}$ (peak height)		Light Intensity	$\log_{10}$
Run 1	Run 2	Run 1	Run 2	(I)	I
0.2180	0.2155	-0.661	-0.667	1.00	0.000
0.1625	0.1740	-0.789	-0.759	0.59	-0.229
0.1340	0.1440	-0.873	-0.842	0.42	-0.377
0.1210	0.1170	-0.917	-0.932	0.32	-0.495

Table 4.4

EPR peak height data at various light intensities for the

4-carbomethoxycubyl radical.
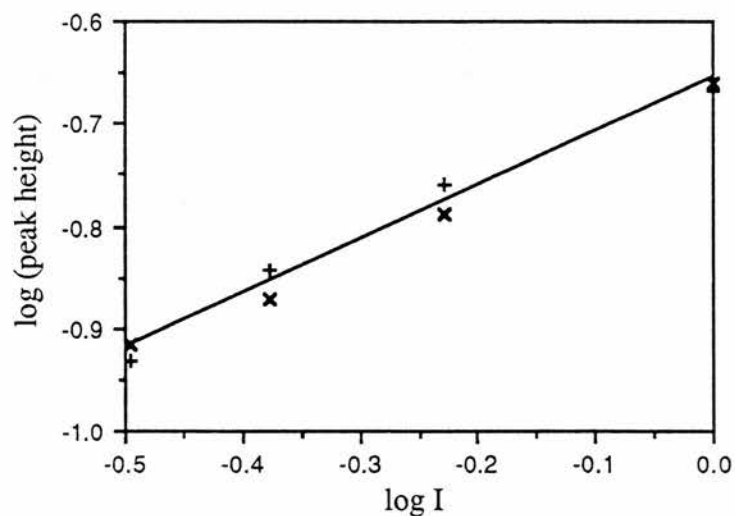
Figure 4.10

The graph of log EPR peak height against log light intensity for the

4-carbomethoxycubyl radical.

Radical	Exponent of Light Intensity
Cubyl	0.57 ± 0.20
4-Fluorocubyl	0.60 ± 0.25
4-Methylcubyl	0.60 ± 0.05
4-Carbomethoxycubyl	0.53 ± 0.05

Table 4.5

The exponent of light intensity for four cubyl radicals.

producing cubylcubanes is likely to be the dominant termination procedure (Figure 4.11). There is also the possibility that cross-combination and cross-disproportionation with other radicals may contribute to the termination of the cubyl radical (Figure 4.12).
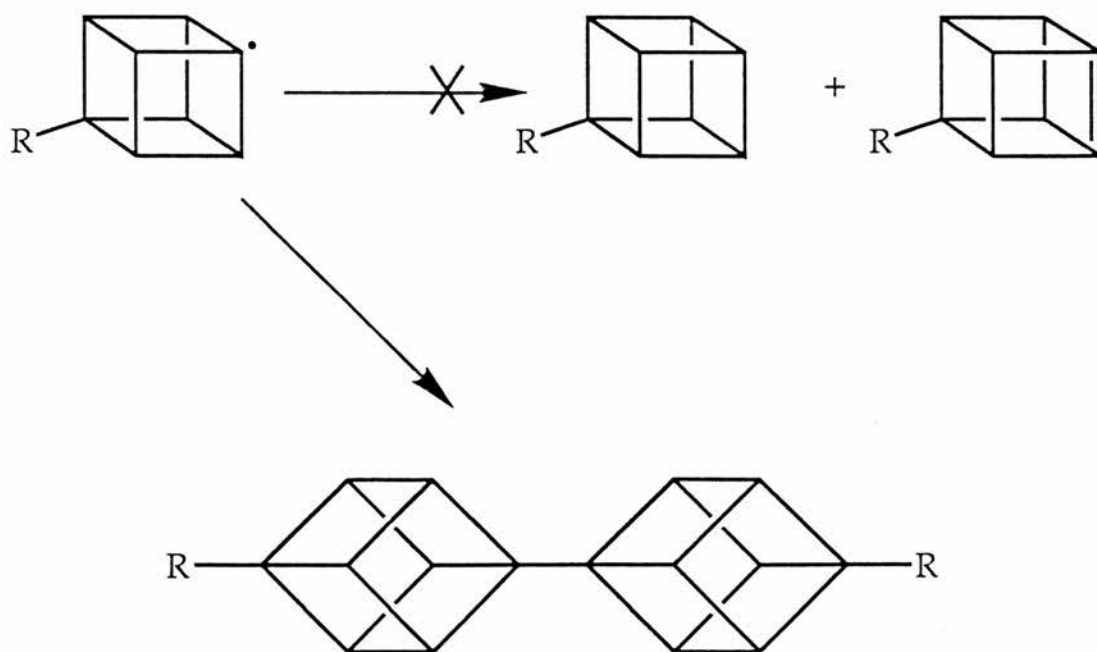
Figure 4.11

The second order termination of cubyl radicals.
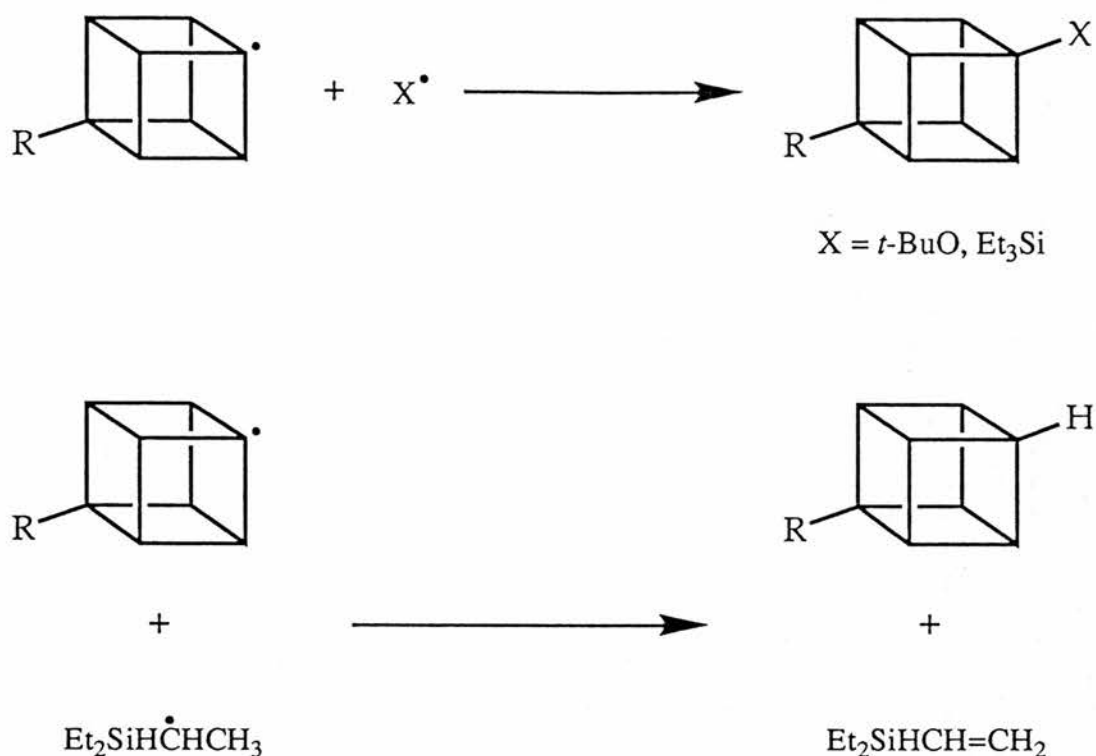
Figure 4.12

The cross-termination of cubyl radicals.

All of the reaction mixtures were examined by GC-MS. After short periods of photolysis, the main products were *tert*-butanol and the silane oxidation product $Et_3SiOSiEt_3$. The 4-methylcubyl bromide containing system was continually monitored for up to 48 hours of photolysis, by which time all the reactant had been consumed. This produced a complex range of products, with a large proportion of intractable tar. Despite this the cross-disproportionation product methylcubane was identified as a minor component, but the formation of cubyl dimers and cross-combination products could neither be confirmed nor disproved.
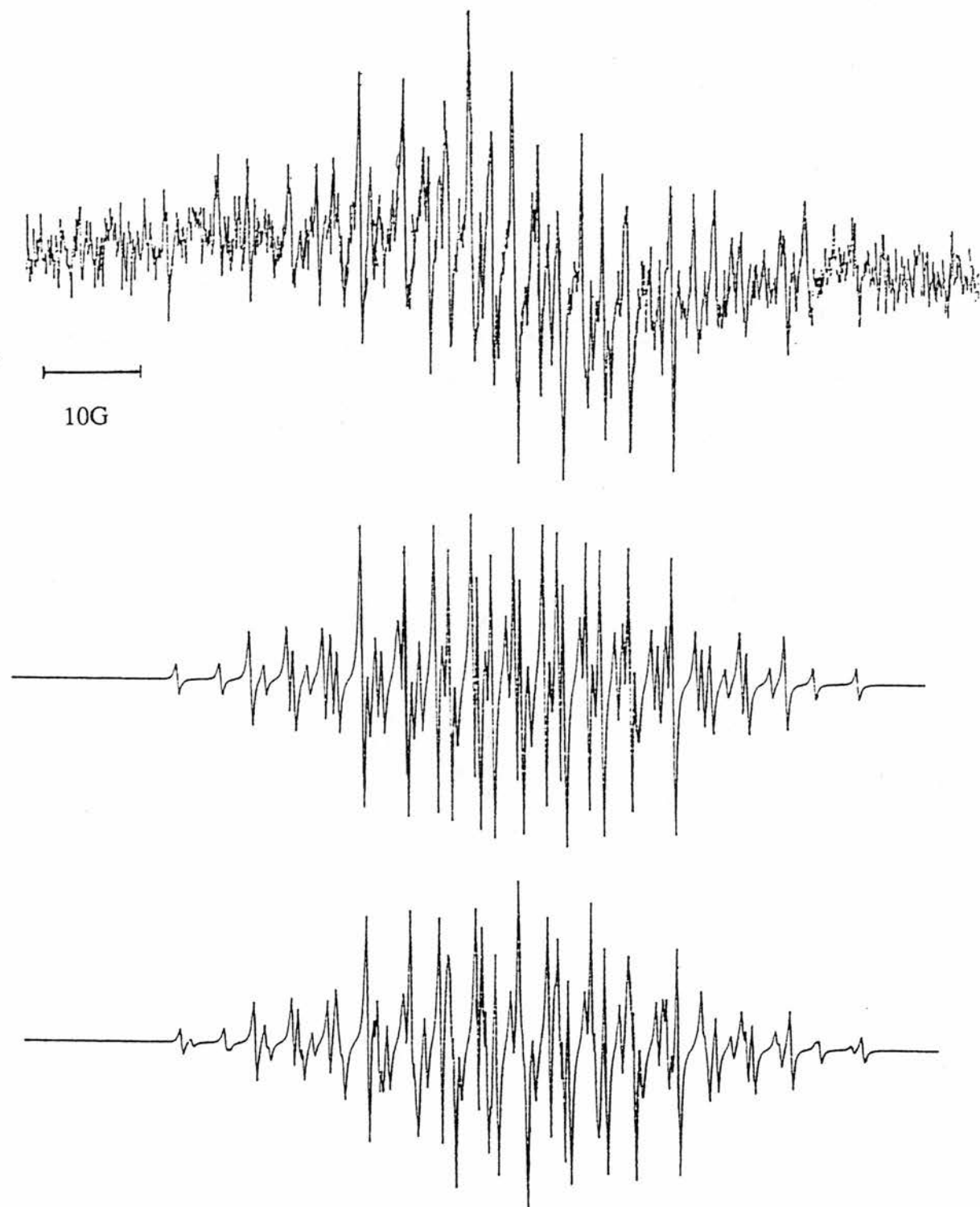
Figure 4.13

Upper: 9.3 GHz EPR spectrum obtained by bromine abstraction from 4-chlorocubyl
bromide in cyclopropane at -120°C.

Middle: Computer simulation of the upper spectrum comprising of 100% ^{35}Cl.

Lower: Computer simulation with 75% ^{35}Cl (a=4.3G) and 25% ^{37}Cl (a=3.6G).
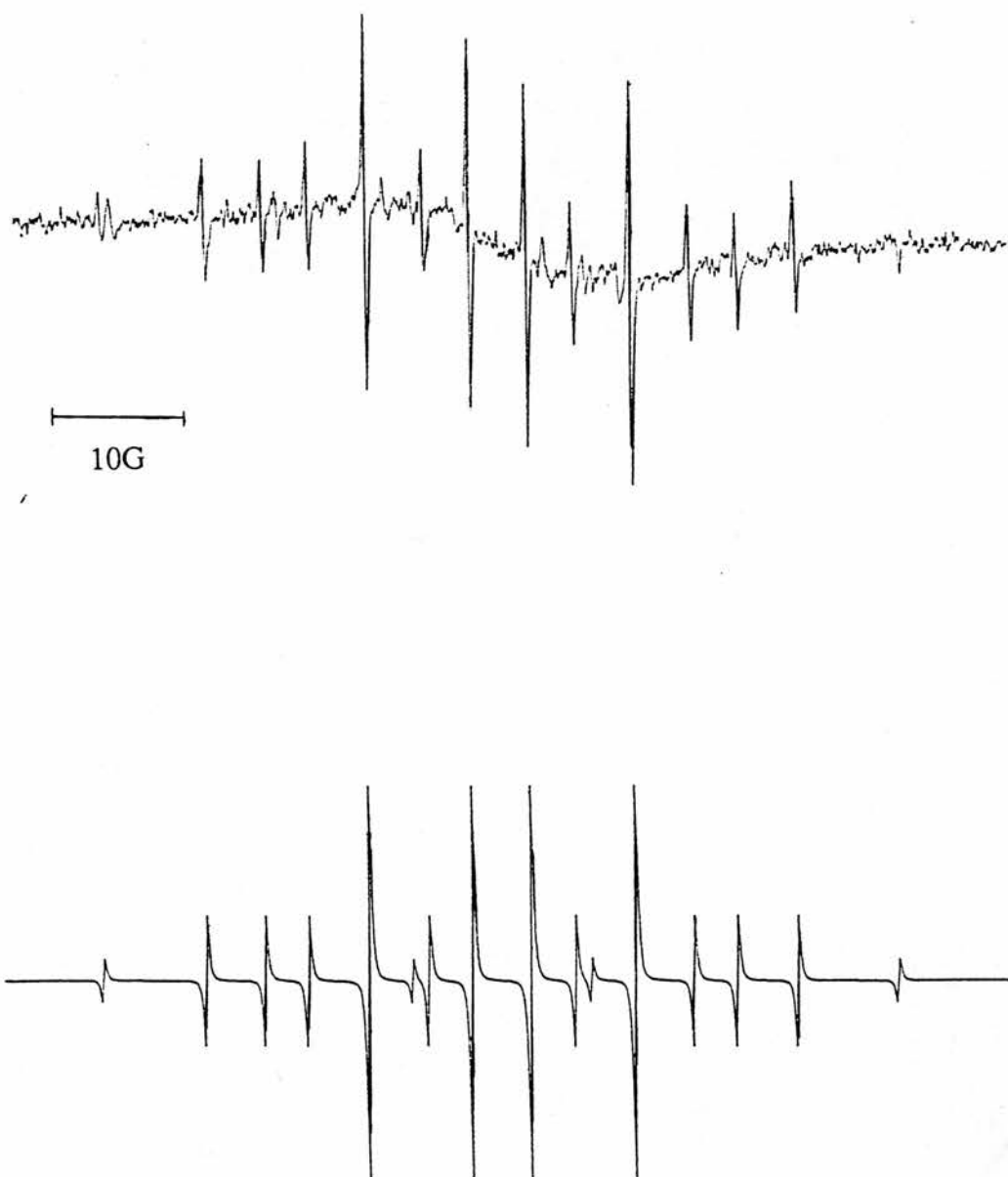
Figure 4.14

Upper: 9.3 GHz EPR spectrum obtained by bromine abstraction from

4-carbomethoxycubyl bromide, in cyclopropane at -120°C.

Lower: Computer simulation of the 4-carbomethoxycubyl radical,

using hfs from Table 4.2.
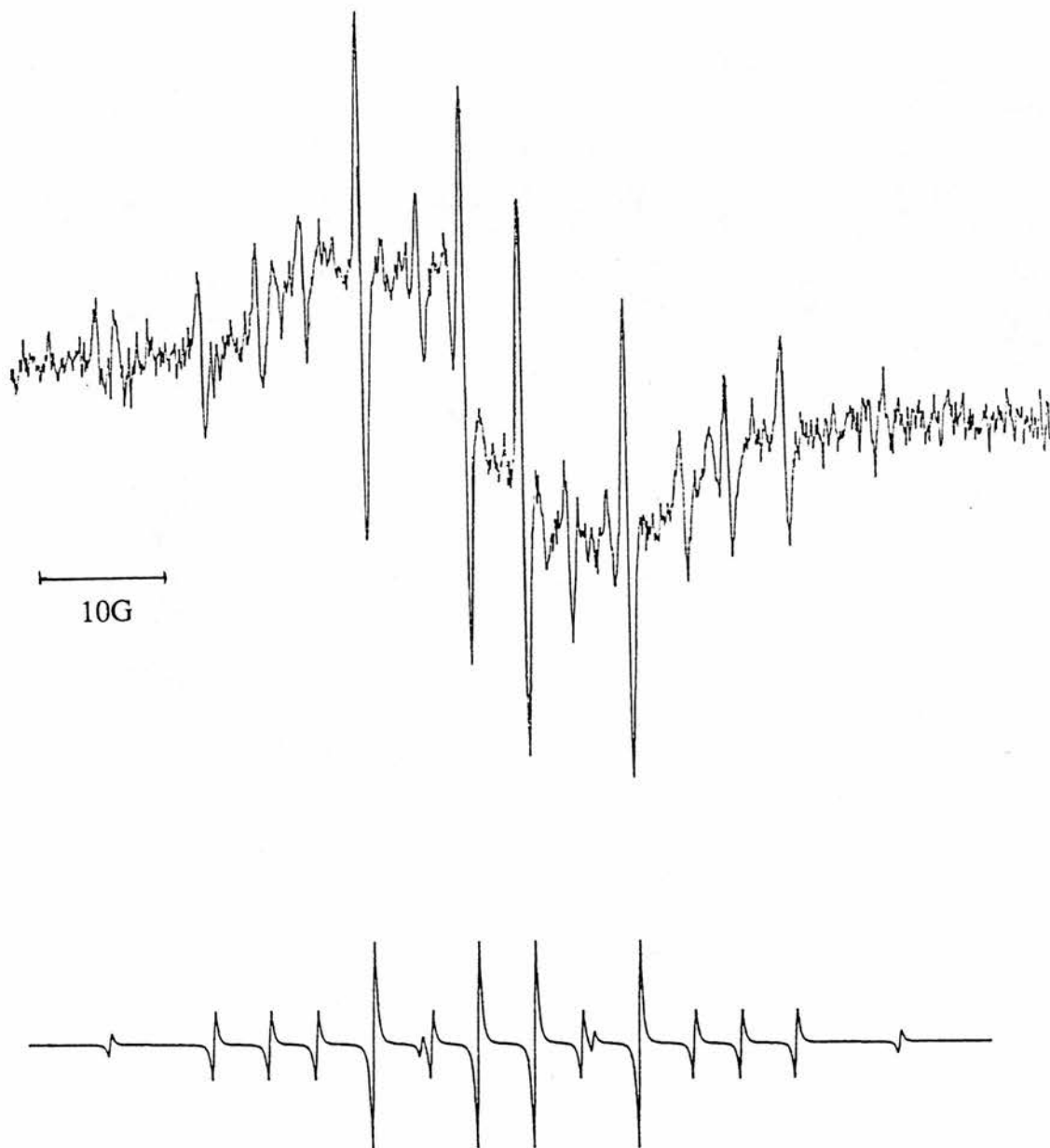
Figure 4.15

Upper: 9.3 GHz EPR spectrum obtained by bromine abstraction from 4-methylcubyl-

bromide, in cyclopropane at -120°C.

Lower: Computer simulation of the 4-methylcubyl radical, using hfs from Table 4.2.
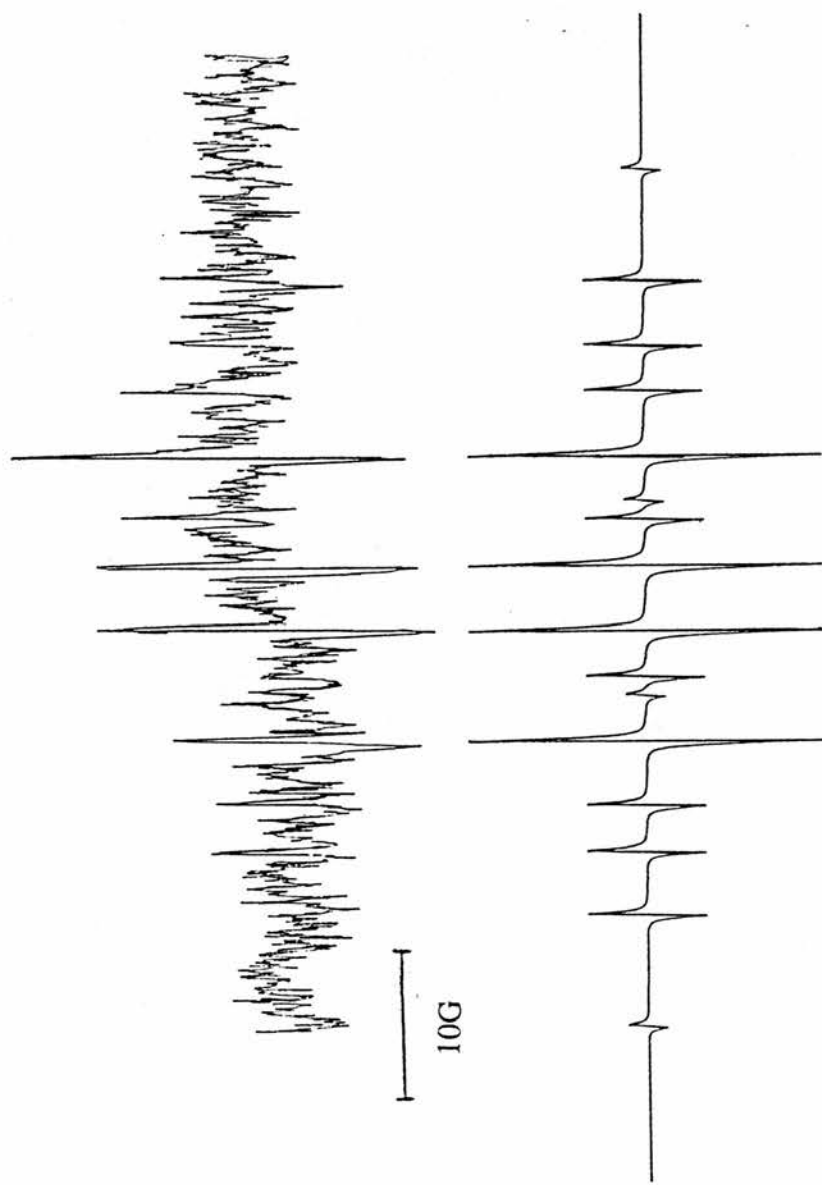
Figure 4.16

Upper: 9.3 GHz EPR spectrum obtained by bromine abstraction from 4-phenylcubyl bromide, in cyclopropane at -120ºC.

Lower: Computer simulation of the 4-phenylcubyl radical, using hfs from Table 4.2.
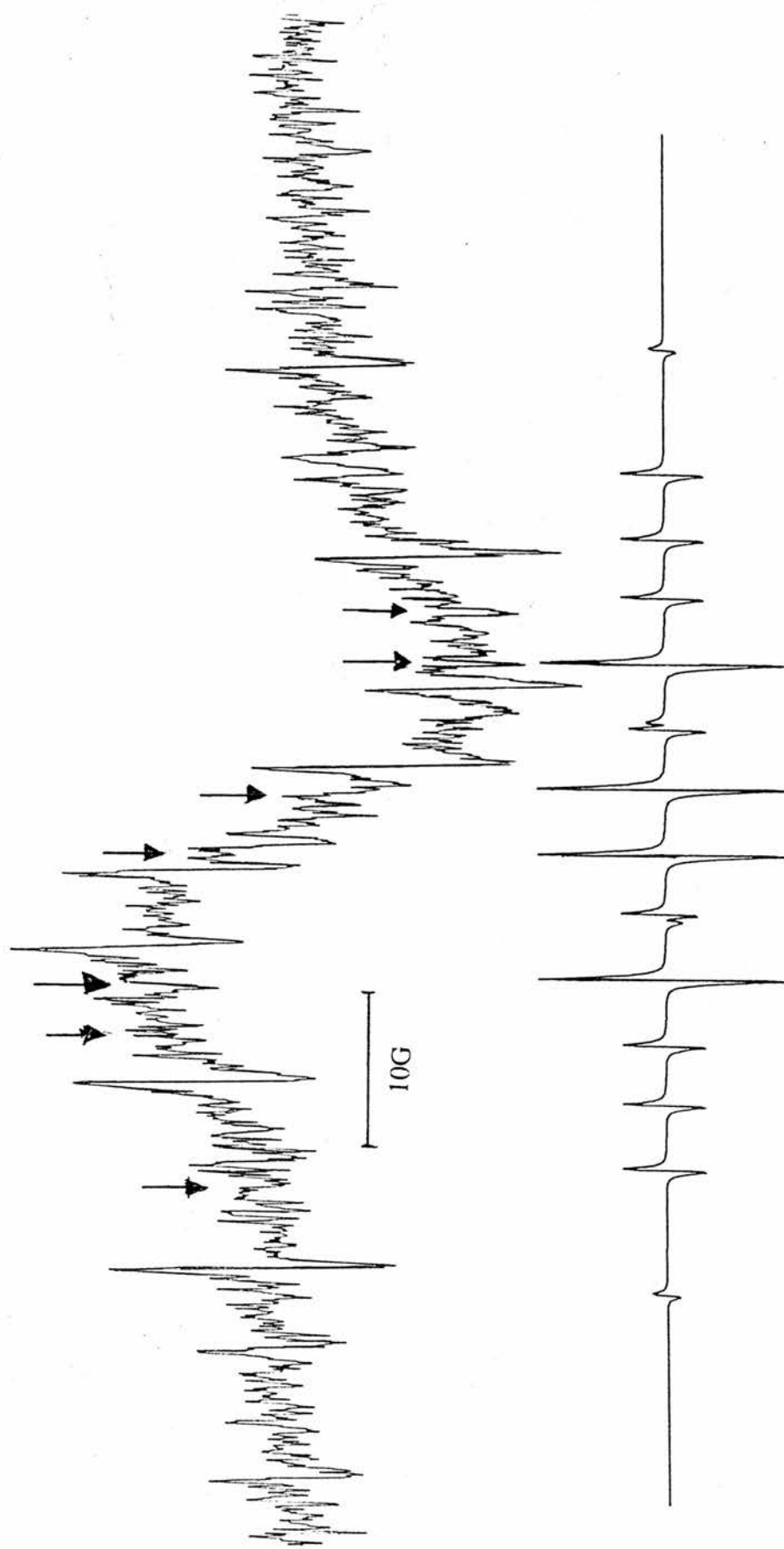
Figure 4.17

Upper: 9.3 GHz EPR spectrum obtained by bromine abstraction from 4-bromocubyl bromide, in cyclopropane at -120°C.   The dominant species is the 1-(diethylsilyl)-ethyl radical, with the 4-bromocubyl radical (indicated) in low concentration.

Lower: Computer simulation of the 4-bromocubyl radical, using hfs from Table 4.2.

112
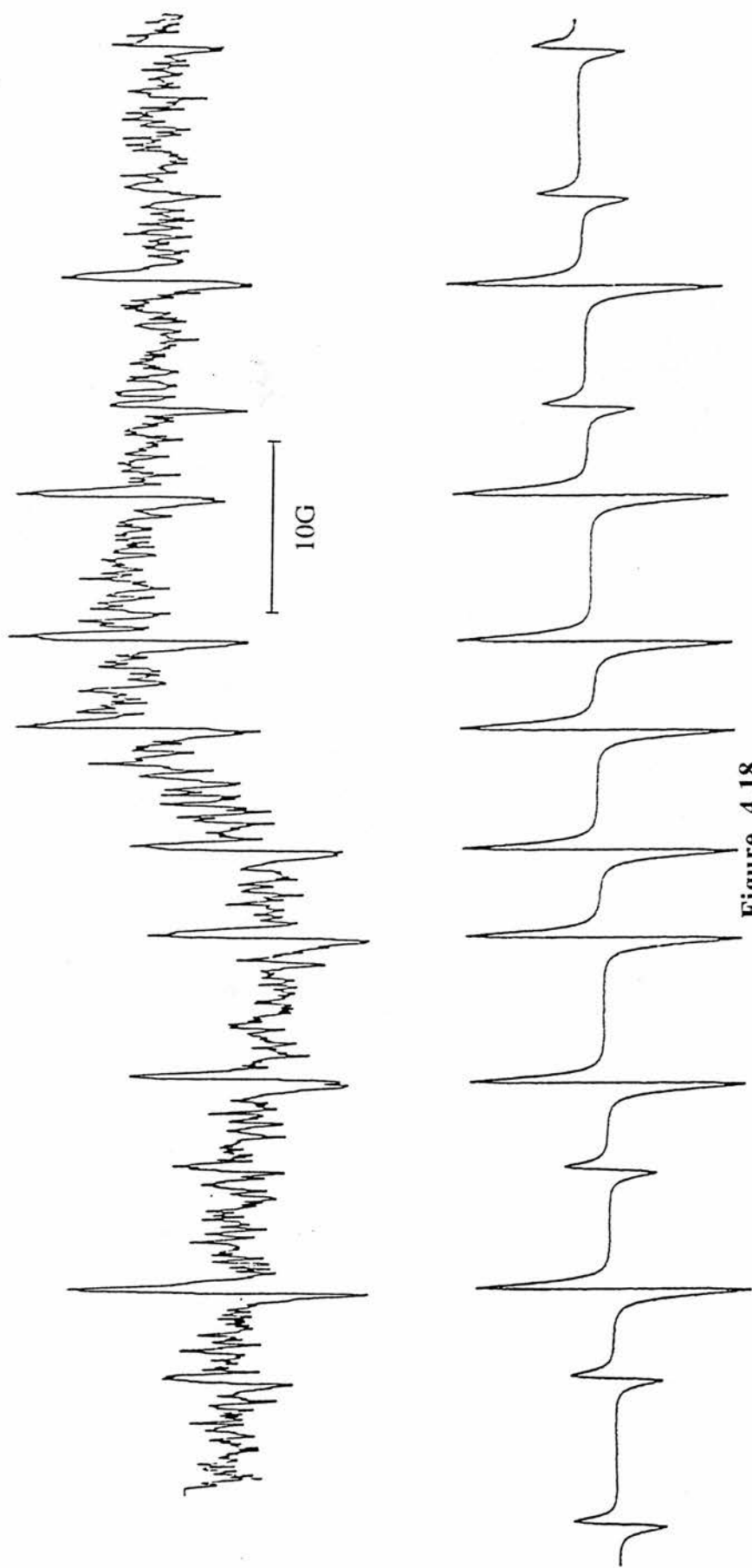
Upper: 9.3 GHz EPR spectrum obtained by abstraction of a secondary hydrogen from triethylsilane, by cubyl radicals, in cyclopropane at -120°C.

Lower: Computer simulation of the 1-(diethylsilyl)-ethyl radical.

Figure 4.18

4.3   Bromine Abstraction from Compounds with
Structures Related to Cubane

In addition to the 4-substituted bromocubanes two other polycyclic bromides, norcubyl bromide and 2-bromotetracyclo[3.3.0.0^{2,8}.0^{3,6}]octane[96], were examined by bromine atom abstraction (Figure 4.19). These two compounds are structurally similar to cubane, and are thus included in this section for comparison with the cubyl radicals.

(a)

(b)
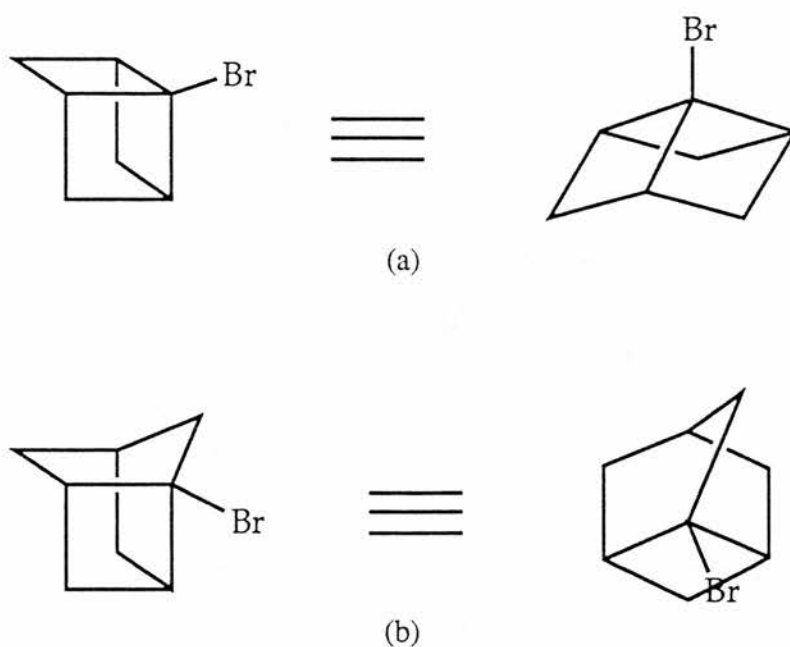
Figure 4.19

Norcubyl bromide (a) and

2-bromotetracyclo[3.3.0.0^{2,8}.0^{3,6}]octane (b).

Triethylsilyl radicals in cyclopropane were again used to abstract the bromine atoms from both species. As was observed with the cubyl radicals, the polycyclic bridgehead radicals produced initially degraded rather quickly, with the tetracyclo-octane radical proving to be impossible to observe.

The EPR spectrum of the norcubyl radical (Figure 4.20) was a complex set of signals produced by couplings to three groups of three hydrogen atoms, labelled H$_a$,

H_b and H_c for clarity (Figure 4.21). The complete spectrum was not recorded, but there were sufficient data for a fully reliable interpretation and simulation. The hfs of this radical were tentatively assigned and compared with typical values for the corresponding couplings of the cubyl radical hydrogens (Table 4.6).
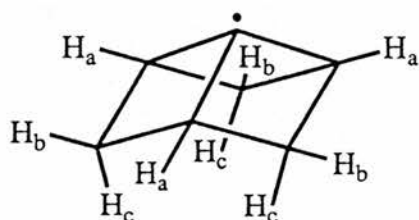
Figure 4.21

The three hydrogen environments in the norcubyl

radical, tentative assignments.

Norcubyl Hydrogen	Norcubyl hfs / G	Corresponding cubyl hfs / G
H_a	10.6	10 to 12.5 (H_β)
H_b	8.25	6 to 8 (H_γ)
H_c	0.8	---

Table 4.6

Norcubyl Radical hfs, g-value=2.0027±0.001.

As can be seen the splittings of the norcubyl radical are of a comparable magnitude to the analogous hydrogen atoms of the cubyl radical. This is hardly surprising, as the structure of norcubane is essentially that of cubane less one carbon atom, that is one corner of the cube missing. Obviously the geometry will not be identical to that of a cube, as the absence of the carbon atom allows the molecule to

"relax" and become less constrained. This change in geometry is reflected by the differences in hfs, in particular of the H_b hydrogen. The H_c hydrogen has no cubyl counterpart, but it does have a particularly low splitting constant when compared to its fellow γ-hydrogen H_b. The high coupling to the H_b hydrogen is due to it being in a W-plan[97] configuration with respect to the orbital of the unpaired electron. This arrangement is recognised in EPR[98] and NMR[99] spectroscopy as producing large long range couplings. In contrast to this is the H_c hydrogen is anti-W-plan with respect to the radical centre and as a result the coupling is correspondingly small.

The norcubyl radical signal was sufficiently strong for the exponent of light intensity to be roughly determined by the use of calibrated gauzes in the light beam as before. The data obtained from this are presented in Table 4.7, with the resulting graph being displayed in Figure 4.22. This produced a value of 0.40±0.30 for the exponent of light intensity, thereby showing that the termination was predominantly bimolecular.

Attempts to observe the tetracyclooctane radical by bromine abstraction failed. The only radical observed was the 1-(diethylsilyl)ethyl radical (identical to that shown

EPR Peak Height / M		$\log_{10}$ (peak height)		Light Intensity	$\log_{10}$
Run 1	Run 2	Run 1	Run 2	(I)	I
0.071	0.063	-1.149	-1.201	1.00	0.000
0.048	0.049	-1.319	-1.310	0.59	-0.229
0.046	0.043	-1.337	-1.366	0.42	-0.377
0.037	0.040	-1.432	-1.398	0.32	-0.495

Table 4.7

EPR peak height data at various light intensities

for the norcubyl radical.
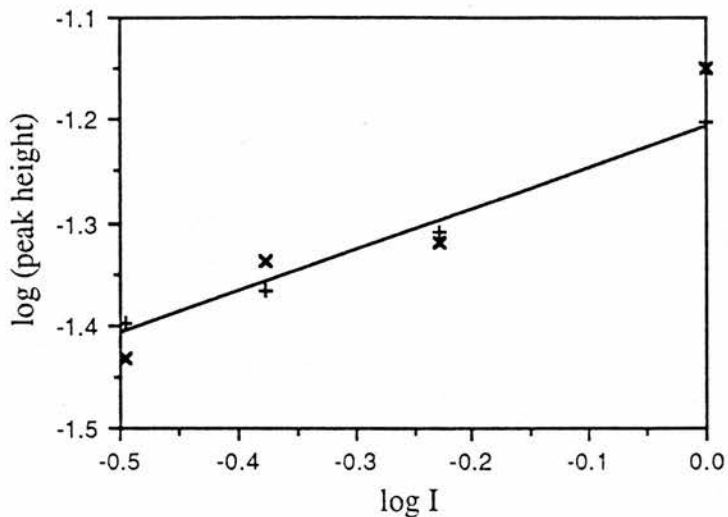
Figure 4.22

The graph of the log (EPR peak height) against log (light intensity)
for the norcubyl radical.

in Figure 4.18). Thus it would appear that this radical is too reactive to be observed in this manner.

It is interesting that both the norcubyl and tetracyclooctane radical, which contain less strain than the cubyl radicals, nevertheless follow the cubyl radical in abstracting secondary hydrogen atoms from the ethyl groups of triethylsilane.
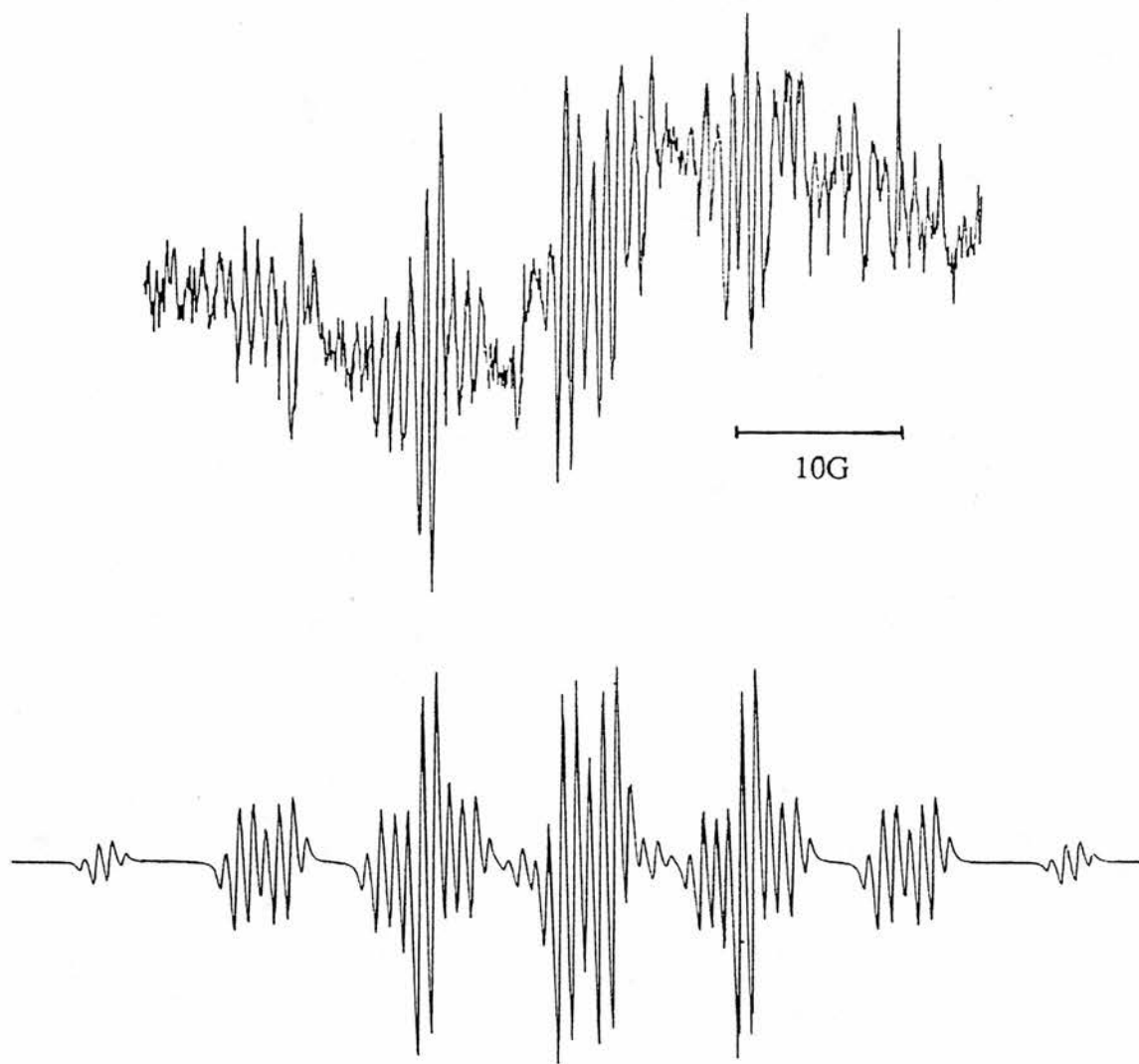
Figure 4.20

Upper: 9.3 GHz EPR spectrum obtained by bromine abstraction from

norcubyl bromide, in cyclopropane at -120°C.

Lower: Computer simulation of the norcubyl radical, using hfs from Table 4.6.

The Cubylcarbinyl Radical

As was explained in Section 3.5, Eaton and Yip generated the cubylcarbinyl radical by the abstraction of bromine from cubylcarbinyl bromide using tri-*n*-butyltin hydride[81].   They also isolated two olefins as the final products from the rearrangement of this radical and subsequently postulated a scheme for the rearrangement (Figure 3.12).

Following on from Eaton and Yips' work, we looked at the abstraction of bromine from cubylcarbinyl bromide with triethylsilyl radicals. The bromide is fairly unstable and rearranges to the homocubyl bromide quite easily (Figure 3.11), and thus it was freshly prepared (Figure 4.23) prior to being utilised in the radical experiments.

On bromine abstraction in *n*-propane solution, a spectrum was visible down to -175°C with no change except for some line broadening.   This spectrum was satisfactorily simulated with the following hfs: $a(1H)=16.4G$, $a(1H)=14.2G$, $a(2H)=13.7G$, $a(1H)3.0G$ and $a(1H)=0.4G$ at -125°C (Figure 4.28). These hfs were
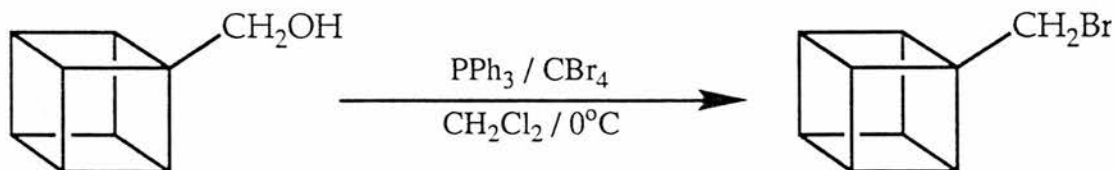
Figure 4.23

Preparation of cubylcarbinyl bromide from cubylcarbinol.

assigned and compared with the known hfs of the structurally related methylenecyclobutyl radical[100] (Figure 4.24). The similarity between the splittings of these two radicals is striking, confirming the identity of the tricycloallyl radical (B) as the first detectable intermediate in the rearrangement of the cubylcarbinyl radical.
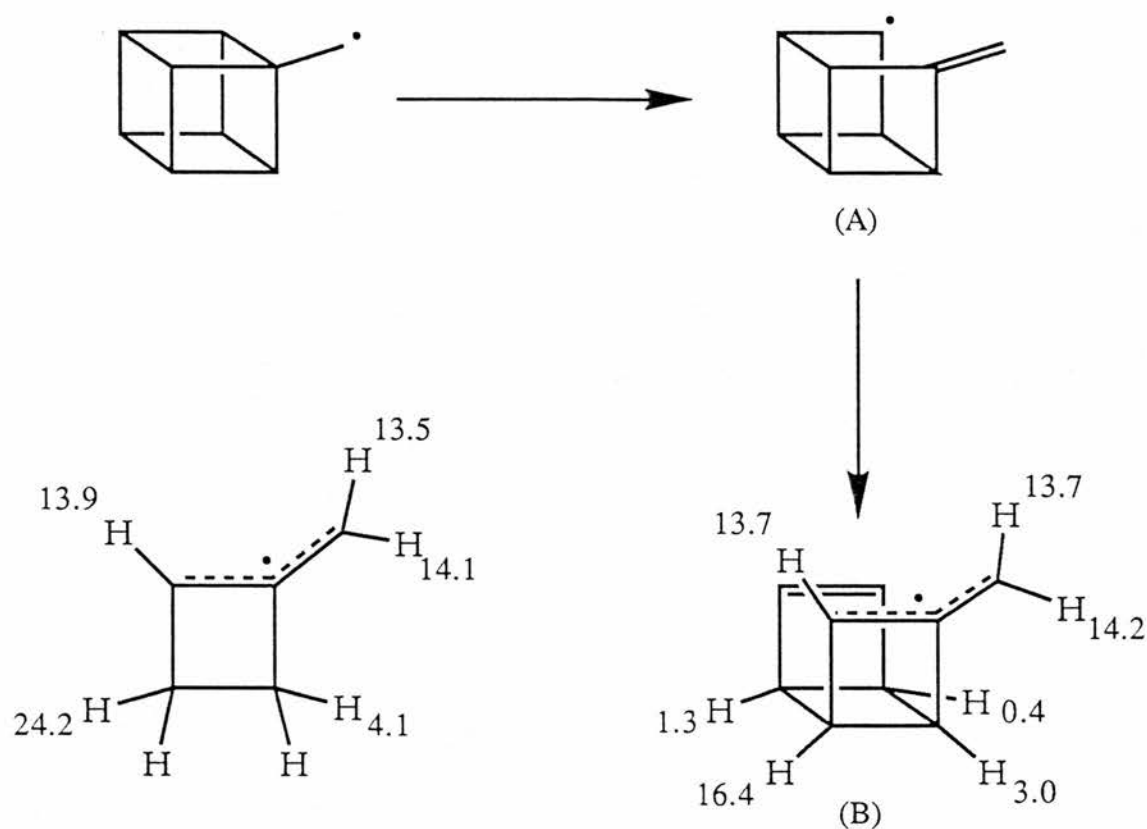
Figure 4.24

Rearrangement of the cubylcarbinyl radical to the tricycloallyl radical (B),

and a comparison of the hfs of the latter with those of the

methylenecyclobutyl radical.

The tricycloallyl radical contains several distant but favourably placed hydrogen atoms, these being *trans* with respect to the radical π-system, and as expected, these hydrogens produce long range hfs. The fact that this radical can be seen down to -175°C under EPR conditions makes it possible to estimate an activation energy of ≤ 4.5 kcal mol^{-1} for the rearrangement of the cubylcarbinyl radical. With a normal pre-exponential factor of 10^{13} s^{-1}, the rate constant for the rearrangement is $\geq$ 5×10^9 s^{-1} at 25°C, which is in reasonable agreement with the value of 2×10^{10} s^{-1} at 25°C calculated by Eaton and Yip[81], confirming that this is in fact one of the fastest known β-scissions in solution.

That the tricycloallyl radical is the first intermediate detected is of no surprise.

The first β-scission produces a tetracyclo radical (A), but this is not observed as it undergoes a more rapid β-scission to produce the tricycloallyl radical (B). This is due to the bond in the tetracyclo species (A) which undergoes β-scission being in a fixed conformation with optimum overlap with the SOMO at the radical centre. In addition, this β-scission produces a resonance stabilised allyl radical, thus adding a further driving force for rearrangement. Taking into account these points one would not expect the tetracyclo radical to be observed, either in this case or with the α-hydroxy-substituted cubylcarbinyl radical covered later in this section. That the cubylcarbinyl radical rearranges so rapidly was expected, because the relief of ring strain plays a major role in β-scission reactions. The cubylcarbinyl structure has a strain energy (SE) of 166 kcal mol^{-1}, with the tricycloallyl structure having a much lower SE of approximately 83 kcal mol^{-1}, giving a massive release of strain, that is

Radical	k (25°C) /s	E_a[a] kcal mol^{-1}	ΔSE[b] kcal mol^{-1}
Cyclobutyl-carbinyl[82b-c,101]	4.7×10^3	11.7	26.5
Bicyclo[2.1.1]hexyl-carbinyl[102]	1.7×10^5	9.3	31.1
Bicyclo[1.1.1]pentyl-carbinyl[102]	1.3×10^7	7.1	41.1
Cubyl carbinyl[81]	2×10^{10}	3.7[c]	83
Cubylcarbinyl[d]	$\geq 5 \times 10^9$	≤ 4.5	83

Table 4.8

Rate parameters and strain relief of cylcobutylcarbinyl type radical rearrangements.
[a]All log (A/s^{-1}) values 13±1. [c]Calculated from the rate constant at 25°C by assuming log (A/s^{-1})=13.0. [d]This work.

$\Delta SE=83$ kcal mol^{-1}.   The rate constants, activation energies and release of strain energy (ΔSE) of four leading types of cyclobutylcarbinyl radical rearrangements are compared in Table 4.8.   It is obvious that the rate constants increase with decrease in the activation energies , as the relief of strain increases (Figure 4.25).
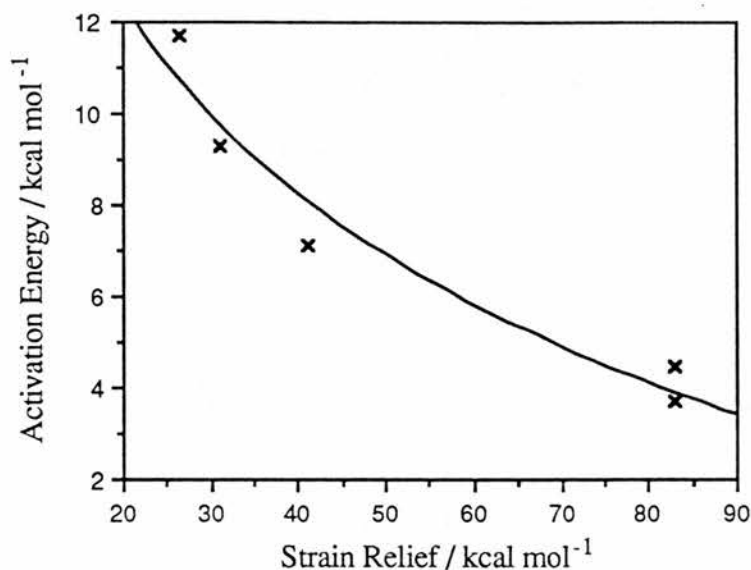
Figure 4.25

The graph of the activation energy of the rearrangement versus the release of strain on

rearrangement, for cyclobutylcarbinyl type radicals.

On raising the temperature of the sample the EPR spectrum rapidly weakened, making the spectroscopic observation of further rearrangements impossible.   At -20°C a set of four central lines in what was obviously a new radical became visible, but the signal to noise ratio was too poor for the complete spectrum to be observed. These four lines had the identical spacing of the four central lines of the substituted cyclobutenyl radical derived from rearrangement of the α-hydroxy-substituted radical (later in this section), and in this case it is attributed to the cyclobutenyl radical displayed in Figure 4.26.

On the introduction of a silyl ether or similar oxygen functionality, such as an
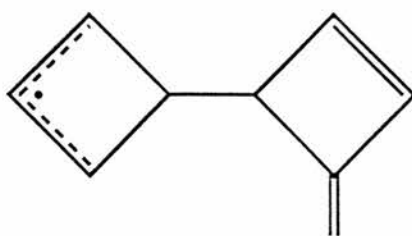
Figure 4.26

hydroxyl group, at the radical centre, the rate of β-scission of cyclopropylcarbinyl radicals is reduced by a factor of about ten[103]. Therefore, in order to determine if this would be the case with the rate of cubylcarbinyl β-scission and thus make it possible to spectroscopically observe the cubylcarbinyl radical, cubylcarbinol was used as the radical precursor. To this end, *tert*-butoxyl radicals were used to selectively abstract an α-hydrogen of the -CH₂OH group. These hydrogens are removed in preference to the cubyl radicals in this case as, unlike in the methylcubane case (Section 4.1), the exocyclic methylene hydrogens are activated due to the adjacent hydroxy group.

The spectrum obtained at -120°C in cyclopropane was attributed to the α-hydroxycubylcarbinyl radical and verified by computer simulation (Figure 4.29),

Radical	$a(H_\alpha)$	$a(H\ 2,6,8)$	$a(H\ 3,5,7)$	$a(OH)$
α-Hydroxycubyl-carbinyl	14.1	2.80	1.25	1.25
α-Deuteroxycubyl-carbinyl	14.1	2.80	1.25	----a

Table 4.9

EPR hfs of substituted cubylcarbinyl radicals in cyclopropane at -120°C.

hfs in G, *g*-factors 2.003 ± 0.001

[a]Deuterium hfs not resolved.

the hfs being shown in Table 4.9. The 14.1G doublet hfs is of an expected magnitude for the H_α of an α-hydroxy carbon-centred radical. The spectrum also displays two sets of quartet splittings from the two sets of three equivalent cubyl hydrogens, in addition to the smaller doublet splitting from the hydroxyl hydrogen. This interpretation was confirmed by examining the deuterium substituted cubylcarbinol, produced by shaking the cubylcarbinol EPR sample with deuterium oxide. The spectrum of the α-deuteroxycubylcarbinyl radical was well simulated, using hfs from Table 4.9, although no splitting due to the -OD deuterium was observed. The triplet hfs from the deuterium nucleus were not seen as it would be approximately one sixth that of the hydroxyl hydrogen splittings, that is $a(D)=0.2G$, which is within the spectral line width of 0.4G and therefore not resolved.

In both the α-hydroxy- and α-deuteroxy-cubylcarbinyl radical cases the spectral intensity was reduced on warming the solution to -115°C, with the pattern becoming more complex as a result. This is presumably due to the formation of the hydroxy substituted tricycloallyl radical (Figure 2.27). By -65°C only a single radical was present once again, but the spectral amplitude was very weak and a good spectrum could not be obtained. Both the protio- and deuterio- precursors produced the same spectrum, these being a triplet of doublets due to $a(2H)=15.3G$, $a(1H)=4.2G$ and $a(1H)=2.5G$ at -65°C (Figure 4.30). These couplings are similar to those of the cyclobutenyl radical[104], and would be consistent with the spectrum of the substituted cyclobutenyl radical (Figure 4.27).

Thus three of the intermediates in the rearrangement pathway of the cubylcarbinyl radical have been characterised by EPR spectroscopy, confirming the proposed mechanism (Figures 3.12 and 4.27).

The spectra of the α-hydroxy- and α-deuteroxy-cubylcarbinyl radicals were too weak and complex for any accurate measurement of the rearrangement rate constant to be made by kinetic EPR. However, the activation energy for the rearrangement of the α-hydroxycubylcarbinyl radical to the tricycloallyl species can be estimated to be approximately 7.5 ± 1.0 kcal mol^{-1} from the temperature at which both
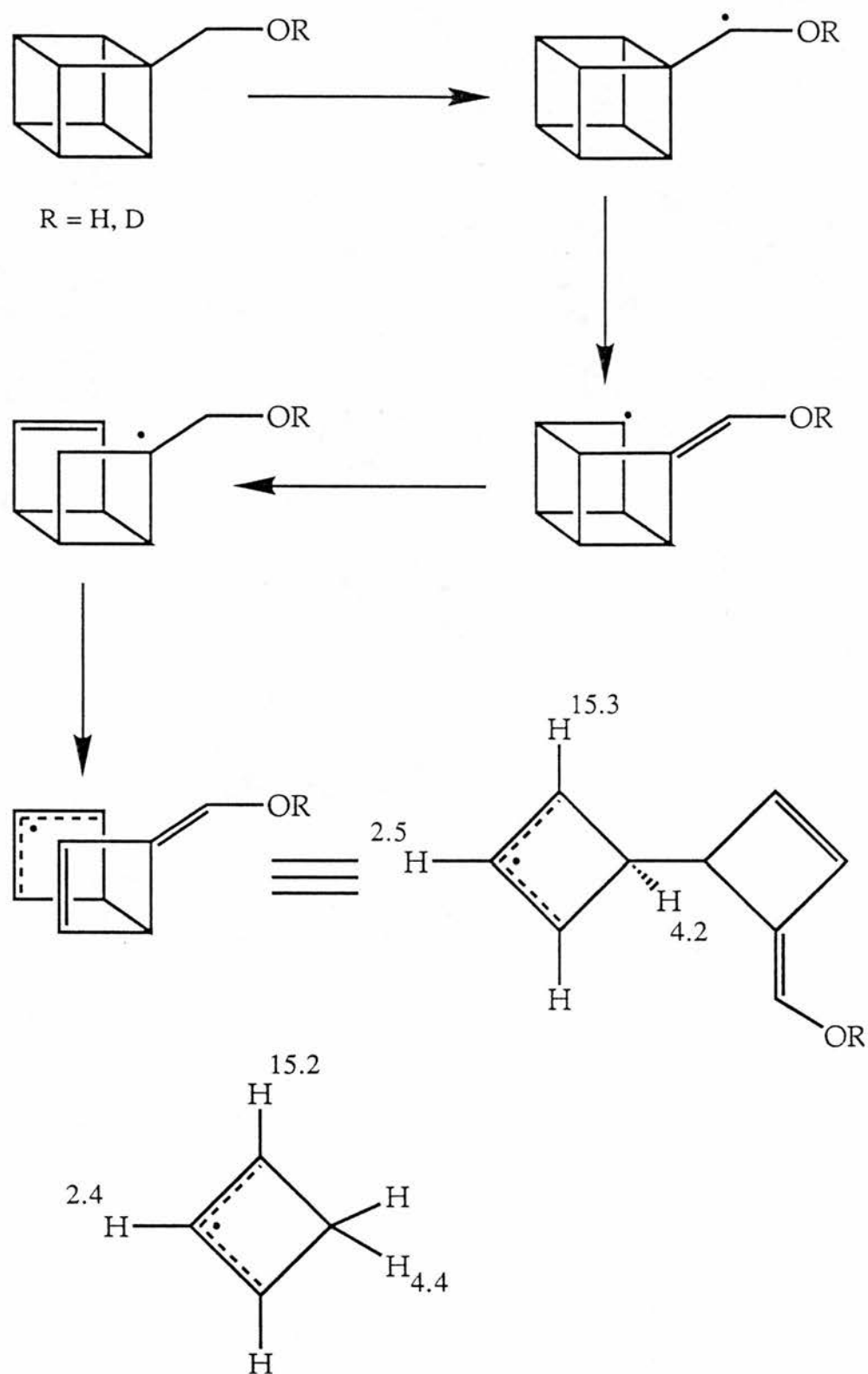
Figure 4.27

The rearrangement of the α-hydroxy- and α-deuteroxy-cubylcarbinyl radicals to

produce substituted cyclobutenyl radicals and the hfs of the cyclobutenyl radical.

the unrearranged and rearranged radicals were present in equal concentrations[105], that is, at about -105ºC. Thus with a normal A-factor of 10^{13} s^{-1}, the rate constant is 3 x 10^7 s^{-1} at 25ºC. The final β-scission, of the tricycloallyl radical to the cyclobutenyl radical, was not clearly distinguished by EPR spectroscopy. The formation of the latter, however, was complete by -65ºC, indicating that the activation energy for this final step of the rearrangement is ≤ 9.5 kcal mol^{-1}. Therefore it can be seen that the introduction of an hydroxy group in the α-position to the radical centre of the cubylcarbinyl radical has the effect of reducing the rate of the first β-scission of its rearrangement by a factor of almost one thousand. But despite this, the overall rate to the final product of the cascade is approximately the same as for the parent hydrocarbon.

All of the samples were examined by GC-MS, but little information was elicited. Neither of the two product cyclobutenes (Figure 3.12) were observed. This was to be expected since with the use of triethylsilane and *tert*-butyl peroxide to abstract the bromine atom (or just the peroxide to abstract a hydrogen), there is no readily available hydrogen atom to quench the final radical to form these products. This hydrogen is however available when tri-*n*-butyltin hydride is used , hence these products are observed when this is the bromine abstractor[81].
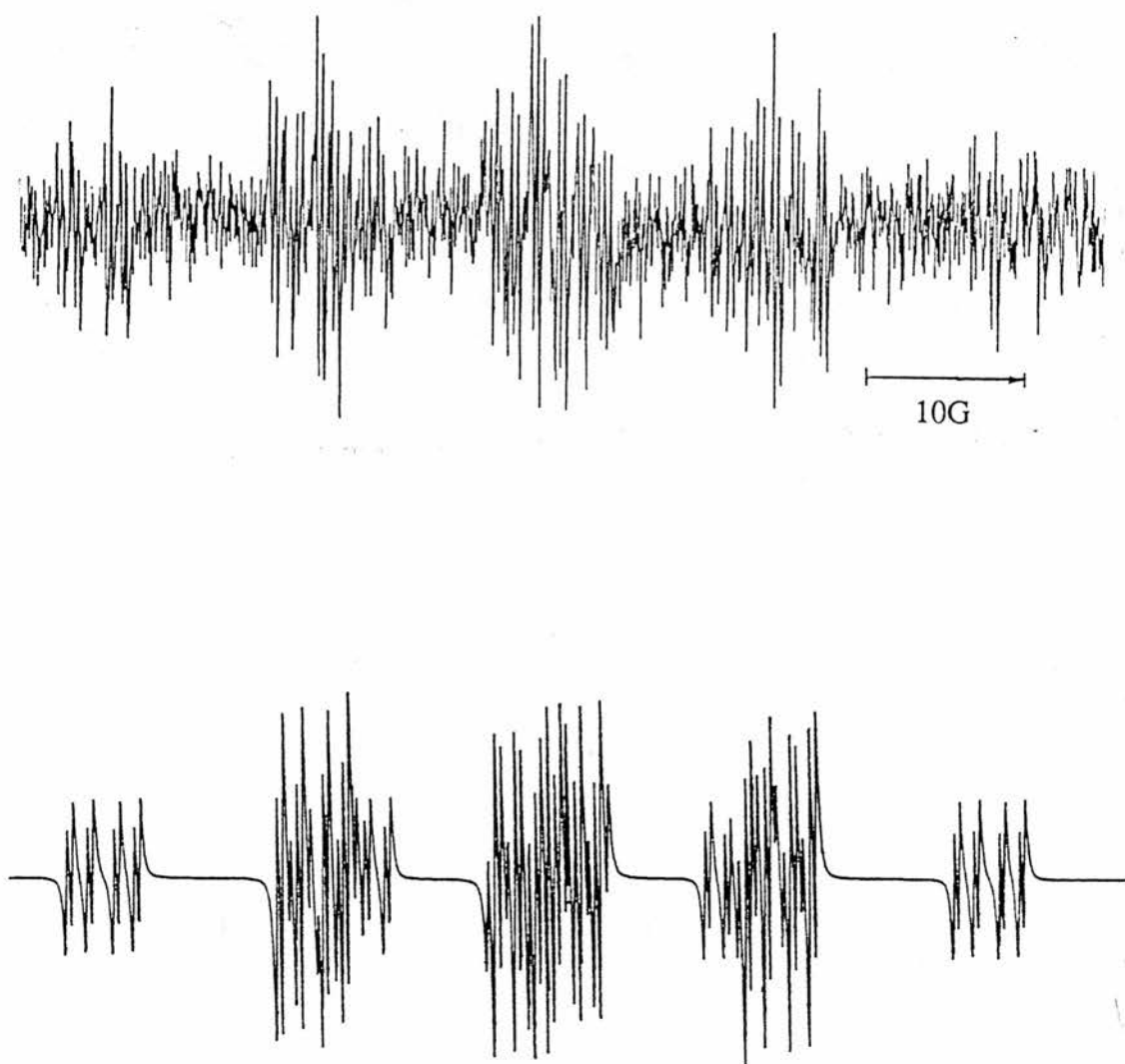
Figure 4.28

Upper: 9.3 GHz EPR spectrum obtained by bromine abstraction from

cubylcarbinyl bromide in cyclopropane at -120°C.

Lower: Computer simulation of the tricycloallyl radical using the hfs given in the text.
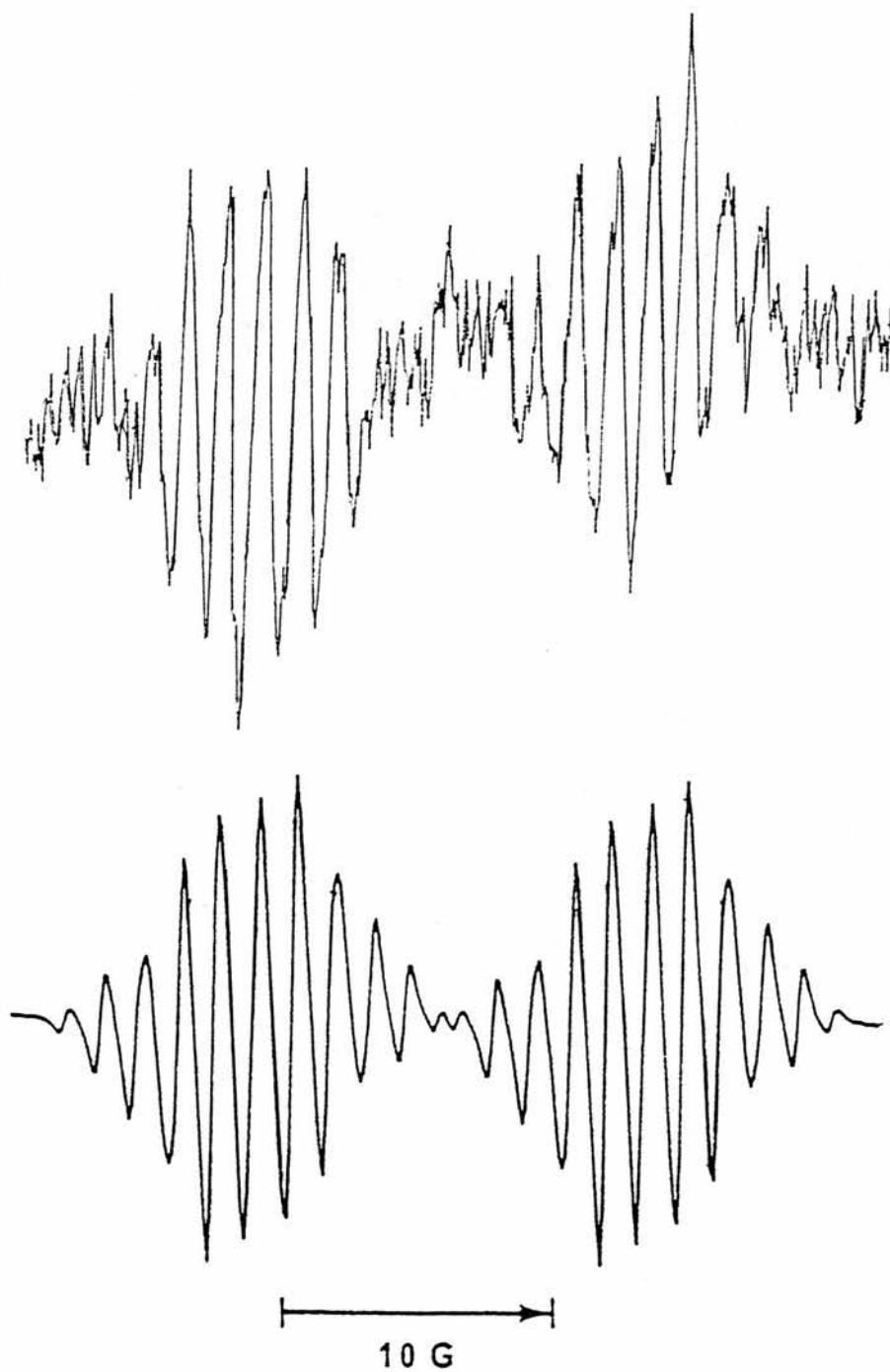
Figure 4.29

Upper: 9.3 GHz EPR spectrum obtained by hydrogen abstraction from

cubylcarbinol in cyclopropane at -120°C.

Lower: Computer simulation of the α-hydroxycubylcarbinyl radical

using the hfs in Table 4.9.
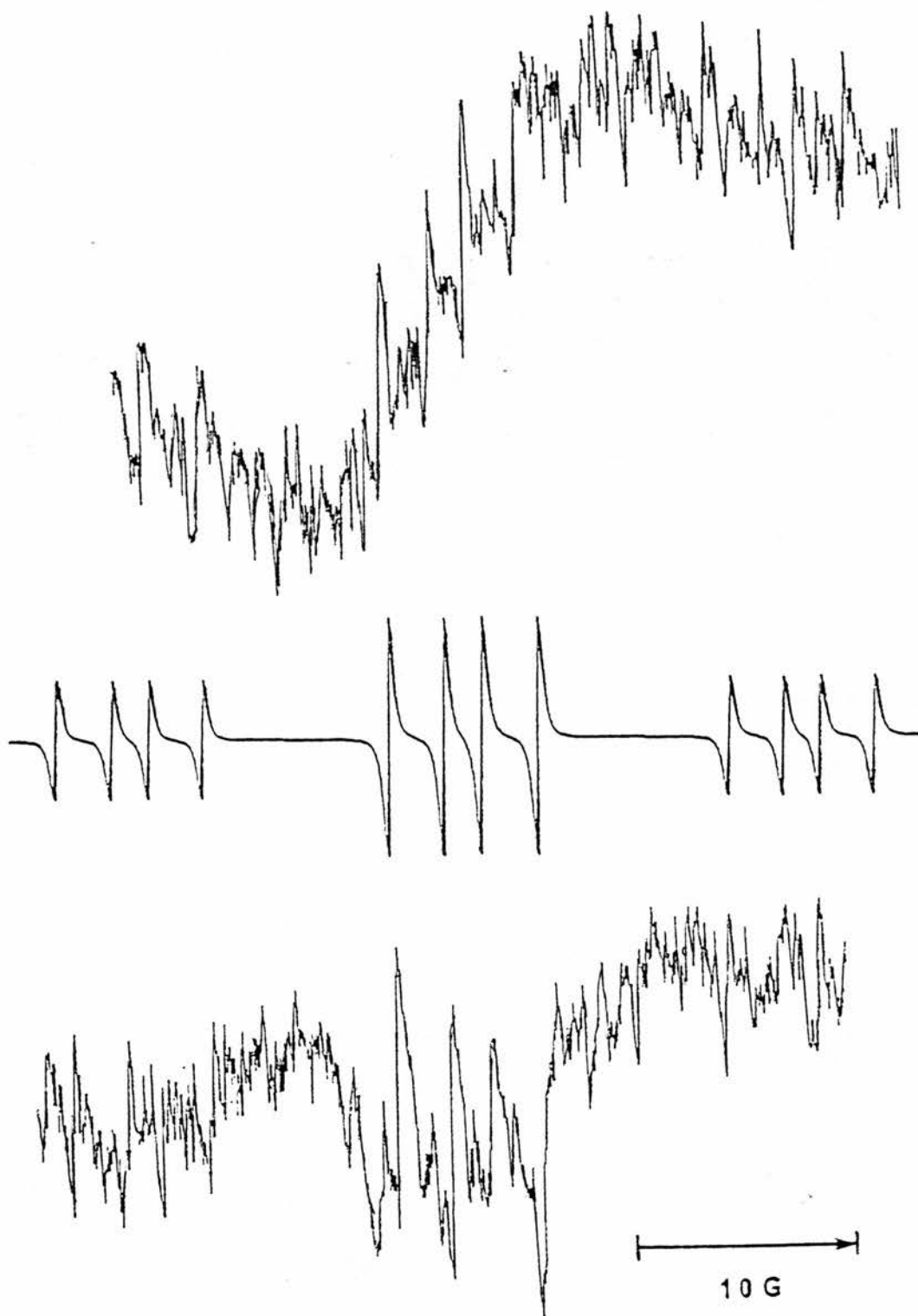
Figure 4.30

Upper: 9.3 GHz EPR spectrum obtained on warming the α-hydroxycubylcarbinyl radical to -65°C in cyclopropane. Middle: Computer simulation of the substituted cyclobutenyl radical. Lower: 9.3 GHz EPR spectrum obtained on warming the α-deuteroxycubylcarbinyl radical to -65°C in cyclopropane.

129

4.5 Conclusions

It has been demonstrated for the abstraction of hydrogen atoms from cubanes by *tert*-butoxyl radicals, that

$$k_H(\text{Cubyl-Me}) > k_H(\text{Cubyl-H}) > k_H(\text{Cubyl-A})$$
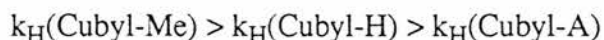
where A is an electron-withdrawing substituent such as a carbomethoxy group or a bromine atom. The cubyl hydrogen atoms of the methylcubane are abstracted in preference to the methyl hydrogens in a statistical manner. Therefore it is implied that the cubyl carbon-hydrogen bond is somewhat weaker than might be expected. 4-Substituted cubyl radicals can easily be generated from 1-bromo-4-substituted cubanes by the abstraction of the bromine with triethylsilyl radicals, but no radicals are observed with tin centred radicals. Under EPR conditions, cubyl radicals show a tendency to decay by bimolecular combination or cross-disproportionation reactions. The latter is the abstraction of a secondary methylenic hydrogen from triethylsilane by the cubyl radical, producing the hitherto unobserved 1-(diethylsilyl)ethyl radical, $Et_2SiC \cdot (H)CH_3$.

The rearrangement of the cubylcarbinyl and α-hydroxycubylcarbinyl radicals were shown to occur via a cascade of three β-scissions, and three out of the four reactive intermediates in this rearrangement were spectroscopically observed and characterised. The exceptionally rapid rate of the first β-scission of the parent hydrocarbon radical was confirmed and it was shown that the α-hydroxy-substituent reduced this rate by almost three orders of magnitude.

4.6 Experimental Section

The ^1H NMR spectra were obtained on a Varian Gemini-200 spectrometer (200MHz). EPR spectra were recorded with a Bruker ER 200D spectrometer operating with 100kHz modulation. Samples were prepared in Spectrosil tubes, degassed and photolysed in the spectrometer cavity by light from a 500W super pressure mercury lamp.

130

Cubylcarbinyl Bromide[81]: Cubylcarbinol (0.30 g, 2.24 mmol) and triphenyl-phosphine (1.19 g, 4.54 mmol) were stirred in dry methylene chloride (4 mL, passed through basic alumina and stored over sodium carbonate), at 0°C using an ice-water bath. A solution of carbon tetrabromide (0.86 g, 2.59 mmol) in dry methylene chloride (3 mL) was added dropwise at 0°C. The mixture was then stirred at room temperature for five hours. The reaction mixture was poured into pentane (35 mL) at -10°C, and filtered while cold. The residue was triturated with pentane (2 x 10mL). The pentane solutions were clarified and evaporated to dryness to produce a viscous oil. The oil was sucked dry and distilled on a high vacuum line at 0.1 Torr using a hair dryer to produce gentle heating. This produced colourless cubylcarbinyl bromide (0.18 g, 40.77%): ^1H NMR δ(CDCl$_3$): 4.00(m,1H), 3.89(m, 6H), 3.68(s, 2H) ppm.

EPR Spectra. The bromocubane (*ca.* 5 mg) was dissolved in di-*tert*-butyl peroxide (*ca.* 30 μL) and triethylsilane (*ca.* 20 μL). This solution was placed in a quartz tube and degassed on a high vacuum line by a series of freeze-pump-thaw cycles. The solvent (cyclopropane, *n*-propane or dichlorodifluoromethane) was distilled in and the tube sealed. Experiments were also carried out with hexamethylditin in place of triethylsilane, but this produced no well defined spectra. In the hydrogen abstraction experiments samples were prepared in a similar way but with no triethylsilane or hexamethylditin.

Chapter Five

Homolytic Reactions Of Cubane

5.0   Bridgehead Homolytic Reactions

The concept that certain substitution reactions can take place by means of electrically neutral radicals was originally put forward by D.H. Hey in 1934[106], and subsequently developed by Hey and Waters[107]. Reactions of this kind are classified as homolytic substitution reactions, thereby distinguishing them from the heterolytic substitution reactions brought about by electrophilic and nucleophilic species. The former, homolytic, process involves the combination of two entities which each contribute one electron (that is free neutral radicals and/or free atoms of diatomic molecules) to the new bond, as opposed to both electrons being supplied by only one of the two combining species (such as charged ions). The intermediate, or transition state, thus formed then eliminates an electrically neutral species (Figure 5.1).

$$R^{\bullet} \; + \; MX \longrightarrow [RM^{\bullet}X]$$

$$RM \; + \; X^{\bullet}$$
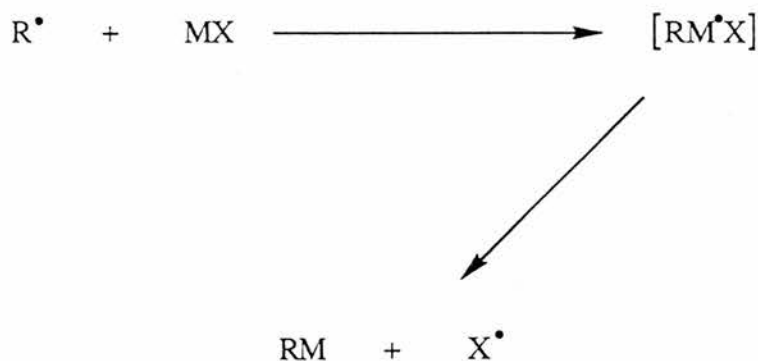
Figure 5.1

The S_H2 Reaction.

Bimolecular homolytic substitution (S_H2) reactions at saturated carbon atoms are rare, and the attacking radical must, with a few exceptions, be a halogen atom for this reaction to replace hydrogen abstraction. The main source of S_H2 reactions is

with highly strained cyclopropane structures which will rapidly undergo an intramolecular type of substitution by halogen atoms[108], and the pseudo-halogen *bis*(trifluoromethyl)aminoxyl[109] (Figure 5.2). In the latter case the displacement step involves scission of the highly strained three-membered ring.
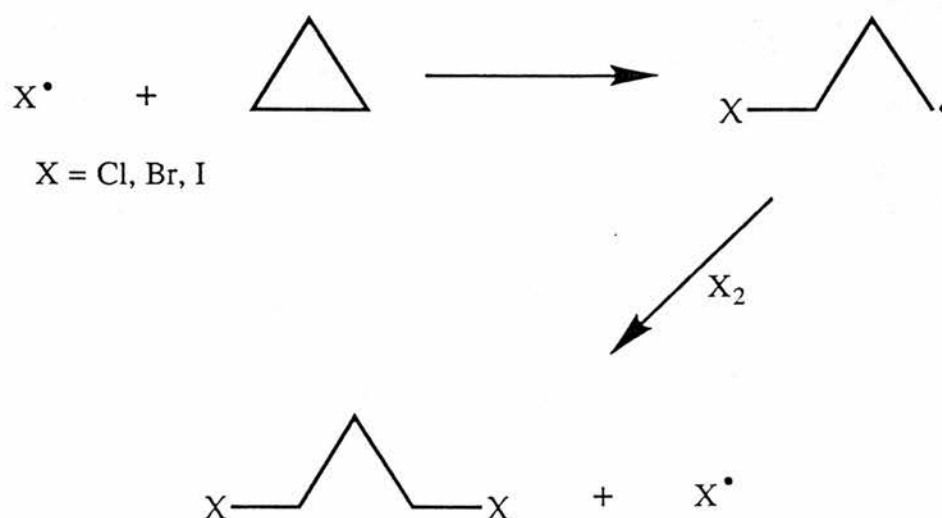
Figure 5.2

Homolytic substitution resulting in addition to cyclopropane.

Cyclobutane has a ring strain of 110 kJ mol^{-1} which is only a little less than that of cyclopropane (115 kJ mol^{-1})[110], so one might expect it to behave with halogen atoms in a similar fashion to cyclopropane. But this is not the case. Both chlorination[111] and bromination[112] of cyclobutane and its derivatives[113] proceed by straightforward abstraction of hydrogen. In fact the only S_H2 reaction of a cyclobutane ring which has been observed is that of fluorination of perfluorocyclobutane, which involves vibrationally excited species[114]. However, the potential for this type of process was increased with the discovery that halogen atoms will take part in homolytic reactions at the bridgehead carbon atoms in polycycloalkanes as long as they contain fused cyclobutane rings.

Photobromination of *cis*-bicyclo[2.2.0]hexane (Figure 5.3) proceeds rapidly

and cleanly, producing only two major products (*trans*-1,4-dibromocyclohexane and *cis*-1,4-dibromocyclohexane)[115] with just a minor amount of *trans*-1,2-dibromocyclohexane (due to a minor degree of electrophilic bromination). The mono-brominated products accounted for less than one percent of the total products. This high specificity in the formation of the 1,4-dibromocyclohexanes is indicative of an S_H2 attack by bromine atoms at the bridgehead carbon atoms as the initial step in the reaction.

57%   40%
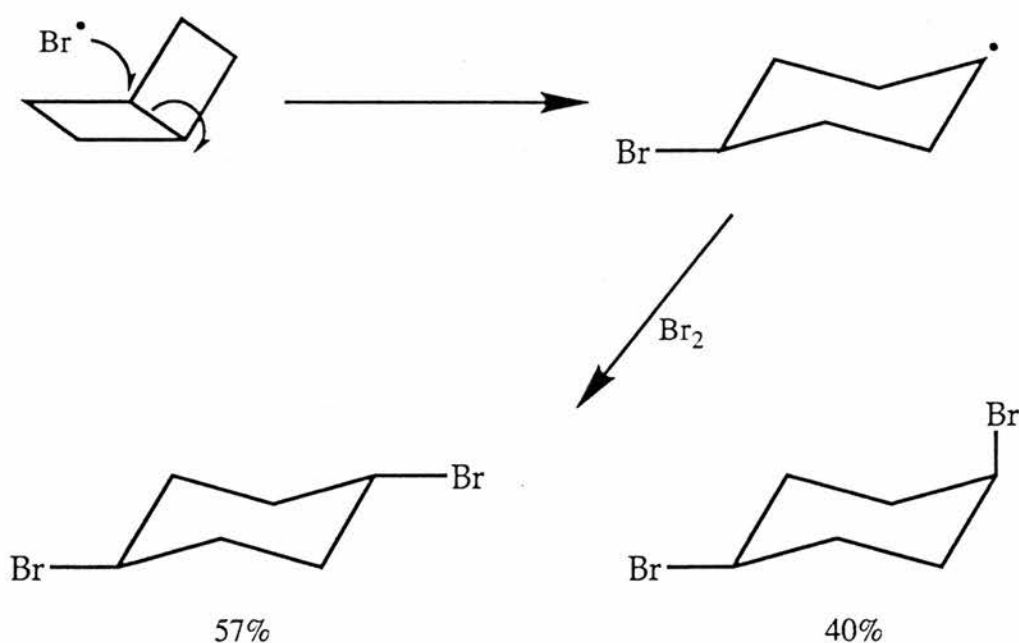
Figure 5.3

Photobromination of *cis*-bicyclo[2.2.0]hexane

showing the major products[115].

Chlorination of *cis*-bicyclo[2.2.0]hexane is not by any means as clean as the bromination. It produces a complex mixture of monochlorides and a whole range of unidentified dichlorides[116]. This demonstrated that in addition to the main hydrogen abstraction reactions of the photochlorination there may also be a contribution from the S_H2 process.

cis-Bicyclo[2.2.0]hexane has a high ring strain (217 kJ mol^{-1})[117], but this is not the only factor involved in producing this homolytic substitution behaviour. Spiro[3.3]heptane (Figure 5.4) is similar to *cis*-bicyclo[2.2.0]hexane in that it too is made up of two four-membered rings and possesses a high strain energy (approximately 220 kJ mol^{-1}). However, bromination of spiro[3.3]heptane took place exclusively by hydrogen abstraction and no S_H2 processes were observed[118]. An electron diffraction study has measured the C-1 to C-4 bond length in *cis*-bicyclo-[2.2.0]hexane at 1.577 Angstroms[119], which is unusually long. Theoretical studies have also indicated that this bond is bent and contains significantly less s-character than the carbon-carbon bonds of cyclobutane[117,120] (or spiro[3.3]heptane). Similarly the [n.2.2]propellanes, where n=2[121], 3[122] and 4[122], undergo halogenation across the central carbon-carbon bond. Thus it is expected that the S_H2 reaction will be standard for the photohalogenation of structures containing condensed cyclobutane rings.
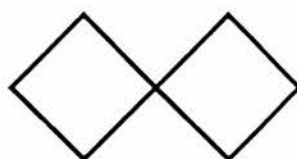
Figure 5.4

Spiro[3.3]heptane.

Even more amazing than the homolytic reactions of *cis*-bicyclo[2.2.0]hexane are these in which [1.1.1]propellanes take part in[123] (Figure 5.5). A whole range of radicals, including MeCO•, CCl$_3$•, PhS•, PhSe•, Bu^{t}O• and halogen atoms, have been seen to cleave the inter-ring bond to yield the substituted bicyclo[1.1.1]pentanes. This procedure is also a method for producing the bridgehead bicyclo[1.1.1]pentyl radical which in some instances substitutes at the quaternary carbon atom of the [1.1.1]propellane, with the dimers and even oligomers being isolated. Bicyclo-

[1.1.0]butane behaves in a comparable fashion, although with fewer initiating radicals, and in the cases of bicyclo[2.1.0]pentane and the [n.2.2]propellanes the inter-ring bond is only cleaved by halogen atoms.
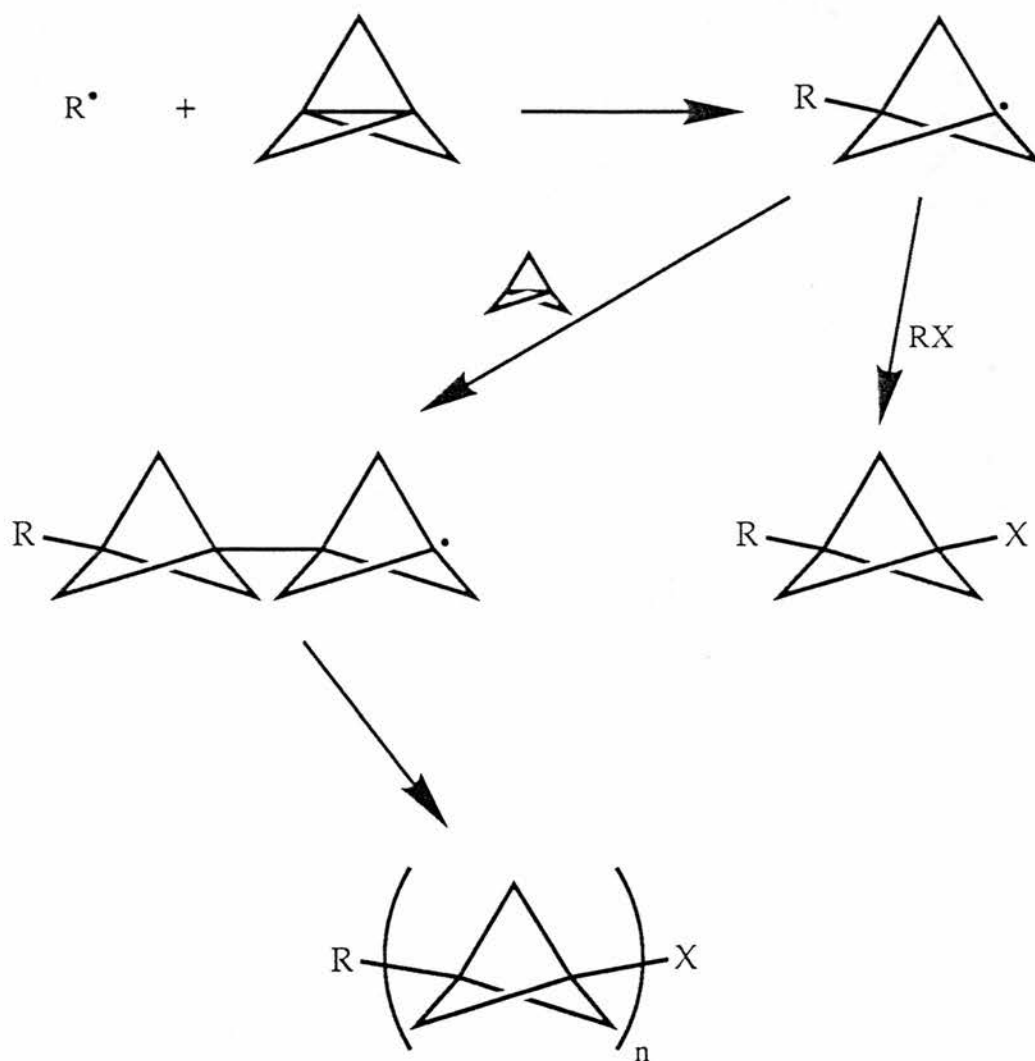
Figure 5.5

Homolytic substitution reactions involving [1.1.1]propellane.

5.1 Bimolecular Homolytic Substitution of Cubane

As mentioned above, [1.1.1]propellane undergoes a greater range of homolytic reactions than bicyclo[1.1.0]butane. The bridgehead carbon atoms of

[1.1.1]propellane are at the junction of three three-membered rings, as opposed to two three-membered rings in bicyclo[1.1.0]butane. A similar comparison can be made between cubane and *cis*-bicyclo[2.2.0]hexane. The bridgehead carbon atoms are at the juncture of three four-membered rings in cubane, whereas in *cis*-bicyclo[2.2.0] hexane they are between two four-membered rings. Therefore, based on this simple comparison, it seems reasonable to expect that as *cis*-bicyclo[2.2.0]hexane undergoes homolytic photobromination then cubane should also. Other points which favour the homolytic process in the case of cubane are its additional ring strain and the s-character of its carbon-carbon bonds. The exocyclic carbon-hydrogen bonds of cubane have a high s-character, with the result that the endocyclic carbon-carbon bonds have low s-character (Section 3.3). This (low s-character of the bonds) is expected to make them more susceptible to homolytic cleavage. The cubane structure contains a ring strain of approximately 21 kcal mol^{-1} per carbon-carbon bond, compared to 6.5 kcal mol^{-1} per bond in cyclobutane, which adds an extra driving force for the bond to cleave. Thus the homolytic substitution of cubane by free radical halogenation appeared to be a viable proposition and an experimental examination undertaken.

When one or two equivalents of molecular bromine, dissolved in degassed carbon tetrachloride, was added to a solution of cubane in degassed carbon tetrachloride at 25°C and photolysed with a tungsten lamp, the bromine colour faded and a white solid precipitated. Examination by NMR of the carbon tetrachloride solution remaining after filtration revealed the presence of unreacted cubane (especially when only one equivalent of bromine was used), but no bromocubane, which would be expected to form if the process involved the abstraction of a hydrogen atom. The white solid was purified by crystallisation and examined by NMR which showed that it was a highly symmetrical compound. This compound was eventually identified as *cis, cis*-tetrabromo-*syn*-tricyclo[4.2.0.0^{2,5}]octane and fully characterised (Experimental Section). A mechanism by which it may form is put forward in Figure 5.6.

The first S_H2 attack by a bromine atom induces homolytic cleavage of the cubane carbon-carbon bond, thereby forming a tetracyclo radical which rapidly undergoes a β-scission to produce the tricyclo[4.2.0.0^{2,5}]oct-3-enyl radical. This
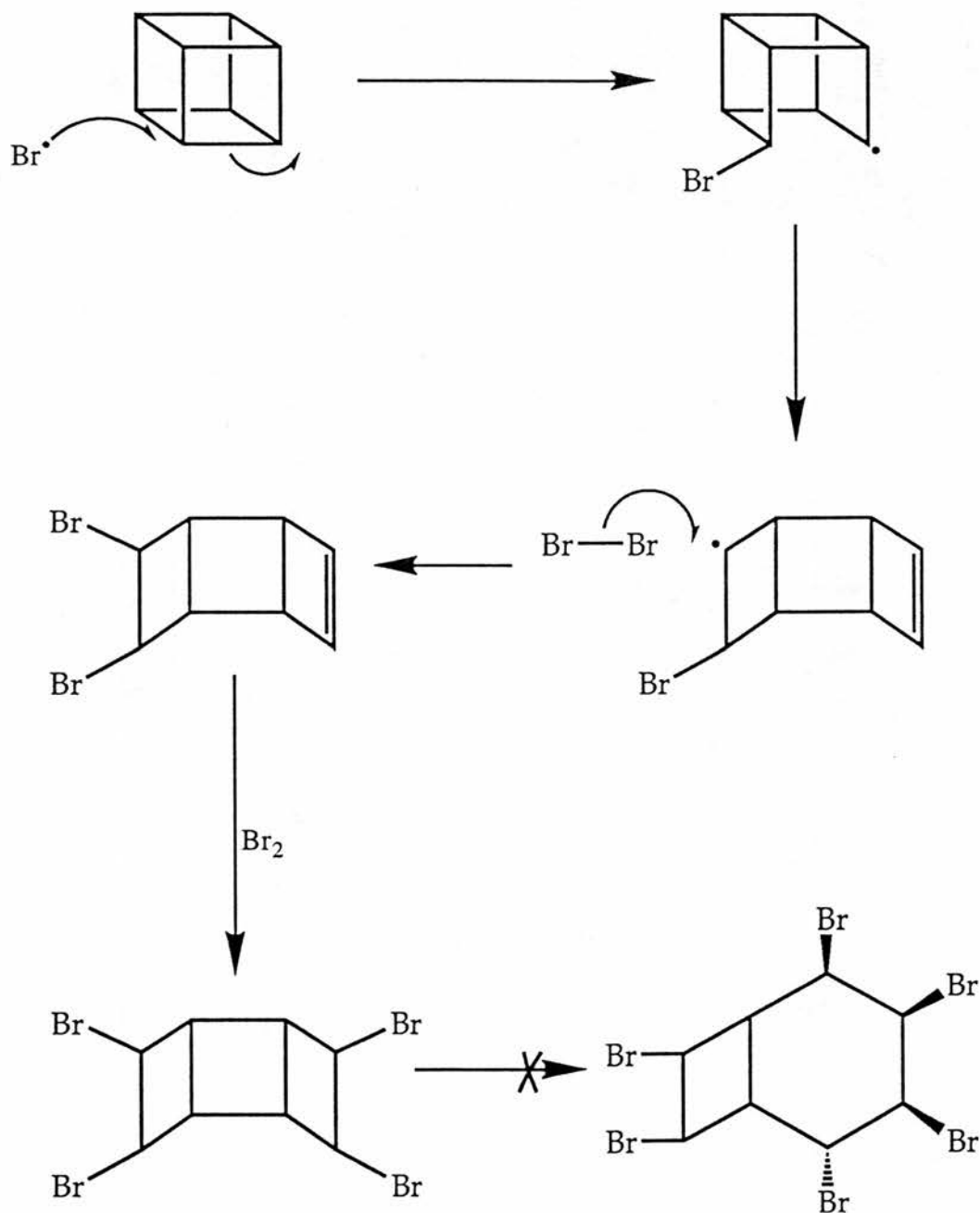
Figure 5.6

Homolytic substitution of cubane by bromine resulting in addition to

produce *cis,cis*-tetrabromo-*syn*-tricyclo[4.2.0.0^{2,5}]octane.

latter tricyclo radical is quickly trapped by bromine atom transfer from molecular bromine before it has the opportunity to rearrange further. The *syn* ring structure of the tricyclo[4.2.0.0^{2,5}]oct-3-enyl radical species shields the inner side of the structure and thus effectively prevents the bromine molecule from approaching *trans* to the carbon-hydrogen bond already in existence. As a result the dibromotricyclooctene is produced stereospecifically with the *cis* arrangement of the pair of bromine atoms. It should be noted that this *cis*-dibromotricyclooctene was never isolated, even when only one equivalent of bromine was used. The reason presumably is that the molecule rapidly adds a second bromine molecule, once again in a stereospecific manner (in the *cis* mode) due to one side of the double bond being screened by the *syn* cage structure. This deduction is totally consistent with the observation of unreacted cubane, and no dibromo products, in the solution after bromination had run its course. Thus, the production of one isomer only of the tetrabromo-*syn*-tricyclooctane follows logically from the initial S_H2 step. The conformation of this structure was irrefutably verified by X-ray crystal structure. A three dimensional image of this structure, based on the crystal structure data, is shown in Figure 5.7, with selected bond lengths and angles. The *syn* cage structure of the tetrabromotricyclooctane is obvious, as is the *cis* conformation of the two -CHBr-CHBr- fractions of the molecule.

The tetrabromo-*syn*-tricyclooctane product itself appears capable of undergoing a further homolytic substitution reaction to form the hexabromo compound (Figure 5.6), but none of this was isolated. This does not mean that this reaction does not occur, it may simply be that this step is too slow to observe, both because of the poor solubility of the tetrabromo product in the carbon tetrachloride and the crowded nature of the hexabromo compound.

E.W. Della and N.J. Head, our co-workers in Australia, looked at the chlorination of cubane in order to discover if it too involved an S_H2 process. They observed five major components, chlorocubane predominated with lesser quantities of cubane and a pair of isomeric dichlorocubanes also being identified. GC-MS analysis
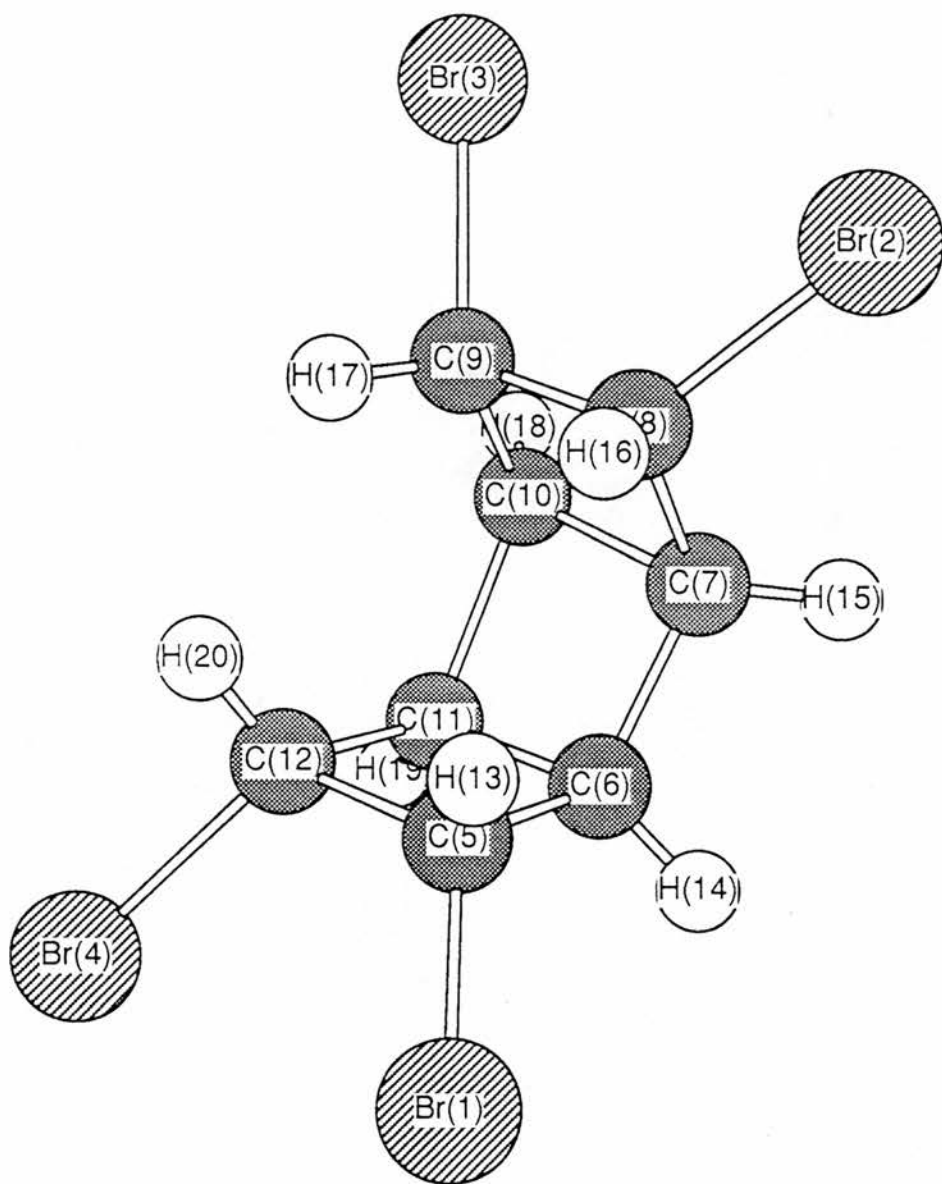
Figure 5.7

The structure of *cis, cis*-tetrabromo-*syn*-tricyclo[4.2.0.0^{2,5}]octane

Bond Lengths/Å		Bond Angles		Dihedral Angles	
Br(1)-C(5)	1.91	Br(1)-C(5)-C(12)	116.80	Br(1)-C(5)-C(6)-C(7)	-150.75
C(5)-C(6)	1.48	Br(1)-C(5)-C(6)	116.48	C(5)-C(6)-C(7)-C(8)	-1.05
C(5)-C(12)	1.60	C(12)-C(5)-C(6)	88.48	Br(1)-C(5)-C(12)-Br(4)	-0.45
C(6)-C(7)	1.52	C(5)-C(6)-C(11)	92.35		
		C(5)-C(6)-C(7)	123.70		
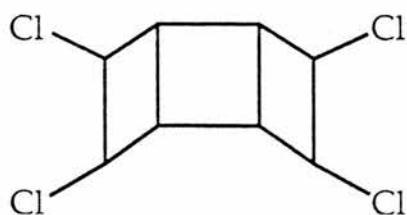
Figure 5.8

cis,cis-tetrachloro-*syn*-tricyclo[4.2.0.0^{2,5}]octane.

revealed the presence of a whole range of products with strong evidence for a tetrachloride, possibly the *cis,cis*-tetrachloro-*syn*-tricyclo[4.2.0.0^{2,5}]octane (Figure 5.8), in 2.3% yield. Therefore it can be seen that the main mode of reaction of the chlorine atoms was by hydrogen abstraction. The complexity of the chlorination of cubane, in comparison to the bromination, is in agreement with the behaviour of cyclopropane on halogenation. That is, the chlorination of cyclopropane was more complex than the bromination and hydrogen abstraction replaced the S_H2 process as the dominant reaction.
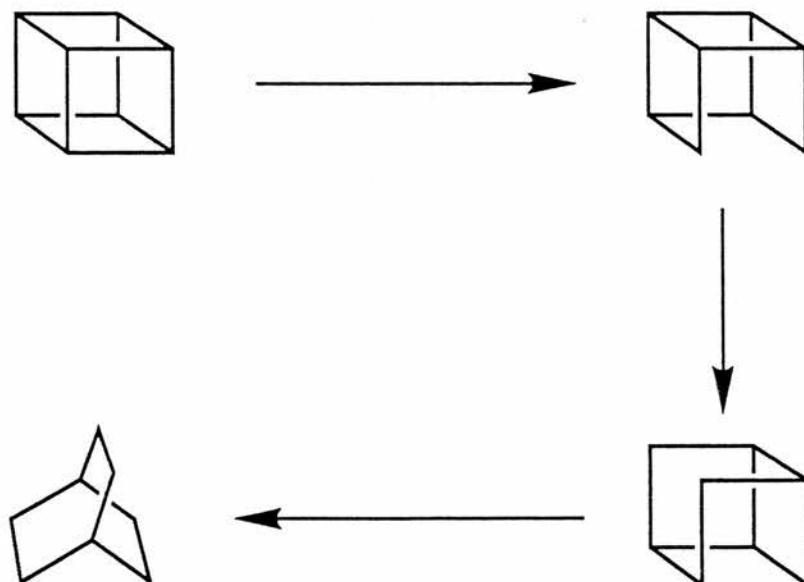
Figure 5.9

Sequential hydrogenolysis of cubane.

The ring opening sequence produced by the S_H2 bromination of cubane is in contrast with that brought about by hydrogenation[30]. As mentioned in Chapter Three, three cubane carbon-carbon bonds can undergo hydrogenolysis sequentially, these bonds being those which are the most highly strained. The opening of the cubane cage is thereby produced (Figure 5.9) in a very different way to that by bromination. Hydrogenolysis proceeds according to the release of the maximum amount of strain from the molecule, resulting in the relatively strain free bicyclo-[2.2.2]octane, whereas the bromination product is still a highly strained structure.

5.2   Conclusions

Unlike the species discussed in Chapter Four bromine atoms do not abstract hydrogen atoms from the cubane skeleton. They directly substitute at the cubyl carbon atom, thereby initiating a sequence of rearrangements which is terminated by the rapid bromine atom transfer to the tricyclo[4.2.0.0^{2,5}]oct-3-enyl radical to produce *cis,cis*-tetrabromo-*syn*-tricyclo[4.2.0.0^{2,5}]octane. In contrast to this is the behaviour of chlorine atoms with cubane. Chlorine atoms react with cubane almost entirely by the abstraction of hydrogen, with the possibility only of a small degree (2.3%) of homolytic substitution.

Thus the bromination of cubane is another example of an S_H2 reaction involving four-membered rings, further reinforcing the idea that homolytic substitution reactions are general for compounds containing condensed four-membered rings.

5.3   Experimental Section

[1]H (200MHz) and ^{13}C (50MHz) NMR were measured using a Varian Gemini-200 spectrometer. Mass spectra were recorded on a Kratos M25 RF spectrometer. Elemental analyses were carried out by the Australian Microanalytical Service[124]. Crystal structure data was measured by Dr. A.H. White at the University of Western Australia with a Nonius CAD-4 diffractometer, graphite monochromated

Mo *K*α radiation, ω/2θ scan mode, using the XTAL System of Crystallographic Programs (Hall and Stewart, 1990) for all computer calculations.

Photobromination of Cubane[124]. Bromine (90.0 mg, 0.56 mmol) in dry carbon tetrachloride (1 mL) was added to a solution of cubane (32.0 mg, 0.31 mmol) in degassed dry carbon tetrachloride (2mL) in an NMR tube. This was left exposed to daylight for 24 hours. The white solid (*cis, cis*-tetrabromo-*syn*-tricyclo-[4.2.0.0^{2,5}]-octane) which precipitated was filtered and recrystallised from methylene chloride (39.2 mg, 30%): melting point 223-224°C (decomposed); ^{1}H NMR δ(CDCl$_3$) 3.44 (s, 4H), 5.28 (s, 4H); ^{13}C NMR δ(CDCl$_3$) 47.46 (CH), 49.97 (CH); EIMS m/z (relative intensity) 266 (4), 264 (8), 262 (5), 185 (22), 184 (53), 183 (24), 182 (49), 169 (21), 104 (100), 103 (100), 78 (95), 77 (82), 69 (37), 52 (38), 51 (3), 50 (45); Elemental Analysis calculated for C$_8$H$_8$Br$_4$: C 22.7%, H 1.9%, found to be : C 22.6%, H 2.1%. The structure was confirmed by an X-ray diffraction study. The crystal was a colourless prism of poor quality and gave poor data (final R=0.117), but fully confirmed the structure as *cis, cis*-tetrabromo-*syn*-tricyclo-[4.2.0.0^{2,5}]-octane. The supernatant liquid was examined by ^{1}H and ^{13}C NMR which showed cubane but no other significant products, and in particular no bromocubane.

Photochlorination of Cubane (carried out by Nicholas J. Head, Flinders University, South Australia). Chlorine gas was passed through carbon tetrachloride (10 mL) at 0°C for 1 hour. The solution was allowed to attain room temperature. An aliquot was removed and found to be 2.3M in chlorine by titration[125]. To cubane (50.0 mg, 0.48 mmol) in an NMR tube was added dropwise the chlorine solution (0.4 mL, 0.92 mmol). A vigorous reaction ensued leaving a colourless solution. GC-MS analysis showed the solution to contain cubane (14.0%) , chlorocubane (28.0%) (identified by comparison of its mass spectrum and retention time with that of an authentic sample): EIMS m/z (relative intensity) [C$_8$H$_6$Cl$_2$-1]$^+$: 173 (0.3), 171

(0.4), 148 (6), 146 (8), 114 (5), 112 (17), 102 (100); and a species tentatively assigned as *cis, cis*-tetrachloro-*syn*-tricyclo[4.2.0.0^{2,5}]octane (2.3%): EIMS <u>m/z</u> (relative intensity) [C$_8$H$_8$Cl$_4$]$^+$: 213 (6), 211 (4), 209 (22), 177 (10), 175 (63), 173 (100), 147 (52), 113 (94).

Part Two References

1. Heath, T. *A History Of Greek Mathematics* ; Oxford University Press, London, 1976; Vols. I and II.

2. Rauscher, G. ; Clark, T. ; Poppinger, D. ; Schleyer, P. von R. *Angew. Chem., Int. Ed. Engl.*, **1978**, *17*, 276.

3. (a) Maier,G. ; Pfriem, S. ; Schaffer,U. ; Matusch,R. *Angew. Chem., Int. Ed. Engl.*, **1978**, *17*, 520.   (b) Maier, G. ; Pfriem, S. *Angew. Chem., Int. Ed. Engl.*, **1978**, *17*, 519.

4. (a) Eaton, P.E. ; Cole, T.W., Jr. *J. Am. Chem. Soc.*, **1964**, *86*, 962.   (b) Eaton, P.E. ; Cole, T.W., Jr. *J. Am. Chem. Soc.*, **1964**, *86*, 3157.

5. (a) Ternansky, R.J. ; Balogh, D.W. ; Paquette, L.A. *J. Am. Chem. Soc.*, **1982**, *104*, 4503.   (b) Paquette, L.A. ; Ternansky, R.J. ; Balogh, D.W. ; Kentgen, G. *J. Am. Chem. Soc.*, **1983**, *105*, 5446.   (c) Fessner, W.-D. ; Murty, B.A.R.C. ; Worth, J. ; Hunkler, D. ; Fritz, H. ; Prinzbach, H. ; Roth, W.D. ; Schleyer, P. von R. ; McEwan, A.B. ; Maier, W.F. *Angew. Chem., Int. Ed. Engl.*, **1987**, *26*, 452.

6. (a) Sheulin, P.B. ; Wolff, A.P. *J. Am. Chem. Soc.*, **1971**, *92*, 5291.   (b) Staab, H.A. ; Wehninger, E. ; Thorwart, W. *Chem. Ber.*, **1972**, *105*, 2590; and References therein.

7. Engler, E.M. ; Andose, J.D. ; Schleyer, P. von R. *J. Am. Chem. Soc.*, **1973**, *95*, 8005.   By subtraction of ΔH_f from the strain-free enthalpy of formation herein.

8. Gasteiger, J. ; Dammer, O. *Tetrahedron*, **1978**, *34*, 2939.

9. Paquette, L.A. ; Ternansky, R.J. ; Balogh, D.W. *J. Am. Chem. Soc.*, **1982**, *104*, 4502.

10. (a) Paquette, L.A. ; Balogh, D.W. ; Usha, R. ; Kountz, D. ; Christoph, G.G. *Science*, **1981**, *211*, 575.   (b) Paquette, L.A. ; Balogh, D.W. *J. Am. Chem. Soc.*, **1982**, *104*, 774.

11. Gleiter, R. ; Heilbronner, E.; Hekman, M. ; Martin, H.-D. *Chem. Ber.*, **1973**, *106*, 28.

12. Bodor, N. ; Chen, B.H. ; Worley, S.D. *J. Electron Spectrosc.*, **1974**, *4*, 65.

13. Spanget-Larsen, J. ; Gleiter, R. ; Paquette, L.A. ; Carmody, M.J. ; Dagenhandt, C.R. *Theor. Chim. Acta.*, **1978**, *50*, 145.

14. Osawa, E. ; Aigami, K. ; Inamoto, Y. *J. Org. Chem.*, **1977**, *42*, 2621.

15. Pelosi, L.F. ; Miller, W.T. *J. Am. Chem. Soc.*, **1976**, *98*, 4311.

16. Barborak, J.C. ; Watts, L. ; Pettit, R. *J. Am. Chem. Soc.*, **1966**, *88*, 1328.

17. Eaton, P.E. ; Cole, T.W., Jr. *J. Chem. Soc., Chem. Commun.*, **1970**, 1493.

18. Chenier, P.J. *J. Chem. Educ.*, **1978**, *55*, 286.

19. Chapman, N.B. ; Key, J.M. ; Toyne, K.J. *J. Org. Chem.*, **1970**, *35*, 3860.

20. Luh, T.-Y. ; Stock, L.M. *J. Org. Chem.*, **1972**, *37*, 338.

21. Marchand, A.P. *Chem. Rev.*, **1989**, *89*, 1011.

22. (a) Moriarty, R.M. ; Khosrowshahi, J.S. ; Dalecki, T.M. *J. Chem. Soc., Chem. Commun.*, **1987**, 675.   (b) Moriarty, R.M. ; Khosrowshahi, J.S. ; Awasthi, A.K. ; Penmasta, R. *Synth. Commun.*, **1988**, *18*, 1179.

23. Eaton, P.E. ; Cunkle, G.T. *Tetrahedron Lett.*, **1986**, *27*, 6055.

24. (a) Eaton, P.E. ; Castaldi, G. *J. Am. Chem. Soc.*, **1985**, *107*, 724.   (b) Eaton, P.E. ; Cunkle, G.T. ; Marchioro, G. ; Martin, R.M. *J. Am. Chem. Soc.*, **1987**, *109*, 948.

25. Della, E.W. ; Tsanaktisidis, J. *Organometallics*, **1988**, *7*, 1178.

26. Marchand, A.P. *Tetrahedron*, **1988**, *44*, 2377.

27. Kybett, B.D. ; Carroll, S. ; Natalis, P. ; Bonnell, D.W. ; Margrave, J.L. ; Franklin, J.L. *J. Am. Chem. Soc.*, **1966**, *88*, 626.

28. Eaton, P.E. *Tetrahedron*, **1979**, *35*, 2189.

29. Klunder, A.J.H. ; Ariaans, G.J.A. ; Van der Loop, E.A.R.M. ; Zwanenburg, B. *Tetrahedron*, **1986**, *42*, 1903.

30. (a) Stober, R. ; Musso, H. *Angew. Chem., Int. Ed. Engl.*, **1977**, *16*, 415.

(b) Stober, R. ; Musso, H. ; Osawa, E. *Tetrahedron*, **1986**, *42*, 1757.

31. Klunder, A.J.H. ; Zwanenburg, B. *Tetrahedron*, **1973**, *29*, 1683.

32. Klunder, A.J.H. ; Zwanenburg, B. *Tetrahedron*, **1975**, *31*, 1419.

33. (a) Martin, H.-D. ; Pfohler, P. ; Urbanek, T. ; Walsh, R. *Chem. Ber.*, **1983**, *116*, 1415. (b) Martin, H.-D. ; Urbanek, T. ; Pfohler, P. ; Walsh, R. *J. Chem. Soc., Chem. Commun.*, **1985**, 964.

34. Eaton, P.E. ; Krebs, E.-P. *unpublished results*.

35. Gassman, P.G. ; Yamaguchi, R. ; Koser, G.F. *J. Org. Chem.*, **1978**, *43*, 4392.

36. Cassar, L. ; Eaton, P.E. ; Halpern, J. *J. Am. Chem. Soc.*, **1970**, *92*, 6366.

37. Cassar, L. ; Eaton, P.E. ; Halpern, J. *J. Am. Chem. Soc.*, **1970**, *92*, 3515.

38. (a) Klunder, A.J.H. ; Zwanenburg, B. *Tetrahedron*, **1972**, *28*, 4131. (b) Edward, J.T. ; Farrell, P.G. ; Langford, G.E. ; *J. Am. Chem. Soc.*, **1976**, *98*, 3075.

39. Abeywickrema, R.S. ; Della, E.W. *J. Org. Chem.*, **1980**, *45*, 4226.

40. (a) Eaton, P.E. ; Shankar, B.K.R. ; Price, G.D. ; Pluth, J.J. ; Gilbert, E.E. ; Alster, J. ; Sandus, O. *J. Org. Chem.*, **1984**, *49*, 185. (b) Eaton, P.E. ; Wicks, G.E. *J. Org. Chem.*, **1988**, *53*, 5353.

41. Della, E.W. ; Tsanaktsidis, J. *Aust. J. Chem.*, **1986**, *39*, 2061.

42. Dunn, G.L. ; Hoover, J.R.E. (Smith, Kline, and French Laboratories), British Patent 1 068 655 ; US Patents 3 418 368, 3 538 160, 3 542 868, and 3 562 317 ; *Chem. Abstr.*, **1968**, *68*, 2640m.

43. Gregory, W.A. (E.I. du Pont de Nemours and Co.), US Patent 3 558 704 ; *Chem. Abstr.*, **1971**, *74*, P141105c.

44. Fleischer, E.B. *J. Am. Chem. Soc.*, **1964**, *86*, 3889.

45. Della, E.W. ; Hine, P.T. ; Patney, H.K. *J. Org. Chem.*, **1977**, *42*, 2940.

46. Luh, T.-T. ; Stock, L.M. *J. Am. Chem. Soc.*, **1974**, *96*, 3712.

47. Edward, J.T. ; Farrell, P.G. ; Langford, G. *J. Am. Chem. Soc.*, **1976**, *98*, 3085.

48.   (a) Bodor, N. ; Dewar, M.J.S. ; Worley, S.L. *J. Am. Chem. Soc.*, **1970**, *92*, 19.   (b) Bischof, P. ; Eaton, P.E. ; Gleiter, R. ; Heilbronner, E. ; Jones, T.B. ; Musso, J. ; Schmelzer, A. ; Stober, R. *Helv. Chim. Acta.*, **1978**, *61*, 547.

49.   (a) Rice, S.A. ; Jortner, J. *unpublished results.*   (b) King, J.M. *M.S. Thesis*, **1975**, University of Atlanta, Atlanta.

50.   Gross, M.L. *Org. Mass Spectrom*, **1972**, *6*, 827.

51.   Cole, T.W., Jr. ; Mayers, C.J. ; Stock, L.M. *J. Am. Chem. Soc.*, **1974**, *96*, 4555.

52.   Edward, J.T. ; Farrell, P.G. ; Langford, G.E. *J. Org. Chem.*, **1977**, *42*, 1957.

53.   Muller, N. ; Pritchard, D.E. *J. Chem. Phys.*, **1959**, *31*, 768, 1471.

54.   Fleming, I. ; Williams, D.H. *Tetrahedron*, **1967**, *23*, 2747.

55.   Sternhell, S. *Quart. Rev., Chem. Soc.*, **1969**, *23*, 236.

56.   Kevill, D.N. ; Malcolm, J.D.S. ; Moriarty, R.M. ; Tuladhar, S.M. ; Penmasta, R. ; Awasthi, A.K. *J. Chem. Soc., Chem. Commun.*, **1990**, 623.

57.   The pyramidalisation angle is defined as $90-\theta$, where θ is any one of the three equal angles between the three bonds from the cation carbon and the z-axis which passes through it (taking the x and y axes to be in the plane of a planar cation); cf. Radziszewski, P. ; Jawdosiuk, M. ; Kovacic, P. ; Michl, J. *J. Am. Chem. Soc.*, **1984**, *106*, 7996.

58.   Eaton, P.E. ; Maggini, M. *J. Am. Chem. Soc.*, **1988**, *110*, 7230.

59.   Klunder, A.J.H. ; Zwanenburg, B. *Tetrahedron*, **1972**, *28*, 4131.

60.   Reddy, D.S. ; Sollot, G.P. ; Eaton, P.E. *J. Org. Chem.*, **1989**, *54*, 722.

61.   (a) Eaton, P.E. ; Yang, C.-X. ; Xiong, Y. *J. Am. Chem. Soc.*, **1990**, *112*, 3225.   (b) Moriarty, R.M. ; Tuladhar, S.M. ; Penmasta, R. ; Awasthi, A.K. *J. Am. Chem. Soc.*, **1990**, *112*, 3228.

62.   Hrovat, D.A. ; Borden, W.T. *J. Am. Chem. Soc.*, **1990**, *112*, 3227.

63.   Wiberg, K.B. ; Hess, B.A., Jr. ; Ashe, A.A.III In *Carbonium Ions* ; Olah,

G.A., Schleyer, P. v.R., Eds. ; Wiley-Interscience: New York, **1972**; Vol. III, pp 1295 ff.

64.   Mergelsberg, I. ; Langhals, H. ; Ruchardt, C. *Chem. Ber.*, **1983**, *116*, 360.

65.   Koenig, T. ; Balle, T. ; Snell, W. *J. Am. Chem. Soc.*, **1975**, *97*, 662.

66.   Lloyd, R.V. ; Wood, D.E. *J. Am. Chem. Soc.*, **1975**, *97*, 5986.

67.   Lisle, J.B. ; Williams, L.F. ; Wood, D.E. *J. Am. Chem. Soc.*, **1976**, *98*, 227.

68.   Krusic, P.J. ; Meakin, P. *J. Am. Chem. Soc.*, **1976**, *98*, 228.

69.   Walton, J.C. *J. Chem. Soc., Perkin Trans. 2*, **1987**, 231.

70.   Bank, S. ; Cleveland, W.K.S. ; Griller, D. ; Ingold, K.U. *J. Am. Chem. Soc.*, **1979**, *101*, 3409.

71.   Della, E.W. ; Elsey, G.M. ; Head, N.J. ; Walton, J.C. *J. Chem. Soc., Chem. Commun.*, **1990**, 1589.

72.   For a recent review of bridgehead radicals see Walton, J.C. *Chem. Soc. Rev.*, **1992**, 105.

73.   (a) Lorand, J.P. ; Chodroff, S.D. ; Wallace, R.W. *J. Am. Chem. Soc.*, **1968**, *90*, 5266.   (b) Fort, R.C., Jr. ; Franklin, R.E. *J. Am. Chem. Soc.*, **1968**, *90*, 5267.   (c) Humphrey, L.B. ; Hodgson, B. ; Pincock, R.E. *Can. J. Chem.*, **1968**, *46*, 3099.

74.   Herwig, K. ; Lorenz, P. ; Ruchardt, C. *Chem. Ber.*, **1975**, *108*, 1421.

75.   (a) Baker, F.W. ; Holtz, H.D. ; Stock, L.M. *J. Org. Chem.*, **1963**, *28*, 514. (b) Herwig, K. ; Ruchardt, C. *Chem. Ber.*, **1972**, *105*, 363.

76.   Luh, T.-Y. ; Stock, L.M. *J. Org. Chem.*, **1978**, *43*, 3271.

77.   Giese, B. *Angew. Chem., Int. Ed. Engl.*, **1976**, *15*, 173.

78.   Knight, L.B., Jr. ; Arrington, C.A. ; Gregory, B.W. ; Cobranchi, S.T. *J. Am. Chem. Soc.*, **1987**, *109*, 5521.

79.   Reddy, D.S. ; Maggini, M. ; Tsanaktsidis, J. ; Eaton, P.E. *Tetrahedron Lett.*, **1990**, *31*, 805.

80.   MINDO/3 shows the difference in the heats of formation of the cubylcarbinyl

cation and the homocubyl cation to be about 18 kcal mol^{-1}, in favour of the latter; the corresponding radicals differing by about 20 kcal mol^{-1}, in the same direction.

81.   Eaton, P.E. ; Yip, Y.C. *J. Am. Chem. Soc.*, **1991**, *113*, 7692.

82.   (a) Castaing, M. ; Pereyre, M. ; Ratier, M. ; Blum, P.M. ; Davies, A.G. *J. Chem. Soc.*, **1979**, 287.   (b) Beckwith, A.L.J. ; Moad, G. *J. Chem. Soc.*, **1980**, 1083.   (c) Ingold, K.U. ; Maillard, B. ; Walton, J.C. *J. Chem. Soc.*, **1981**, 970.

83.   Newcomb, M. ; Manek, M.B. *J. Am. Chem. Soc.*, **1990**, *112*, 9662.

84.   Newcomb, M. ; Glenn, A.G. *J. Am. Chem. Soc.*, **1989**, *111*, 275.

85.   (a) Della, E.W. ; Head, N.J. *J. Org. Chem.*, in press.   (b) Della, E.W. ; Tsanaktsidis, J. *Aust. J. Chem.*, **1989**, *42*, 61.   (c) Key, J. Ph.D. Dissertation, University of Hull, East Yorkshire, 1968.

86.   Della, E.W. ; Head, N.J. ; Mallon, P. ; Walton, J.C. *J. Am. Chem. Soc.*, submitted 1992.

87.   Cole, T.W., Jr. Ph.D. Dissertation, University of Chicago, Chicago, Illinois, 1966.

88.   McMillen, D.F. ; Golden, D.M. *Ann. Rev. Phys. Chem.*, **1982**, *33*, 493.

89.   McKinley, A.J. ; Michl, J. ; Eaton, P.E. ; Zhou, J.P. Unpublished Work.

90.   Seetula, J.A. ; Russell, J.J. ; Gutman, D. *J. Am. Chem. Soc.*, **1990**, *112*,1347.

91.   (a) Bernlohr, W. ; Flamm-ter Meer, M.A. ; Kaiser, J.H. ; Schmittel, M. ; Beckhaus, H.-D. ; Ruchardt, C. *Chem. Ber.*, **1986**, *119*, 1911.   (b) Walton, J.C. *Mag. Res. Chem.*, **1987**, *25*, 998.

92.   Bromocubane and 4-fluorocubanyl bromide were looked at by E.W. Della and J.C. Walton in previous work, but it has been included here for comparison. See reference 71.

93.   Kawamura, T. ; Tsumura, M. ; Yokomichi, Y. ; Yonezawa, T. *J. Am. Chem. Soc.*, **1977**, *99*, 8251.

94. (a) Krusic, P.J. ; Kochi, J.K. *J. Am. Chem. Soc.*, **1969**, *91*, 3938. (b) Jackson, R.A. *J. Chem. Soc., Perkin Trans. 2*, **1983**, 523.

95. Barker, P.J. ; Davies, A.G. ; Henriques, R. ; Nedelec, J.-Y. *J. Chem. Soc., Perkin Trans. 2*, **1982**, 745.

96. Freeman, P.K. ; Ziebarth, T.D. *J. Org. Chem.*, **1976**, *41*, 949.

97. Russell, G.A. *Radical Ions*, Kaiser, E.T. , Kevan, L, Ed.s, Interscience, New York.

98. King, F.W. *Chem. Rev.*, **1976**, *76*, 157.

99. (a) Meinwald, J. ; Lewis, A. *J. Am. Chem. Soc.*, **1961**, *83*, 2769. (b) Jefford, C.W. ; Waegell, B. ; Ramey, K. *J. Am. Chem. Soc.*, **1965**, *87*, 2191.

100. Lunazzi, L. ; Placucci, G. ; Grossi, L. *J. Chem. Soc., Perkin Trans. 2*, **1980**, 1063.

101. Maillard, B. ; Walton, J.C. *J. Chem. Soc., Perkin Trans. 2*, **1985**, 443.

102. Della, E.W. ; Schiesser, C.H. ; Taylor, D.K. ; Walton, J.C. *J. Chem. Soc., Perkin Trans. 2*, **1991**, 1329.

103. Nonhebel, D.C. ; Suckling, C.J. ; Walton, J.C. *Tetrahedron Lett.*, **1982**, *23*, 4477.

104. Krusic, P.J. ; Jesson, J.P. ; Kochi, J.K. *J. Am. Chem. Soc.*, **1969**, *91*, 4566.

105. Griller, D. ; Ingold, K.U. *Acc. Chem. Res.*, **1980**, *13*, 317.

106. Hey, D.H. *J. Chem. Soc.*, **1934**, 1966.

107. Hey, D.H. ; Waters, W.A. *Chem. Rev.*, **1937**, *21*, 169.

108. (a) Tedder, J.M. ; Walton, J.C. *Adv. Free-Radical Chem.*, **1980**, *6*, 155. (b) Thaler, W.A. *Methods Free-Radical Chem.*, **1969**, *2*, 121. (c) Poutsma, M.L. *Methods Free-Radical Chem.*, **1969**, *1*, 79.

109. Anpo, M. ; Chatgilialoglu, C. ; Ingold, K.U. *J. Org. Chem.*, **1983**, *48*, 4104.

110. Benson, S.W. *"Thermochemical Kinetics"*, Second Edn., Wiley, New York,

1976, p.273.

111. Walling, C. ; Mayahi, M.F. *J. Am. Chem. Soc.*, **1959**, *81*, 1485.

112. Ferguson, K.C. ; Whittle, E. *Trans. Faraday Soc.*, **1971**, *67*, 2618.

113. (a) Nevill, W.A. ; Frank, D.A. ; Trepka, R.D. *J. Org. Chem.*, **1962**, *27*, 422. (b) Ashton, D.S. ; Tedder, J.M. *J. Chem. Soc., Perkin Trans. 2*, **1972**, 2965. (c) Ashton, D.S. ; Singh, H. ; Tedder, J.M. ; Walton, J.C. ; Watt, E.A. *J. Chem. Soc., Perkin Trans. 2*, **1973**, 125.

114. Levy, J.B. ; Kennedy, R.C. *J. Am. Chem. Soc.*, **1974**, *96*, 4791.

115. Walton, J.C. *J. Chem. Soc., Chem. Commun.*, **1987**, 1252.

116. Srinivasan, R. ; Sonntag, F.I. *Tetrahedron Lett.*, **1967**, 603.

117. Wiberg, K.B. ; Wendoloski, J.J. *J. Am. Chem. Soc.*, **1982**, *104*, 5679.

118. Roberts, C. ; Walton, J.C. ; Maillard, B. *J. Chem. Soc., Perkin Trans. 2*, **1986**, 305

119. Andersen, B. ; Srinivasan, R. *Acta. Chem. Scand.*, **1972**, *26*, 3468.

120. (a) Harano, K. ; Ban, T. ; Yasuda, M. ; Osawa, E. ; Kanematsu, K. *J. Am. Chem. Soc.*, **1981**, *103*, 2310. (b) Wiberg, K.B. ; Bader, R.F. ; Lau, C.D.H. *J. Am. Chem. Soc.*, **1987**, *109*, 985, 1001.

121. Eaton, P.E. ; Temme III, G.H. *J. Am. Chem. Soc.*, **1973**, *95*, 7508.

122. Eaton, P.E. ; Nyi, K. *J. Am. Chem. Soc.*, **1971**, *93*, 2786.

123. (a) Wiberg, K.B. ; Waddell, S.T. ; Laidig, K. *Tetrahedron Lett.*, **1986**, 1553. (b) Friedli, A.C. ; Kaszynski, P. ; Michl, J. *Tetrahedron Lett.*, **1989**, 455. (c) Kaszynski, P. ; Michl, J. *J. Am. Chem. Soc.*, **1988**, *110*, 5225. (d) Murthy, G.S. ; Hassenruck, K. ; Lynch, V.M. ; Michl, J. *J. Am. Chem. Soc.*, **1989**, *111*, 7262.

124. The photobromination was repeated by our Australian co-workers due to insufficient starting cubane being present in St. Andrews. Hence the elemental analysis and crystal structure were carried out in Australia.

125. Taylor, N.W. ; Hildebrand, J.H. *J. Am. Chem. Soc.*, **1923**, *45*, 682.

Part Three:

The Behaviour of

Fullerene Radicals.

Chapter Six

Introduction to the Chemistry and Properties
of Fullerenes

In 1985, during their mass spectral studies of laser ablated graphite, Kroto, Smalley and co-workers[1] observed a stable carbon cluster molecular ion, which appeared to consist of sixty carbon atoms.   The structure which they subsequently postulated was made up of pentagons and hexagons only, which closed to form a cage.   This structure was based upon the geodesic domes designed by R. Buckminster Fuller, the American engineer and philosopher, and named Buckminsterfullerene.[1]   Thus a new class of closed-caged carbon molecules, now termed "Fullerenes", was born.   Other names put forward for the C_{60} molecule have been: soccerballene, soccerene, footballene, carbon-s-icosahedron,[2] follene-60[3] (derived from the Latin "follis" meaning football) and the slang term "buckyballs". However, here we will refer to C_{60} as fullerene-60 and C_{70} as fullerene-70, and so on for other molecules in the fullerene series.

As has previously been mentioned, synthetic organic chemists are now able to synthesise three out of the five Platonic solids, these being tetrahedrane, cubane and dodecahedrane (Chapter 3).   In contrast, similar attention has not been given to the synthesis of the members of the family of Archimedean solids.   Archimedean solids are defined as being semi-regular polyhedra which are facially regular (*i.e.* each face is a regular polygon), but the faces are not all of the same sized polygon.   Despite this, the vertices are all congruent, that is, they are all identical.   For example, in the fullerene-60 structure every vertex joins two hexagons and one pentagon.

It can be proved geometrically that only thirteen non-trivial Archimedean solids exist; thus fullerene-60 is just one of a number of Archimedean solids which may be realised in molecular form by assembling sp^2 hybridized carbon atoms.   Of these thirteen, only seven have three-fold coordinated vertices, that is, three edges

meeting at each vertex. These are the obvious candidates for aromatic molecules made up exclusively of carbon. Three of these contain three-membered rings which, from the point of view of chemical bonding, are unfavourable and can therefore be ruled out. Of the four remaining, there is the truncated icosahedron which is composed of sixty vertices arranged in twelve pentagonal and twenty hexagonal rings (thus observing the Euler principle, which states that twelve pentagons are required to close a network and that hexagons alone will not suffice). This structure already being realised in fullerene-60 (Figure 6.1) possesses a large aromatic delocalisation energy. The remaining three structures all contain four-membered rings connected to hexagonal rings, and in two cases connected to larger rings. The mathematical names of these solids are: the truncated octahedron (24 vertices); the truncated cuboctahedron (48 vertices); and the truncated icoidodecahedron (120 vertices). The structure of the latter, dubbed "Archimedene", has been postulated by Haymet[4].

Fullerene-60 is a mustard coloured solid that appears brown or black as the thickness of the film increases. It is sparingly soluble in several organic solvents (such as methylene chloride and tetrahydrofuran), especially in aromatic hydrocarbons (eg. benzene and toluene) and forms magenta coloured solutions. Fullerene-70 is a reddish brown solid, with thick films being a greyish black and its solutions a deep red (likened to red port wine). Solutions of mixtures of fullerene-60 and -70 are red because fullerene-70 is more intensely coloured than fullerene-60. Both compounds are crystalline with high melting points (greater than 280 °C).

Due to the shape of fullerene-60, and to a lesser extent fullerene-70, it is not unreasonable to envisage the crystal structure as closely packed. This is demonstrated by the rate at which fullerenes dissolve. Despite both fullerene-60 and -70 being ultimately quite soluble (fullerene-60 the more so), they are in fact slow to dissolve (regardless of solvent), reflecting the efficiency of the close packing achieved. Fullerene-60 crystalises in the form of both needles and plates. The needles arise from a series of overlapping plates, whereas the plates are a mixture of squares, triangles and trapezia.
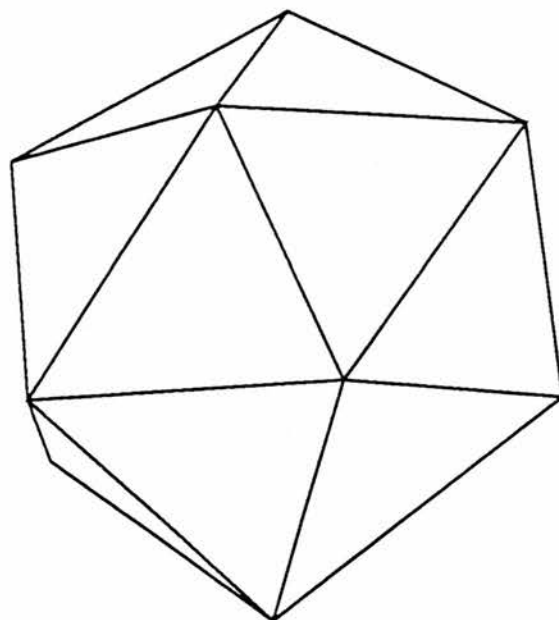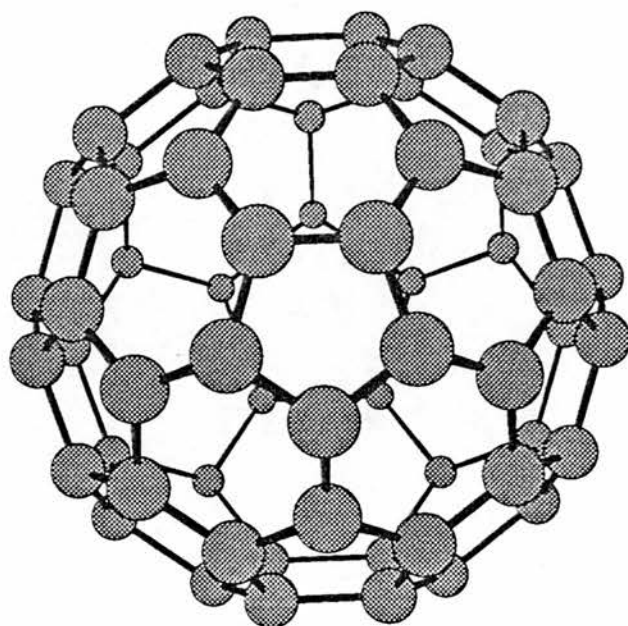
Figure 6.1.

Fullerene-60, the truncated icosahedron (top).

The icosahedron, the underlying symmetry of fullerene-60 (bottom).

Finally, it should be pointed out that the rate at which work concerning the fullerenes is published is phenomenal. Consequently this section may be outdated in certain areas, as it reviews the literature to the end of March 1992.

156

6.1 Methods of Preparation of Fullerene-60 and -70

In the original work of Kroto et al.[1], which showed how conditions could be achieved to produce a signal in which the fullerene-60 peak was dominant, the pulsed nozzle / laser vaporization technique[5] was used to produce carbon clusters from a graphite target. These clusters were expanded in a supersonic molecular beam, photoionized using an excimer laser and detected by time-of-flight mass spectrometry (TOF-MS).

Several other studies have been carried out which demonstrate that a variety of types of carbonaceous target materials also produce a dominant fullerene-60 signal, by TOF-MS, when vaporized using a focussed pulse laser. Materials such as carbon films (Creasy and Brenna[6]), polymers such as polyimides (Creasy and Brenna[7], and Campbell et al.[8,9]), coal (Greenwood et al.[10]), polycyclic aromatic hydrocarbons (Lineman et al.[11]), soot (So and Wilkins[12]) and diamond (McElvany, Dunlap and O'Keefe[13]) have been used. These results indicate that the fullerenes are produced by the nucleation of atomic / molecular carbon vapour and are not formed as a result of a process involving ablation of large fragments of material from the surface of the target.

Despite the obvious importance of the laser vaporization technique in the discovery of the fullerenes, it is of little use in the production of fullerene-60 in gram quantities. The primary process of fullerene production which is utilised at present is that of evaporation of graphite electrodes in an inert atmosphere, usually of helium (generally at about 100 torr), as pioneered by Kratschmer, Lamb and co-workers.[14] Following on from this work, many fullerene generators have been designed and constructed, all based on the 'carbon-arc' method employed by Kratschmer et al.[14], and suitable for bulk preparation of fullerene-60.[15-22] All these reactors burn rods of graphite, although of differing dimensions, and in some cases at a different pressure of helium to the usual 100 torr. The design varies from the "Simple Benchtop Reactor" of Fred Wudl[22] to the more complex reactors of Parker et al.[21] and Haufler et al.[20] (the latter having the option of computer control of the 'feeding' of the

graphite rods). As a result of these variations, the rate of production of fullerene-60 varies from 100 mg per day for the original Kratschmer preparation[14], to up to 10 g per day claimed by Haufler et al.[20] for their larger reactor (which uses 6 mm graphite rods). In addition to this, the ratio of fullerene-60 to fullerene-70 produced also varies. Ratios of from 3:1[21] (60:70) to 17:3[16,17] have been reported, implying that conditions can be manipulated in order to produce a greater or smaller proportion of fullerene-70, as desired.

In all of these cases the soot formed is collected from the reactor and extracted with benzene, or toluene, in order to obtain a fullerene-60, and -70, rich soot extract. To begin with this was further purified by repeated sublimation[14], however, the method now favoured is that of column chromatography, using neutral alumina and eluting with hexane and a hexane-toluene mixture. This produces pure samples of fullerene-60 and -70, although it is limited to relatively small amounts of material due to the poor solubility of the fullerenes in hexane. Consequently other methods of separation have been looked into, such as phenylglycine-based HPLC columns[17] and the use of graphite as the stationary phase in liquid chromatography[23]. Both of these reportedly give good separation of fullerene-60 and -70.

Typical yields for the 'contact-arc' generation of fullerene-60 are in the range of *ca.* 8 to 15%. However, the Wudl Benchtop reactor gives a yield of only 3 to 4%, but this reactor has other advantages (see Chapter Seven for further details on this particular reactor). It should be pointed out that these yields are based on the amount of carbon rod used.

Finally, one other form of preparation which has been reported is that of burning benzene (Howard et al.[24]). This particular method arose as a result of the suggestion[25-28] that fullerenes might have been formed in sooting flames, and the subsequent detection, in flames[29], of all-carbon ions with mass/charge ratio suggestive of fullerenes. This process produces fullerene-60 and -70 in yields and ratios which are dependent on the temperature, pressure, carbon/oxygen ratio and residence time in the flame. By careful control of these conditions the highest yield

obtained is 3g of fullerenes from 1kg of fuel burned (approximately 0.3%). The ratio of fullerene-60 to fullerene-70 also varies by a great deal, over the range of 3.85 to 0.18.

With an optimum yield of *ca.* 0.3% this latter method does not seem to be destined to usurp that of 'carbon-arc' generation as the favoured mode of fullerene production. However, if the yield could be improved with the fullerene-60 to fullerene-70 ratio less than one (preferably near to the 0.18 value reported), then this could become an important route to fullerene-70.

6.2   Spectroscopic Characterisation of Fullerene-60 and -70

Fullerene-60 was first observed by TOF-MS as the dominant cluster present in a whole range of carbon clusters. Seven years later, mass spectrometry is still an excellent method for assessing the purity of fullerene-60 and -70 (C_{60}^{+} ion at m/z = 720 and the C_{70}^{+} ion at m/z = 840) , and in particular observing the presence of higher fullerenes.

TOF-MS has been used by many groups to look at fullerene-60, using a variety of techniques to desorb molecules from the sample[14,30]. Other methods of mass spectrometry utilised in characterising fullerenes include fast atom bombardment (FAB-MS)[15] and electron impact mass spectrometry (EI-MS)[16]. The latter in particular produces extraordinarily clear spectra.

Due to the exceptionally high symmetry exhibited by fullerene-60, point group I_h (the highest finite point group symmetry), it is reasonable to assume that it should have a simple IR spectrum. Normal coordinate calculations[31-37] suggest that fullerene-60 should have a spectrum consisting of only four allowed vibrations. Kratschmer et al. observed four weak features in the IR spectrum of the soot extract from arc-processed carbon, but since then pure fullerene-60 has been separated and examined by IR[38,39]. As expected, four bands are observed: (cm^{-1}) 527s, 576.5m, 1182.5m, 1429m[39].

Fullerene-70 is not as symmetrical as fullerene-60, having only D_{5h} symmetry, and as a result has a much more complex spectrum, with twelve IR bands being observed[39].

Important information in verifying the structures of fullerene-60 and -70 is of course derived from their ^{13}C NMR spectra. The ^{13}C NMR spectrum of fullerene-60 consists of a single line at approximately 143 ppm[15,16] in benzene-d[6] and 142.5 ppm in carbon tetrachloride[30], and is unaltered by proton decoupling. This is considerably downfield from the peak for the corresponding positions in naphthalene (133.7 ppm), acenaphthylene (128.65 ppm) and benzo-[g,h,i]-fluoranthene (126.85, 128.05 and 137.75 ppm)[40] (Figure 6.2 displays these structures). This shift is not unexpected however, as strain is known to produce downfield shifts which may be attributed to strain-induced hybridisation changes.

(a)   (b)

(c)
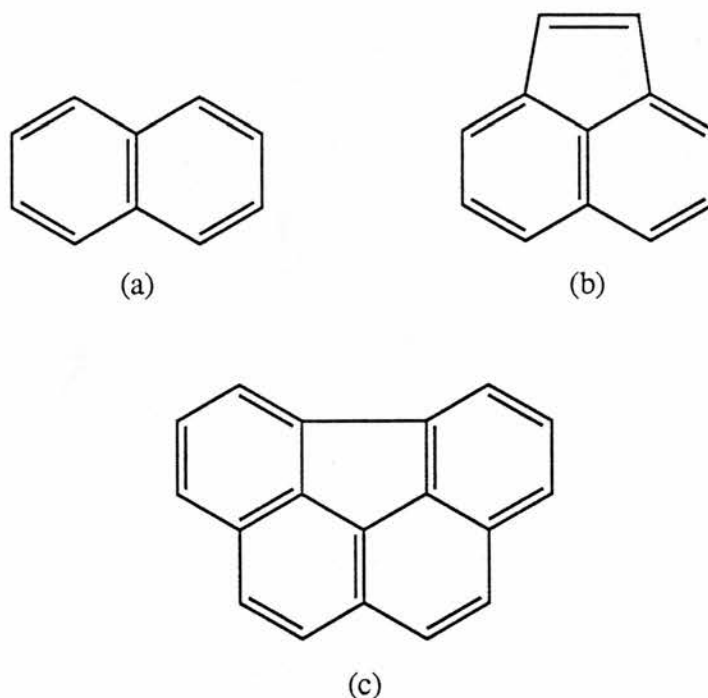
Figure 6.2.

(a) Naphthalene; (b) Acenaphthylene; (c) Benzo-[g,h,i]-fluoranthene.

Fullerene-70 has five carbon environments, these being shown in Figure 6.3, with the relative abundance of these environments and ^{13}C NMR data [15,16] shown in Table 6.1.

(a) (b) (c)　(d)　(e)　(d)　(c) (b) (a)
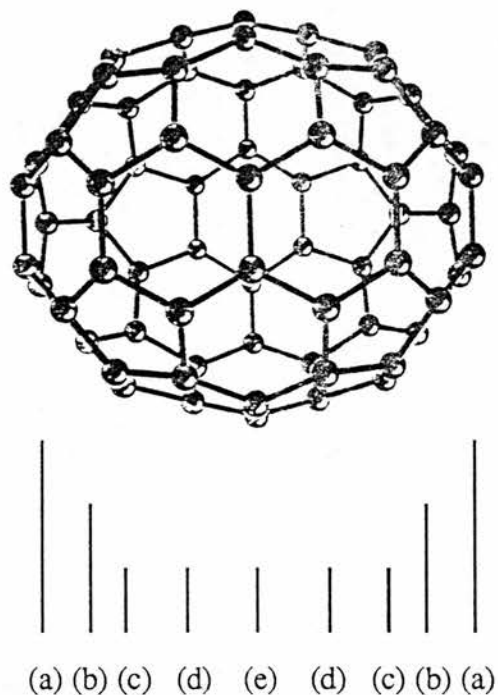
Figure 6.3.

Fullerene-70, with the five different

carbon environments labelled (a) to (e).

Carbon Environment	Number of Carbons	^{13}C NMR δ
(a)	10	150.07
(b)	10	146.82
(c)	20	147.52
(d)	20	144.77
(e)	10	130.28

Table 6.1: The carbon environments and ^{13}C data for fullerene-70.

Solid state ^{13}C NMR measurements have also been made on both fullerene-60 and -70[41,42], and have produced excellent spectra both without sample spinning (the fullerenes themselves rotating rapidly on a molecular level) and with spinning at the magic angle. The ^{13}C MAS NMR spectrum of fullerene-60 shows a single line at 144.1 ppm (with a linewidth of less than 0.5 ppm), and fullerene-70 displays lines at 151.4, 148.8, 148.1, 146.2, 131.7 ppm, these being comparable with the results obtained from ^{13}C solution NMR.

Thus the structure proposed for fullerene-60 and -70 is vindicated by the mass spectrum, IR and ^{13}C NMR data . Other structural studies of crystalline fullerene-60 have shown that at room temperature, fullerene-60 molecules are disordered with respect to each other (orientationally speaking) and the crystal structure may be regarded as a face-centred cubic configuration of fullerene-60 spheres[41,42]. Other spectroscopic data on fullerene-60 include the visible[43], UV[38,43] and vacuum UV[43] absorption spectra. Also the crystal structure of the 1:1 adduct $C_{60}(OsO_4)(4\text{-}tert\text{ -butylpyridine})_2$[44], in which the heavy atom causes the rapid rotation of fullerene-60 to stop at room temperature (thereby allowing the crystal structure to be obtained), irrefutably displays the truncated icosahedral structure of fullerene-60.

6.3 Cyclic Voltammetric and Electron Spin Resonance Studies

The cyclic voltammetry (CV) of both fullerene-60 and -70 has been investigated quite extensively[17,47,48]. Surprisingly they both exhibit remarkably similar CV behaviour. This may be explained, in terms of electron affinity and ionization potential, as follows. The high electron affinity (*ca.* 2.8 eV[49]) and ionisation potential (*ca.* 7.5 to 7.72 eV[50]) of fullerene-60 may be ascribed to two factors. Firstly, if a carbon atom was negatively charged as a result of electron capture, then that atom would have a higher degree of sp^3 character and longer bond lengths compared to its neighbours and would therefore reduce the strain energy of the cage structure. On the other hand, electron loss would produce a positively

charged atom, which would have more sp^2 character and shorter bond lengths and would thereby increase the strain energy. Secondly, if one viewed fullerene-60 as being a sphere made up of pyracylene units (Figure 6.4), then it would be expected to be electronegative, as pyracylene has a reasonably large electron affinity and its LUMO is a NBMO[51]. In contrast to fullerene-60, fullerene-70 is more highly strained and has fewer pyracylene groups. Therefore the greater strain relief (on becoming C_{70}^-) undergone by fullerene-70 would have a tendency to increase its electron affinity relative to fullerene-60. However, the fewer pyracylene units present would have precisely the opposite effect. Thus, if these two effects were to be in operation and essentially cancel each other, then both fullerene-60 and -70 would have similar CV, which appears to be the case.

Both fullerene-60 and -70 undergo four one electron reductions (the first three being shown in Figure 6.5), all of which are reversible in a conventional electrochemical cell. The first two reductions have been shown to be fully reversible one electron transfer processes (in methylene chloride), presumably:-

$$(C_{60} / C_{70}) \xrightleftharpoons{e^-} (C_{60} / C_{70})^- \xrightleftharpoons{e^-} (C_{60} / C_{70})^{2-}$$

Pyracylene   "Fullerene-60"

Figure 6.4.

163
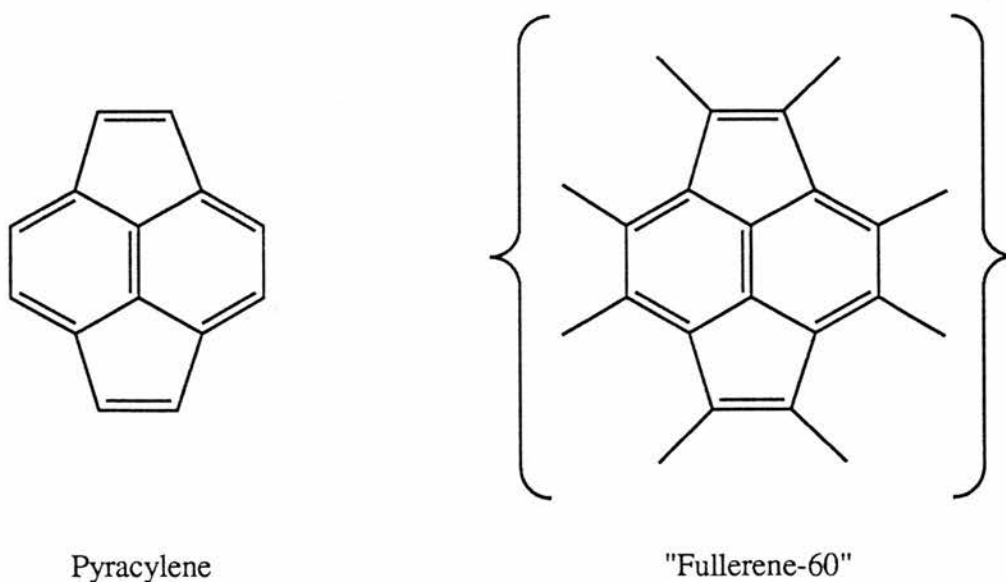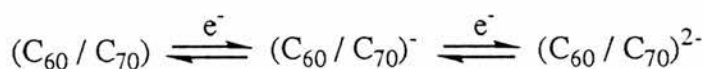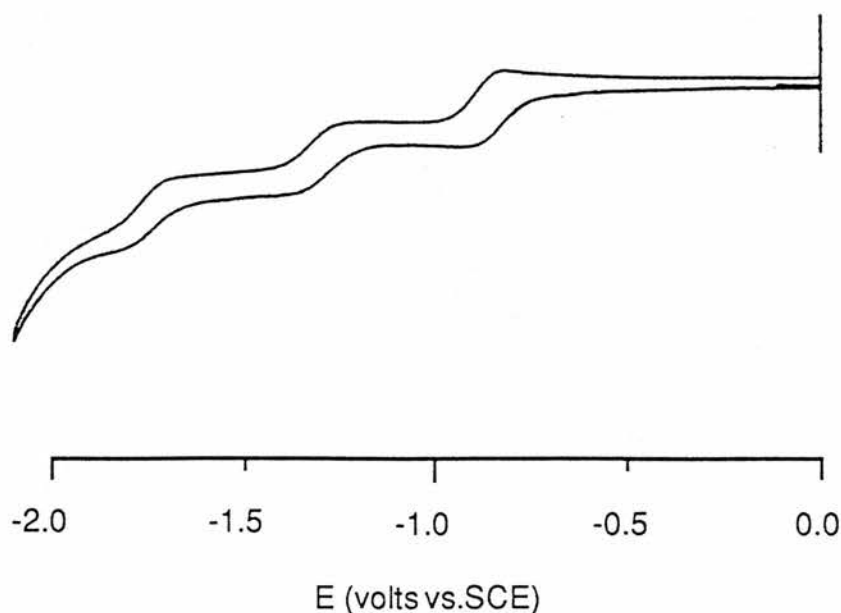
Figure 6.5

Cyclic voltammetry of fullerene-60 at a platinum microelectrode in
CH_2Cl_2, with no supporting electrolyte, at 100 mV/S.

Fullerene-60 in methylene chloride or nitrobenzene does not appear to undergo electrochemical oxidation, up to +1.50 V (NHE). However, this is not surprising when one considers the somewhat high ionisation potential of fullerene-60. Fullerenes which are more likely to undergo oxidation would be those which have a metal atom enclosed within the cage structure itself ($C_{60}M$). There is strong evidence for the generation of such molecules where the encapsulated metal atom is La, Ca, Ba, Sr, Ni, Rb, Na, K, Cs and U, provided by supersonic cluster beam experiments[30,49,52].

The information obtained from the CVs of fullerenes-60 and -70 prompted people to look toward the generation of free radicals associated with these structures. The first to report any such results were Wudl et al.[53] on the fullerene-60 salt $C_{60}^{\cdot-}$ $Ph_4P^+.(Ph_4PCl)_2$, deposited as a microcrystalline powder on bulk electrolysis of fullerene-60. The ESR spectrum of this salt in the solid state produces a 45 G wide symmetric line at $g = 1.9991$ (±0.0002), and the linewidth is drastically affected by temperature. This shift of the g-value into the realm inhabited by transition metal

and rare-earth compounds and the temperature dependence of the linewidth is also displayed by electrochemically generated $C_{60}\cdot^-$ (at 100 K)[54], free from other species. The increase in linewidth at higher temperatures makes the fullerene-60 radical anion undetectable in liquid solutions. These effects may be explained by the large spin-orbit coupling, which is hinted at by the short triplet lifetime and small singlet-triplet splitting observed by Arbogast *et al.*[55].

The radical monoanions and dianions of both fullerene-60 and -70 (C_{60}^- and C_{70}^-) have also been generated[48] electrochemically and the EPR of their frozen methylene chloride glasses examined. At 120 K the fullerene-60 radical anion shows slight anisotropy only, whereas the fullerene-70 radical anion displays a great deal more, with three g -values being easily distinguishable. This property is a result of the lower symmetry of fullerene-70 and is also exhibited by the dianions, which appear to be diradicals[48]. However, the EPR spectrum of C_{60}^{2-} is a quintet (centred at $g = 2.003$), which is more complex than the triplet that one would expect to result from simple dipolar coupling, if one were to assume that C_{60}^{2-} was an S=1 diradical. This may however be due to exchange coupling, spectral simulation studies being needed to verify this idea.

Finally, fullerene-60 has been exposed to a variety of reactive, neutral radicals[54], generated photochemically, to produce unusually persistent radical adducts. Intense ESR absorptions are produced in each case, with multiple addition of the radicals being expected (FAB-MS showing up to 11 phenyl groups present on the fullerene-60 cage when the radical was $C_6H_5\cdot$). When the solutions are frozen to approximately 100 K, two shoulders on the main ESR signal may be discerned (with a further two being visible at 4 K), which are assumed to be a consequence of the presence of a triplet species. The triplets are either ground state or almost degenerate with a ground state singlet, as the triplet is clearly visible at 4 K.

6.4 Reactions of Fullerenes

Both the organic and inorganic chemistry of the fullerenes have been probed

and will be dealt with here (with the exception of metal-doped fullerenes, as these have important electronic effects and are therefore covered in Section 6.5).

The first reaction involving fullerene-60 which gave a discrete product, as opposed to a range of isomers or products, was that of osmylation[56,57]. Osmium tetroxide is a strong, selective oxidant, which adds across one of the double bonds of fullerene-60 leaving the osmium bound via two oxygen atoms. The ligands on the osmium may be varied in order to adjust the solubility and crystal quality of the resulting adduct. The adduct so formed side steps the orientational disorder present in fullerene-60, thereby allowing an ordered crystal to develop. This gave rise to the first crystal structure obtained of a fullerene containing species[46], as previously mentioned.

Metal complexes with fullerene-60 bound directly to the metal atom are also known[58]. In such complexes, fullerene-60 behaves as an electron-deficient alkene, as demonstrated by its ruthenium chemistry[59]. This discovery led to the investigation of low-valent transition-metal complexes of fullerene-60 (low-valent transition-metal complexes being known to bind to electron-poor alkenes). Therefore complexes such as $(Et_3P)_2M(\eta^2-C_{60})$, with M=Pt, Pd, and Ni, have been examined, all of which bind directly to carbon atoms on the cage structure. Fullerene-60 has two types of bond: those at the border of a six-membered ring and a five-membered ring (6-5), and those which fuse two six-membered rings (6-6). In the osmium adduct the two oxygens are bound at a 6-6 ring bond, as is platinum in its complexes[59,60]. Also the complex $(Ph_3P)_2(CO)ClIr(\eta^2-C_{60})$ has been structurally characterised by Balch et al.[61], and the iridium is shown to bind to fullerene-60 in the same way. That metals should bind at these sites is easily accounted for as the 6-6 ring bonds are shorter than the 6-5 ring bonds and have more double bond character[62-64]. It was subsequently found that up to six metals could be attached to one fullerene-60 molecule to give complexes of the kind $[(Et_3P)_2M]_6(\eta^2-C_{60})$, with M=Pt, Pd and Ni[60]. The metal atoms are arranged in an octahedral array about the exterior of the fullerene-60 core (having an almost ideal T_h point group symmetry). Increasing the

amount of metallic substitution on fullerene-60 makes the species more difficult to reduce. This is presumably brought about as a result of the presence of π -back bonding from the metal to fullerene-60. Also, upon reduction the complexes become unstable, releasing the metal species into solution and yielding the free fullerene-60 anions.

Since fullerene-60 was discovered there has been speculation as to the possible lubricant properties of the fully fluorinated fullerene $C_{60}F_{60}$, and as a result the halogenation of fullerene-60 has been much studied. Fluorination has been investigated by Selig et al.[65] and Holloway et al.[66], both favouring the use of fluorine gas. Despite this similarity however, both groups produce derivatives of fullerene-60 displaying differing degrees of fluorination. Selig and co-workers report a total reaction time of 20 hours at room temperature and produce $C_{60}F_{36}$ as the main product; Holloway et al. expose fullerene-60 to fluorine gas for approximately 7 to 8 days at 70°C, producing a derivative with a single line ^{19}F NMR spectrum, identified as $C_{60}F_{60}$. This difference in products may be assigned to the slightly stronger conditions (ca. 70°C) and longer reaction time employed by the latter method, whereas the former method ceases at 36 fluorine atoms due to some intrinsic stability in this particular structure (this stability being overcome by the latter method). Fullerene-60 also undergoes chlorination[67,68] and bromination[68], although to a lesser extent than fluorination. When exposed to liquid chlorine (at -35°C), fullerene-60 appears to undergo the addition of twelve chlorine atoms[67], whereas at 250°C, in the presence of gaseous chlorine, an average of 24 atoms are added. Although subsequent substitution of these with methoxy groups implies that 26 chlorines are present (Figure 6.6). Bromination on the other hand appears to be much simpler, with only two or four bromine atoms being added at room temperature or 50°C (based on the weight increase). All these chlorinations and brominations are reversible, heating the derivative resulting in the liberation of the halogen and the fullerene-60.

In comparison to $C_{60}F_{36}$, $C_{60}H_{36}$ has also been prepared[17]. This is achieved by the Birch reduction (Li / NH$_3$ / Bu^{t}OH) of fullerene-60, EI-MS showing the
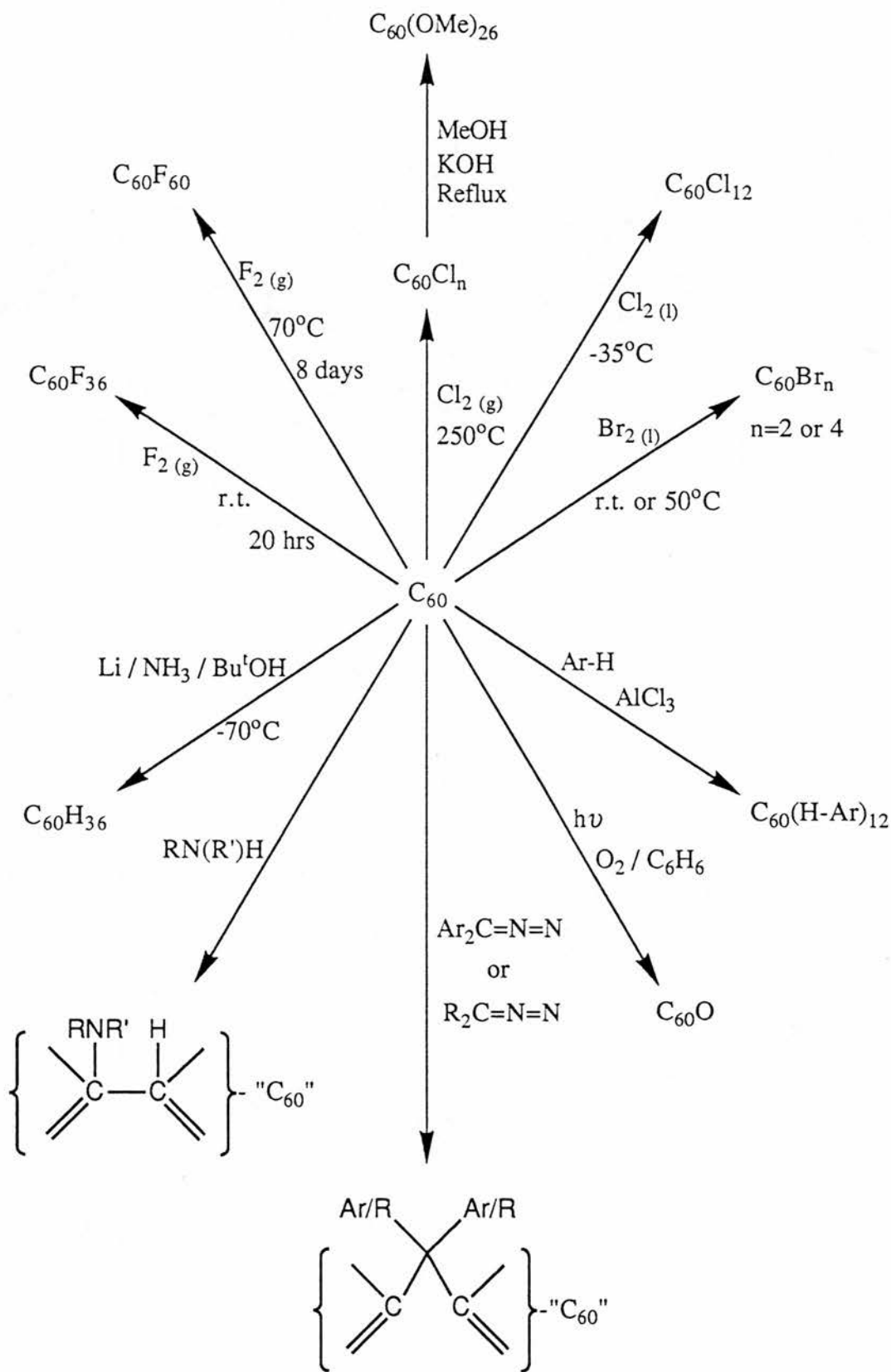
Figure 6.6.

Summary of the major aspects of the organic chemistry of fullerene-60.

product to be $C_{60}H_{36}$. In this case, the explanation for the extent of addition is simple. The addition of 36 hydrogens leaves exactly one unconjugated double bond in each pentagon of fullerene-60, the Birch reduction being known to only attack conjugated double bonds[69].

Another aspect of the organic chemistry of fullerenes which has attracted attention is that of the addition of aromatics to the fullerene ball. Olah *et al.*[70] have demonstrated that a variety of polyarenefullerenes are accessible using $AlCl_3$-catalysed addition. The reaction proceeds by the initial addition of $AlCl_3$ to the fullerene producing the cation which electrophilically adds to the aromatic. FAB-MS shows that the main product is $C_{60}(H-Ar)_{12}$, this being observed for both Ar = C_6H_5- and $CH_3C_6H_5$-. A second and more specific method of attaching aromatic and alkyl groups to the ball is that of Wudl and co-workers, using diazoalkanes[71,72]. The diazoalkane adds across a 6-6 ring bond of fullerene-60 to produce a five-membered ring which then eliminates nitrogen. The resulting three-membered ring is then believed to open at the 6-6 ring bond of fullerene-60 to give the final derivative (see Figure 6.6 for clarification). An interesting result of this work is that it should be possible to extend the preparation, and by judicious choice of diazoalkane, to produce two types of polymer: one with fullerenes as part of the backbone, so-called "pearl necklace" polymers; and the other being a polymer with the fullerene derivatives as pendant groups, "charm bracelet" polymers.

Other aspects of the organic chemistry of fullerenes which have been examined, albeit to a somewhat lesser extent are: the addition of amines across a fullerene-60 double bond (predominantly giving six amino groups per fullerene-60 ball)[73]; the preparation of a fullerene-60 epoxide, $C_{60}O$, by Creegan *et al.*[74]; the polymethylation of fullerene-60 using lithium metal and methyl iodide[75] and the preparation of methylene and oxygen adducts of both fullerene-60 and -70[76].

6.5　　　　Electronic Properties of Fullerene-60

Fullerene-60 in various compounds has been found to act as a ferromagnet,

insulator, conductor, semi-conductor and superconductor, a most unusual ability indeed.

When mixed with an excess of the strong organic reducing agent tetrakis(dimethylamino)ethylene (TDAE), a microcrystalline precipitate of $C_{60}(TDAE)_{0.86}$ is produced[77]. $C_{60}(TDAE)_{0.86}$ is found to be a soft organic ferromagnet with a Curie temperature of 16.1 K (the highest for any known molecular ferromagnet consisting of first-row elements only) and a remenence of essentially zero. This is attributed to a completely three dimensional system with no domain pinning sites.

Fullerene-60 itself displays a reasonable photoconductivity[78], as do organic semi-conductors such as phthalocyanine, and is in fact a direct band gap semi-conductor (like gallium arsenide). However, unlike gallium arsenide, the fullerene-60 molecule spins freely and at random. This element of disorder within the ordered bulk of fullerene-60 itself is expected to lead to a new class of semi-conductors. Fullerene-60 films can also be grown on crystalline substrates, such as gallium arsenide, which opens the door to the possibility of applications in the field of microelectronics.

When doped with alkali metals, fullerene-60 behaves as an insulator, conductor and even a superconductor at the appropriate temperature, depending on the extent of the doping. Generally the doping is achieved by exposing the fullerene to alkali metal vapour, either under a vacuum or a partial pressure of helium[79,80]. The only exception to this is Cs_xC_{60}, which is produced by using binary alloys of caesium as the dopant[81], as Cs_6C_{60} is formed by the direct reaction of caesium vapour with fullerene-60. Thus are produced derivatives which are conductors of electricity at room temperature[79]. The alkali metals potassium and rubidium give rise to the highest conductivities, 500 Scm^{-1} and 100 Scm^{-1} respectively. Other metals looked at as the dopant include lithium, sodium and caesium.

On cooling, it was found that potassium doped fullerene-60 becomes superconducting at 18 K[80]. Subsequent research demonstrated that the composition

of the superconducting phase is in fact K_3C_{60}[82], which has a face-centred cubic structure with the metal ions situated in all of the interstitial octahedral and tetrahedral 'holes' within the fullerene-60 lattice[83]. Other metal-doped derivatives have been examined and found to exhibit superconductivity, with the highest onset temperature, 43 K, at present being displayed by the thallium/rubidium doped derivative. The composition of these and the other metal-doped fullerenes[81,84,85] are shown in Table 6.2, with their transition temperatures (T_c).

It should be noted that the interface between the crystalline film of fullerene-60 and K_3C_{60} is stable, which consequently may lead to the production of intricately layered microelectronic devices.

Should the fullerene-60 be overdoped however, then the conductivity diminishes, with M_4C_{60} and M_6C_{60} becoming insulating[86]. This change to

Composition	T_c (K)
K_3C_{60}	18[80]
Rb_2C_{60}	28[84]
Rb_3C_{60}	28[84]
Rb_4C_{60}	28[84]
Cs_xC_{60}[a]	30[81]
$Cs_1Rb_2C_{60}$	31[85]
$Cs_2Rb_1C_{60}$	33[85]
$Rb_xTl_yC_{60}$[b]	43[b]

Table 6.2

The composition and transition temperatures of the superconducting

phases of alkali metal-doped fullerene-60 derivatives.

[a] x=1.2 - 3.1, but is expected to be shown to be 3; [b] indicated

by recent work at Allied-Signal, Inc., as yet unpublished.

insulating behaviour may be due to "overcrowding" of the lattice and thus a change in the structure, with M_6C_{60} having a body-centred cubic lattice.

So it can be seen that in less than twelve months fullerene-60 has been exploited to produce a whole range of novel new compounds with a variety of electronic properties and potential uses, with this new class of molecular solid affording boundless possibilities.

6.6 The Fullerene Family Series

The formation of "giant fullerenes"[87] of formula up to C_{400} have been observed by laser vapourisation of graphite[88], polycyclic aromatic hydrocarbons[89] and higher oxides of carbon[90]. Then, with the arrival of fullerene-60 in gram quantities, came the opportunity to look into the synthetic accessibility of the higher fullerenes. The fullerene class of carbon allotropes are defined as being of the composition C_{20+2m}, in the form of hollow three-dimensional cages made up of twelve pentagonal rings and m hexagonal rings.

The higher fullerenes can be extracted from the fullerene-rich "soot", produced from a carbon-arc, by the judicious choice of extracting solvent. Using 1,2,3,5-tetramethylbenzene, for instance, one can extract all the fullerenes up to fullerene-200[21] (using continuous soxhlet extraction), and up to fullerene-212 with 1,2,4-trichlorobenzene[91]. Also the use of certain solvents in sequence can be of great help when trying to isolate these higher fullerenes. For example, extraction with hexane will remove almost all of the fullerene-60 and -70 present, and subsequent extraction of the "soot" with heptane will produce a sample rich in fullerenes -60, -70, -78 and -84 (in the ratios 4:2:1:2 respectively)[21].

Recently, improved chromatographic techniques have led to the isolation and structural characterisation of three new fullerenes, these being the chiral D_2-C_{76}[92], C_{2v}-C_{78}, chiral D_3-C_{78}[93] and a fraction containing several isomers of fullerene-84[94]. Like fullerene-60 and -70, these fullerenes also produce deeply coloured solutions (in aprotic solvents). A solution of D_2-C_{76} being a bright yellow-green colour; C_{2v}-C_{78}

a chestnut-brown; D_3-C_{78} a golden-yellow and the fullerene-84 fraction being an olive-greenish colour.

That only a couple of structures for an individual larger fullerene may be isolated is interesting, as the number of possible structures is astronomical. For example, Manolopoulos and Fowler have calculated that there are 21 822 fullerene structures for fullerene-78[95]. However, when one applies the 'isolated pentagon rule' (IPR), that is, no two pentagonal rings should share a common edge, this number drops dramatically. The number of IPR-satisfying isomers for fullerene-78 is only five, with twenty-four for fullerene-84 and forty-six for fullerene-90, the number of structures obviously increasing with fullerene size[96].

Yet another interesting product of fullerene formation is the production of chiral molecules from achiral graphite. The chirality thereby produced stems from the helicity in the absence of a single chiral centre. For example, fullerene-76 has D_2 symmetry with a spiralling double helical arrangement of two identical edge-sharing helical fragments.

Cyclic voltammetric studies have been carried out on fullerene-76 and C_{2v}-C_{78}[97], showing that these molecules are capable of both accepting and releasing electrons. In THF, fullerene-76 displays four reversible reduction steps and two reversible oxidation steps; C_{2v}-C_{78} also displays four reversible reduction steps, but only one oxidation step. In this way it has been shown that fullerene-76 is both a better donor and better acceptor than either fullerene-60 or fullerene-70.

Thus it can be seen that research on the higher fullerenes not only produces results which are the same as those obtained from the studies on fullerene-60 and -70 but superior. At present two chiral fullerenes have been isolated and many more are expected to be found in the future. CV studies[97] have shown that chemical transformations and electron transfer processes involving cationic intermediates, that are not feasible with fullerene-60 and -70, are possible with the larger carbon structures of the higher fullerenes.

Finally, some mention should be made concerning the potential uses of fullerenes in the real world. But first it should be pointed out that applications have not been established as yet because fullerenes have been available for only a very short period of time. Despite this, there are expected to be a wide range of uses for the fullerenes and their derivatives. Their ability to accept and release electrons, for example, makes them of use as charge carriers in batteries. The uses of polyfluorinated fullerenes as lubricants and the mechanical properties of other derivatives are also worth looking into in depth. Then there are the most exciting physical properties, in particular the superconductivity and ferromagnetism of alkali metal derivatives having obvious uses in the electronics industry.

Chapter Seven

The Radical Behaviour of Fullerenes 60 and 70.

Fullerenes 60 and 70 were prepared by the kind permission of Dr. Fred Wudl, University of Santa Barbara, using the simple benchtop reactor designed in his own labs.[22] Upon the separation of pure fullerenes their reactions with organic radicals and the behaviour of the subsequent fullerene radical adducts thereby produced was investigated.

7.0 The Simple Fullerene Benchtop Reactor[22]

The reactor itself is shown schematically in Figure 7.1, with the key features being labelled. The major points of interest are that the graphite rods were gravity-fed and that the soot was contained and collected within a 4 dm^3 Pyrex kettle reactor which allowed observation of the process, in order to check that the apparatus was functioning correctly. This apparatus consumed a graphite rod of approximately 150 mm in length and 3 mm in diameter in about 10 minutes, with a current of 55 A. The bottom graphite rod, of 12 mm diameter, was not significantly degraded.

At the beginning of each new run a fresh 3 mm diameter graphite rod was sharpened (using a pencil sharpener), which ensured more efficient arcing, and fitted to the electrode as shown. The lower 12 mm graphite rod was cleansed of any "slag", which may have built up during the previous run, by scraping with a scalpel. Thus the surface of the lower electrode was maintained as a concave indentation of fresh graphite. Failure to remove this "slag" resulted in the upper graphite rod burning in a non-uniform manner, and it also made starting the arc difficult. The apparatus was then connected to a cylinder of ultrapure helium, and to a 5 dm^3 two-necked flask (ballast), the other end of which was connected to a high vacuum oil pump via a 2.5 cm outside diameter frit to prevent contamination of the oil pump with soot. The apparatus was purged five times by helium pump filling cycles. The
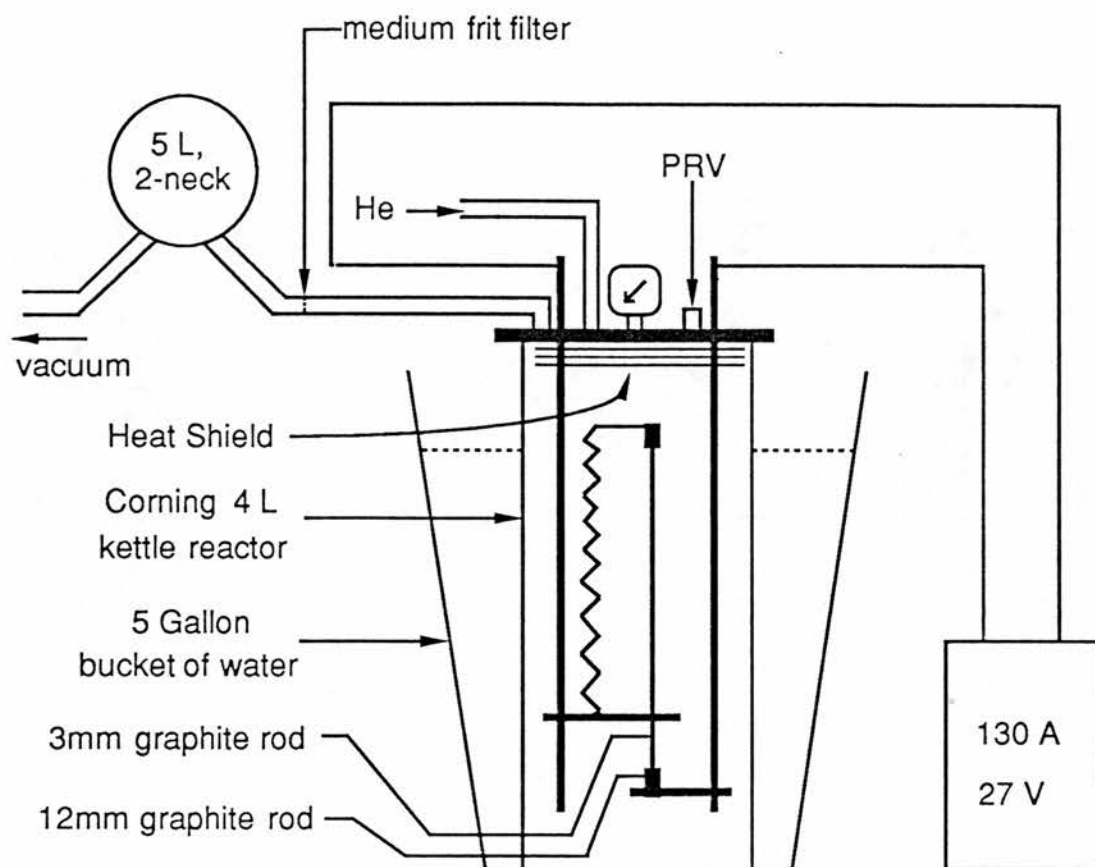
Figure 7.1

Schematic of the simple fullerene benchtop reactor.

reactor was then brought to a 100 Torr pressure of helium. Cold water was placed in

the bucket surrounding the reactor to act as a heat sink (note, care was taken in doing

this, as the electrical power supply was in close proximity to the reactor and therefore

the water). The power supply was set to 130 A (3.5 kW at 27V), AC, and switched

on. Once the graphite rods had begun to arc the power was reduced to 55 A. Note

that protective goggles were worn during this procedure to protect the eyes from the

intense light produced by the arcing of the graphite rods. When the upper rod had

been consumed the power was switched off and the apparatus left standing for twenty

minutes to cool down. Once cool the pressure release valve (PRV) was slowly

opened and the reactor brought to atmospheric pressure. The soot deposited on the

electrodes and heat shield was brushed off and into the kettle reactor, where the

majority of the soot was deposited. Whilst handling the reactor and soot in this way in between runs a mask was worn over the mouth and nose to prevent inhalation of the soot. This procedure was then repeated and further runs carried out.

Twelve such runs were carried out during the course of a normal working day, after which the kettle was removed and extracted with approximately 1 dm^3 of benzene. This benzene extract was filtered through a sinter funnel and the benzene was removed at reduced pressure to produce a soot extract rich in fullerenes 60 and 70.

Using the "Simple Benchtop Reactor" in this way, 23.5 g of graphite rod was consumed and produced 0.50 g (2.13%) of soot extract. This extract was separated into pure fullerene 60 and 70 using a column of neutral alumina. The soot was loaded onto the neutral alumina (Brockmann type 1, 100-250 mesh) by addition of alumina to a toluene solution of the extract and subsequent removal of the toluene at reduced pressure. This "loaded alumina" was then placed on a column of neutral alumina and eluted with 60-80 petroleum ether until the fullerene 60 had been removed (the fullerene 60 being visible as a purple band on the column). The column was then eluted with 10% toluene in 60-80 petroleum ether to remove the fullerene 70 (visible as a red band). This produced 0.28 g (0.39 mmol, 1.19%) of pure fullerene 60 and 0.06 g (0.07 mmol, 0.26%) of pure fullerene 70 (percentage yields are based on the amount of graphite consumed in the reactor). The purity was checked by FAB-MS, giving accurate masses of 720 amu and 840 amu for the samples of fullerene 60 and fullerene 70 respectively. The fullerene 60 was also examined by cyclic voltammetry, producing the CV shown in Figure 6.5 (Chapter Six). This shows the first three one electron reductions of fullerene 60 which are fully consistent with the results of other CV studies[47,48].

7.1   Addition of Alkyl Radicals to Fullerene 60 and 70

Benzyl, ethyl and methyl radicals were generated in solution with the corresponding fullerene in the cavity of the ESR spectrometer. The sources of these

radicals and the solvents used are shown in Table 7.1.

Radical	Source	Solvent
$C_6H_5CH_2^{\bullet}$	$C_6H_5CH_3 / (Bu^tO)_2$	Toluene
$CH_3CH_2^{\bullet}$	CH_3CH_2Br	t-Butylbenzene
$CH_3^{\bullet}$	$(CH_3COO)_2$	Benzene

Table 7.1

The addition of benzyl radicals, produced by abstracting hydrogen from toluene with t-butyl radicals, to both fullerene 60 and 70 produced very persistent radicals with similar spectra. At temperatures above 200 K an intense singlet was observed (Figure 7.5) with both fullerenes (ΔB=1.8 G for fullerene 60 and 2.2 G for fullerene 70) which continued to grow as the sample is irradiated. On shuttering the light source the peak height of the signal decreased; however, both fullerene radicals displayed a high stability and the signal decayed slowly. This is demonstrated by Figures 7.1 and 7.2 where the peak height of these "benzylfullerene" radical adducts
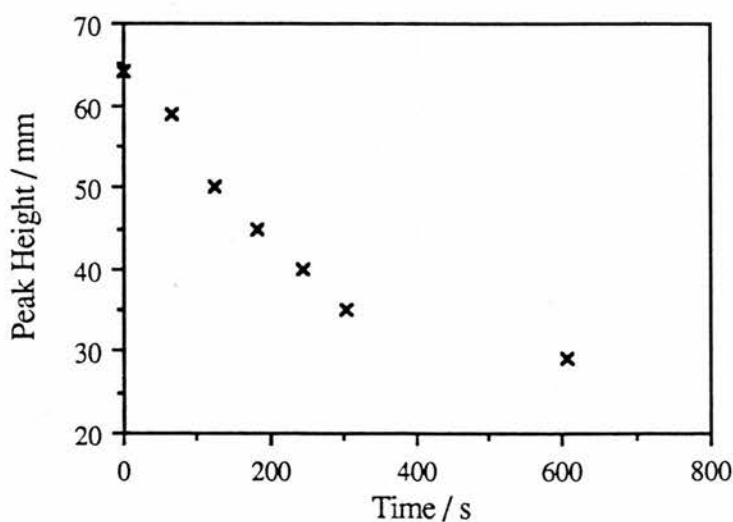

Figure 7.1

Decay curve for $PhCH_2C_{60}^{\bullet}$ radical adducts.
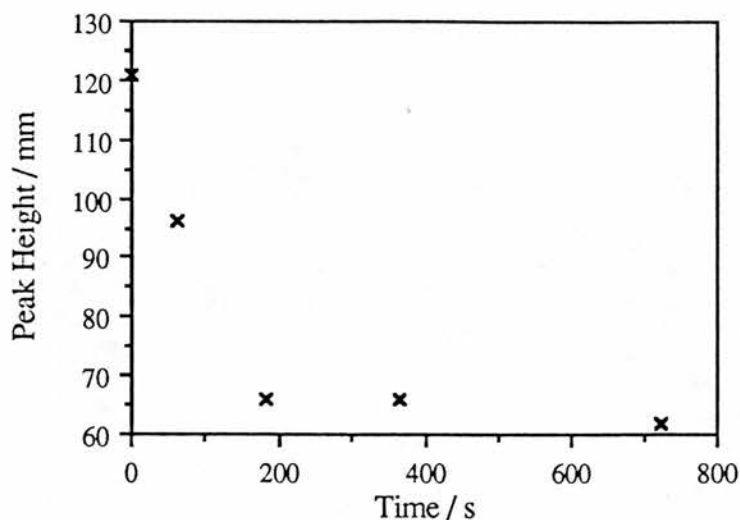
Figure 7.2

Decay curve for $PhCH_2C_{70}\cdot$ radical adducts.
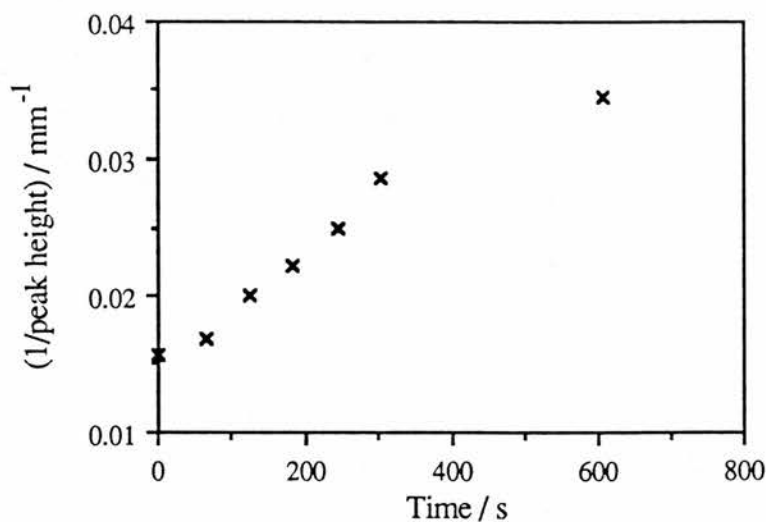
Figure 7.3

A graph of 1/peak height vs. time showing the process to be second order.

is plotted against time after the light source was shuttered. In order to discover the nature of the decay of the radicals the inverse of the peak height was plotted against the time (Figure 7.3). This produced a straight line, indicating a second order process. However, after approximately 350 seconds the graph deviates from a straight line relationship. A possible explanation of this behaviour can be given with

reference to the equilibrium shown in Figure 7.4. Initially, the concentration of the dimer is very small compared to that of the radical. Therefore the dissociation of the

$$PhCH_2\text{-}C_{60}^{\bullet} \rightleftharpoons PhCH_2\text{-}C_{60}\text{—}C_{60}\text{-}CH_2Ph$$
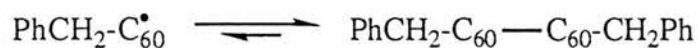
Figure 7.4

dimer to the radical is unimportant. However given time the concentration of the dimer will increase and that of the radical decrease. As time proceeds therefore the dissociation of the dimer becomes more important until the production of the radical in this way becomes observable (*ie.* the decay of the radical with time is retarded). At this point (*ca.* 400s for $PhCH_2C_{60}^{\bullet}$) the decay appears to depart from second order.

10G

Figure 7.5

9.3GHz EPR Spectra of the fullerene radical produced by addition of benzyl radicals to fullerene 60 (left) and fullerene (70), in toluene at 270K.

Fullerene 70 is believed to behave in the same way, however the data obtained are a little ambiguous because a good straight line relationship was not obtained.

On reducing the temperature of observation of these radicals to below 160 K a change in their spectra was observed. With both fullerene 60 and 70 a pair of shoulders, with a separation of 10.4 G in the case of fullerene 60 and 10.3 G for fullerene 70, appeared on either side of the central signal, producing a broad triplet (Figure 7.6).
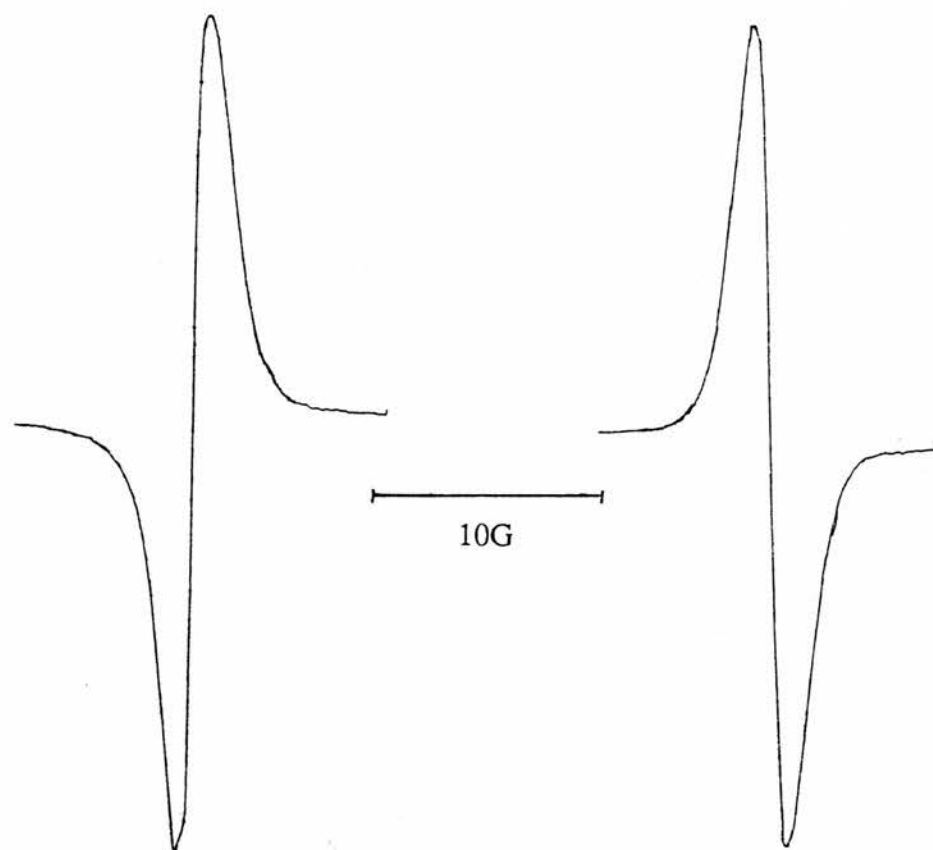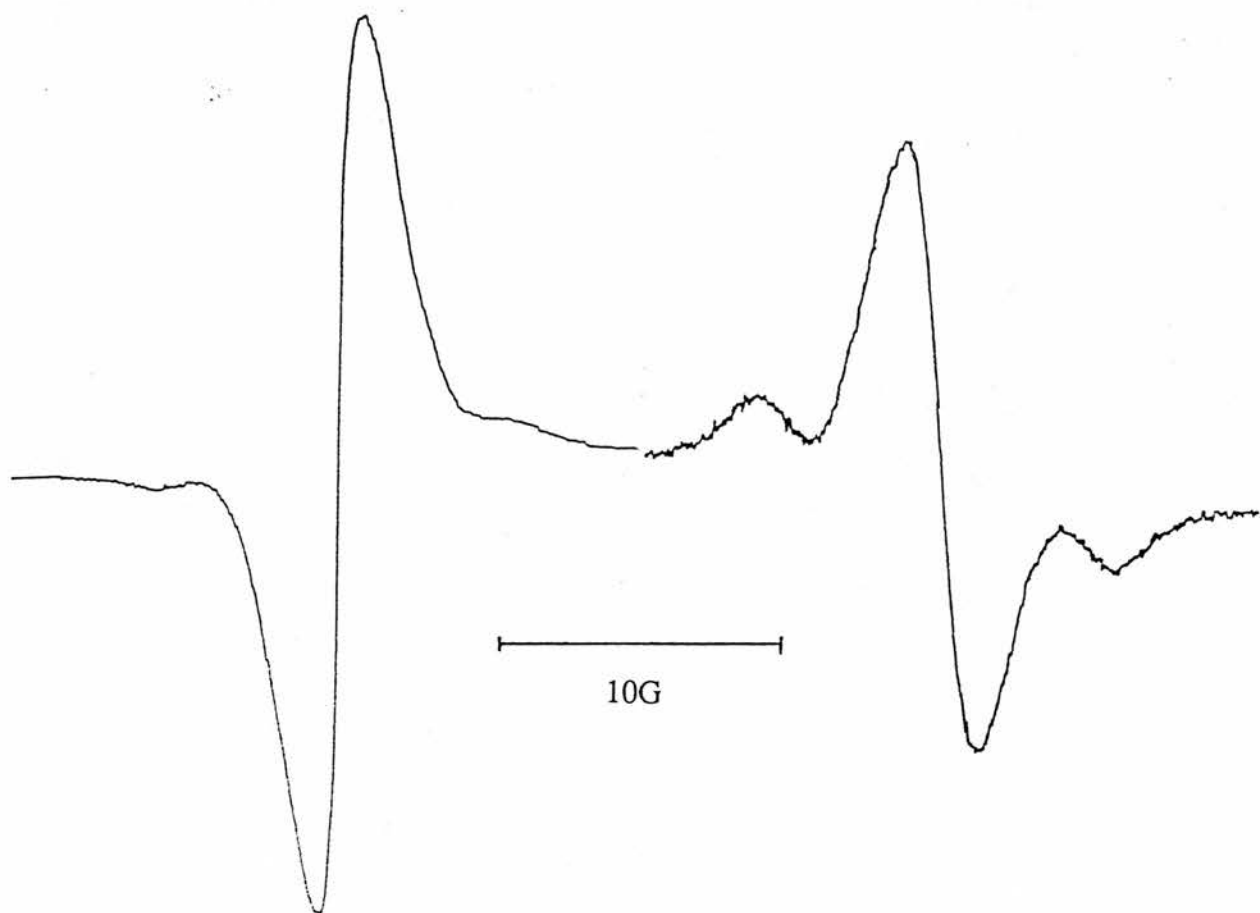

Figure 7.6

9.3GHz EPR Spectra of the fullerene radical produced by addition of benzyl radicals to fullerene 60 (left) and fullerene (70), in toluene at 115K.

Possible explanations for these triplets are: (i) the presence of two unpaired electrons on the same fullerene molecule[54]; and (ii) that the reduced temperature

freezes out the rotation of the fullerene molecule such that there are two fullerene radical centres in close spacial proximity with each other, thereby producing a triplet.

The addition of ethyl and methyl radicals to the fullerene produced the same results, with identical spectra. Ethyl radicals were produced by direct photolysis of ethyl bromide, whereas the methyl radicals were produced by photoelimination of carbon dioxide from diacetyl peroxide. The diacetyl peroxide was freshly prepared from acetyl chloride (Figure 7.7) and stored at -5° C until needed. Morton and Preston *et al.* have recently published their findings[98] with the addition of benzyl and ethyl radicals to fullerene 60 in solution, in which they observed hyperfine coupling from the alkyl hydrogens (benzyl producing a triplet of triplets [interaction with the *ortho* protons of the benzene and the methylene protons], and ethyl a triplet of quartets). The fact that we do not observe this detail may be attributed to a small amount of oxidation of the fullerenes used.
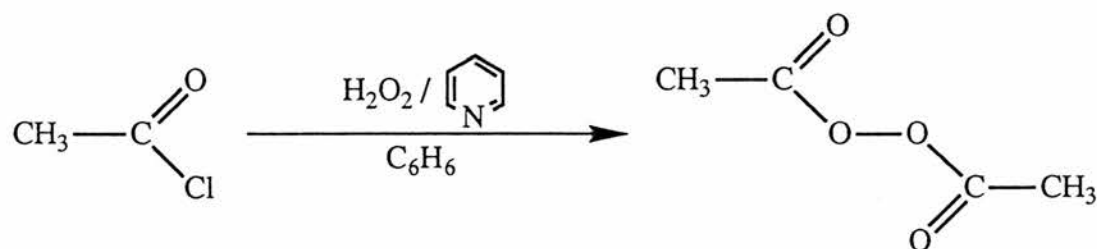

Figure 7.7

Preparation of diacetyl peroxide.

The samples from all of the EPR experiments were examined by FAB-MS, in search of some indication of dimer formation. However no noteworthy information could be extracted, and no peaks corresponding to any of the dimers could be identified, with peaks corresponding to the C_{60}^+ or C_{70}^+ ions only being visible.

7.2   Addition of Trihalomethyl Radicals to Fullerenes 60 and 70

Trichloromethyl and fluorodichloromethyl radicals were generated by direct photolysis of carbon tetrachloride (or bromotrichloromethane) and fluorotrichloromethane respectively. The addition of these radicals to fullerenes 60 and 70 was then investigated.

When exposed to the fullerenes the trichloromethyl radicals in solution (at 268K to 344K) produced similar results to the alkyl radicals , *ie.* an intense singlet ($\Delta B=2.0$ G in the case of fullerene 60 and 5.0G for fullerene 70). As the temperature of these samples was increased, in the absence of photolysis, then so did the intensity of the radical signal. According to Morton and Preston[99] this is due to the thermolysis of the dimer produced by the combination of two fullerene radical adducts, back to the radical adduct (Figure 7.8). Therefore by measuring the intensity of the singlet at different temperatures (Table 7.2), in the absence of photolysis, one can obtain a value for the dissociation energy of the dimer from an

$$CCl_3\text{-}C_{60}\text{---}C_{60}\text{-}CCl_3 \underset{\longleftarrow}{\overset{\text{Heat}}{\longrightarrow}} 2\ CCl_3\text{-}\overset{\centerdot}{C}_{60}$$
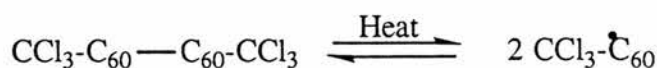
Figure 7.8

Peak Height / mm	Temperature / K	ln (peak height)	1000/Temp. / K^{-1}
102	344	4.62	2.90
75	330	4.32	3.03
57	320	4.04	3.12
58	312	4.06	3.20
22	290	3.09	3.45
13	268	2.56	3.73

Table 7.2

Peak intensity data for the $CCl_3\text{-}C_{60}^{\centerdot}$ radical adduct.
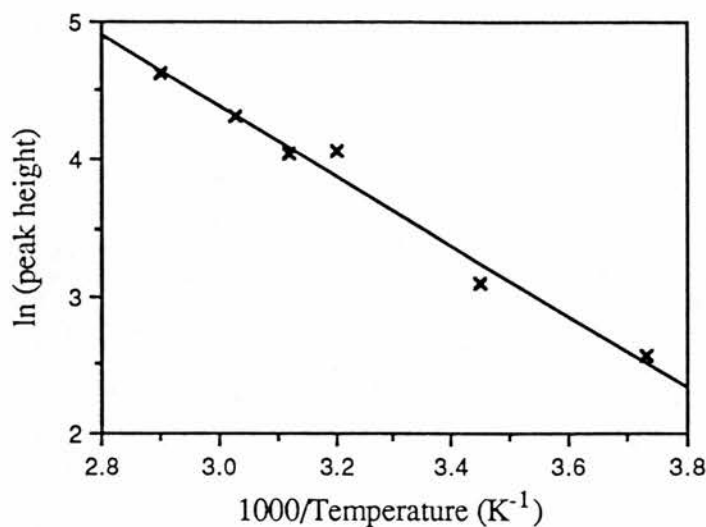
Figure 7.9

Arrhenius type plot for the CCl_3-C_{60}· radical adduct.

Arrhenius type plot, with ln (peak height) against 1000/T (Figure 7.9). This produces a straight line with the gradient being related to the heat of dissociation as shown below.

$$\text{Gradient} = -\frac{\Delta H}{R}$$

From the data in Figure 7.9 a value of 21.4 kJ mol^{-1} (5.1 kcal mol^{-1}) for the dissociation energy of the dimer was obtained. Despite its small magnitude we found this result to be reproducible, with the experiment being repeated several times to afford comparable values for ΔH. This is in stark contrast to the more realistic value of 17.1 kcal mol^{-1} obtained by Morton and Preston *et al.* with trichloromethyl radicals[99]. The reasons for this discrepancy are unclear and we can find no fault in our calculations.

When the spectrometer gain was increased dramatically then ^{13}C satellites became apparent (Figure 7.11). The hfs and percentage intensity, relative to the central ^{12}C signal, of these satellites are given in Table 7.3.

hfs / G	Percentage Intensity
30.5	1.2
18.8	1.7
9.3	4.2
4.5	3.8[a]

Table 7.3

[a]Tentative assignment due to the poor resolution of this peak in the EPR spectra.

The natural abundance of ^{13}C is 1.1%. Therefore the 30.5 G and 18.8 G splittings must be due to couplings to single carbon atoms, and the 9.3 G to four carbon atoms. Due to overlapping with the central signal the relative intensity of the 4.5 G coupling was unclear and an estimate has therefore been made based on the "half-peak" visible in the spectra. This indicates that the coupling is to three carbon
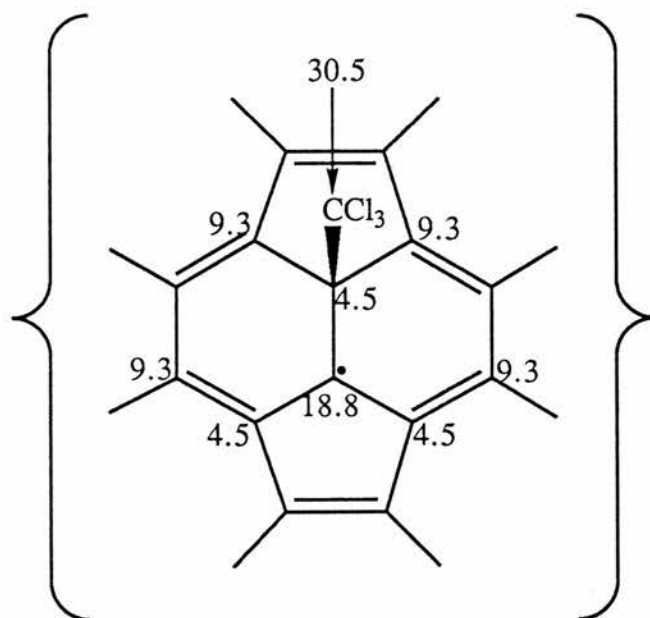
Figure 7.10

The ^{13}C satellites in the CCl_3-$C_{60}^{\bullet}$ radical adduct.

atoms, which is in agreement with studies of the $(CD_3)_3C-C_{60}^{\bullet}$ radical adduct[98] which shows a coupling, of a similar magnitude, to three equivalent carbon atoms. The specific carbon atoms involved in these couplings are shown in Figure 7.10. These assignments are totally consistent with the results of Morton and Preston and co-workers with trichloromethyl radicals and fullerene 60[100], although they did not observe the 4.5 G splitting.
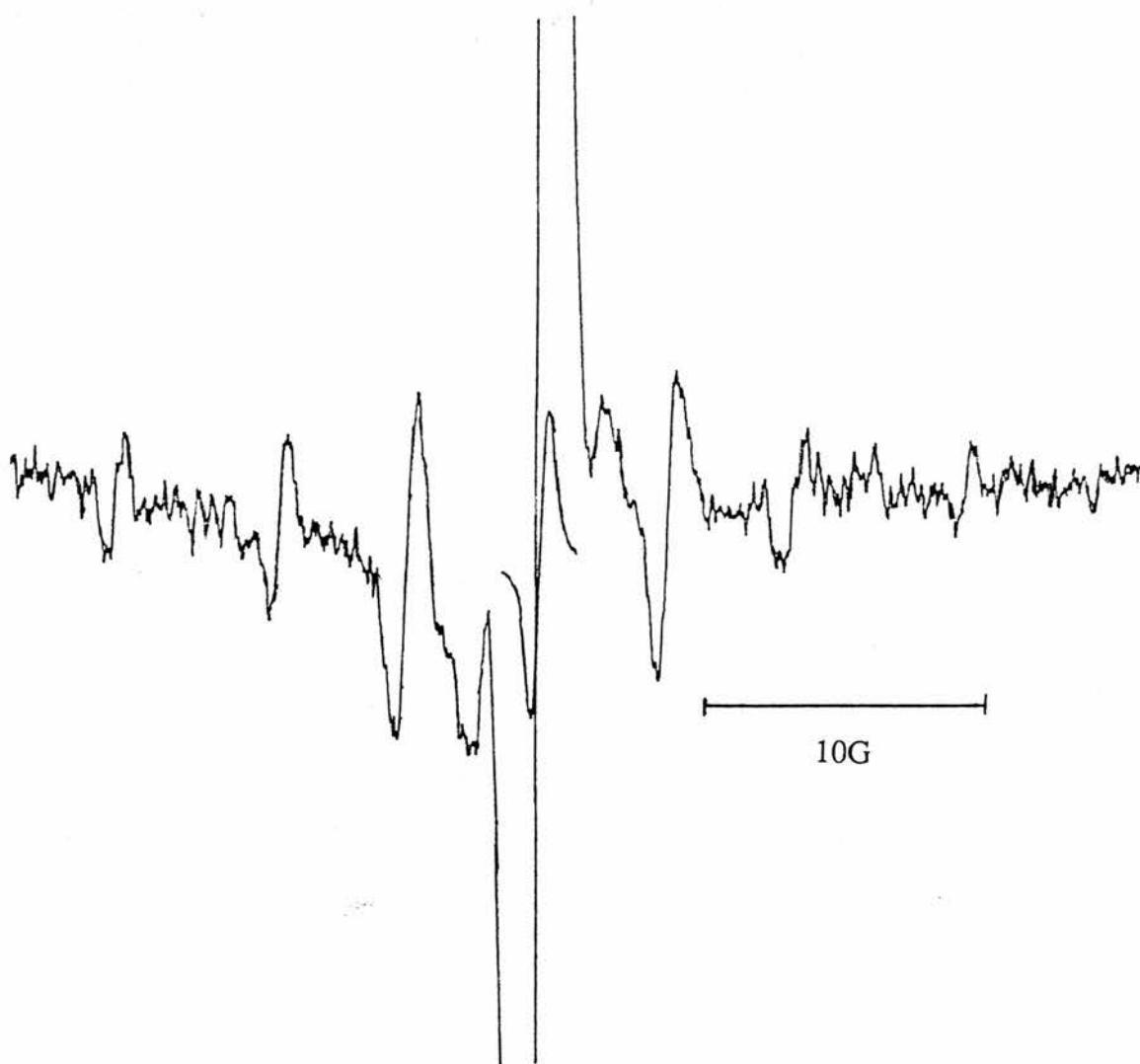
Figure 7.11

9.3GHz EPR spectra of the $CCl_3-C_{60}^{\bullet}$ radical

adduct in carbon tetrachloride at 330K.

Fullerene 70 has five carbon atom environments (see Chapter Six, Figure

6.3), and therefore one would expect to observe ^{13}C satellites produced by the five corresponding radicals to overlap and produce a complex spectrum. However on examination of fullerene 70 with trichloromethyl radicals at higher temperatures with high spectrometer gain, only a singlet as previously observed was obtained, with no resolution of the five fullerene 70 radicals or any ^{13}C satellites. Whilst our work was in progress Morton and Preston observed three dominant forms of R-C_{70}[.] radical adducts with a variety of R groups[101]. This we assume was due to the presence of an impurity in the fullerene which was scavenging the radical and thus preventing it from being observed in high resolution.

The addition of fluorodichloromethyl radicals to fullerenes 60 and 70 produced complex EPR spectra made up of more than one radical species (Figure 7.12). One of these species appeared to be a doublet (with an hfs of 3.1G) whilst the other was a singlet of varying breadth, probably due to the multiple addition of FCl_2C[.] to the fullerene. The coupling of this doublet is compared to the couplings of hydrogen atoms in similar positions on fullerene 60, relative to the radical centre (Table 7.4). Also included are couplings to fluorine atoms in two radicals where the fluorine atom is a similar distance from the radical centre as it would be in the

Radical	Hfs / G
$CFCl_2$-C_{60}[.a]	3.1 (1F)[a]
CH_3CH_2-C_{60}[.]	0.28 (2H)[98]
$PhCH_2$-C_{60}[.]	0.42 (2H)[98]
$CF_3CF_2CF_2$[.]	3.6 (3F)[102]
$CF_3CH_2CH_2$[.]	0.35 (3F)[102]
$CH_3CH_2CH_2$[.]	0.27 (3H)[102]

Table 7.4

Comparison of fluorine splittings in $CFCl_2$-C_{60}[.] to other representative radicals.

[a]Tentative assignment.

$CFCl_2$-$C_{60}^{\bullet}$ radical adduct[102] (*ie.* two C-C bonds between the radical centre and the C-F bond).

Direct comparison of these values produces no obvious similarity between these fluorine couplings and those assigned to the $CFCl_2$-$C_{60}^{\bullet}$ radical adduct. However, taking the ratio of the couplings observed with the $CFCl_2$-$C_{60}^{\bullet}$ and CH_3CH_2-$C_{60}^{\bullet}$ radical adducts and comparing these to the ratio of those between $CF_3CF_2CF_2^{\bullet}$ and $CH_3CH_2CH_2^{\bullet}$ (the analogous alkyl and fluoroalkyl radicals) we obtain values of 11:1 and 13:1 respectively. The fully fluorinated *n*-propyl radical is used in preference to the $CF_3CH_2CH_2^{\bullet}$ as the radical centre of the former is not planar (as is the case with the fullerene 60 radicals) but pyramidal. These ratios are comparable, which would tend to support the argument that the 3.1G splitting is a result of coupling to the fluorine in $CFCl_2$-$C_{60}^{\bullet}$, but is by no means conclusive.
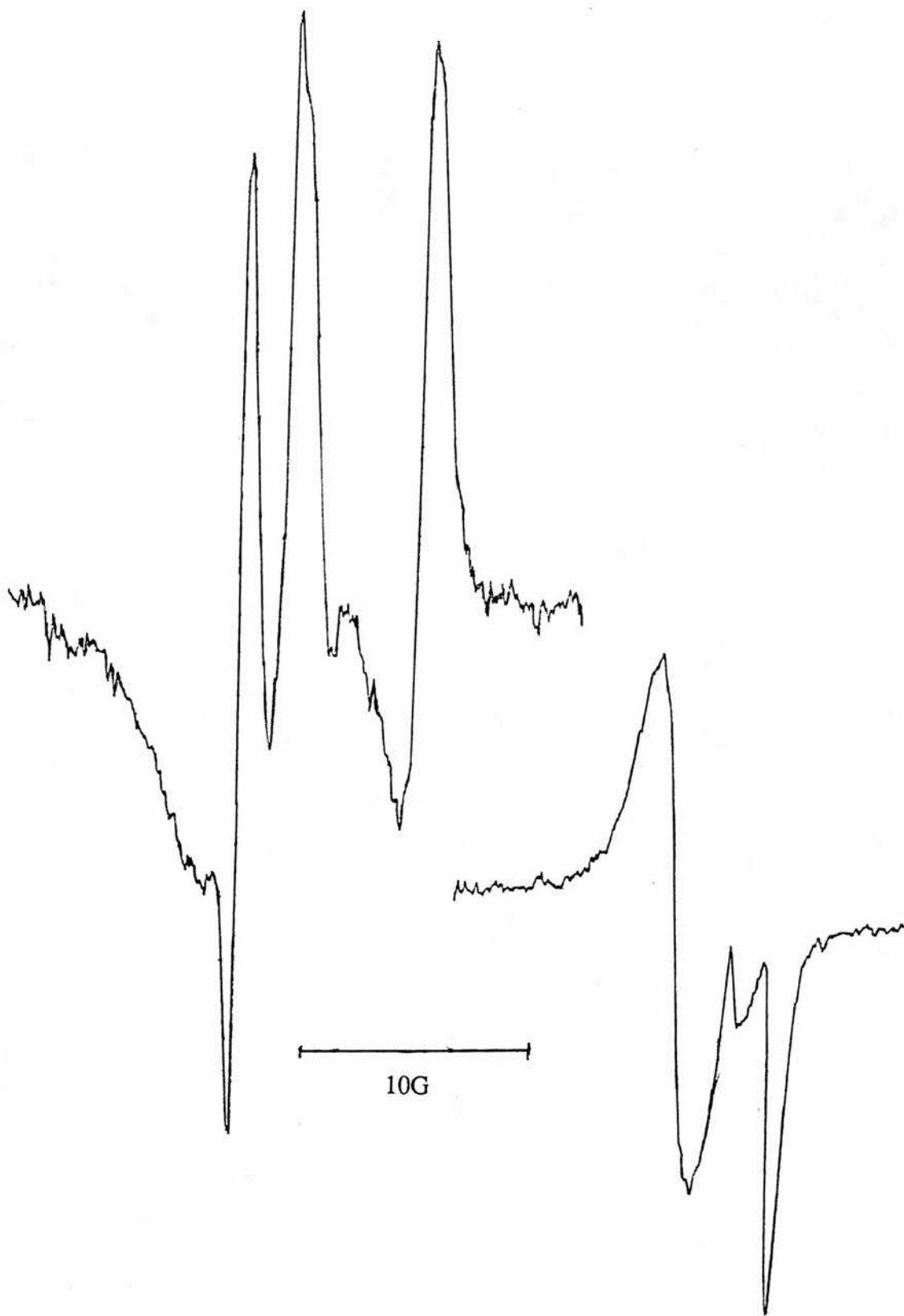
Figure 7.12

9.3GHz EPR spectra obtained on photolysis of a solution of fullerene 60 (left)

or 70 (right) in fluorotrichloromethane at 370K and 350K respectively.

7.3 Addition of the 1,3-Cyclopentane Diradical to Fullerene 60

The 1,3-cyclopentane diradical was produced by photoelimination of nitrogen from 2,3-diazabicyclo[2.2.1]hept-2-ene. This diradical was generated in benzene solution in the presence of fullerene 60 in order to determine if the cyclopentane diradical would add to two separate fullerene molecules to produce two fullerene 60 radical groups bridged by the cyclopentane (Figure 7.13), or whether a fullerene diradical would be formed. The result could then be compared to the triplet spectrum produced by the $PhCH_2$-$C_{60}^{\bullet}$ radical adduct at low temperature.
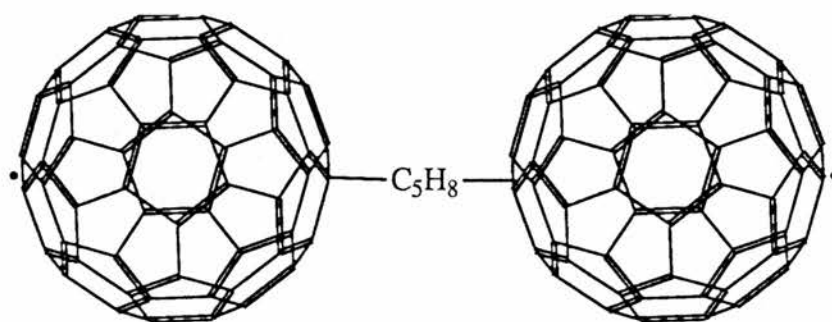
Figure 7.13

The 2,3-diazabicyclo[2.2.1]hept-2-ene was prepared from cyclopentadiene via 2,3-dicarboethoxy-2,3-diazabicyclo[2.2.1]heptane[103] (Figure 7.14), with an overall yield of 60%.

Fullerene 60 and 2,3-diazabicyclo[2.2.1]hept-2-ene were dissolved in benzene and photolysed in the cavity of the EPR spectrometer. At low temperatures (120K) a broad singlet (ΔB=4.5G) was observed (Figure 7.15), with no indication of shoulders forming on either side of the signal. At higher temperatures (280K) the spectra become more complex (Figure 7.16). At this temperature it appears that another radical-containing species is also present in addition to the original one observed at low temperatures. This second radical species is probably produced by the decay of the original radical to another radical species. This would explain the absence of the second radical at low temperature and its appearance at higher

temperatures. Further EPR examination and analysis of the products by FAB-MS produced no information concerning the identity of this second radical species, or the decay products produced, with only fullerene 60 being identifiable.
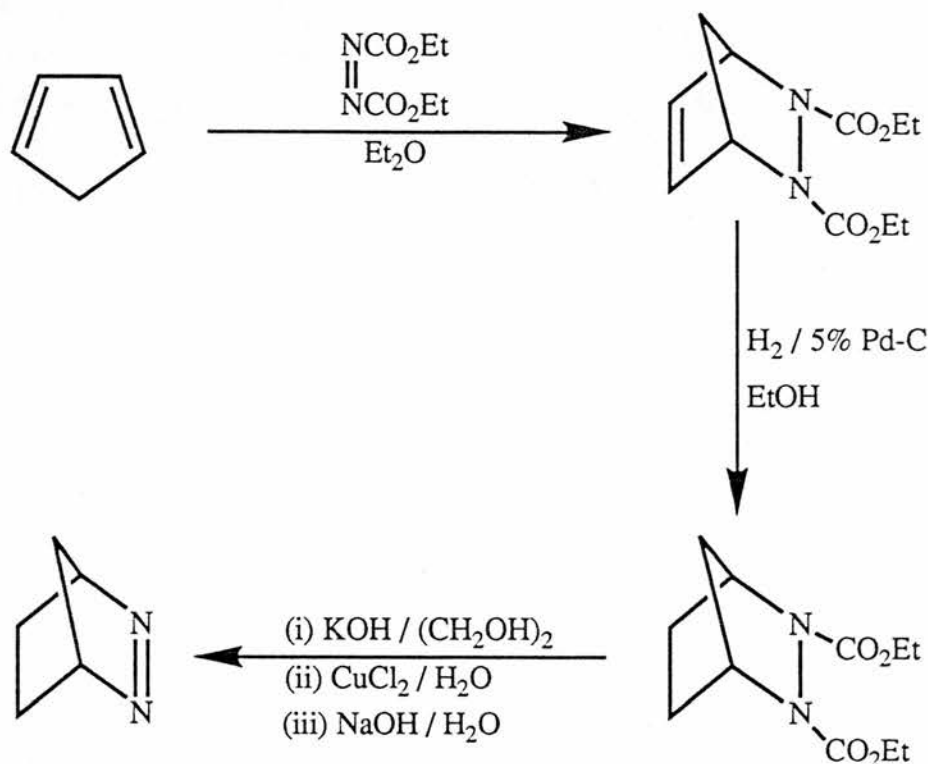
Figure 7.14

Preparation of 2,3-diazabicyclo[2.2.1]hept-2-ene.

The apparent simplicity of the initial radical produced, *ie.* a singlet, must be due to a species with only one radical centre. An explanation which accounts for this is that the diradical adds to fullerene 60 to produce a new diradical which then rapidly abstracts a single hydrogen atom from the solvent or 2,3-diazabicyclo[2.2.1]hept-2-ene before it can be observed. Thus a single mono-radical was produced which decays at higher temperatures to produce a second radical species.

10G
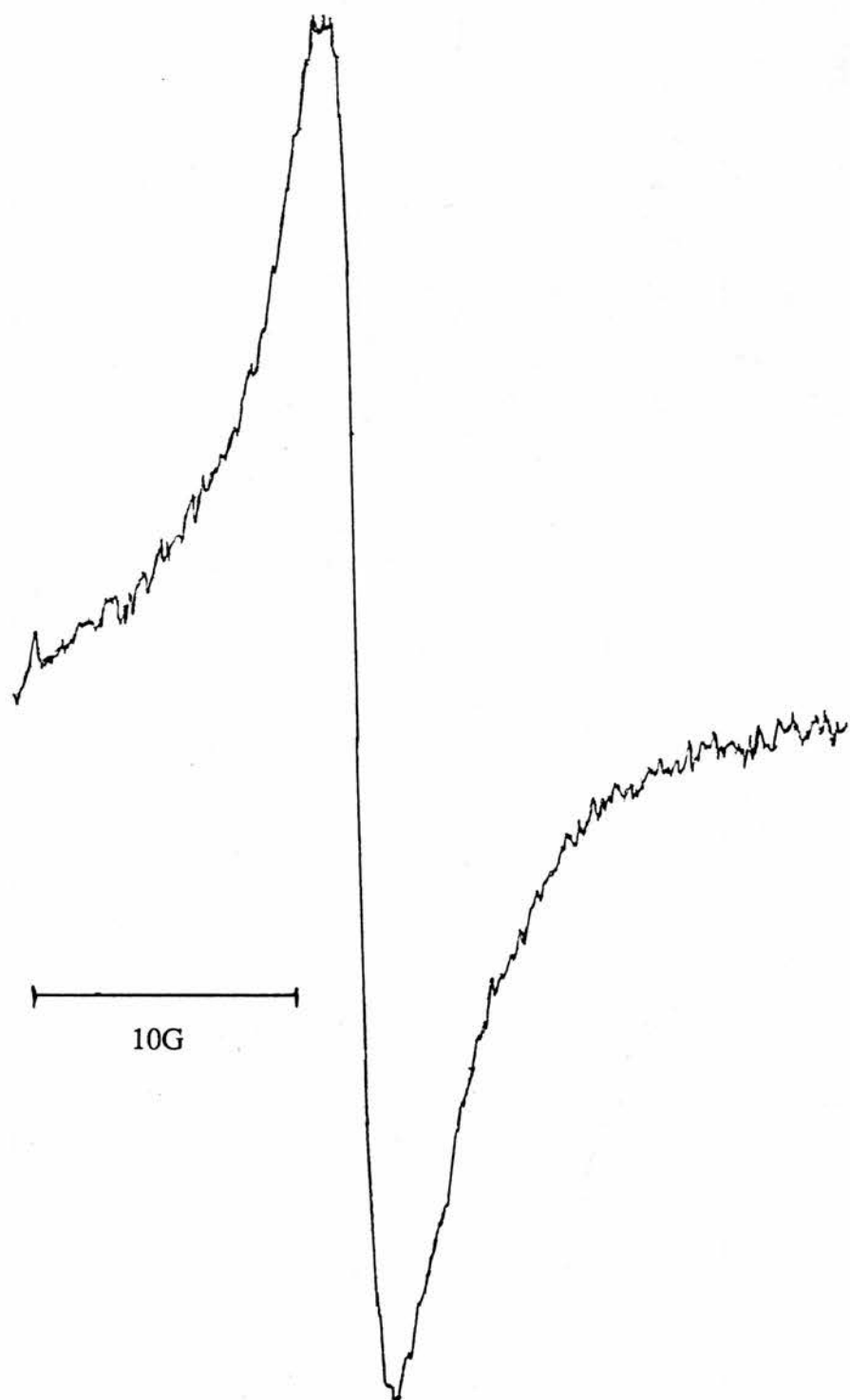
Figure 7.15

9.3GHz EPR spectra obtained by photolysis of a solution of fullerene 60

and 2,3-diazabicyclo[2.2.1]hept-2-ene in benzene at 120K.
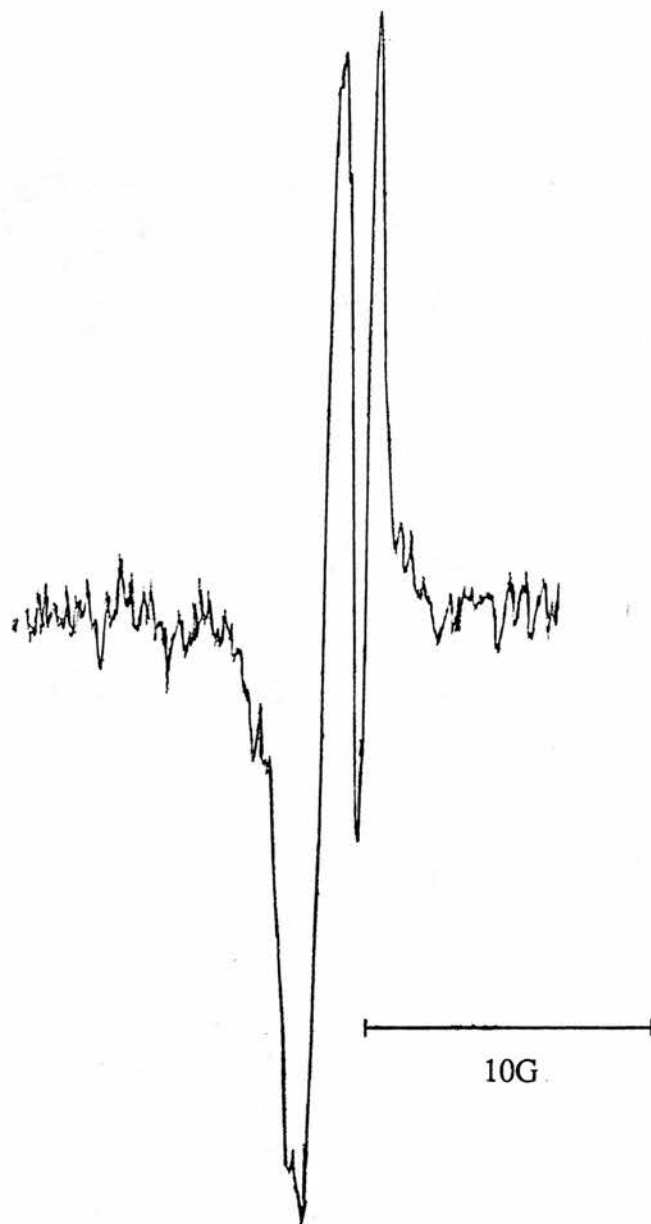
Figure 7.16

9.3GHz EPR spectra obtained by photolysis of a solution of fullerene 60
and 2,3-diazabicyclo[2.2.1]hept-2-ene in benzene at 280K.

7.4   Bromine Atom Abstraction from Brominated Fullerene 60

Fullerene 60 was dibrominated by exposure to neat bromine at $5^{\circ}C$[68]. Hexamethylditin was used to abstract bromine from the dibromofullerene 60 in *tert*-butylbenzene. This produced a broad and poorly defined, singlet ($\Delta B = ca.$ 2.9 G) in the EPR spectrum over a range of temperatures varying from 240 K to 345 K (Figure 7.17).

A singlet is what would be expected for the abstraction of one bromine atom from the dibromofullerene. The absence of any triplets indicates that only one of the bromine atoms has been abstracted, with the other remaining intact.
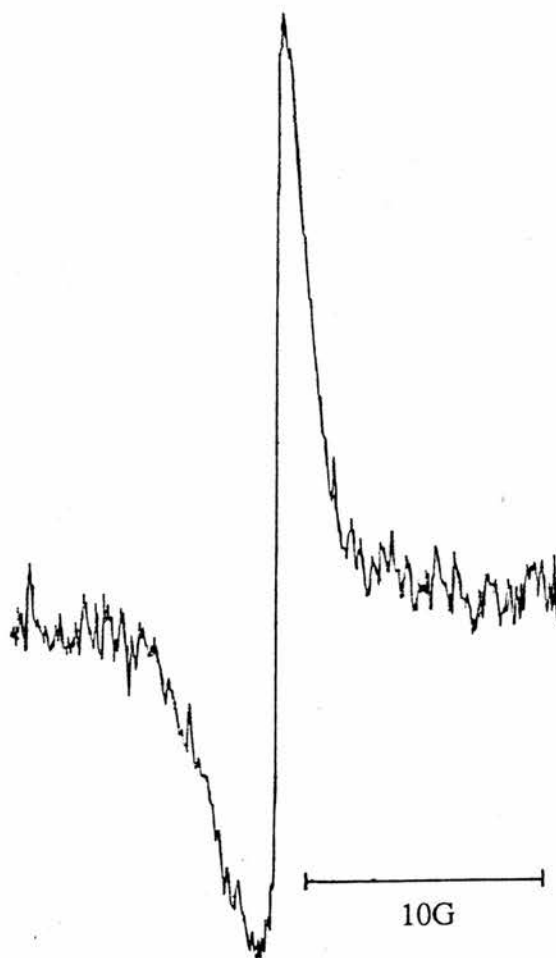
Figure 7.17

9.3GHz EPR spectra obtained by photolysis of a solution of $C_{60}Br_2$ and $(CH_3)_6Sn_2$ in *tert*-butylbenzene at 345K.

Once more FAB-MS of the sample after photolysis yielded no information concerning the products formed by this radical and only the fullerene 60 peak was observed.

7.5 Conclusions

In order to obtain high quality EPR spectra with fullerenes it is important to ensure that the fullerene has not undergone any oxidation, however minor. To achieve this it is recommended that the fullerene is sublimed at approximately 700°C (as done by Morton and Preston and co-workers) prior to use. In our work the fullerenes were passed through a short pad of neutral alumina using toluene, which is known to reduce oxidised fullerene back to the fullerene. From our results however, it is apparent that this is insufficient when using a technique as sensitive as EPR spectroscopy. Despite this problem, it was obvious that the $R\text{-}C_{60}{}^{\bullet}$ and $R\text{-}C_{70}{}^{\bullet}$ radical adducts are exceptionally persistent, with half-lives in the region of four minutes.

7.6 Experimental Section

EPR spectra were recorded using a Bruker ER200D EPR Spectrometer operating at 100kHz modulation. Samples were prepared in spectrosil tubes and degassed by bubbling nitrogen through the sample for 5 minutes.

FAB-MS were recorded at the SERC mass spectrometry service centre, Department of Chemistry, University College of Swansea.

Diacetyl Peroxide. Acetyl chloride (5.00g, 63.69mmol) was stirred at 0° C in 20ml of benzene. 27.5% Hydrogen peroxide (3.94g, 31.84mmol) was added dropwise to this, followed by dropwise addition of pyridine (5.04g, 63.72mmol). The resulting solution was stirred at 0°C for 1 hour and filtered. The benzene solution was washed with dilute hydrochloric acid (5%), saturated sodium bicarbonate solution, water and dried over magnesium sulphate.

The resulting solution was concentrated to about 10mls and stored in a freezer.

^{1}H NMR (200MHz) δ(C_6H_6+$CDCl_3$) 2.12 (3H).

The benzene solution was used as produced for EPR samples.

2,3-Dicarboethoxy-2,3-diazabicyclo[2.2.1]hept-5-ene[103]. Cyclopenta-diene dimer was cracked and distilled to produce the monomer which was used immediately.

A solution of cyclopentadiene (3.79g, 57.34 mmol) in 9ml of diethyl ether was added to a solution of diethylazodicarboxylate (10.00g, 57.42 mmol) in 9ml of diethyl ether. The resulting solution was left to stand for 24 hours. The ether was then removed and the residue distilled at reduced pressure using a kugelrohr apparatus. This produced 12.18g (50.70mmol, 88.4%) of the desired product at 135 to 140°C and 0.5 mmHg. ^{1}H NMR (200 MHz) δ($CDCl_3$) 1.23 (t, 6H), 1.70 (m, 2H), 4.16 (q, 4H), 5.10 (br s, 2H), 6.48 (s, 2H).

2,3-Dicarboethoxy-2,3-diazabicyclo[2.2.1]heptane[103]. A solution of 2,3-dicarboethoxy-2,3-diazabicyclo[2.2.1]hept-5-ene (12.18g, 50.70mmol) in 25ml of dry ethanol was hydrogenated at atmospheric pressure over 5% palladium-on-charcoal (0.15g). The solution was then filtered through hyflo, the solvent removed and the residue distilled at reduced pressure. This yielded a viscous oil at 125 to 130°C and 0.4mmHg, 10.66g (44.00 mmol, 86.8%), which proved to be the desired product. ^{1}H NMR (200MHz) δ($CDCl_3$) 1.16 (m, 6H), 1.52 (t, 2H), 1.65 (m, 4H), 4.1 (br q, 4H), 4.45 (br s, 2H).

2,3-Diazabicyclo[2.2.1]hept-2-ene. 55ml of ethylene glycol was degassed by bubbling dry nitrogen through it, whilst stirring and with slight heating, for 20 minutes. Potassium hydroxide (11.66g, 207.81 mmol) was added to this in four portions. The solution was then heated up to 125°C, under a dry nitrogen atmosphere, and 2,3-dicarboethoxy-2,3-diazabicyclo[2.2.1]heptane (10.66g,

44.00mmol) was then added as quickly as the addition funnel would allow. This was then stirred at 125°C for 1 hour. Once cool the reaction mixture was poured into 50ml of ice and water and 20ml of concentrated hydrochloric acid. The acidified reaction mixture was heated to 40°C and neutralised using 5M ammonium hydroxide.

This solution was then slowly stirred and 2ml of 2M cupric chloride solution added. This produced an immediate colour change to brick red, followed by rapid formation of a red precipitate (the cuprous chelate of 2,3-diazabicyclo[2.2.1]hept-2-ene). The pH was then increased back up to 5-6 with 5M ammonium hydroxide solution and the precipitate filtered. Another 2ml of 2M cupric chloride solution was then added and the process repeated until the filtrate remained clear red at pH 3-4 and produced no further precipitate at pH 6, where the solution was green.

The precipitate was washed with 40ml of 20% ammonium chloride solution, twice with 95% ethanol (2x30ml) and twice with cold water (2x25ml). The precipitate was then sucked dry on the filter funnel.

This precipitate was placed in a flask with 16ml of water and a solution of sodium hydroxide (3.44g, 86.00 mmol) in 8ml of water was added slowly with stirring. The suspension thereby produced was continuously extracted with pentane. The pentane extracts were dried over anhydrous potassium carbonate. Removal of the solvent yielded 3.30g (34.33 mmol, 78.0%) of white crystalline product. M.p. 98 to 99°C. ^{1}H NMR (200MHz) δ(CDCl$_3$) 0.88 (m,2H), 1.11 (m, 2H), 1.48 (m, 2H), 5.10 (s, 2H). ^{13}C NMR (50.0MHz) δ(CDCl$_3$) 20.11 (CH$_2$), 40.35 (CH$_2$), 75.82 (CH). EIMS m/z (relative intensity) 96 (1), 86 (7), 84 (12), 68 (52), 67 (100), 66 (7), 65 (6), 53 (38), 42 (17), 41 (33), 40 (36), 39 (48).

Bromination of Fullerene 60. Using the procedure of Olah et al.[68] fullerene 60 was dibrominated as follows. Fullerene 60 (10mg, 0.014mmol) and bromine (15.6mg, 0.097mmol) were sealed in a sample bottle and left to stand at 5°C for 15 hours. The bromine was then allowed to evaporate with the sample then being pumped dry at the oil pump for 2 hours. The dibromofullerene 60 thereby produced

was stored in a sealed tube and kept in the dark.

Part Three References

1. Kroto, H.W. ; Heath, J.R. ; O'Brien, S.C. ; Curl, R.F. ; Smalley, R.E. *Nature*, **1985**,*318*, 162.

2. Bochvar, D.A. ; Gal'pern, E.G. *Dokl. Akad. Nauk SSSR*, **1973**, *209*, 610. *Dokl. Chem. (Engl. Transl.)*, **1973**, *209*, 239. Stanvevich, I.V. ; Nikerov, M.V. ; Bochvar, D.A. *Russ. Chem. Rev. (Engl. Transl.)*, **1984**, *53*, 640.

3. Larsson, S. ; Volosov, A. ; Rosen, A. *Chem. Phys. Lett.*, **1987**, *137*, 501.

4. Haymet, A.D.J. *Chem. Phys. Lett.*, **1985**, *122*, 421-424.

5. Dietz, T.G. ; Duncan, M.A. ; Powers, D.E. ; Smalley, R.E. *J. Chem. Phys.*, **1981**, *74*, 1236.

6. Creasy, W.R. ; Brenna, J.T. *J. Chem. Phys.*, **1990**, *92*, 2269.

7. Creasy, W.R. ; Brenna, J.T. *Chem. Phys.*, **1988**, *126*, 453.

8. Campbell, E.E.B. ; Ulmer, G. ; Busmann, H.-G. ; Hertel, I.V. *Chem. Phys. Lett.*, **1990**, *175*, 505.

9. Campbell, E.E.B. ; Ulmer, G. ; Hasselberger, B. ; Busmann, H.-G. ; Hertel, I.V. *J. Chem. Phys.*, **1990**, *93*, 6900.

10. Greenwood, P.F. ; Strachan, M.G. ; El-Nakat, H.J. ; Willet, G.D. ; Wilson, M.A. ; Attalla, M.I. *Fuel*, **1990**, *69*, 257.

11. Lineman, D.N. ; Somayajula, K.V. ; Sharkey, A.G. ; Hercules, D.M. *J. Phys. Chem.*, **1989**, *93*, 5025.

12. So, H.Y. ; Wilkins, C.L. *J. Phys. Chem.*, **1989**, *93*, 1184.

13. McElvany, S.W. ; Dunlap, B.I. ; O'Keefe, J. *J. Chem. Phys.*, **1987**, *86*, 715.

14. Kratschmer, W. ; Lamb, L.D. ; Fostiropoulos, K. ; Huffman, D.R. *Nature*, **1990**, *347*, 354.

15. Taylor, R. ; Hare, J.P. ; Abdul-Sada, A. ; Kroto, H. *J. Chem. Soc., Chem. Commun.*, **1990**, 1423.

16. Ajie, H. ; Alvarez, M.M. ; Anz, S.J. ; Beck, R.D. ; Diederich, F. ; Fostiropoulos, K. ; Huffman, D.R. ; Kratschmer, W. ; Rubin, Y. ; Schriver, K.E. ; Sensharma, D. ; Whetten, R.L. *J. Phys. Chem.*, **1990**, *94*, 8630.

17. Haufler, R.E. ; Conceicao, J. ; Chibante, L.P.F. ; Chai, Y. ; Byrne, N.E. ; Flanagan, S. ; Haley, M.M. ; O'Brien, S.C. ; Pan, C. ; Xiao, Z. ; Billups, W.E. ; Ciufolini, M.A. ; Hauge, R.H. ; Margrave, J.L. ; Wilson, L.J. ; Curl, R.F. ; Smalley, R.E. *J. Phys. Chem.*, **1990**, *94*, 8634.

18. Hare, J.P. ; Kroto, H. ; Taylor, R. *Chem. Phys. Lett.*, **1991**, *177*, 394.

19. Pradeep, T. ; Rao, C.N.R. *Mat. Res. Bull.*, **1991**, *26*, 1101.

20. Haufler, R.E. ; Chai, Y. ; Chibante, L.P.F. ; Conceicao, J. ; Jin, C. ; Wang, L.-S. ; Maruyama, S. ; Smalley, R.E. *Mat. Res. Soc. Symp. Proc.*, **1990**.

21. Parker, D.H. ; Wurz, P. ; Chatterjee, K. ; Lykke, K.R. ; Hunt, J.E. ; Pellin, M.J. ; Hemminger, J.C. ; Gruen, D.M. ; Stock, L.M. *J. Am. Chem. Soc.*, **1991**, *113*, 7499.

22. Koch, A.S. ; Khemani, K.C. ; Wudl, F. *J. Org. Chem.*, **1991**, *56*, 4543.

23. Vassallo, A.M. ; Palmisano, A.J. ; Pang, L.S.K. ; Wilson, M.A. *J. Chem. Soc., Chem. Commun.*, **1992**, 60.

24. Howard, J.B. ; McKinnon, J.T. ; Makarovsky, Y. ; Lafleur, A.L. ; Johnson, M.E. *Nature*, **1991**, *352*, 139.

25. Zhang, Q.L. ; O'Brien, S.C. ; Heath, J.R. ; Liu, H. ; Curl, R.F. ; Kroto, H.W. ; Smalley, R.E. *J. Phys. Chem.*, **1986**, *90*, 525.

26. Kroto, H.W. ; McKay, K. *Nature*, **1988**, *331*, 328.

27. Curl, R.F. ; Smalley, R.E. *Science*, **1988**, *242*, 1017.

28. Kroto, H.W. *Science*, **1988**, *242*, 1139.

29. Gerhadt, P. ; Loffler, S. ; Homann, K.H. *Chem. Phys. Lett.*, **1987**, *137*, 306.

30. Johnson, R.D. ; Meijer, G. ; Bethune, D.S. *J. Am. Chem. Soc.*, **1990**, *112*, 8983.

31. Stanton, M.D. ; Newton, R.E. *J. Phys. Chem.*, **1988**, *92*, 2141.

32.   Wu, Z.C. ; Jelski, D.A. ; George, T.F. *Chem. Phys. Lett.*, **1987**, *137*, 291.

33.   Cyvin, S.J. ; Brensdal, E. ; Cyvin, B.N. ; Brunvoll, J. *Chem. Phys. Lett.*, **1988**, *143*, 377.

34.   Weeks, D.E. ; Harter, W.G. *Chem. Phys. Lett.*, **1988**, *144*, 366.

35.   Brensdal, E. *Spectrosc. Lett.*, **1988**, *21*, 319.

36.   Weeks, D.E. ; Harter, W.G. *J. Chem. Phys.*, **1989**, *90*, 4744.

37.   Slanina, Z. ; Rudzinski, J.M. ; Togaso, M. ; Osawa, E. *J. Mol. Struct.*, **1989**, *202*, 169.

38.   Kratschmer, W. ; Fostiropoulos, K. ; Huffman, D.R. *Chem. Phys. Lett.*, **1990**, *170*, 167.

39.   Hare, J.P. ; Dennis, T.J. ; Kroto, H.W. ; Taylor, R. ; Allaf, A.W. ; Balm, S. ; Walton, D.R.M. *J. Chem. Soc., Chem. Commun.*, **1991**, 412.

40.   Breitmaier, E. ; Haas, G. ; Voelter, W. *Atlas Of Carbon-13 NMR Data.*, Heyden, London, **1979**.

41.   Yannoni, C.S. ; Johnson, R.D. ; Meijer, G. ; Bethune, D.S. ; Salem, J.R. *J. Phys. Chem.*, **1991**, *95*, 9.

42.   Tycko, R. ; Haddon, R.C. ; Dabbagh, G. ; Glarum, S.H. ; Douglass, D.C. ; Mujsce, A.M. *J. Phys. Chem.*, **1991**, *95*, 518.

43.   Fischer, J.E. et al. *Science*, **1991**, *252*, 1288.

44.   Heiney, P.A. et al *Phys. Rev. Lett.*, **1991**, *66*, 2911.

45.   Achiba, Y. ; Nakagawa, T. ; Matsui, Y. ; Suzuki, S. ; Shiromaru, H. ; Yamauchi, K. ; Nishiyama, K. ; Kainosho, M. ; Hoshi, H. ; Maruyama, Y. ; Mitani, T. *Chem. Lett.*, **1991**, 1233.

46.   Hawkins, J.M. ; Loren, S. ; Meyer, A. ; Nunlist, R. *J. Am. Chem. Soc.*, **1991**, *113*, 7770.

47.   Allemand, P.-M. ; Koch, A. ; Wudl, F. ; Rubin, Y. ; Diederich, F. ; Alvarez, M.M. ; Anz, S.J. ; Whetten, R.L. *J. Am. Chem. Soc.*, **1991**, *113*, 1050.

48.   Dubois, D. ; Kadish, K.M. ; Flanagan, S. ; Haufler, R.E. ; Chibante, L.P.F. ; Wilson, L.J. *J. Am. Chem. Soc.*, **1991**, *113*, 4634.

49. Curl, R.F. ; Smalley, R.E. *Science*, **1988**, *242*, 1017.

50. Zimmerman, J.A. ; Eyler, J.R. ; Bach, S.B.H. ; McElvany, S.W. *J. Chem. Phys.*, **1991**, *94*, 3556.

51. Trost, B.M. ; Bright, G.M. ; Frihart, C. ; Britelli, D. *J. Am. Chem. Soc.*, **1971**, *93*, 737.

52. Weiss, F.D. ; Elkind, J.L. ; O'Brien, S.C. ; Curl, R.F. ; Smalley, R.E. *J. Am. Chem. Soc.*, **1988**, *110*, 4464.

53. Allemand, P.-M. ; Srdanov, G. ; Koch, A. ; Khemani, K. ; Wudl, F. ; Rubin, Y. ; Diederich, F. ; Alvarez, M.M. ; Anz, S.J. ; Whetten, R.L. *J. Am. Chem. Soc.*, **1991**, *113*, 2780.

54. Krusic, P.J. ; Wasserman, E. ; Parkinson, B.A. ; Malone, B. ; Holler, E.R., Jr. ; Keizer, P.N. ; Morton, J.R. ; Preston, K.F. *J. Am. Chem. Soc.*, **1991**, *113*, 6274.

55. Arbogast, J.W. ; Darmanyan, A.P. ; Foote, C.S. ; Rubin, Y. ; Diederich, F.N. ; Alvarez, M.M. ; Anz, S.J. ; Whetten, R.L. *J. Phys. Chem.*, **1991**, *95*, 11.

56. Hawkins, J.M. ; Lewis, T.A. ; Loren, S.D. ; Meyer, A. ; Heath, J.R. ; Shibato, Y. ; Saykally, R.J. *J. Org. Chem.*, **1990**, *55*, 6250.

57. Hawkins, J.M. *Acc. Chem. Res.*, **1992**, *25*, 150.

58. Fagan, P.J. ; Calabrese, J.C. ; Malone, B. *Acc. Chem. Res.*, **1992**, *25*, 134.

59. Fagan, P.J. ; Calabrese, J.C. ; Malone, B. *Science*, **1991**, *252*, 1160.

60. Fagan, P.J. ; Calabrese, J.C. ; Malone, B. *J. Am. Chem. Soc.*, **1991**, *113*, 9408.

61. Balch, A.L. ; Catalano, V.J. ; Lee, J.W. *Inorg. Chem.*, **1991**, *30*, 3980.

62. Haser, M. ; Almlof, J. ; Suseria, G.E. *Chem. Phys. Lett.*, **1991**, *181*, 497.

63. Yannoni, C.S. ; Bernier, P.P. ; Bethune, D.S. ; Meijer, G. ; Salem, J.R. *J. Am. Chem. Soc.*, **1991**, *113*, 3190.

64. David, W.I.F. ; Ibberson, R.M. ; Matthewman, J.C. ; Prassides, K. ; Dennis, T.J.S. ; Hare, J.P. ; Kroto, H.W. ; Taylor, R. ; Walton, D.R.M. *Nature*, **1991**, *353*, 147.

65. Selig, H. ; Lifshitz, C. ; Peres, T. ; Fischer, J.E. ; McGhie, A.R. ; Romanow, W.J. ; McCauley, J.P., Jr. ; Smith III, A.B. ; *J. Am. Chem. Soc.*, **1991**, *113*, 5475.

66. Holloway, J.H. ; Hope, E.G. ; Taylor, R. ; Lanley, G.J. ; Avent, A.G. ; Dennis, T.J. ; Hare, J.P. ; Kroto, H.W. ; Walton, D.R.M. *J. Chem. Soc., Chem. Commun.*, **1991**, 966.

67. Tebbe, F.N. ; Becker, J.Y. ; Chase, D.B. ; Firment, L.E. ; Holler, E.R. ; Malone, B.S. ; Krusic, P.J. ; Wasserman, E. *J. Am. Chem. Soc.*, **1991**, *113*, 9900.

68. Olah, G.A. ; Bucsi, I ; Lambert, C. ; Aniszfeld, R. ; Trivedi, N.J. ; Sensharma, D.K. ; Prakash, G.K.S. *J. Am. Chem. Soc.*, **1991**, *113*, 9385.

69. Kaiser, E.M. *Synthesis*, **1972**, 391.

70. Olah, G.A. ; Bucsi, I ; Lambert, C. ; Aniszfeld, R. ; Trivedi, N.J. ; Sensharma, D.K. ; Prakash, G.K.S. *J. Am. Chem. Soc.*, **1991**, *113*, 9387.

71. Wudl, F. *Acc. Chem. Res.*, **1992**, *25*, 157.

72. Suzuki, T. ; Li, Q. ; Khemani, K.C. ; Wudl, F. ; Almarsson, O. *Science*, **1991**, *254*, 1186.

73. Hirsch, A. ; Li, Q. ; Wudl, F. *Angew. Chem., Int. Ed. Engl.*, **1991**, *30*, 1309.

74. Creegan, K.M. ; Robbins, J.L. ; Robbins, W.K. ; Millar, J.M. ; Rexford, D.S. ; Tindall, P.J. ; Cox, D.M. ; Smith III, A.B. ; McCauley, J.P., Jr. ; Jones, D.R. ; Gallagher, R.T. *J. Am. Chem. Soc.*, **1992**, *114*, 1103.

75. Bausch, J.W. ; Prakash, G.K.S. ; Olah, G.A. *J. Am. Chem. Soc.*, **1991**, *113*, 3205.

76. Wood, J.M. ; Kahr, B. ; Hoke II, S.H. ; Dejarme, L. ; Cocks, R.G. ; Ben-Amotz, D. *J. Am. Chem. Soc.*, **1991**, *113*, 5907.

77.   Allemand, P.-M. ; Khemani, K.C. ; Koch, A. ; Wudl, F. ; Holczer, K. ;
        Donovan, S. ; Gruner, G. ; Thompson, J.D. *Science*, **1991**, *253*, 301.

78.   Minami, N. *Chem. Lett.*, **1991**, 1791.

79.   Haddon, R.C. ; Hebard, A.F. ; Rosseinsky, M.J. ; Murphy, D.W. ; Duclos,
        S.J. ; Lyons, K.B. ; Miller, B. ; Rosamillia, J.M. ; Fleming, R.M. ; Kortan,
        A.R. ; Glarum, S.H. ; Makhija, A.V. ; Muller, A.J. ; Eick, R.H. ; Zahurak,
        S.M. ; Tycko, R. ; Dabbagh, G. ; Thiel, F.A. *Nature*, **1991**, *350*, 320.

80.   Hebbard, A.F. ; Rosseinsky, M.J. ; Haddon, R.C. ; Murphy, D.W. ;
        Glarum, S.H. ; Palstra, T.T.M. ; Ramirez, A.P. ; Kortan, A.R. *Nature*,
        1991, *350*, 600.

81.   Ketty, S.P. ; Chen, C.-C. ; Lieber, C.M. *Nature*, **1991**, *352*, 223.

82.   Holczer, K. ; Klein, O. ; Huang, S.-M. ; Kaner, R.B. ; Fu, K.-J. ; Whetten,
        R.L. ; Diederich, F. *Science*, **1991**, *252*, 1154.

83.   Stephens, P.W. ; Mihaly, L. ; Lee, P.L. ; Whetten, R.L.; Huang, S.-M. ;
        Kaner, R. ; Diederich, F. ; Holczer, K. *Nature*, **1991**, *351*, 632.

84.   Rosseinsky, M.J. ; Ramirez, A.P. ; Glarum, S.H.; Murphy, D.W. ; Haddon,
        R.C. ; Hebard, A.F. ; Palstra, T.T.M. ; Kortan, A.R. ; Zahurak, S.M. ;
        Makhija, A.V. *Phys. Rev. Lett.*, **1991**, *66*, 2830.

85.   Tanigaki, K. ; Ebbesen, T.W. ; Saito, S. ; Mizuki, J. ; Tsai, J.S. ; Kubo, Y. ;
        Kuroshima, S. *Nature*, **1991**, *352*, 222.

86.   Haddon, R.C. *Acc. Chem. Res.*, **1992**, *25*, 127.

87.   Kroto, H. *Pure Appl. Chem.*, **1990**, *62*, 407.

88.   Rohlfing, E.A. ; Cox, D.M. ; Kaldor, A. *J. Chem. Phys.*, **1984**, *81*, 3322.

89.   So, H.Y. ; Wilkins, C.L. *J. Phys. Chem.*, **1989**, *93*, 1184.

90.   Rubin, Y. ; Kahr, M. ; Knobler, C.B. ; Diederich, F. ; Wilkins, C.L. *J. Am.
        Chem. Soc.*, **1991**, *113*, 495.

91.   Diederich, F. ; Ettl, R. ; Rubin, Y. ; Whetten, R.L. ; Beck, R. ; Alvarez, M. ;
        Anz, S. ; Sensharma, D. ; Wudl, F. ; Khemani, K.C. ; Koch, A. *Science*,
        1991, *252*, 548.

92.   Ettl, R. ; Chao, I. ; Diederich, F. ; Whetten, R.L. *Nature*, **1991**, *353*, 149.

93.   Diederich, F. ; Whetten, R.L. ; Thilgen, C. ; Ettl, R. ; Chao, I. ; Alvarez, M.M. *Science*, **1991**, *254*, 1768.

94.   Kikuchi, K. ; Nakahara, N. ; Honda, M. ; Suzuki, S. ; Saito, K. ; Shiromaru, H. ; Yamauchi, K. ; Ikemoto, I. ; Kuramochi, T. ; Hino, S. ; Achiba, Y. *Chem. Lett.*, **1991**, 1607.

95.   Fowler, P.W. ; Manolopoulos, D.E. ; Batten, R.C. *J. Chem. Soc., Faraday Trans.*, **1991**, *87*, 3103.

96.   Manolopoulos, D.E. ; Fowler, P.W. *Chem. Phys. Lett.*, **1991**, *187*, 1.

97.   Li, Q. ; Wudl, F. ; Whetten, R.L. ; Thilgen, C. ; Diederich, F. *J. Am. Chem. Soc.*, submitted.

98.   Morton, J.R. ; Preston, K.F. ; Krusic, P.J. ; Hill, S.A. ; Wasserman, E. *J. Phys. Chem.*, **1992**, *96*, 3576.

99.   Morton, J.R. ; Preston, K.F. ; Krusic, P.J. ; Hill, S.A. ; Wasserman, E. *J. Am. Chem. Soc.*, **1992**, *114*, 5454.

100.   Morton, J.R. , Steacie Institute for Molecular Sciences, NRCC, Ottawa, private communication to Dr. J.C. Walton.

101.   Keizer, P.N. ; Morton, J.R. ; Preston, K.F. *J. Chem. Soc., Perkin Trans II*, **1992**, in print.

102.   Brendt, A. ; Fischer, H. ; Paul, H. Landolt-Bernstein Numerical Data and Functional Relationships in Science and Technology, Vol. 9, *Magnetic Properties of Free Radicals*, Fischer, H. ; Hellwege, K.-H. Eds., p.245, p.23 and p.12, Springer-Verlag, Berlin 1977.

103.   Cohen, S.G ; Zand, R, ; Steel, C. *J. Am. Chem. Soc.*, **1961**, *83* , 2895.